UNIVERSITY OF TURIN

Department of Clinical and Biological Sciences

Doctoral School of Life and Health Sciences

PhD in Experimental Medicine and Therapy

Cycle XXXIII

PhD Thesis

Role of Hepcidin/Ferroportin1 pathway in iron homeostasis moving from canonical organs to the brain

Tutor: **Candidate**

Prof. Marco De Gobbi   Mariarosa Mezzanotte

Co-tutor:

Dott.ssa Antonella Roetto

Coordinator:

Prof. Pasquale Pagliaro

A.A: 2017-2021
SDS: MED/09

Index

1 Introduction

The relevance of iron to nearly all living organisms is indisputable. Iron is a transition metal essential for all organisms and physiologically the most abundant required in various fundamental biological processes essential for life. Iron is critical to normal cellular function and works as a cofactor in many biological pathways, including oxygen transport, oxidation reduction reactions, ATP production, DNA biosynthesis and repair (Chifman *et al.*, 2014). A common peculiarity among transition metals, including iron, is their ability of interconversions between the divalent cation or ferrous (Fe^{2+}) and trivalent cation or ferric (Fe^{3+}) states (Papanikolaou and Pantopoulos, 2005). The ability to accept and donate electrons makes it an essential component of oxygen-binding molecules (Hemoglobin and Myoglobin), cytochrome, in the electron transport chain and as a cofactor in a variety of enzymes (Papanikolaou and Pantopoulos, 2005). This property turns iron, at the same time, into an extremely harmful metal because under aerobic conditions, iron can readily catalyze the generation of toxic radicals through the Fenton reaction, in which hydrogen peroxide (H_2O_2) is converted to the highly reactive hydroxyl radical ($\cdot OH$) which can damage membrane lipids, proteins and DNA and cause cell death and tissue damage (Gammella *et al.*, 2016).

Since body iron losses are not regulated, systemic iron balance is controlled on the one hand by dietary iron uptake, and on the other hand by iron release from recycling macrophage and hepatocytes (Dev and Babitt, 2017).

1.1 Iron metabolism

Iron intake, in form of heme and non-heme iron, occurs through the diet. Only 1-2 mg of iron are absorbed daily in the gut and the same amount is lost in the urine, feces, sweat and sloughed cells. A large amount of iron is destined to red blood cell haemoglobin ($\sim$20-25 mg iron/day). The reticuloendothelial macrophages provide to recycled iron in the process of erytrophagocytosis; in these cells, as well as in hepactocytes, iron is mainly stored (Ganz, 2013) (Figure 1).

Heme iron is introduced into the enterocyte via a Heme carrier protein 1 (HCP1), a heme receptor localized on the brush border of intestinal cells. Heme is broken up into free iron and biliverdin by heme oxygenase (HMOX). The released iron then enters the low-molecular weight pool and is transferred outside from the enterocyte in the same manner as inorganic non-heme iron. HCP1 and the major transport facilitator for feline leukemic virus, subgroup C (FLVCR), have been shown to export

cytoplasmic heme in human erythroid cells, suggesting that intact heme may also be transported out of the enterocyte (Chiabrando et al., 2014).

Inorganic iron is absorbed by duodenal enterocytes via the Divalent Metal Transporter 1 (DMT1) (Andrews, 1999; Gunshin *et al.*, 1997) after reduction of iron from ferric (Fe^{3+}) to ferrous (Fe^{2+}) by duodenal cytochrome b (DcytB) localized in the apical membrane of enterocytes (McKie, 2008). The fundamental role of DMT1 in intestinal iron intake has been proven by using animal models with intestine deletion of DMT1 that provoke postnatal anaemia and systemic iron reduction (Gunshin *et al.*, 2005).

Depending on the body needs, in enterocytes, unused iron can be stored inside ferritin protein or exporter to bloodstream by Ferroportin (Fpn1), the only iron exporter (McKie *et al.*, 2000). The exported ferrous iron is then oxidized to ferric iron by Hephaestin (HEPH), a membrane ferroperoxidase (Petrak and Vyoral, 2005) and binds to circulating plasma Transferrin (Tf) (Fuqua *et al.*, 2012) (Figure 2).
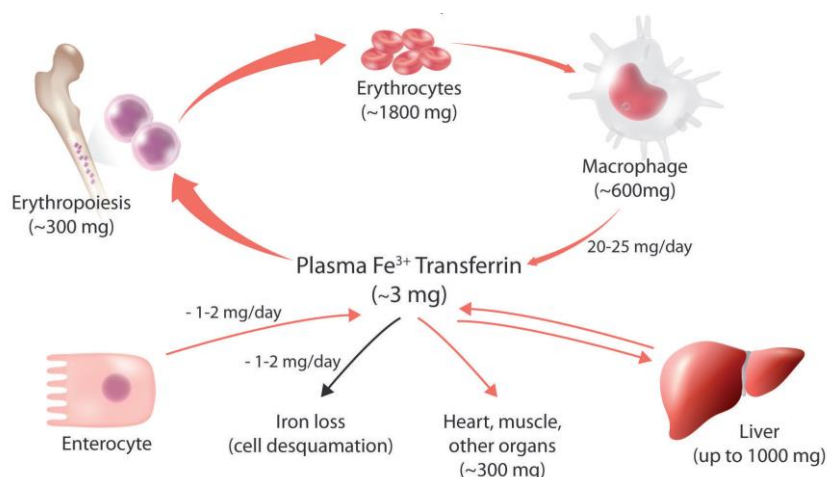
Figure 1: The iron cycle: pathways of iron traffic between human cells and tissues. Approximate daily fluxes of iron are also indicated. Iron losses result from sloughing of skin and mucosal cells as well as blood loss. Importantly, there exists no regulated excretion pathway to control systemic iron homeostasis (Camaschella *et al.*, 2020)

Holo-transferrin (Tf-Fe^{2+}) binds to Transferrin Receptor 1 (TfR1) on the cell surface and is internalized through a receptor-mediated endocytosis. Iron in the endosome, is released from Tf and reduced by metalloreductase Steap3 (Six transmembrane epithelial antigen of the prostate 3) (Ohgami *et al.*, 2005). After reduction, Fe^{2+} is transported into the cytosol by DMT1 or ZIP14 (ZRT, IRT-like protein) (Zhao *et al.*, 2010). Both apo-Tf and TfR1 return to the cell surface, where the iron-depleted Tf is released allowing TfR1 to bind other iron-loaded Tf for another round of internalization.

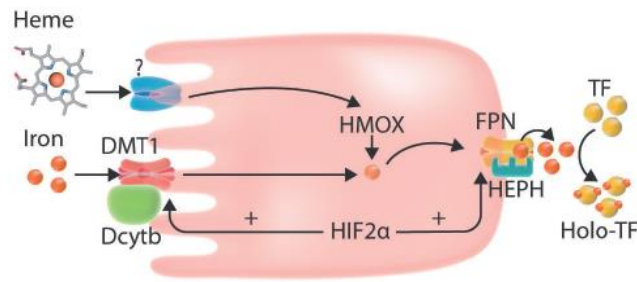TfR1 is important to maintain homeostatic intestinal epithelium, acting independently of its iron-absorption function (Chen et al., 2015a). Moreover, hepatocyte-specific ablation of TfR1 in mice models show that TfR1 is redundant at least in hepatocytes for basal iron supply, but it is essential to regulates Hepcidin (Hepc) responses according to the iron increase (Fillebeen et al., 2019).

The homolog of TfR1, Transferrin receptor 2 (TfR2), mainly expressed in hepatocytes and erythroblasts, is able to bind Tf, even if with low affinity compared to TfR1(Kawabata et al., 1999). Indeed, in iron overload condition, Tf-Fe^{2+} binds TfR2 causing Hepcidin (Hepc) upregulation in hepatocytes while in erythroid cells TfR2 binds erythropoietin receptors, inducing an erythropoietin reduction (Camaschella et al., 2016). The opposite situation occurs during iron deficiency.

1.2 Systemic iron homeostasis: Hepcidin-Ferroportin1 (Hepc-Fpn1) axis

1.2.1 BMP/SMAD pathway

The key regulator of systemic iron homeostasis is Hepcidin (Hepc) a small peptide of 25 amino acid, secreted by liver hepatocytes. Hepc secretion is regulated at the transcriptional level by different stimuli including systemic iron availability, hepatic iron stores, erythropoietic activity, hypoxia, and inflammatory/infectious states (Nicolas *et al.*, 2002). Physiologically, during iron overload conditions Hepc is upregulated, displaying a regulatory response to iron overload, while during iron deficiency condition the Hepc synthesis is reduced. Hepc controls iron export to the plasma by inducing lysosomal degradation of the iron exporter Ferroportin1 (Fpn1) in enterocytes, macrophages and hepatocytes (Nemeth *et al.*, 2004). The Hepc-Fpn1 interaction implies that when Hepc levels are low (iron-depleted states), Fpn1 and iron release by macrophages and duodenal crypt cells result up-regulated while when Hepc levels are high, Fpn1 and iron release by these cells are down-regulated (Figure 3).
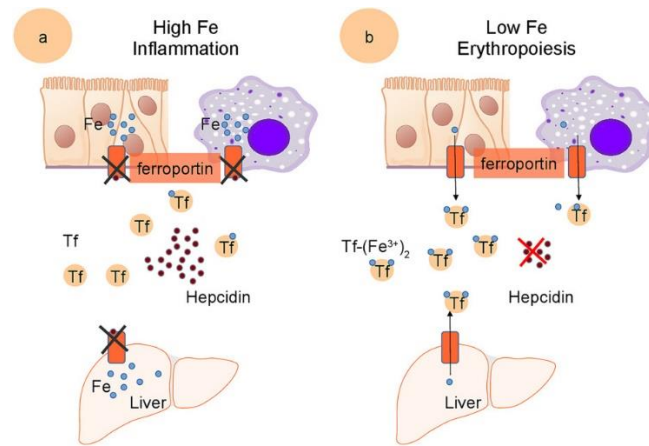
Different hemochromatosis proteins are involved in Hepc regulation: hereditary hemochromatosis protein (HFE), Transferrin receptor type 1 and 2 (TfR1 and TfR2), Hemojuvelin (Hjv), bone morphogenetic protein (BMP). These proteins coordinate the SMAD pathway signaling through the binding of Bone morphogenetic proteins to their receptors (Babitt et al., 2006) (Figure 4).

In particular, Bone morphogenetic protein 2 (BMP2), BMP6 and two types of BMP receptors, type I (BMPRI) and type II (BMPRII) are involved in this pathway activation. BMP2 and BMP6, the iron dependent proteins, work as a heterodimer activating Hepc *in vivo* (Xiao et al., 2020).

When iron levels are high, the BMP6 expression increases and bounds to BMP receptors, BMPR1-2, on the surface of hepatocytes in presence of the co-receptor Hemojuvelin (HJV). BMP6 activates the signal transduction through SMAD1/5/8 phosphorylation (pSMADs), the formation of a complex with SMAD4 (pSMADs/SMAD4) that translocates into the nucleus where it activates HEPC gene transcription (Daher and Karim, 2017). On the other hand, in conditions of low iron levels, Hepc expression is inhibited. Transmembrane serine protease matriptase 2, codified by TMPRSS6 gene (Du *et al.*, 2008), is the key protein involved in this mechanism. It downregulates BMP/SMAD signaling to Hepc since it cleaves and forms a soluble form of Hjv, one of the Hepc positive regulators, inactivating it (Silvestri *et al.*, 2008).

Serum iron level can stimulate Hepc in a BMP6 independent way that involves saturated Tf, marker of increased iron availability. HFE, TfR1 and TfR2 are involved in this signal transduction too.

When Transferrin saturation increases, the SMAD 1/5/8 phosphorylation is induced by a mechanism involving HFE protein (Corradini *et al.*, 2011). Since HFE competes with Tf for binding to TfR1, when circulating holo-transferrin raises, HFE dissociates from TfR1 and it is able to interacts with TfR2 and HJV in order to induce BMP-SMAD signaling to Hepc (Core *et al.*, 2014).

In addition to iron, the Hepc expression is induced, by inflammatory/infection situations. Interleukin-6 (IL6)/Janus Kinase 2 (JAK2) pathway, is the main pathway that takes place in induction of Hepc promoter in inflammatory conditions (Daher and Karim, 2017). In addition, Hepc is controlled by negative regulators: Erythroferrone (Erfe) and Platelet-derived growth factor-BB (PDGF-BB) are candidate factors of Hepc inhibition exerted when erythropoiesis is compromised or in hypoxic conditions, respectively (Papanikolaou and Pantopoulos, 2017) (Figure 4).
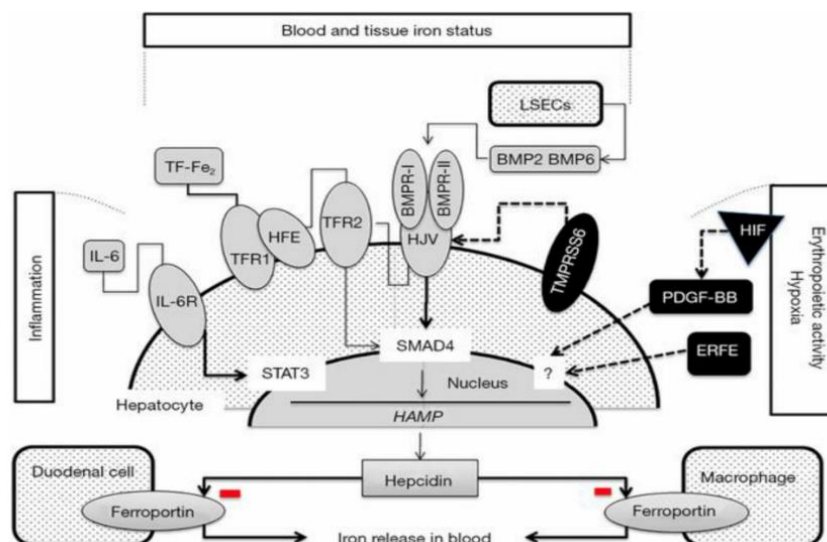
Figure 4: Regulatory pathways of hepcidin synthesis: schematic representation of Hepcidin production. HAMP refers to the HEPC gene encoding Hepcidin (Piperno et al., 2020).

1.2.2 Transferrin receptor 2 (TfR2)

As mentioned before, TfR2 physically forms a complex with hemochromatosis protein, HFE, in the cell membrane (Goswami and Andrews, 2006) and works as a component of the iron sensing machinery in hepatocytes aimed to control Hepcidin expression (Wu *et al.*, 2014). In fact, TfR2 mutations cause a non-response of Hepc to iron overload and a rare form of hereditary hemochromatosis (HFE3) characterized by iron overload and low Hepc levels (Camaschella *et al.*, 2000).

TFR2 gene is transcribed in two different isoforms, alpha and beta (see TfR2 β paragraph). The alpha isoform has a predominant role compared to the beta one in hepatic and erythroid tissues. In this context TfR2 alpha is a partner of erythropoietin receptor (EpoR) in erythroid cells (Forejtnikovà *et al.*, 2010). The mouse model with selective bone marrow TfR2 deletion, shows increased erythroblast erythropoietin (Epo) sensitivity and erythrocytosis (Nai *et al.*, 2015). TfR2 and EpoR are co-expressed during the maturation process of erythroid progenitors and it is required for efficient EpoR expression and/or stabilization on the cell membrane (Forejtnikovà *et al.*, 2010). As a sensor of iron-bound

transferrin, if on one hand erythroid TfR2 regulates erythropoiesis, hepatic TfR2 regulates Hepc synthesis, modulating iron uptake related to body needs. Indeed, TfR2 is also expresses in osteoclasts and osteoblasts as a regulator of bone homeostasis (Rauner *et al.*, 2019), drawing a connecting line between iron metabolism, red cell production and bone turnover.

After TFR2 cloning, different targeted mice have been created; Fleming and colleagues generated a germinal knockout (KO) introducing a premature stop codon (Y245X) (Fleming *et al.*, 2002) in the murine TfR2 coding sequence. This mutation, is orthologous to the human mutation Y250X, responsible to type 3 hemochromatosis (Camaschella *et al.*, 2000). In addition to TfR2 total KOs, hepatocytes-specific (TfR2 LCKO) knockout (Roetto *et al.*, 2010; Wallace *et al.*, 2007), double knockout for TfR2 and other iron genes, for example HFE (Latour *et al.*, 2016), have been generated (Table 1). The common feature of these models is inappropriate Hepc expression and a liver iron overload phenotype. Interestingly, TfR2 KO mice have milder iron overload compared to TfR2 LCKO (Roetto *et al.*, 2010; Wallace *et al.*, 2007) slightly higher Hemoglobin levels (Roetto *et al.*, 2010) and moderate macrocytosis. Moreover, Roetto et al generated a floxed knock-in model (Tfr2 KI), specifically lacking the TfR2 beta-isoform, that is known to be expressed in the spleen (Kawabata *et al.*, 1999; Roetto *et al.*, 2010), (see TfR2 β paragraph).

Classification of hereditary hemochromatosis mouse models	Mouse Genotype	Mouse phenotype
Hfe KO	Hfe -/-	Increased body iron, splenic iron retention, decreased hepcidin
	HfeAlfpCre+	Increased plasma iron and liver iron, decreased spleen iron
	HfeVillinCre +	Low hepcidin expression, increased duodenal iron absorption
	HfeLysMCre+	No significant changes (10 weeks old mice) Decreased liver Hepc mRNA expression (45 weeks) Increased Fpn1 expression in isolated macrophages (45 weeks)
Tfr2 KO	Tfr2 -/-	Reduced hepatic hepcidin levels and liver iron overload
	Tfr2AlfpCre+	Reduced hepatic hepcidin levels and more severe iron overload in the liver
Hfe-Tfr2 Double KO	Hfe -/- Tfr2 -/-	Lower hepcidin levels and more severe iron deposition compared to single Hfe or Tfr2 KO mice
	Hfe-Tfr2 LysMCre +	?

Table 1: Hereditary hemochromatosis mouse model. Hfe total KO (Hfe -/-); Tfr2 total KO (Tfr2 -/-); Enterocyte-specific KO (HfeVillinCre+); Hepatocyte-specific KO (HfeAlfpCre+); Macrophage-specific KO (HfeLysMCre+).

Furthermore, combined deletion of Hfe and TfR2 in mice models resulted in lower Hepc levels and more severe iron deposition compared to single Hfe or TfR2 knockout mice (Wallace *et al.*, 2007). And what about macrophage-specific Hfe-TfR2 double knockout mouse? Preliminary studies conducted by Roetto et al in collaboration with Vujic et al show that double KO mice at 10 weeks of age do not have abnormal serum iron parameters and hepatic iron overload. Nevertheless, they present a reduction of Hepc expression in the spleen concomitant to an increased expression and production of Fpn1; this means, an increase of iron flux from the spleen. Since macrophages are the main cells involved in iron storage and release in spleen and bone marrow, splenic and bone marrow macrophages were analysed. Interestingly, they are found to abnormally introduce and retain iron, since the iron importer TfR1, is significantly increased in these cells while iron exporter Fpn1 is decreased (unpublished data). These findings demonstrate that Hfe and TfR2 explicate an extrahepatic function in iron metabolism regulation.

The analysis of the wide amount of literature describing iron metabolism and its related proteins, TfR2 in particular, in canonical organs as liver, heart but also in extrahepatic regions, gave me the opportunity to participate in the writing of a comprehensive and detailed review published during my PhD School and reported below.

✚   *Publication: The Functional Versatility of Transferrin Receptor 2 and Its Therapeutic Value*

The Functional Versatility of Transferrin Receptor 2 and Its Therapeutic Value

Antonella Roetto *, Mariarosa Mezzanotte and Rosa Maria Pellegrino

Department of Clinical and Biological Sciences, University of Torino, 10043 Orbassano, Torino, Italy; mariarosa.mezzanotte@unito.it (M.M.); rosamaria.pellegrino@unito.it (R.M.P.)
* Correspondence: antonella.roetto@unito.it; Tel.: +39-011-6705462

Abstract: Iron homeostasis is a tightly regulated process in all living organisms because this metal is essential for cellular metabolism, but could be extremely toxic when present in excess. In mammals, there is a complex pathway devoted to iron regulation, whose key protein is hepcidin (Hepc), which is a powerful iron absorption inhibitor mainly produced by the liver. Transferrin receptor 2 (Tfr2) is one of the hepcidin regulators, and mutations in *TFR2* gene are responsible for type 3 hereditary hemochromatosis (HFE3), a genetically heterogeneous disease characterized by systemic iron overload. It has been recently pointed out that Hepc production and iron regulation could be exerted also in tissues other than liver, and that Tfr2 has an extrahepatic role in iron metabolism as well. This review summarizes all the most recent data on Tfr2 extrahepatic role, taking into account the putative distinct roles of the two main Tfr2 isoforms, Tfr2α and Tfr2β. Representing Hepc modulation an effective approach to correct iron balance impairment in common human diseases, and with Tfr2 being one of its regulators, it would be worthwhile to envisage Tfr2 as a therapeutic target.

Keywords: Tfr2; iron metabolism; hepcidin; erythropoiesis; SNC

1. Tfr2 Gene and Proteins

Tfr2 is a type II transmembrane glycoprotein, a member of the transferrin receptor family and homologous to Tfr1 [1].

It is encoded by *TFR2*, a 2471 bp long gene localized on the long arm of human chromosome 7 (7q22.1) that consists of 18 exons, and gives origin to two main variants regulated by different specific promoters: Tfr2α and Tfr2β (Figure 1).

Tfr2α results from the transcription of all exons, and is prevalently and highly expressed in hepatocytes and erythroid cell lines. Tfr2α cDNA is 2.3 kb long (AF067864), and the Tfr2α is a protein of about 89 kDa encompassing 801 amino acids [2]. As Tfr1, Tfr2α has a short cytoplasmic tail (aa 1–80) that contains a consensus sequence YQRV for endocytosis, a transmembrane domain (aa 81–104) with four cysteines (aa 89–98 and 108–111), involved in disulphide bonds, likely responsible for *TFR2* homodimerization, and a large extracellular domain (aa 105–801) comprising a protease-associated domain and two RGD motifs that bind di-ferric Tf (Fe_2Tf). Furthermore, an N-terminal mitochondrial targeting sequence (MTS) has been found in Tfr2 intracellular domain [3]. In vitro analysis demonstrated that Tfr2α on cell membranes can be shed and give origin to a soluble form, and that this process is inhibited by Fe_2Tf [4]; however, this form could not be found in animal or human sera.

Tfr2α transcription is upregulated in mouse embryonic fibroblast cells (NIH3T3) by erythroid GATA1, EKLF, and cEBP/α transcriptional factors, while FOG1 seems to inhibit GATA1

enhancement [5]. Also, hepatic Hnf4α stimulates Tfr2α transcription, since it is significantly decreased in liver-specific HNF4α-null mice [6]. There is no Tfr2α IRE/IRP-dependent post-transcriptional regulation [7], while the hepatic tetraspanin CD81 is able to interact with Tfr2α and induce its degradation [8].

Tfr2β has an in-frame transcription start site in exon 4, so the Tfr2β cDNA (NM_001206855.1) transcript lacks exons 1–3, and presents 142 additional untranslated base pairs at its 5′ end. Tfr2β is ubiquitously expressed at low level, and mostly expressed in spleen, heart, and brain. The resulting protein lacks the cytoplasmic and the transmembrane domain [2]. Since no signal peptide involved in the secretory pathway could be evidenced in Tfr2β isoform, it is supposed to be a cytosolic 60 kDa protein identical to the Tfr2α extracellular domain. At the moment, no transcriptional/translational regulatory pathway is known for Tfr2β isoform (Figure 1).
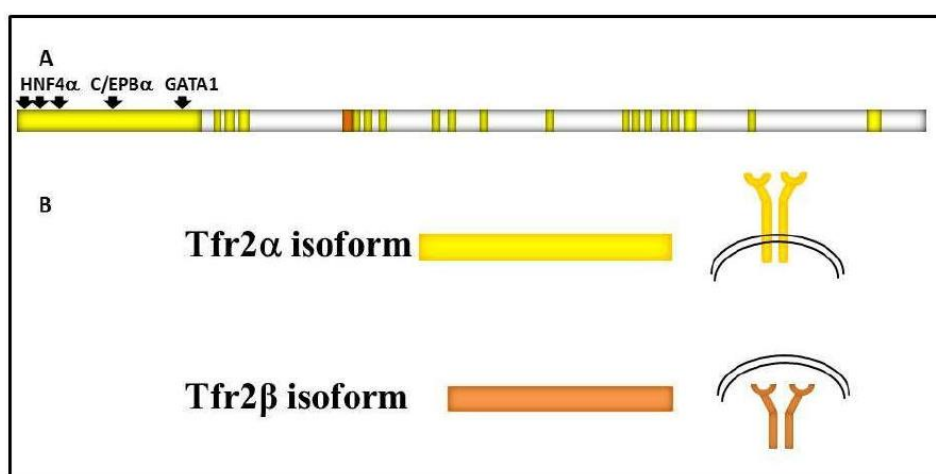

Figure 1. Schematic representation of: (**A**) *TFR2* gene structure. *TFR2* 18 exons are in bright yellow, *TFR2α* promoter is shown upstream of the gene, and transcriptional factors binding sites are highlighted by black arrows. 5′ untranslated region (142 bp long) of *TFR2β* transcript is shown in orange; (**B**) the two main transcripts and of Tfr2α and Tfr2β isoforms, that are identical in the common sequence, and the two protein localizations, on the cell surface or in the cytosol, respectively.

1.1. Tfr2 and HFE3

Inactivating mutations of *TFR2* gene (OMIM: 604720) lead to type 3 hereditary hemochromatosis (*TFR2*-HHC or HFE3), a rare recessive disorder characterized by increased transferrin saturation and serum ferritin concentration and iron overload [9].

HFE3 is one of the 5 different forms of hereditary hemochromatosis, a genetically heterogeneous disorder due to the deregulation of iron protein hepcidin (Hepc) [10] (Table 1). *TFR2*-HHC presents an earlier age of onset than type 1 hereditary hemochromatosis (*HFE-HHC*), and some pediatric patients have been reported so far. However, the majority of the affected individuals are young adults with abnormal serum iron indices [11].

Most of the mutations involved in HFE3 pathogenesis cause an inactivation of both Tfr2 isoforms, but some of them, occurring in exons from 1 to 3, impair the production of the Tfr2α isoform only [12–14]. Three patients with homozygote mutation M172K, that impairs Tfr2β translation initiation codon, were identified, all presenting typical hemochromatosis symptoms (cirrhosis, hypogonadism, cardiomyopathy, arthritis) at an average age of 38 ± 5 years [13,15].

Unfortunately, few clinical data are available on patients with these mutations to allow an exhaustive genotype/phenotype analysis.

Table 1. Hereditary hemochromatosis (HHC types) and their relationship with hepcidin.

HH type	Acronym	Inheritance	Gene	Protein	Function
HFE1	HFE-HHC	AR	HFE	Hfe	Hepc regulator
HFE2a	HJV-HHC	AR	HJV	Hemojuvelin	Hepc regulator
HFE2b	HEPC-HHC	AR	HAMP	Hepc	Fe absorption inhibitor
HFE3	TFR2-HHC	AR	TFR2	Tfr2	Hepc regulator
HFE4	FPN1-HHC	AD	SLC40A1	Fpn1	Hepc receptor

1.2. Systemic Iron Metabolism: The Hepc-Fpn1 Axis and the Proteins Involved in Hepc Regulation

In mammals, the hepatocyte-secreted hormone Hepc regulates systemic iron homeostasis [16]. Hepc is codified by *HAMP* gene, which encodes for an 84 amino acids precursor protein, from which active 20–25 amino acids peptides are generated [17]. It is expressed primarily in the liver, although low levels of Hepc transcripts have been also reported in other organs [18].

How *HAMP* gene expression is regulated is mostly unknown. There are no IRE elements in its transcript, but the transcriptional factor CCAAT/enhancer binding protein-α is highly expressed in the liver, and seems to stimulate *HAMP* expression, while the hepatocyte nuclear factor 4-α (HNF-4) represses Hepc expression [19].

The molecular processes involved in hepatic Hepc regulation are quite complex. Basal Hepc expression is regulated through the bone morphogenetic protein 6 (Bmp6) and Smad protein signaling pathway. In iron excess condition, Bmp6, produced and secreted by liver sinusoidal endothelial cells (LSECs) [20], binds to bone morphogenetic protein receptors, ALK2 and/or ALK3 [21], activin receptor type 2A (Actr2a) [22], Hemojuvelin (Hjv) and Neogenin [23]. The protein complex activates signals transducers Smad1/5/8, leading to their interaction with the common mediator Smad4. As a consequence of this interplay, Smad4 translocates into the nucleus and promotes Hepc transcription [16].

More recently, it has been demonstrated that bone morphogenetic protein 2 (Bmp2), expressed in LSECs, can also trigger Hepc transcription increase [24].

A second Hepc regulatory pathway involves di-ferric Tf (Fe2Tf) as the signaling of increased iron availability, transferrin receptor 1 (Tfr1), hemochromatosis type 1 protein (Hfe), and transferrin receptor 2 (Tfr2). It has been demonstrated that Fe2Tf competes with Hfe for binding Tfr1 then, when circulating, Fe2Tf increases as a consequence of iron raising, Hfe dissociates from Tfr1 and binds Tfr2 [25]. Hfe/Tfr2 complex is then responsible for Hepc response to iron increase, through the activation of Erk1/2 and MAPK cascade that has been proposed to potentially converge on the Bmps/Smad1/5/8-mediated pathway [26].

The hierarchy of the two pathway activations, and their relationship, are still not completely defined. In vitro data support the hypothesis that the complex Hfe/Tfr2 interacts with membrane Hjv (mHjv) on cell surface, thereby, the link between the two signaling pathways occurs [27]. It has been found, in vivo, that both Hfe and Tfr2 knock-out (KO) mice present lower pErk1/2 [28] and pSmad1/5/8 proteins [29,30], meaning that these two proteins regulate both signal translation pathways. Hepatic Hepc upregulation is inhibited by matriptase 2 (MT-2 or Tmprss6), that acts as Hepc inhibitor cleaving mHjv expressed on the plasma membrane [31]. *TMPRSS6* gene expression has been found to be induced by chronic dietary iron loading and Bmp6 injection [32], and its interaction with Neogenin facilitates mHjv cleavage and inactivation in transfected cells [23] (Figure 2).

On the contrary, in iron deficient conditions, this signaling pathway is inhibited by soluble Hjv (sHjv) and Tmprss6, which physically interacts with mHjv, causing its fragmentation.

Hepc expression in hepatocytes is systemically regulated by multiple signals: body iron availability, such as iron-loaded transferrin and hepatic iron stores, erythropoietic activity, hypoxia, and inflammation [33]. Hepc secreted by hepatocytes regulates iron release from duodenal enterocytes, splenic macrophages, and hepatocytes, which are responsible for dietary iron absorption, contain large amounts of iron from erythrocyte recycling, and act as an iron reservoir and export iron when needed, respectively. Hepc exerts its function, binding the iron exporter ferroportin 1 (Fpn1) [34] and stimulating complex internalization and degradation, leading, de facto, to cellular retention of iron [35]. Elevated plasma Hepc, as in inflammatory state, downregulates iron efflux from several cell types, and this leads to an overall reduction in plasma iron. On the contrary, low Hepc, as seen in iron-depleted or erythropoietic expansion conditions, causes an increased iron release by macrophages and by the basolateral site of villi duodenal cells.

A potent Hepc inhibitor signal is iron demand for erythropoiesis, mediated by three Hepc modulators (Gdf15, Twgs1, Erfe). Their roles and precise mechanisms in Hepc regulation are still not completely clear, but Erfe, in particular, has emerged as a potent Hepc negative regulator in conditions of acute erythropoietic demand, acting in conjunction with erythropoietin (Epo) signaling, as well as in anemia of inflammation (AI) condition [36].
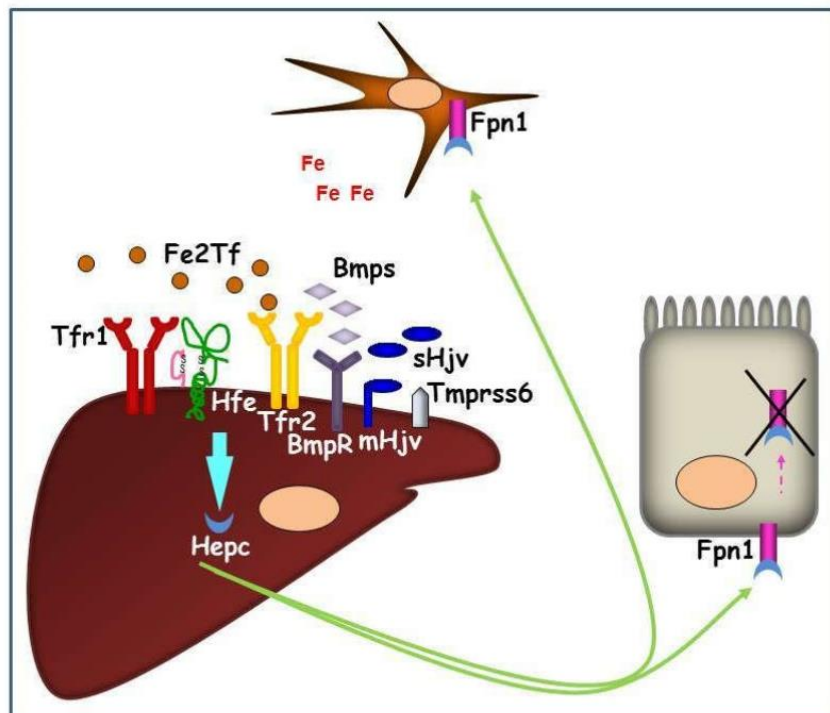
Figure 2. Graphic representation of the hepatic Hepc pathway in conditions of systemic iron increase. The iron signaling proteins (Fe2Tf and Bmps) interact with iron sensors (Tfr1, Hfe, Tfr2, BmpRs) and their co-activator (mHjv) to promote Hepc production. Hepc, secreted by hepatocytes, is transported in plasma and binds iron exporter Fpn1 on duodenal and reticuloendothelial cell surfaces causing its internalization and intracellular degradation. As a consequence, iron remains entrapped in these cells, systemically reducing the metal availability.

HAMP expression is induced by inflammation and infection. This acute phase response involves a different pathway from the ones described above, and is mainly mediated by interleukin 6 (IL-6) inflammatory cytokine, and requires the signal transducer and activator of transcription 3

(STAT3) activation, and the binding of STAT3 to a STAT3-binding motif in the Hepc promoter [37]. In addition, cytokine IL-22, involved in immunological response to extracellular infections, as well as Toll-like receptor 5 (TLR5) agonist flagellin, seem to upregulate Hepc, strengthening the hypothesis of a possible Hepc role in innate immunity [38].

Conversely, *HAMP* expression is repressed by hypoxia both in vitro and in vivo in animal models [33] and humans [39,40]. The mediator of Hepc response to hypoxia seems to be the hypoxia inducible factor (HIF), even though it is not clear if it acts directly or indirectly on Hepc regulation [16]. The fact that Hepc inhibitor, Tmprss6, presents a hypoxia responsive element (HRE) in its promoter [41] might make Tmprss6 the linking protein between hypoxia and iron homeostasis.

Mutations in *HAMP* gene and in genes codifying for Hepc regulatory proteins (*HFE*, *TFR2*, and *HJV*) cause the lack of upregulation of Hepc as a response to increased liver iron stores. In fact, inappropriately low levels of liver Hepc are observed in patients and mouse models of hereditary hemochromatosis [42,43]. These conditions promote a continuous dietary iron absorption that leads to iron overload. On the contrary, inappropriately high Hepc has been found in animal models and patients with iron resistant iron deficient anemia (IRIDA), a genetic disorder due to mutations in *TMPRSS6* gene [44–46].

2. Tfr2 in Liver

In the liver, Tfr2α is a sensor of circulating iron, but the knowledge about the Tfr2α hepatic function is still incomplete. It is known that Tfr2α localizes in caveolar microdomains [47], membrane structures involved in the recruitment of receptors that can be activated by ligand binding [48]. Also, Tfr2α localizes in lipid raft domains on the exosomal cell membrane, where it is internalized by clathrin-mediated endocytosis, if transferrin saturation (TS) is low [49].

Tfr2α protein regulation occurs mainly through its stabilization on the cell membrane as a consequence of the binding to Fe2Tf [50,51]. An in vitro study showed that, in the presence of Fe2Tf, Tfr2α has an increased half-life and is recycled, while in presence of apo-Tf membrane, Tfr2α is mainly subjected to lysosomal degradation [52]. It has been recently demonstrated that CD81 is also able to induce Tfr2α degradation, but the correlation between this Tfr2α regulatory route and Hepc pathway is still obscure [8].

Therefore, increased TS has an opposite effect on the two Tfrs via two different mechanisms: it causes a decrease of Tfr1, regulated by the IRE/IRP system, but a stabilization of Tfr2α on the cell surface [1].

This supports the hypothesis that Tfr2α exerts its function(s) as a signaling receptor more than as an iron importer.

According to the available in vitro data, hepatic Tfr2α interacts, on the cell membrane, with two main iron proteins, Tfr1 and Hfe.

The current model assumes that Tfr2α, in conjunction with HFE and Tfr1, is a partner of a sensor complex of circulating iron that activates Hepc in response to elevated TS [53]. In physiological conditions (TS 30–35%) Hfe and the complex Tf/Tfr1 are bound on the plasma cells; when TS increases in response to increased iron availability, loaded Tf impairs Hfe binding to Tfr1/Tf complex, leading it to bind Tfr2α, that is stabilized on the membrane by the same Fe^{2}Tf. The resulting complex Tfr2α/Fe2Tf/Hfe causes the activation of Hepc transcription [25]. On the HuH7 hepatoma cell surface, this Tfr2α/HFE interaction occurs within a multiprotein complex, that also includes mHjv [27]. It remains to be demonstrated if this complex activates the intracellular signaling to upregulate Hepc expression, also, in vivo.

In the presence of Fe2Tf, Tfr2α is able to activate Erk1/2 and p38 MAPK kinase signaling transduction pathway [47], since Tfr2 KO mice present a decrease of pErk1/2 [28]. Furthermore, the Smad1/5/8 pathway also seems to be involved in Tfr2α-mediated signal transduction, since pSmad1/5/8 is decreased in Tfr2 KO animals, as well [29].

Erk 1/2 phosphorylation could be increased also by Hfe overexpression, and both Tfr2 and Hfe cause an increase of the pro-hormone convertase furin [29], previously demonstrated to be involved

in Hepc regulation [54]. Whether it is the sole and/or the main Tfr2 dependent Hepc regulatory pathway is still not clear.

3. TFR2 Mouse Models

The first Tfr2 KO animal model was generated by targeted mutagenesis, introducing a premature stop codon (Y245X) in the murine Tfr2 coding sequence [55]. This mutation is homologous to the Y250X variant, originally detected in humans and responsible for HFE3 [9]. Even young homozygous Y245X mice maintained on a standard diet had high liver iron concentration, in agreement with the observation of early iron overload in HFE3 patients [11]. As in humans, heterozygous animals were normal. The histological distribution of iron resembles the features of HFE3, with the typical liver periportal accumulation.

Subsequently, different murine models of Tfr2 inactivation were developed, including Tfr2 total (Tfr2 KO) and liver-specific (Tfr2 LCKO) knockouts [56,57] as well as a Tfr2/Hfe double KO [28]. All these models are characterized by an inadequate hepatic Hepc expression and liver iron overload with variable severity. However, when generated in the same genetic background, Tfr2 KO mice were shown to have a more severe iron overload than Hfe KO, although less severe than the Tfr2/Hfe double KO [58]. These observations are in agreement with the model of Tfr2/Hfe proteins' cooperation in the liver.

In a double Tfr2/Hjv KO mouse model, plasma Hepc and Hepc transcription was lower than in Tfr2, and similar to Hjv single KOs, respectively. The same was true for the Tfr2/Hfe double KO [59]. Also, a recent study on a mouse model with inactivation of both Bmp6 and Tfr2 (Tfr2/Bmp6 double KO) demonstrated that loss of functional Tfr2 further represses Hamp expression, Smad5 phosphorylation, and plasma Hepc amount in Bmp6 KO mice. The same results were obtained in the Hfe/Bmp6 double KO, and the Hfe/Bmp6/Tfr2 triple KO [60]. All these data support the hypothesis that Tfr2 and Hfe act downstream Bmp6 and upstream Hjv in Hepc regulatory pathway.

Last, Tfr2 germinal vs liver-specific KO animals highlighted a distinct function of Tfr2 outside the liver in maintaining iron balance. In fact, Tfr2 KO mice have less severe iron overload, slightly higher hemoglobin (Hb) levels [57,61], and moderate macrocytosis than Tfr2 LCKO [56,57].

To study the specific function of Tfr2β isoform in iron metabolism, a specific mouse model was generated, introducing the M167K substitution in the Tfr2 protein [57]. This mutation, homologous to the one found in naturally mutant individuals with HFE3, substitutes the start codon methionine of the Tfr2β isoform, with a lysine. Interestingly, this knock-in mouse model (Tfr2 KI), specifically lacking the Tfr2β-isoform ($\alpha^+\beta^0$), is characterized by normal transferrin saturation, liver iron concentration, Hepc, and Bmp6 levels, but shows transient anemia at a young age. In addition, adult Tfr2 KI animals accumulate iron in the spleen, due to a significant reduction of iron exporter Fpn1 mRNA, thus suggesting a possible regulatory effect of Tfr2β isoform on splenic Fpn1 expression. These data are further supported by the results obtained in Tfr2 macrophage-specific KO mouse model. These animals present normal systemic iron parameters, but lower Fpn1 transcript and protein in peritoneal macrophages [62]. Recent studies demonstrated that Tfr2β is well expressed in reticuloendothelial cells of different tissues, where it exerts its role in modulating iron availability in these tissues, acting on Fpn1 transcription (see below). Since Fpn1 protein has several regulatory systems both at the transcriptional [63,64] and post-transcriptional level through IRE/IRP system [7], and origins from different Fpn1 transcripts with or without IREs [65], it remains to be clarified how and when Tfr2β acts on Fpn1 regulation.

4. Tfr2 in Extrahepatic Tissues

4.1. Tfr2 in the Erythropoietic Compartment

A Tfr2α erythropoietic role was firstly hypothesized in genome-wide association studies that identified Tfr2α polymorphisms affecting hematologic parameters [66,67]. These data were further strengthened by the identification of Tfr2α as a component of the erythropoietin receptor (EpoR)

15

complex in erythroid progenitor cells. Tfr2α was shown to be crucial for efficient transport of EpoR to the cell surface and for its terminal differentiation, since human erythroid progenitors with silenced Tfr2α showed a delayed differentiation [68]. Another hint was provided by the increased Hb content present only in Tfr2 germinal KO, but not in liver-specific KO mice. Since both mouse models manifest comparable iron overload, the lack of enhanced hemoglobinization in Tfr2 LCKO mice suggests that the erythroid function of Tfr2α is preserved [68]. Also, double Tmprss6/Tfr2 KO mice develop erythrocytosis while, in double Tmprss6/Tfr2 LCKO mice, where Tfr2α is functional in erythroid cells, red blood cells (RBC) number is normal [61].

Recently, a mouse model lacking Tfr2 in bone marrow cells (Tfr2[BMKO]) was developed injecting BM cells from Tfr2 KO mice in lethally irradiated C57/BL6 mice. Tfr2[BMKO] mice manifest reduced mean corpuscular value (MCV) and low Hepc levels as a typical response to iron deficiency, but an enhanced terminal erythropoiesis, demonstrated by increased RBC and Hb content [69]. Interestingly, erythropoiesis and Epo level in these mice do not change in a mild dietary restriction setting, as happens for WT animals, where the Epo level is drastically increased.

As a whole, these data suggest that the lack of Tfr2 confers increased Epo sensitivity to erythroid progenitor cells, a hypothesis that is further supported by the induction of Epo target genes, like Hamp regulator Erfe [70], in these animals.

A similar animal model was recently developed crossing Tfr2 floxed mice with Vav-Cre expressing mice to obtain Tfr2 silencing in erythroid compartment [62]. Results differed from previous work since decreased RBC and splenomegaly were observed, but these discrepancies might be explained by the different procedures used to create the two mouse models since, in the first case, Tfr2 is silenced in all bone marrow (BM) cell lines after a BM transplant procedure while, in the latter, only the erythroid cell lines are Tfr2null.

In another study, Tfr2 erythropoietic role was further investigated studying the erythropoiesis of two Tfr2 mice with one or both Tfr2 isoforms silenced (Tfr2 KI and Tfr2 KO), and with normal or increased iron availability [57]. The evaluations were performed in bone marrow and spleen, in young and adult animals to unravel the erythropoietic role of Tfr2 isoforms at different ages, and in the two main erythropoietic organs. It resulted that the lack of Tfr2 in Tfr2 KO mice leads to macrocytosis with low reticulocyte number and increased Hb value, together with an anticipation of erythropoiesis in young mice both in BM and in the spleen [71], probably because the increased systemic iron amount present in these animals allows them to reach mature erythropoiesis even at a young age.

Although different animals and approaches were used in these studies, and partially contradictory results were obtained, they all demonstrate that erythropoiesis is impaired by a lack of Tfr2 in BM, independently from its activity in hepatic tissues.

Moreover, results obtained studying Tfr2 KI ($\alpha^+\beta^0$) mice [57] demonstrated, for the first time, the involvement of Tfr2β in favoring iron availability for erythropoiesis. In fact, the sole lack of Tfr2β, in normal systemic iron condition, causes an increased but immature splenic erythropoiesis seen only in young mice, as if they had insufficient iron availability during animal growth, that is normalized in animal adult age. Decreased iron availability for erythropoiesis in Tfr2 KI young mice is demonstrated by increased ferritin (Ft) and decreased divalent metals transporter 1 (DMT1) in their splenic monocyte, the increase of Erfe transcription in BM and spleen, and the low hepatic Hepc transcription that could, in turn, be responsible for the increased splenic Fpn1 amount in these animals [71].

This effect, due to Tfr2β absence, in aged matched Tfr2 KO ($\alpha^0\beta^0$) mice, was compensated by the increased amount of circulating iron available that may be used for erythrocyte production (Figure 3A).
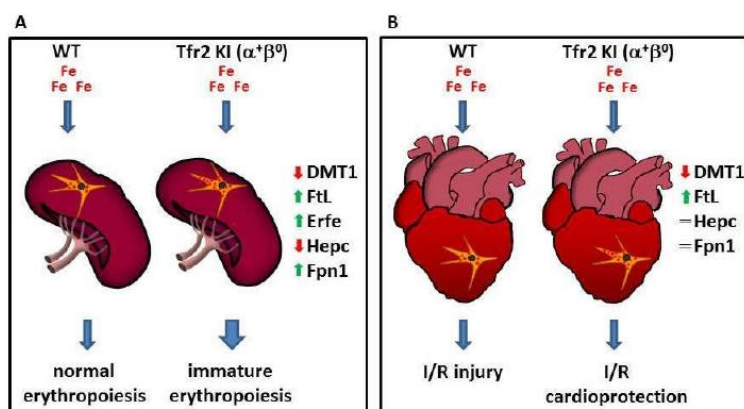
Figure 3. Schematic model illustrating Tfr2β function in regulation iron export from reticulo-endothelial (REL) cells. Lack of Tfr2β causes an increased iron retention in REL cells that (**A**) causes the onset of an immature erythropoiesis in the spleen, and (**B**) induces a cardioprotection against the effect of the reperfusion of oxygenated solutions after an ischemic event in heart (see text).

4.2. Tfr2β in the Heart

The cardiac muscle is a major site of oxygen consumption, so an adequate intracellular iron pool is essential to its aerobic activity. This is demonstrated by the finding that deletion of cardiac Tfr1 in mice causes fatal energetic failure in cardiomyocytes [72]. Cardiomyocytes express relatively high levels of Hepc and Fpn1, despite the fact that these cells have no role in systemic iron control [73].

Studies on mouse models demonstrated that the cardiac Hepc/Fpn1 axis is essential for heart cells' autonomous control of the intracellular iron pool that guarantees a normal cardiac functionality [73], and that Hepc/Fpn1 appears to protect the heart from the effects of systemic iron deficiency [74].

On the other side, cardiomyocytes are particularly susceptible to ROS-mediated damage because they are rich in mitochondria and consume large amounts of oxygen [75]. Therefore, when labile iron pool (LIP) expansion occurs, oxidative stress can affect cardiac functions, as it happens in severe juvenile HHC forms [10].

Although ubiquitously expressed, Tfr2β is highly transcribed in heart [2], such that a role for Tfr2β isoform in cardiac iron management has been postulated.

Indeed, in the hearts of two Tfr2β null mice with normal or increased systemic iron amount, Tfr2 KI and Tfr2 LCKO [57], the silencing of Tfr2β induces a selective activation of different proteins involved in cell survival, antioxidant enzymes, and kinases involved in cardioprotective pathways that are usually activated by stressful stimuli.

In particular, Tfr2 KI and Tfr2 LCKO mice develop a greater resistance against acute ischemia/reperfusion (I/R) challenge, irrespective of animals' systemic iron content, via the activation of the RISK or SAFE/GSK3β cardioprotective pathways, respectively. The iron imbalance present in these mice hearts was demonstrated by the finding that both models present the activation of antioxidant proteins, pro-apoptotic markers, and catalase, even before I/R [76]. They also have a slightly increased synthesis of cardiac ferritins, similarly to what happens in ischemic preconditioning, in which a small increase of ferritin protects cardiac cells from iron-mediated oxidative damage associated with ischemia/reperfusion injury [77].

Since previous data demonstrated a significant decrease of Fpn1, and an increased iron deposit in splenic macrophages in Tfr2β-null mice [57,71], one might hypothesize that Tfr2β isoform inactivation, in the heart, causes an iron retention in cardiac reticuloendothelial cells that is able to

induce cardioprotective pathways activation and to reduce iron availability to form free oxygen radicals during the reperfusion phase (Figure 3B).

4.3. Tfr2 in the Central Nervous System (CNS)

Iron levels in the brain vary during life. The iron amount increases with aging in the striatum and the brain stem [78] and it is present in most CNS cell types: neurons, oligodendrocytes, microglia, and astrocytes [79]. A well-regulated iron homeostasis is important for brain development and function. Iron deficiency negatively impacts neurodevelopmental processes [80], and is also implicated in a number of psychiatric and neurological conditions, learning disabilities, attention deficit hyperactivity disorder (ADHD), and pediatric restless legs syndrome (RLS) [81,82]. On the contrary, brain iron overload is present in Alzheimer's and Huntington's neurodegenerative disorders, as well as in Parkinson's disease (PD) [83]. Nevertheless, the exact role of iron in these diseases' onset/worsening is still debated, and it remains to be clarified whether brain iron overload is directly involved in their pathogenesis, or it is a secondary effect that contributes to their clinical symptoms' progression.

The main sites of brain iron uptake are the brain vascular endothelial cells (BVECs) present in the blood–brain barrier (BBB) [84]. As in other organs, there are two main pathways responsible for CNS cells' iron uptake, the Tf-Tfr1 pathway, and the NTBI transport pathway. Traditionally, Tf-Tfr1 is considered a major pathway, and works as in all the other cell types of the organism, through a receptor-mediated endocytosis of plasma Tf circulating in the ventricles [85].

The NTBI transport pathway has been recently revaluated as a significant way to introduce iron in CNS, and it could be done through vesicular or non-vesicular mechanism. In the first case, Tf homologues, such as lactoferrin and melanotransferrin, might be involved in Tfr-mediated iron transport; moreover, the newly characterized Ft receptors, Tim 2 and Scara5, can introduce iron inside the cells through a Ft-FtR pathway. Non-vesicular iron uptake can be exerted by iron importer DMT1, that is present in endothelial cells of the brain microvasculature, as well as other importers like IN4/5/6 [86].

In CNS, the iron exporter Fpn1 is found in BVECs, neurons, oligodendrocytes, astrocytes, the choroid plexus, and ependymal cells and microglia, together with ceruloplasmin (CP) or hephaestin (Hp), the two ferroxidases that cooperate with Fpn1 to facilitate iron export [87]. Fpn1 could be the main protein responsible for iron release from CNS cells, even if other proteins and mechanisms have been brought into play for these processes [86].

Inside brain cells, the majority of iron is bound to ferritin heteropolymers (Ft H/L) [88]. Their cellular distribution and ratio varies with iron status, age, and disease conditions [89].

CNS iron homeostasis is intracellularly modulated by (IRE/IRPs) system [90], and by local and systemic Hepc. Injection of Hepc into the mouse lateral cerebral ventricle decreases Fpn1 protein levels and treatment of primary cultured rat neurons with Hepc decreases Fpn1 expression and reduces these cells release of iron [91]. More recently, it was demonstrated that injection of adenovirus expressing Hepc (ad-hepcidin) in brain ventricles reduces brain iron in iron-overloaded rats through the downregulation of iron transporter [92]. This data indicates that Hepc/Fpn1 axis is present and acts in CNS, as in the other districts of the organism.

It remains a matter of debate whether Hepc acting in brain is locally produced or comes from the systemic circulation crossing the BBB or both [93].

Similar to other Hepc regulatory proteins, Tfr2 gene expression has been shown in total brain extracts [2,94], in brain tumor cell lines [95], or in specific neuronal subtypes as dopaminergic neurons [3]. Furthermore, a transcriptome study on Tfr2-null mice revealed that several genes involved in the control of neuronal functions are abnormally transcribed [96]. Of note, the same experimental approaches, applied to Hfe-null mice, revealed that a consistent percentage of transcripts are modified in the same way in the two models [96]. This highlights the possibility of a cooperation between Tfr2α and Hfe protein in CNS iron regulation, as in the rest of the organism.

Immunofluorescence studies using a Tfr2α-specific antibody demonstrate that the protein is significantly produced in mouse hippocampus, amygdala, central nucleus, and in the hypothalamic paraventricular nucleus [97].

A recent study assessed the situation of iron in the brain of Tfr2 KO mouse model vs WT sib pairs subjected to an iron-enriched diet (IED). They both are iron overloaded animals, so one could distinguish the effects of Tfr2 silencing from those due to Tfr2-independent iron load modifications.

It has been demonstrated that Tfr2 causes a lack of brain Hepc response to the systemic rise of iron levels, with altered iron mobilization and/or cellular distribution in the nervous tissue [98].

Moreover, Tfr2 KO mice present a selective over activation of neurons in the limbic circuit and the emergence of an anxious-like behavior.

Also, microglial cells showed sensitivity to iron perturbations of Tfr2 KO mice, being more reactive, dystrophic, and with a high level of apoptosis [97]. In light of these data, Tfr2 appears to be a key regulator of brain iron homeostasis, and could have a role in the regulation of the brain regions that are involved in the anxiety onset, mainly, the basolateral and central nucleus subregions of the amygdala [98].

5. Tfr2 in Intracellular Iron Trafficking

It is still under debate if Tfr2α contributes to iron introduction inside the cells. When the protein was characterized, it was reported that, in vitro, it was able to introduce iron inside cells [2], but its contribution to intracellular iron amount in vivo seems to be quite negligible, since Tfr1-deficient mice present severe iron deficiency not compensated by the presence of Tfr2 [1].

Conversely, Tfr2α seems to have a role in intracellular iron trafficking, at least in specific cell types. The first evidence about it was found in dopaminergic neurons, where a novel Tf/Tfr2α-mediated iron transport pathway to the mitochondria has been reported [3]. Disruption of this Tf/TfR2α-dependent system has been associated with PD, and this finding highlights the role of iron accumulation in this movement disorder [3]. In this regard, a protective association between some Tf and TfR2α genetic haplotypes and PD was reported, suggesting that Tf or a Tf/TfR2α complex may play a role in the etiology of these disorders [99].

More recently, a similar TfR2α function in iron delivery to mitochondria has been convincingly demonstrated in erythroid cells. In an intermediate stage of human erythroid cell maturation, Tfr2α was present in cytoplasmic multi-organellar complexes, formed by lysosomes surrounded by mitochondria, and found to be co-regulated with several proteins, among which, ionic channels and proteins involved in lysosomal modification and in mitochondrial membrane contacts to other intracellular organelles [100]. Therefore, Tfr2α in lysosomes has been proposed to be involved in iron delivery from these organelles to mitochondria, for Hb synthesis. Considering the abovementioned evidence about a specific role for Tfr2α in erythropoiesis, this data might represent one of the molecular processes at the basis of Tfr2α erythropoietic function/s (Figure 4).

In light of the above data, Tfr2α involvement in iron delivery to the mitochondria, notably, seems to work at least in the two compartments in which this protein is significantly produced: brain and bone marrow. Although a similar mechanism has been evidenced also in cell lines derived from other organs (HeLa and hepatoma cell lines) [52,101], it remains an open question if this TfR2α function is present also in other cell types.
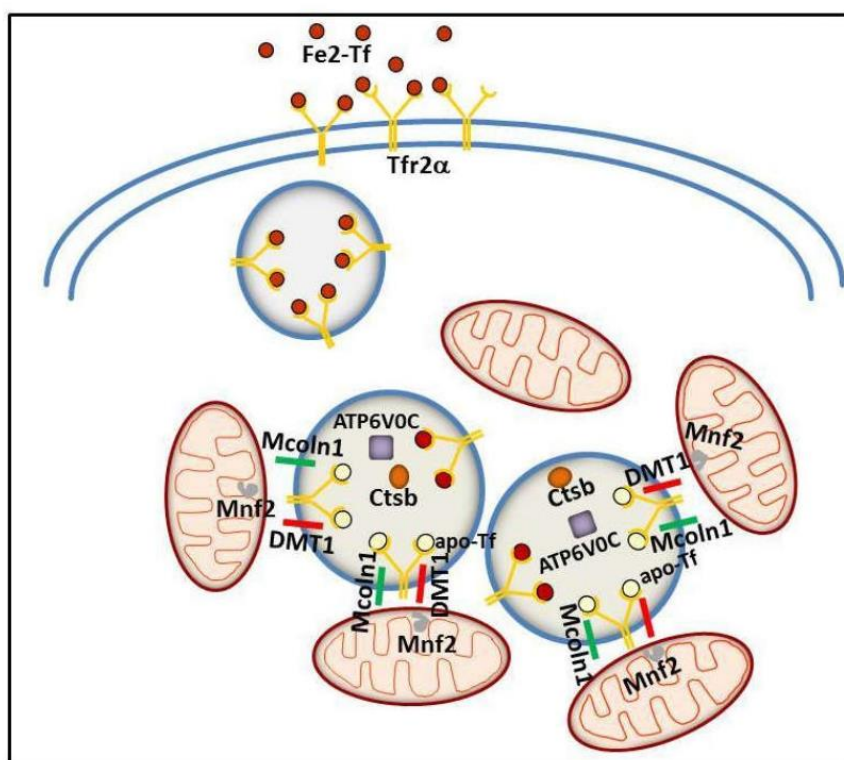
Figure 4. Schematic model illustrating the putative intracellular Tfr2α role in erythroid cells. Tfr2α—together with ATPV0C, a V-ATPase that contributes to vesicular acidification and lysosomal activity; Mcoln1, a lysosomal divalent cation channel; lysosomal cathepsin B (CTSB); and iron importer DMT1—could be involved in iron delivery from lysosome to mitochondria, with the collaboration of Mitofusin-2 (MFN-2), a mitochondrial outer membrane protein involved in mitochondria–endoplasmic reticulum contacts.

6. Tfr2 in Other Diseases

Being a "regulator of the iron regulator" hepcidin, Tfr2 transcriptional analysis was attempted to unravel if the Tfr2 isoforms could be reliable markers for some disorders in which iron perturbations occur.

6.1. Tfr2 in Cancer

Cancer cells need an increased amount of iron for their growth, and iron importers upmodulation confer a selective advantage to these cells.

Since its characterization, the significant transcription of *TFR2* gene appeared evident in BM cancer cells, in particular, erythroid leukemic cells [5], but also in myeloid malignant cells [2], while Tfr2β seemed much more prevalent than the TfR2α isoform in chronic B cells lymphocytic leukemia (B-CLL) cells [102].

Due to high *TFR2* expression in erythroid lineage, and to its functional relationship with the erythropoietin receptor (EpoR) [68], *TFR2* transcription was evaluated in patients with myelodysplastic syndromes (MDS), a hematopoietic disorder with a variable risk to evolve in acute myeloid leukemia (AML), and in which chronic anemia can be corrected by Epo injection [103]. It has been found that Tfr2α and Tfr2β isoforms, as well as EPOR transcript, have a lower level of transcription in BM from high risk MDS patients, such as RAEB2, compared to controls and low risk

MDS cells [104]. Likewise, AML patients with high level of Tfr2α and Tfr2β present an increased survival [105]. Therefore, Tfr2 isoforms might represent good predictive markers for MDS/AML prognosis.

Calzolari et al. 2007 [106] demonstrated *TFR2* expression in colon and ovarian cancer cell lines, as well as in lymphoma and glioblastoma (GBM). Moreover, in glioblastoma TB10 cell line under hypoxic condition, a marked increase of *TFR2* transcription was observed. In these cell lines, *TFR2* high expression is probably correlated with cell proliferation, since Tfr2 silencing inhibited GMB cell growth. Surprisingly, tumor cells from GBM patients with high *TFR2* transcriptional levels present a better prognosis compared to patients with low transcripts. Although, this is probably due to the fact that Tfr2-expressing cells have a highly increased proliferation, so they are more sensitive to temozolomide, the anti-proliferative drug used in GBM therapy, more than to a direct involvement of Tfr2 in the disease course [107].

6.2. Tfr2 in Alzheimer's Disease (AD)

Alzheimer's disease (AD) is another common degenerative disorder in which iron perturbation has been demonstrated [108].

A recent genetic study from 116 AD patients has found that a Tfr2 single nucleotide polymorphism (rs 7385804) and a Tfr2 haplotype, composed by two SNPs (rs 7385804 and rs 4434553) are associated with a decreased AD susceptibility [109].

In the same study, a significant decrease of Tfr2 transcription was found in peripheral blood mononuclear cells (PBMC) from AD patients, compared to healthy controls ($p < 0.001$) [110].

7. Tfr2 as a Therapeutic Target

In our opinion, three might be the major application of Tfr2α as a therapeutic target: (a) as Hepc regulator, it could be a target in disorders in which Hepc amount is, in some way, inadequate to body iron availability; (b) since Tfr2α production is selective in specific organs and cell types, it could represent a selective target to correct iron perturbation in these organs; (c) Tfr2, being a membrane protein that is able to bind plasma Tf and to be internalized with it, this property could be utilized as a vector for drugs.

As mentioned above, TfR2α is involved in regulation of Hepc and, in consequence, in iron modulation according to body/organs needs. Among the Hepc-related disorders there are all the hereditary hemochromatosis forms (Table 1) and the secondary iron overload disorders, like hemoglobinopathy, where abnormally low Hepc amounts lead to iron overload.

In this regard, just published data demonstrate that Tfr2 KO BM transplantation in beta-thalassemia intermedia (β-TI) mouse models significantly improved these animals' erythropoiesis, opening a new way to the therapy of this very common disorder [111].

In IRIDA and anemia of chronic disease (ACD), where abnormally high Hepc causes the onset of an iron deficiency condition [111], Tfr2 downmodulation might be beneficial to decrease Hepc hyperproduction. A preliminary study on mice revealed that Tfr2 silencing, through small interfering RNAs (Tfr2-siRNA) in a single dose, led to a significant Hepc downmodulation, and increased transferrin saturation within 24 h post-administration, persisting for more than two weeks, and to a recovery from anemia in animal models of ACD [112].

Beside the liver, in brain, Tfr2 regulates the production of local Hepc and iron amount in the CNS, since Tfr2 KO mice brain have a blunted Hepc response to brain iron overload [97]. In recent time, it has emerged that brain Hepc production is altered in several neurodegenerative disorders: downmodulated in Alzheimer's and Parkinson's disease [113,114] and upmodulated in restless legs syndrome (RLS) [115]. It might be worthwhile to further investigate if Tfr2 is involved in these Hepc variations, and consider using anti Tfr2 antibodies or siRNA-based therapy to rescue Hepc physiologic values in RLS. Nowadays, siRNA delivery to brain is quite difficult, due to the presence of the BBB, but the ongoing studies on nanoparticles' use, to target siRNA in specific sites, could allow an increase in the efficacy of this therapy [116].

An alternative therapeutic approach aims to deliver blocking antibody in the brain, exploiting the BBB physiologic activities. This is based on the use of anti-Tfr1 antibodies, since Tfr1 is well expressed in BBB endothelial cells and is involved in receptor-mediated transcytosis. Indeed, it has been demonstrated that the bispecific Tfr1/BACE1 (β-amyloid cleaving enzyme-1) antibody resulted in being effective in decreasing β-amyloid concentration in the brain [117].

Due to high Tfr1/Tfr2 homology and the common cellular internalization through a receptor-mediated endocytosis pathway, one could hypothesize a parallel Tfr2-based approach for CNS, blocking antibody delivery. Nevertheless, it should be further confirmed, the presence of Tfr2 on BBB endothelial cells and its involvement in transcytosis.

Recent studies have aimed at exploiting the Tfr1 as a vehicle for drug delivery inside the cells through endocytosis, often utilizing Tfr1 natural ligand, Tf, conjugated with different synthetic molecules [1]. Moreover, since Tfr1 is able to bind and internalize FtH also [118], FtH nanocages conjugated with a PARP inhibitor, olaparib, were developed for breast cancer therapy [119].

Due to its strict homology to Tfr1, one might hypothesize that Tfr2α could also be utilized to deliver drugs inside cells. This approach would be particularly useful for two main Tfr2α features; Tfr2α-selective expression in particular tissues (hepatic, erythroid, and in CNS) and Tfr2α high expression in several tumor cells, sometimes with Tfr1 and sometimes without it. High expression of Tfr1 and Tfr2α were, in fact, detected in tumor and para-cancerous normal liver tissues collected from 41 patients with hepatocellular carcinoma (HCC) [120]. Tfr2α is also highly expressed in brain tumor cells in several cases of anaplastic astrocytoma and glioblastoma, but not in normal brain or endothelial brain cells [121].

Furthermore, in the light of the new data on Tfr2α function in delivery iron to mitochondria, Tfr2α could, possibly, represent a good vehicle for drug delivery in these organelles [122], paving the way to tailored therapies for mitochondrial iron disorders, notably Friedreich's ataxia [123].

Unfortunately, too few functional data are available at the moment on Tfr2β isoform to foresee possible therapeutic applications.

8. Conclusions

The process of body iron homeostasis is complex, and since there is no apparent significant excretory pathway, the amount of iron absorbed from mature duodenal enterocytes and that is recycled by macrophages needs to be tightly regulated. From the last decades, iron pathways have been enriched of new regulatory proteins whose functions remains to be elucidated from the molecular point of view. Each of them could represent a potential target for a focused pharmacological therapy of disorders with iron unbalance, that still represents the most prevalent of diseases all around the world.

References

1. Kawabata, H. Transferrin and transferrin receptors update. *Free Radic. Biol. Med.* **2018**, doi:10.1016/j.freeradbiomed.2018.06.037.
2. Kawabata, H.; Yang, R.; Hirama, T.; Vuong, P.T.; Kawano, S.; Gombart, A.F.; Koeffler, H.P. Molecular cloning of transferrin receptor 2. A new member of the transferrin receptor-like family. *J. Biol. Chem.* **1999**, *274*, 20826–20832.

3.	Mastroberardino, P.G.; Hoffman, E.K.; Horowitz, M.P.; Betarbet, R.; Taylor, G.; Cheng, D.; Na, H.M.; Gutekunst, C.A.; Gearing, M.; Trojanowski, J.Q.; et al. A novel transferrin/TfR2-mediated mitochondrial iron transport system is disrupted in Parkinson's disease. *Neurobiol. Dis.* **2009**, *34*, 417–431, doi:10.1016/j.nbd.2009.02.009.

4.	Pagani, A.; Vieillevoye, M.; Nai, A.; Rausa, M.; Ladli, M.; Lacombe, C.; Mayeux, P.; Verdier, F.; Camaschella, C.; Silvestri, L. Regulation of cell surface transferrin receptor-2 by iron-dependent cleavage and release of a soluble form. *Haematologica* **2015**, *100*, 458–465, doi:10.3324/haematol.2014.118521.

5.	Kawabata, H.; Germain, R.S.; Ikezoe, T.; Tong, X.; Green, E.M.; Gombart, A.F.; Koeffler, H.P. Regulation of expression of murine transferrin receptor 2. *Blood* **2001**, *98*, 1949–1954.

6.	Matsuo, S.; Ogawa, M.; Muckenthaler, M.U.; Mizui, Y.; Sasaki, S.; Fujimura, T.; Takizawa, M.; Ariga, N.; Ozaki, H.; Sakaguchi, M.; et al. Hepatocyte Nuclear Factor 4α controls iron metabolism and regulates transferrin receptor 2 in mouse liver. *J. Biol. Chem.* **2015**, *290*, 30855–30865, doi:10.1074/jbc.M115.694414.

7.	Muckenthaler, M.U.; Galy, B.; Hentze, M.W. Systemic iron homeostasis and the iron-responsive element/iron-regulatory protein (IRE/IRP) regulatory network. *Annu. Rev. Nutr.* **2008**, *28*, 197–213, doi:10.1146/annurev.nutr.28.061807.155521.

8.	Chen, J.; Enns, C.A. CD81 promotes both the degradation of transferrin receptor 2 (TfR2) and the Tfr2-mediated maintenance of hepcidin expression. *J. Biol. Chem.* **2015**, *290*, 7841–7850, doi:10.1074/jbc.M114.632778.

9.	Camaschella, C.; Roetto, A.; Calì, A.; De Gobbi, M.; Garozzo, G.; Carella, M.; Majorano, N.; Totaro, A.; Gasparini, P. The gene TFR2 is mutated in a new type of haemochromatosis mapping to 7q22. *Nat. Genet.* **2000**, *25*, 14–15.

10.	Brissot, P.; Cavey, T.; Ropert, M.; Guggenbuhl, P.; Loréal, O. Genetic hemochromatosis: Pathophysiology; diagnostic and therapeutic management. *Presse Med.* **2017**, *46*, e288–e295, doi:10.1016/j.lpm.2017.05.037.

11.	De Gobbi, M.; Roetto, A. TFR2-Related Hereditary Hemochromatosis. In *GeneReviews®*; Adam, M.P., Ardinger, H.H., Pagon, R.A., Wallace, S.E., Bean, L.J.H., Stephens, K., Amemiya, A., Eds.; University of Washington: Seattle, WA, USA, 2005; pp. 1993–2018, ISSN 2372-0697.

12.	Biasiotto, G.; Belloli, S.; Ruggeri, G.; Zanella, I.; Gerardi, G.; Corrado, M.; Gobbi, E.; Albertini, A.; Arosio, P. Identification of new mutations of the HFE, hepcidin, and transferrin receptor 2 genes by denaturing HPLC analysis of individuals with biochemical indications of iron overload. *Clin. Chem.* **2003**, *49*, 1981–1988.

13.	Roetto, A.; Totaro, A.; Piperno, A.; Piga, A.; Longo, F.; Garozzo, G.; Calì, A.; De Gobbi, M.; Gasparini, P.; Camaschella, C. New mutations inactivating transferrin receptor 2 in hemochromatosis type 3. *Blood* **2001**, *97*, 2555–2260.

14.	Bardou-Jacquet, E.; Cunat, S.; Beaumont-Epinette, M.P.; Kannengiesser, C.; Causse, X.; Sauvion, S.; Pouliquen, B.; Deugnier, Y.; David, V.; Loréal, O.; et al. Variable age of onset and clinical severity in transferrin receptor 2 related haemochromatosis: Novel observations. *Br. J. Haematol.* **2013**, *162*, 278–281, doi:10.1111/bjh.12350.

15.	Majore, S.; Milano, F.; Binni, F.; Stuppia, L.; Cerrone, A.; Tafuri, A.; De Bernardo, C.; Palka, G.; Grammatico, P. Homozygous p.M172K mutation of the TFR2 gene in an Italian family with type 3 hereditary hemochromatosis and early onset iron overload. *Haematologica* **2006**, *91*, ECR33.

16.	Finberg, K.E. Regulation of systemic iron homeostasis. *Curr. Opin. Hematol.* **2013**, *20*, 208–214, doi:10.1097/MOH.0b013e32835f5a47.

17.	Hunter, H.N.; Fulton, D.B.; Ganz, T.; Vogel, H.J. The solution structure of human hepcidin; a peptide hormone with antimicrobial activity that is involved in iron uptake and hereditary hemochromatosis. *J. Biol. Chem.* **2002**, *277*, 37597–37603.

18.	Ganz, T.; Nemeth, E. Hepcidin and iron homeostasis. *Biochim. Biophys. Acta* **2012**, *1823*, 1434–1443, doi:10.1016/j.bbamcr.2012.01.014.

19.	Courselaud, B.; Pigeon, C.; Inoue, Y.; Inoue, J.; Gonzalez, F.J.; Leroyer, P.; Gilot, D.; Boudjema, K.; Guguen-Guillouzo, C.; Brissot, P.; et al. C/EBPalpha regulates hepatic transcription of hepcidin;an antimicrobial peptide and regulator of iron metabolism. Cross-talk between C/EBP pathway and iron metabolism. *J. Biol. Chem.* **2002**, *277*, 41163–41170.

20.	Canali, S.; Zumbrennen-Bullough, K.B.; Core, A.B.; Wang, C.Y.; Nairz, M.; Bouley, R.; Swirski, F.K.; Babitt, J.L. Endothelial cells produce bone morphogenetic protein 6 required for iron homeostasis in mice. *Blood* **2017**, *129*, 405–414, doi:10.1182/blood-2016-06-721571.

23

21. Steinbicker, A.U.; Bartnikas, T.B.; Lohmeyer, L.K.; Leyton, P.; Mayeur, C.; Kao, S.M.; Pappas, A.E.; Peterson, R.T.; Bloch, D.B.; Yu, P.B.; et al. Perturbation of hepcidin expression by BMP type I receptor deletion induces iron overload in mice. *Blood* **2011**, *118*, 4224–4230, doi:10.1182/blood-2011-03-339952.

22. Mayeur, C.; Leyton, P.A.; Kolodziej, S.A.; Yu, B.; Bloch, K.D. BMP type II receptors have redundant roles in the regulation of hepatic hepcidin gene expression and iron metabolism. *Blood* **2014**, *124*, 2116–2123, doi:10.1182/blood-2014-04-572644.

23. Enns, C.A.; Ahmed, R.; Zhang, A.S. Neogenin interacts with matriptase-2 to facilitate hemojuvelin cleavage. *J. Biol. Chem.* **2012**, *287*, 35104–35117, doi:10.1074/jbc.M112.363937.

24. Canali, S.; Wang, C.Y.; Zumbrennen-Bullough, K.B.; Bayer, A.; Babitt, J.L. Bone morphogenetic protein 2 controls iron homeostasis in mice independent of Bmp6. *Am. J. Hematol.* **2017**, *92*, 1204–1213, doi:10.1002/ajh.24888.

25. Schmidt, P.J.; Toran, P.T.; Giannetti, A.M.; Bjorkman, P.J.; Andrews, N.C. The transferrin receptor modulates Hfe-dependent regulation of hepcidin expression. *Cell Metab.* **2008**, *7*, 205–214, doi:10.1016/j.cmet.2007.11.016.

26. Gao, J.; Chen, J.; Kramer, M.; Tsukamoto, H.; Zhang, A.S.; Enns, C.A. Interaction of the hereditary hemochromatosis protein HFE with transferrin receptor 2 is required for transferrin-induced hepcidin expression. *Cell Metab.* **2009**, *9*, 217–227, doi:10.1016/j.cmet.2009.01.010.

27. D'Alessio, F.; Hentze, M.; Muckenthaler, M.U. The hemochromatosis proteins HFE; TfR2; and HJV form a membrane-associated protein complex for hepcidin regulation. *J. Hepatol.* **2012**, *57*, 1052–1060, doi:10.1016/j.jhep.2012.06.015.

28. Wallace, D.F.; Summerville, L.; Crampton, E.M.; Frazer, D.M.; Anderson, G.J.; Subramaniam, V.N. Combined deletion of Hfe and transferrin receptor 2 in mice leads to marked dysregulation of hepcidin and iron overload. *Hepatology* **2009**, *50*, 1992–2000, doi:10.1002/hep.23198.

29. Poli, M.; Luscieti, S.; Gandini, V.; Maccarinelli, F.; Finazzi, D.; Silvestri, L.; Roetto, A.; Arosio, P. Transferrin receptor 2 and HFE regulate furin expression via mitogen-activated protein kinase/extracellular signal-regulated kinase (MAPK/Erk) signaling. Implications for transferrin- dependent hepcidin regulation. *Haematologica* **2010**, *95*, 1832–1840.

30. Corradini, E.; Rozier, M.; Meynard, D.; Odhiambo, A.; Lin, H.Y.; Feng, Q.; Migas, M.C.; Britton, R.S.; Babitt, J.L.; Fleming, R.E. Iron regulation of hepcidin despite attenuated Smad1,5,8 signaling in mice without transferrin receptor 2 or Hfe. *Gastroenterology* **2011**, *141*, 1907–1914, doi:10.1053/j.gastro.2011.06.077.

31. Silvestri, L.; Pagani, A.; Nai, A.; De Domenico, I.; Kaplan, J.; Camaschella, C. The serine protease matriptase-2 (TMPRSS6) inhibits hepcidin activation by cleaving membrane hemojuvelin. *Cell Metab.* **2008**, *8*, 502–511, doi:10.1016/j.cmet.2008.09.012.

32. Meynard, D.; Vaja, V.; Sun, C.C.; Corradini, E.; Chen, S.; López-Otín, C.; Grgurevic, L.; Hong, C.C.; Stirnberg, M.; Gütschow, M.; et al. Regulation of TMPRSS6 by BMP6 and iron in human cells and mice. *Blood* **2011**, *118*, 747–756, doi:10.1182/blood-2011-04-348698.

33. Nicolas, G.; Chauvet, C.; Viatte, L.; Danan, J.L.; Bigard, X.; Devaux, I.; Beaumont, C.; Kahn, A.; Vaulont, S. The gene encoding the iron regulatory peptide hepcidin is regulated by anemia; hypoxia; and inflammation. *J. Clin. Investig.* **2002**, *110*, 1037–1044.

34. Donovan, A.; Lima, C.A.; Pinkus, J.L.; Pinkus, G.S.; Zon, L.I.; Robine, S.; Andrews, N.C. The iron exporter ferroportin/Slc40a1 is essential for iron homeostasis. *Cell Metab.* **2005**, *1*, 191–200.

35. Nemeth, E.; Tuttle, M.S.; Powelson, J.; Vaughn, M.B.; Donovan, A.; Ward, D.M.; Ganz, T.; Kaplan, J. Hepcidin regulates cellular iron efflux by binding to ferroportin and inducing its internalization. *Science* **2004**, *306*, 2090–2093.

36. Papanikolaou, G.; Pantopoulos, K. Systemic iron homeostasis and erythropoiesis. *IUBMB Life* **2017**, *69*, 399–413, doi:10.1002/iub.1629.

37. Wrighting, D.M.; Andrews, N.C. Interleukin-6 induces hepcidin expression through STAT3. *Blood* **2006**, *108*, 3204–3209.

38. Armitage, A.E.; Eddowes, L.A.; Gileadi, U.; Cole, S.; Spottiswoode, N.; Selvakumar, T.A.; Ho, L.P.; Townsend, A.R.; Drakesmith, H. Hepcidin regulation by innate immune and infectious stimuli. *Blood* **2011**, *118*, 4129–4139, doi:10.1182/blood-2011-04-351957.

39. Piperno, A.; Galimberti, S.; Mariani, R.; Pelucchi, S.; Ravasi, G.; Lombardi, C.; Bilo, G.; Revera, M.; Giuliano, A.; Faini, A.; et al. Modulation of hepcidin production during hypoxia-induced erythropoiesis in humans in vivo: Data from the HIGHCARE project. *Blood* **2011**, *117*, 2953–2959, doi:10.1182/blood-2010-08-299859.

40. Talbot, N.P.; Lakhal, S.; Smith, T.G.; Privat, C.; Nickol, A.H.; Rivera-Ch, M.; León-Velarde, F.; Dorrington, K.L.; Mole, D.R.; Robbins, P.A. Regulation of hepcidin expression at high altitude. *Blood* **2012**, *119*, 857–860, doi:10.1182/blood-2011-03-341776.

41. Maurer, E.; Gütschow, M.; Stirnberg, M. Matriptase-2 (TMPRSS6) is directly up-regulated by hypoxia inducible factor-1: Identification of a hypoxia-responsive element in the TMPRSS6 promoter region. *Biol. Chem.* **2012**, *393*, 535–540, doi:10.1515/hsz-2011-0221.

42. Kawabata, H.; Fleming, R.E.; Gui, D.; Moon, S.Y.; Saitoh, T.; O'Kelly, J.; Umehara, Y.; Wano, Y.; Said, J.W.; Koeffler, H.P. Expression of hepcidin is down-regulated in TfR2 mutant mice manifesting a phenotype of hereditary hemochromatosis. *Blood* **2005**, *105*, 376–381.

43. Nemeth, E.; Roetto, A.; Garozzo, G.; Ganz, T.; Camaschella, C. Hepcidin is decreased in TFR2 hemochromatosis. *Blood* **2005**, *105*, 1803–1806.

44. Du, X.; She, E.; Gelbart, T.; Truksa, J.; Lee, P.; Xia, Y.; Khovananth, K.; Mudd, S.; Mann, N.; Moresco, E.M.; et al. The serine protease TMPRSS6 is required to sense iron deficiency. *Science* **2008**, *23*, 320, 1088–1092, doi:10.1126/science.1157121.

45. Finberg, K.E.; Heeney, M.M.; Campagna, D.R.; Aydinok, Y.; Pearson, H.A.; Hartman, K.R.; Mayo, M.M.; Samuel, S.M.; Strouse, J.J.; Markianos, K.; et al. Mutations in TMPRSS6 cause iron-refractory iron deficiency anemia (IRIDA). *Nat. Genet.* **2008**, *40*, 569–571, doi:10.1038/ng.130.

46. Folgueras, A.R.; de Lara, F.M.; Pendás, A.M.; Garabaya, C.; Rodríguez, F.; Astudillo, A.; Bernal, T.; Cabanillas, R.; López-Otín, C.; Velasco, G. Membrane-bound serine protease matriptase-2 (Tmprss6) is an essential regulator of iron homeostasis. *Blood* **2008**, *112*, 2539–2545.

47. Calzolari, A.; Raggi, C.; Deaglio, S.; Sposi, N.M.; Stafsnes, M.; Fecchi, K.; Parolini, I.; Malavasi, F.; Peschle, C.; Sargiacomo, M.; et al. TfR2 localizes in lipid raft domains and is released in exosomes to activate signal transduction along the MAPK pathway. *J. Cell Sci.* **2006**, *119*, 4486–4498.

48. Simons, K.; Toomre, D. Lipid rafts and signal transduction. *Nat. Rev. Mol. Cell Biol.* **2000**, *1*, 31–39.

49. Chen, J.; Wang, J.; Meyers, K.R.; Enns, C.A. Transferrin-directed internalization and cycling of transferrin receptor 2. *Traffic* **2009**, *10*, 1488–1501, doi:10.1111/j.1600-0854.2009.00961.x.

50. Johnson, M.B.; Enns, C.A. Diferric transferrin regulates transferrin receptor 2 protein stability. *Blood* **2004**, *104*, 4287–4293.

51. Chen, J.; Enns, C.A. The cytoplasmic domain of transferrin receptor 2 dictates its stability and response to holo-transferrin in Hep3B cells. *J. Biol. Chem.* **2007**, *282*, 6201–6209.

52. Johnson, M.B.; Chen, J.; Murchison, N.; Green, F.A.; Enns, C.A. Transferrin receptor 2: Evidence for ligand-induced stabilization and redirection to a recycling pathway. *Mol. Biol. Cell* **2007**, *18*, 743–754.

53. Goswami, T.; Andrews, N.C. Hereditary hemochromatosis protein; HFE; interaction with transferrin receptor 2 suggests a molecular mechanism for mammalian iron sensing. *J. Biol. Chem.* **2006**, *281*, 28494–28498.

54. Valore, E.V.; Ganz, T. Posttranslational processing of hepcidin in human hepatocytes is mediated by the prohormone convertase furin. *Blood Cells Mol. Dis.* **2008**, *40*, 132–138.

55. Fleming, R.E.; Ahmann, J.R.; Migas, M.C.; Waheed, A.; Koeffler, H.P.; Kawabata, H.; Britton, R.S.; Bacon, B.R.; Sly, W.S. Targeted mutagenesis of the murine transferrin receptor-2 gene produces hemochromatosis. *Proc. Natl. Acad. Sci. USA* **2002**, *99*, 10653–10658.

56. Wallace, D.F.; Summerville, L.; Subramaniam, V.N. Targeted disruption of the hepatic transferrin receptor 2 gene in mice leads to iron overload. *Gastroenterology* **2007**, *132*, 301–310.

57. Roetto, A.; Di Cunto, F.; Pellegrino, R.M.; Hirsch, E.; Azzolino, O.; Bondi, A.; Defilippi, I.; Carturan, S.; Miniscalco, B.; Riondato, F.; et al. Comparison of 3 Tfr2-deficient murine models suggests distinct functions for Tfr2-alpha and Tfr2-beta isoforms in different tissues. *Blood* **2010**, *115*, 3382–3389, doi:10.1182/blood-2009-09-240960.

58. Fleming, R.E.; Feng, Q.; Britton, R.S. Knockout mouse models of iron homeostasis. *Annu. Rev. Nutr.* **2011**, *31*, 117–137, doi:10.1146/annurev-nutr-072610-145117.

59. Gutschow, P.; Schmidt, P.J.; Han, H.; Ostland, V.; Bartnikas, T.B.; Pettiglio, M.A.; Herrera, C.; Butler, J.S.; Nemeth, E.; Ganz, T.; et al. A competitive enzyme-linked immunosorbent assay specific for murine hepcidin-1: Correlation with hepatic mRNA expression in established and novel models of dysregulated iron homeostasis. *Haematologica* **2015**, *100*, 167–177, doi:10.3324/haematol.2014.116723.

60. Latour, C.; Besson-Fournier, C.; Meynard, D.; Silvestri, L.; Gourbeyre, O.; Aguilar-Martinez, P.; Schmidt, P.J.; Fleming, M.D.; Roth, M.P.; Coppin, H. Differing impact of the deletion of hemochromatosis-associated molecules HFE and transferrin receptor-2 on the iron phenotype of mice lacking bone morphogenetic protein 6 or hemojuvelin. *Hepatology* **2016**, *63*, 126–137, doi:10.1002/hep.28254.

61. Nai, A.; Pellegrino, R.M.; Rausa, M.; Pagani, A.; Boero, M.; Silvestri, L.; Saglio, G.; Roetto, A.; Camaschella, C. The erythroid function of transferrin receptor 2 revealed by Tmprss6 inactivation in different models of transferrin receptor 2 knockout mice. *Haematologica* **2014**, *99*, 1016–1021, doi:10.3324/haematol.2013.103143.

62. Rishi, G.; Secondes, E.S.; Wallace, D.F.; Subramaniam, V.N. Hematopoietic deletion of transferrin receptor 2 in mice leads to a block in erythroid differentiation during iron-deficient anemia. *Am. J. Hematol.* **2016**, *91*, 812–818, doi:10.1002/ajh.24417.

63. Marro, S.; Chiabrando, D.; Messana, E.; Stolte, J.; Turco, E.; Tolosano, E.; Muckenthaler, M.U. Heme controls ferroportin1 (FPN1) transcription involving Bach1, Nrf2 and a MARE/ARE sequence motif at position -7007 of the FPN1 promoter. *Haematologica* **2010**, *95*, 1261–1268, doi:10.3324/haematol.2009.020123.

64. Chiabrando, D.; Fiorito, V.; Marro, S.; Silengo, L.; Altruda, F.; Tolosano, E. Cell-specific regulation of Ferroportin transcription following experimentally-induced acute anemia in mice. *Blood Cells Mol. Dis.* **2013**, *50*, 25–30, doi:10.1016/j.bcmd.2012.08.002.

65. Zhang, D.L.; Hughes, R.M.; Ollivierre-Wilson, H.; Ghosh, M.C.; Rouault, T.A. A ferroportin transcript that lacks an iron-responsive element enables duodenal and erythroid precursor cells to evade translational repression. *Cell Metab.* **2009**, *9*, 461–473, doi:10.1016/j.cmet.2009.03.006.

66. Soranzo, N.; Spector, T.D.; Mangino, M.; Kühnel, B.; Rendon, A.; Teumer, A.; Willenborg, C.; Wright, B.; Chen, L.; Li, M.; et al. A genome-wide meta-analysis identifies 22 loci associated with eight hematological parameters in the HaemGen consortium. *Nat. Genet.* **2009**, *41*, 1182–1190, doi:10.1038/ng.467.

67. Auer, P.L.; Teumer, A.; Schick, U.; O'Shaughnessy, A.; Lo, K.S.; Chami, N.; Carlson, C.; de Denus, S.; Dubé, M.P.; Haessler, J.; et al. Rare and low frequency coding variants in CXCR2 and other genes are associated with hematological traits. *Nat. Genet.* **2014**, *46*, 629–634, doi:10.1038/ng.2962.

68. Forejtnikovà, H.; Vieillevoye, M.; Zermati, Y.; Lambert, M.; Pellegrino, R.M.; Guihard, S.; Gaudry, M.; Camaschella, C.; Lacombe, C.; Roetto, A.; et al. Transferrin receptor 2 is a component of the erythropoietin receptor complex and is required for efficient erythropoiesis. *Blood* **2010**, *116*, 5357–5367, doi:10.1182/blood-2010-04-281360.

69. Nai, A.; Lidonnici, M.R.; Rausa, M.; Mandelli, G.; Pagani, A.; Silvestri, L.; Ferrari, G.; Camaschella, C. The second transferrin receptor regulates red blood cell production in mice. *Blood* **2015**, *125*, 1170–1179, doi:10.1182/blood-2014-08-596254.

70. Kautz, L.; Jung, G.; Valore, E.V., Rivella, S.; Nemeth, E.; Ganz, T. Identification of erythroferrone as an erythroid regulator of iron metabolism. *Nat. Genet.* **2014**, *46*, 678–684, doi:10.1038/ng.2996.

71. Pellegrino, R.M.; Riondato, F.; Ferbo, L.; Boero, M.; Palmieri, A.; Osella, L.; Pollicino, P.; Miniscalco, B.; Saglio, G.; Roetto, A. Altered Erythropoiesis in Mouse Models of Type 3 Hemochromatosis. *Biomed. Res. Int.* **2017**, 2408941, doi:10.1155/2017/2408941.

72. Xu, W.; Barrientos, T.; Mao, L.; Rockman, H.A.; Sauve, A.A.; Andrews, N.C. Lethal cardiomyopathy in mice lacking transferrin receptor in the heart. *Cell Rep.* **2015**, *13*, 533–545, doi:10.1016/j.celrep.2015.09.023.

73. Lakhal-Littleton, S.; Wolna, M.; Carr, C.A.; Miller, J.J.; Christian, H.C.; Ball, V.; Santos, A.; Diaz, R.; Biggs, D.; Stillion, R.; et al. Cardiac ferroportin regulates cellular iron homeostasis and is important for cardiac function. *Proc. Natl. Acad. Sci. USA* **2015**, *112*, 3164–3169, doi:10.1073/pnas.1422373112.

74. Lakhal-Littleton, S.; Wolna, M.; Chung, Y.J.; Christian, H.C.; Heather, L.C.; Brescia, M.; Ball, V.; Diaz, R.; Santos, A.; Biggs, D.; et al. An essential cell-autonomous role for hepcidin in cardiac iron homeostasis. *Elife* **2016**, *5*, e19804, doi:10.7554/eLife.19804.

75. Gammella, E.; Recalcati, S.; Rybinska, I.; Buratti, P.; Cairo, G. Iron-induced damage in cardiomyopathy: Oxidative-dependent and independent mechanisms. *Oxid. Med. Cell. Longev.* **2015**, doi:10.1155/2015/230182.

76. Boero, M.; Pagliaro, P.; Tullio, F.; Pellegrino, R.M.; Palmieri, A.; Ferbo, L.; Saglio, G.; De Gobbi, M.; Penna, C.; Roetto, A. A comparative study of myocardial molecular phenotypes of two Tfrβ null mice: Role in ischemia/reperfusion. *Biofactors* **2015**, *41*, 360–371, doi:10.1002/biof.1237.

77. Chevion, M.; Leibowitz, S.; Aye, N.N.; Novogrodsky, O.; Singer, A.; Avizemer, O.; Bulvik, B.; Konijn, A.M.; Berenshtein, E. Heart protection by ischemic preconditioning: A novel pathway initiated by iron and mediated by ferritin. *J. Mol. Cell. Cardiol.* **2008**, *45*, 839–845, doi:10.1016/j.yjmcc.2008.08.011.

78. Aquino, D.; Bizzi, A.; Grisoli, M.; Garavaglia, B.; Bruzzone, M.G.; Nardocci, N.; Savoiardo, M.; Chiapparini, L. Age-related iron deposition in the basal ganglia: Quantitative analysis in healthy subjects. *Radiology* **2009**, *252*, 165–172, doi:10.1148/radiol.2522081399.

79. Pfefferbaum, A.; Adalsteinsson, E.; Rohlfing, T.; Sullivan, E.V. MRI estimates of brain iron concentration in normal aging: Comparison of field-dependent (FDRI) and phase (SWI) methods. *Neuroimage* **2009**, *47*, 493–500, doi:10.1016/j.neuroimage.2009.05.006.

80. Carlson, E.S.; Fretham, S.J.; Unger, E.; O'Connor, M.; Petryk, A.; Schallert, T.; Rao, R.; Tkac, I.; Georgieff, M.K. Hippocampus specific iron deficiency alters competition and cooperation between developing memory systems. *J. Neurodev. Disord.* **2010**, *2*, 133–143, doi:10.1007/s11689-010-9049-0.

81. Millichap, J.G. Etiologic classification of attention-deficit/hyperactivity disorder. *Pediatrics* **2008**, *12*, e358–e365.

82. Benton, D. The influence of dietary status on the cognitive performance of children. *Mol. Nutr. Food Res.* **2010**, *54*, 457–470, doi:10.1002/mnfr.200900158.

83. Xu, H.; Wang, Y.; Song, N.; Wang, J.; Jiang, H.; Xie, J. New Progress on the Role of Glia in Iron Metabolism and Iron-Induced Degeneration of Dopamine Neurons in Parkinson's Disease. *Front. Mol. Neurosci.* **2018**, *10*, 455, doi:10.3389/fnmol.2017.00455.

84. McCarthy, R.C.; Kosman, D.J. Mechanistic analysis of iron accumulation by endothelial cells of the BBB. *Biometals* **2012**, *25*, 665–675, doi:10.1007/s10534-012-9538-6.

85. Benarroch, E.E. Brain iron homeostasis and neurodegenerative disease. *Neurology* **2009**, *72*, 1436–1440, doi:10.1212/WNL.0b013e3181a26b30.

86. Mills, E.; Dong, X.P.; Wang, F.; Xu, H. Mechanisms of brain iron transport: Insight into neurodegeneration and CNS disorders. *Future Med. Chem.* **2010**, *2*, 51–64.

87. Wang, J.; Jiang, H.; Xie, J.X. Ferroportin1 and hephaestin are involved in the nigral iron accumulation of 6-OHDA-lesioned rats. *Eur. J. Neurosci.* **2007**, *25*, 2766–2772.

88. Morris, C.M.; Candy, J.M.; Keith, A.B.; Oakley, A.E.; Taylor, G.A.; Pullen, R.G.; Bloxham, C.A.; Gocht, A.; Edwardson, J.A. Brain iron homeostasis. *J. Inorg. Biochem.* **1992**, *47*, 257–265.

89. Connor, J.R.; Boeshore, K.L.; Benkovic, S.A.; Menzies, S.L. Isoforms of ferritin have a specific cellular distribution in the brain. *J. Neurosci. Res.* **1994**, *37*, 461–465.

90. Rouault, T.A. Iron metabolism in the CNS: Implications for neurodegenerative diseases. *Nat. Rev. Neurosci.* **2013**, *14*, 551–564, doi:10.1038/nrn3453.

91. Wang, S.M.; Fu, L.J.; Duan, X.L.; Crooks, D.R.; Yu, P.; Qian, Z.M.; Di, X.J.; Li, J.; Rouault, T.A.; Chang, Y.Z. Role of hepcidin in murine brain iron metabolism. *Cell. Mol. Life Sci.* **2010**, *67*, 123–133, doi:10.1007/s00018-009-0167-3.

92. Du, F.; Qian, Z.M.; Luo, Q.; Yung, W.H.; Ke, Y. Hepcidin suppresses brain iron accumulation by downregulating iron transport proteins in iron-overloaded rats. *Mol. Neurobiol.* **2015**, *52*, 101–114, doi:10.1007/s12035-014-8847-x.

93. Vela, D. Hepcidin, an emerging and important player in brain iron homeostasis. *J. Transl. Med.* **2018**, *16*, doi:10.1186/s12967-018-1399-5.

94. Moos, T.; Rosengren Nielsen, T.; Skjørringe, T.; Morgan, E.H. Iron trafficking inside the brain. *J. Neurochem.* **2007**, *103*, 1730–1740.

95. Hänninen, M.M.; Haapasalo, J.; Haapasalo, H.; Fleming, R.E.; Britton, R.S.; Bacon, B.R.; Parkkila, S. Expression of iron-related genes in human brain and brain tumors. *BMC Neurosci.* **2009**, *10*, 36, doi:10.1186/1471-2202-10-36.

96. Acikyol, B.; Graham, R.M.; Trinder, D.; House, M.J.; Olynyk, J.K.; Scott, R.J.; Milward, E.A.; Johnstone, D.M. Brain transcriptome perturbations in the transferrin receptor 2 mutant mouse support the case for brain changes in iron loading disorders, including effects relating to long-term depression and long-term potentiation. *Neuroscience* **2013**, *235*, 119–128, doi:10.1016/j.neuroscience.2013.01.014.

97. Pellegrino, R.M.; Boda, E.; Montarolo, F.; Boero, M.; Mezzanotte, M.; Saglio, G.; Buffo, A.; Roetto, A. Transferrin Receptor 2 Dependent Alterations of Brain Iron Metabolism Affect Anxiety Circuits in the Mouse. *Sci. Rep.* **2016**, *6*, 30725, doi:10.1038/srep30725.

98. Adhikari, A. Distributed circuits underlying anxiety. *Front. Behav. Neurosci.* **2014**, *8*, 112, doi:10.3389/fnbeh.2014.00112.

99. Rhodes, S.L.; Buchanan, D.D.; Ahmed, I.; Taylor, K.D.; Loriot, M.A.; Sinsheimer, J.S.; Bronstein, J.M.; Elbaz, A.; Mellick, G.D.; Rotter, J.I.; et al. Pooled analysis of iron-related genes in Parkinson's disease: Association with transferrin. *Neurobiol. Dis.* **2014**, *62*, 172–178, doi:10.1016/j.nbd.2013.09.019.

100. Khalil, S.; Holy, M.; Grado, S.; Fleming, R.; Kurita, R.; Nakamura, Y.; Goldfarb, A. A specialized pathway for erythroid iron delivery through lysosomal trafficking of transferrin receptor 2. *Blood Adv.* **2017**, *1*, 1181–1194, doi:10.1182/bloodadvances.2016003772.

101. Robb, A.D.; Ericsson, M.; Wessling-Resnick, M. Transferrin receptor 2 mediates a biphasic pattern of transferrin uptake associated with ligand delivery to multivesicular bodies. *Am. J. Physiol. Cell Physiol.* **2004**, *287*, C1769–C1775.

102. Smilevska, T.; Stamatopoulos, K.; Samara, M.; Belessi, C.; Tsompanakou, A.; Paterakis, G.; Stavroyianni, N.; Athanasiadou, I.; Chiotoglou, I.; Hadzidimitriou, A.; et al. Transferrin receptor-1 and 2 expression in chronic lymphocytic leukemia. *Leuk. Res.* **2006**, *30*, 183–189.

103. Gangat, N.; Patnaik, M.M.; Tefferi, A. Myelodysplastic syndromes: Contemporary review and how we treat. *Am. J. Hematol.* **2016**, *91*, 76–89, doi:10.1002/ajh.24253.

104. Di Savino, A.; Gaidano, V.; Palmieri, A.; Crasto, F.; Volpengo, A.; Lorenzatti, R.; Scaravaglio, P.; Manello, A.; Nicoli, P.; Gottardi, E.; et al. Clinical significance of TFR2 and EPOR expression in bone marrow cells in myelodysplastic syndromes. *Br. J. Haematol.* **2017**, *176*, 491–495, doi:10.1111/bjh.13968.

105. Nakamaki, T.; Kawabata, H.; Saito, B.; Matsunawa, M.; Suzuki, J.; Adachi, D.; Tomoyasu, S.; Phillip Koeffler, H. Elevated levels of transferrin receptor 2 mRNA, not transferrin receptor 1 mRNA, are associated with increased survival in acute myeloid leukaemia. *Br. J. Haematol.* **2004**, *125*, 42–49.

106. Calzolari, A.; Oliviero, I.; Deaglio, S.; Mariani, G.; Biffoni, M.; Sposi, N.M.; Malavasi, F.; Peschle, C.; Testa, U. Transferrin receptor 2 is frequently expressed in human cancer cell lines. *Blood Cells Mol. Dis.* **2007**, *39*, 82–91.

107. Calzolari, A.; Larocca, L.M.; Deaglio, S.; Finisguerra, V.; Boe, A.; Raggi, C.; Ricci-Vitani, L.; Pierconti, F.; Malavasi, F.; De Maria, R.; et al. Transferrin receptor 2 is frequently and highly expressed in glioblastomas. *Transl. Oncol.* **2010**, *3*, 123–134.

108. Crichton, R.R.; Dexter, D.T.; Ward, R.J. Brain iron metabolism and its perturbation in neurological diseases. *J. Neural. Transm.* **2011**, *118*, 301–314, doi:10.1007/s00702-010-0470-z.

109. Crespo, Â.C.; Silva, B.; Marques, L.; Marcelino, E.; Maruta, C.; Costa, S.; Timóteo, A.; Vilares, A.; Couto, F.S.; Faustino, P.; et al. Genetic and biochemical markers in patients with Alzheimer's disease support a concerted systemic iron homeostasis dysregulation. *Neurobiol. Aging* **2014**, *35*, 777–785, doi:10.1016/j.neurobiolaging.2013.10.078.

110. Artuso, I.; Lidonnici, M.R.; Altamura, S.; Mandelli, G.; Pettinato, M.; Muckenthaler, M.U.; Silvestri, L.; Ferrari, G.; Camaschella, C.; Nai, A. Transferrin Receptor 2 is a potential novel therapeutic target for beta-thalassemia: Evidence from a murine model. *Blood* **2018**, doi:10.1182/blood-2018-05-852277.

111. Girelli, D.; Nemeth, E.; Swinkels, D.W. Hepcidin in the diagnosis of iron disorders. *Blood* **2016**, *127*, 2809–2013, doi:10.1182/blood-2015-12-639112.

112. Akinc, A.; Chan-Daniels, A.; Sehgal, A.; Foster, D.; Bettencourt, B.R.; Hettinger, J.; Racie, T.; Aubin, J.; Kuchimanchi, S.; Epstein-Barashand, H.; et al. Targeting the hepcidin pathway with RNAi therapeutics for the treatment of anemia. *Blood* **2011**, *21*, 688.

113. Raha, A.A.; Vaishnav, R.A.; Friedland, R.P.; Bomford, A.; Raha-Chowdhury, R. The systemic iron-regulatory proteins hepcidin and ferroportin are reduced in the brain in Alzheimer's disease. *Acta Neuropathol. Commun.* **2013**, *1*, 55, doi:10.1186/2051-5960-1-55.

114. Chen, D.; Kanthasamy, A.G.; Reddy, M.B. EGCG protects against 6-OHDA-induced neurotoxicity in a cell culture model. *Parkinsons Dis.* **2015**, doi:10.1155/2015/843906.

115. Clardy, S.L.; Wang, X.; Boyer, P.J.; Earley, C.J.; Allen, R.P.; Connor, J.R. Is ferroportin–hepcidin signaling altered in restless legs syndrome? *J. Neurol. Sci.* **2006**, *247*, 173–179.

116. Zheng, M.; Tao, W.; Zou, Y.; Farokhzad, O.C.; Shi, B. Nanotechnology-Based Strategies for siRNA Brain Delivery for Disease Therapy. *Trends Biotechnol.* **2018**, *36*, 562–575, doi:10.1016/j.tibtech.2018.01.006.

117. Couch, J.A.; Yu, Y.J.; Zhang, Y.; Tarrant, J.M.; Fuji, R.N.; Meilandt, W.J.; Solanoy, H.; Tong, R.K.; Hoyte, K.; Luk, W.; et al. Addressing safety liabilities of TfR bispecific antibodies that cross the blood-brain barrier. *Sci. Transl. Med.* **2013**, *5*, doi:10.1126/scitranslmed.3005338.

118. Li, L.; Fang, C.J.; Ryan, J.C.; Niemi, E.C.; Lebrón, J.A.; Björkman, P.J.; Arase, H.; Torti, F.M.; Torti, S.V.; Nakamura, M.C.; et al. Binding and uptake of H-ferritin are mediated by human transferrin receptor-1. *Proc. Natl. Acad. Sci. USA* **2010**, *107*, 3505–3510, doi:10.1073/pnas.0913192107.

119. Mazzucchelli, S.; Truffi, M.; Baccarini, F.; Beretta, M.; Sorrentino, L.; Bellini, M.; Rizzuto, M.A.; Ottria, R.; Ravelli, A.; Ciuffreda, P.; et al. H-Ferritin-nanocaged olaparib: A promising choice for both BRCA-mutated and sporadic triple negative breast cancer. *Sci. Rep.* **2017**, *7*, 7505, doi:10.1038/s41598-017-07617-7.

120. Sakurai, K.; Sohda, T.; Ueda, S.; Tanaka, T.; Hirano, G.; Yokoyama, K.; Morihara, D.; Aanan, A.; Takeyama, Y.; Irie, M.; et al. Immunohistochemical demonstration of transferrin receptor 1 and 2 in human hepatocellular carcinoma tissue. *Hepatogastroenterology* **2014**, *61*, 426–430.

121. Voth, B.; Nagasawa, D.T.; Pelargos, P.E.; Chung, L.K.; Ung, N.; Gopen, Q.; Tenn, S.; Kamei, D.T.; Yang, I. Transferrin receptors and glioblastoma multiforme: Current findings and potential for treatment. *J. Clin. Neurosci.* **2015**, *22*, 1071–1076, doi:10.1016/j.jocn.2015.02.002.

122. Murphy, M.P.; Smith, R.A. Drug delivery to mitochondria: The key to mitochondrial medicine. *Adv. Drug Deliv. Rev.* **2000**, *41*, 235–250.

123. Bürk, K. Friedreich Ataxia: Current status and future prospects. *Cerebellum Ataxias* **2017**, doi:10.1186/s40673-017-0062-x.

1.3 Intracellular iron metabolism

1.3.1 The IRE/IRP system

Cellular iron homeostasis is regulated by post-transcriptional feedback mechanisms controlling the expression of proteins involved in iron import, storage, utilization and export which are mainly regulated by the iron response element–iron regulatory protein (IRE–IRP) system. Several mRNAs involved in iron metabolism contain iron-responsive elements (IREs): stem-loop structures located in 5'- or 3'-untranslated regions (UTRs) flanking their coding sequence (CDS). IRE elements are bound by two functionally similar iron regulatory proteins, IRP1 and IRP2 (Muckenthaler *et al.*, 2008). Depending upon whether the IRE elements are located in the 5'-UTR or in the 3'-UTR, the IRE–IRP interaction has opposite effects on the target gene expression. IRE/IRP complexes within the 5′UTR of an mRNA (e.g., FTH1, FTL, ALAS2, ACO2, FPN1) inhibit translation, whereas IRP binding to IREs in the 3′UTR of TFR1 mRNA prevents its degradation.

In low iron states, IRP1 and 2 increase iron uptakes by stabilizing TfR1 mRNA and blocking iron storage and export by suppressing Ferritin and Fpn1translation (Figure 5 on the left). This homeostatic response mediates raised cellular iron intake from Tf and prevents the formation of Ferritin, useless in iron deficiency. In iron-depleted cells, Fe/S clusters convert IRP1 to a cytosolic aconitase, able to interconverts citrate in isocitrate but unable to bind the IRE elements, while IRP2 is degraded in the proteasome in an iron-dependent manner (Figure 5 on the right). As a consequence, the above mentioned iron proteins half-life and stability return to normality (Wilkinson and Pantopoulos, 2014).

It is important to note that IRP 1 and 2 deletion in mice is incompatible with life, while the loss of only the IRP2 form results in mild anaemia, erythropoietic protoporphyria and adult-onset neurodegeneration in mice (Zhang *et al.*, 2014) and in patients (Costain *et al.*, 2019), probably due to a functional iron deficiency.

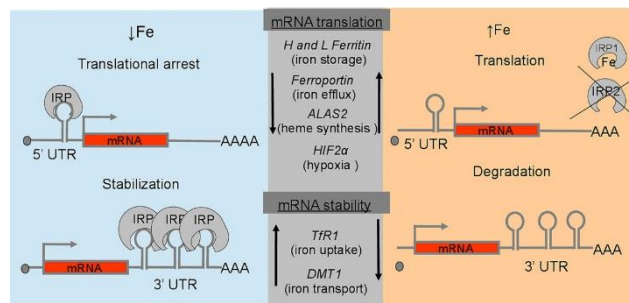**Figure 5: Mechanisms of intracellular iron metabolism.** Intracellular iron homeostasis is predominantly maintained through the post-transcriptional control of several iron metabolism genes via the IRE–IRP system. The iron-sensitive IRE–IRP interaction regulates the translation rate or mRNA stability of mRNAs depending upon the location of the IRE in the 5' or 3' -UTR (Papanikolaou and Pantopoulos, 2017).

1.3.2 Transferrin Receptor2-beta (TfR2-β)

For years, it has been though that TfR1 was the only receptor able to bind Tf until in 1999 Kawabata et al cloned TfR1 homologous, termed Transferrin Receptor 2 (TfR2) (Kawabata *et al.*, 1999). TFR2 gene is transcribed in two isoforms via alternative promoters: the full-length (α) and a shorter form (β) with different functions and cellular distribution (Kawabata *et al.*, 1999). The TfR2 full-length sequence gives rise to the TfR2-α isoform, that codify for a transmembrane protein mostly expressed in hepatocytes and erythroid precursor cell. In contrast, the β isoform lacks exons 1–3 which encodes for the cytoplasmic, transmembrane and part of the extracellular domain of TfR2-α, suggesting that it may be a soluble, intracellular form of TfR2 (Kawabata *et al.*, 1999) (Figure 6).
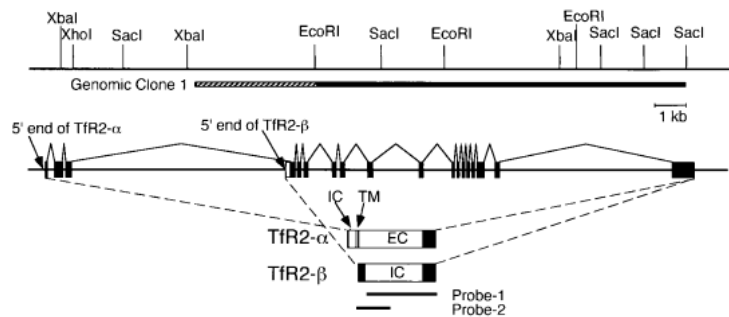

Figure 6: Genomic structure of TfR2 gene. TfR2-α have 18 exons (black box); while Tfr2-β lacks exons 1-3. IC: intracellular domain; TM: transmembrane domain; EC: extracellular domain (Kawabata *et al.*, 1999).

TfR2-α works as an iron sensor and, in the liver, it is involved in the SMAD pathway activation that regulates Hepc expression (Hentze *et al.*, 2010) while the β isoform have a central role in iron efflux in spleen reticuloendothelial cells (Roetto *et al.*, 2010). Moreover, the β isoform is expressed ubiquitously *(e.g.,* spleen, liver, heart, prostate) (Kawabata *et al.*, 1999). TfR2-β function is unclear, but different studies suggest its involvement in iron metabolism, especially in monocytes/macrophages. An available mouse model with specific deletion of TfR2-β (KI), show a normal transferrin saturation, liver iron amount, Hepc and BMP6 levels but show a transient anaemia at the age between 14 days and 10 weeks. On the other hand, adult mice develop an evident splenic iron accumulation, with a moderate reduction of Fpn1 expression in the total spleen but significantly impaired in macrophages. These findings suggest a regulatory effect of TfR2-β on Fpn1 expression in this organ and these cell types (Roetto *et al.*, 2010). In the same mouse model, TfR2-*β* deletion provokes an increased and immature splenic erythropoiesis compared to age-matched WT mice (Pellegrino *et al.*, 2017).

To corroborate these findings, mice lacking TfR2 in macrophages were developed (Rishi *et al.*, 2016). Consistently, peritoneal macrophages of knockout mice had significantly decrease of Fpn1 expression

and production even if no systemic iron alterations were found (Rishi *et al.*, 2016). Moreover, it has been shown that TfR2-β isoform is expressed in the heart, where its deletion leads to a cardio protection phenotype after ischemic/reperfusion damage via enhancing expression of Ferritin-H, Heme oxygenase 1 and Hypoxia inducible factor (HIF)-2α (Boero *et al.*, 2015). These findings suggest that TfR2-β modulation could have beneficial effects on tissue and cells iron metabolism and it could represent a therapeutic option for these damages.

1.3.3 Ferritin Light and Heavy Chains (Ft-L and Ft-H)

The major iron storage protein Ferritin plays a fundamental and decisive role to cope with iron deficiency, and that it is crucial in iron metabolism and iron-related toxicity, if not correctly coordinated. This protein allows to remove iron excess and it stores it in the cell in a safe way in order to reduce cell damage and oxidative stress. Ferritins was identified in 1937 from horse spleen by Laufberger who purified it crystallization with cadmium salts (Laufberger *et al.,*1937).

Ferritins bind iron (Fe^{2+}) and carry out two important functions: first, they sequester iron in a non-toxic form inside its large cavity that can be bind up to 4500 Fe atoms (Arosio *et al.*, 2009); second, under condition of cellular iron demand, ferritins can release iron to be used for metabolic process (De Domenico *et al.*, 2009) (Figure 7). Cytosolic ferritins are composed of 24 chains of Heavy (H), with ferroxidase activity, and Light (L) isoforms able to facilitate iron hydrolysis and mineralization and, vice versa, to accelerate iron passage from ferroxidase cavity to the iron core and optimizes iron sequestering process (Santambrogio *et al.*, 1993). The chains of ferritin co-assemble to form heteropolymers with a specific ratio depending on the organ/tissue type: liver and spleen, the main iron storage organs, are rich in L-subunits while heart and brain, organs with high ferroxidase activity, are rich in H-subunits (Harrison and Arosio, 1996).
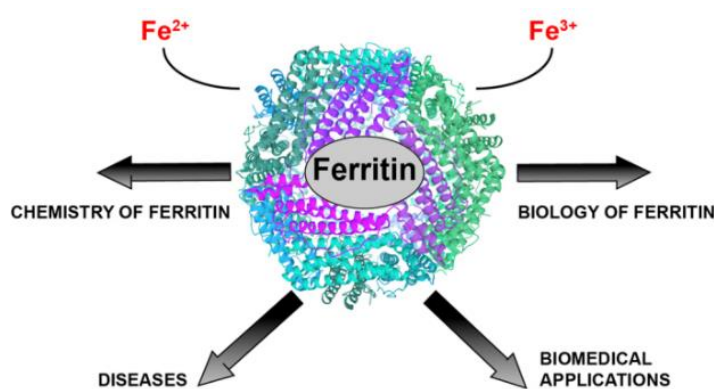

Figure 7: Ferritin shell. (Plays *et al.*, 2021).

While the interaction Ferritin-Fe^{2+} *in vitro* is direct, the iron transport to ferritin *in vivo* is a more complex mechanism. It has been studied and identified the cytosolic chaperon Poly (rC) binding protein 1 (PCBP1), able to delivers iron to ferritin (Ryu *et al.*, 2017). As a matter of fact, it has been experimentally proven that PCBP1 depletion in hepatoma cells fails ferritin iron incorporation; the opposite situation occurs if PCBP1 is overexpressed (Philpott *et al.*, 2017). Moreover, Ft-L and H expression in mammals are regulated by intracellular iron through the IRE-IRP system as previously explained (Muckenthaler *et al.,* 2008) and "the IRE/IRP system paragraph".

Inside the cells, ferritin degradation can occur through different way: ferritin is degraded in the lysosome under iron chelation stimulus (Deferasirox) (Dowdle *et al.,* 2014) or in the proteosomal pathway induced by overexpression of Fpn1 (De Domenico *et al.,* 2006) or through an evolutionarily conserved degradation pathway, with a selective process named "ferritinophagy" that involved the protein Nuclear receptor Coactivator 4 (NCOA4) (Dowdle *et al.,* 2014; Mancias *et al.,* 2014) (see Nuclear receptor Coactivator 4 paragraph).

Since the interaction between NCOA4 and ferritin is Ft-H specific during ferritinophagy (Mancias et al., 2014), NCOA4 favors Ft-H-rich ferritin heteropolymers degradation over Ft-L polymers as demonstrated in wild-type mice brain during aging (Mezzanotte *et al.*, 2021) (in revision). Thus, the expression of Ft-H and NCOA4 may have an impact on the rate of iron release in different tissues and organs. Moreover, data on transgenic mice expressing Ft-H from a tetracycline-inducible promoter showed that Ft-H expression can change according to iron amount, inducing an iron deficiency phenotype. This means that Ft-H regulates tissue iron balance (Wilkinson *et al.,* 2006).

A soluble form of ferritin is found in blood plasma, coming from macrophages (Cohen *et al.*, 2010), mostly represented by Ft-L subunits (Wang *et al.*, 2010). Serum ferritin amount is related to iron stores: when low, it is a marker of iron deficiency, while when its levels are high, it is a marker of iron overload and/or inflammation (Daru *et al.*, 2017), reflecting *de facto* macrophage ferritin amount. Nevertheless, function and origin of serum ferritin is still unknown.

1.3.4 Nuclear receptor Coactivator 4 (NCOA4)

It has been recently demonstrated that, in condition of iron deficiency and/or increased iron requirement, cells can recover it, through ferritinophagy mediated by Nuclear receptor Coactivator 4 (NCOA4) (Dowdle *et al.,* 2014; Mancias *et al.,* 2015). Protein NCOA4 interacts and co-activates different nuclear receptors and controls DNA replication origin preserving, in this way, genome stability (Bellelli *et al.,* 2014).

In 2014, Mancias and collaborators identified NCOA4 on the surface of autophagosomes, where it binds ferritin and delivers it to autophagosomes via interacting with ATG8 like proteins (GABARAP and GABARAPL1), causing in this way the iron release in the cytoplasm, (Dowdle *et al.*, 2014; Mancias *et al.*, 2014). Moreover, biochemical experiments showed that NCOA4 interacts directly with Ft-H isoform via a conserved surface arginine (R23) on Ft-H and a conserved C-terminal domain in NCOA4 (Mancias *et al.*, 2015).

Interestingly, NCOA4 levels are regulated by intracellular iron status (Mancias *et al.*, 2015) because: *i*) in cellular iron overload condition, NCOA4 levels are low, supporting ferritin accumulation and iron storage; *ii*) in cellular iron deficiency condition, NCOA4 levels are high to promote ferritinophagy and iron is released to be used by the cell (Mancias *et al.*, 2014). Recent works showed that the amount of NCOA4 changes as a consequence of the interaction with an E3 ubiquitin protein ligase (HERC2) (Mancias *et al.*, 2015; Quiles Del Rey and Mancias, 2019). Only when iron levels increase, HERC2 binds to NCOA4 and leads it to degradation via ubiquitin-proteasome system increasing in this way the amount of ferritin proteins for iron storage (Mancias *et al.*, 2015) (Figure 8).
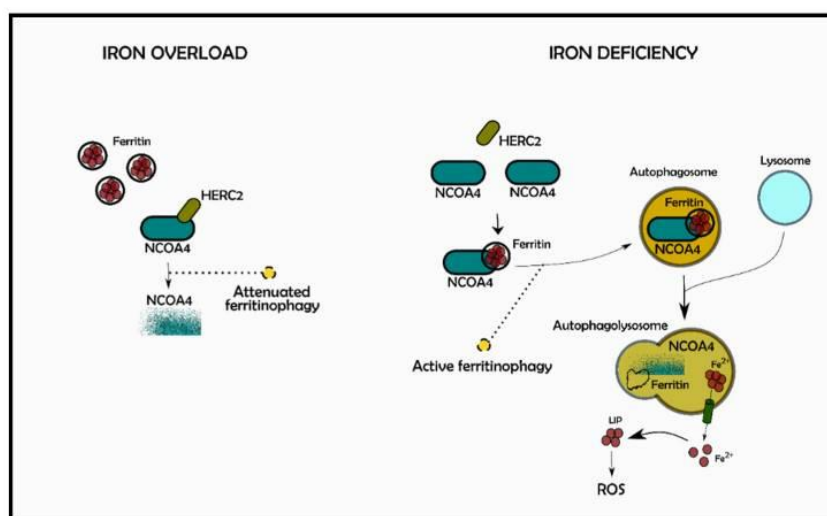

Figure 8: NCOA4-mediated ferritinophagy. Intracellular iron is regulated by ferritinophagy. During iron overload (on the left), NCOA4 is degraded by the binding with HERC2 and, as a consequence, ferritin degradation decreases. The opposite situation occurs during iron deficiency (on the right), where NCOA4 bind ferritin, thus activating ferritinophagy via lysosomal degradation. NCOA4 (Nuclear Receptor Coactivator 4); HERC2 (E3 ubiquitin protein ligase) LIP (Labile Iron Pool); ROS (Reactive oxygen species) (Mancardi *et al.,* 2021).

A systemic NCOA4 knockout mouse model designed by Bellelli (Bellelli *et al.*, 2014) develops an iron overload phenotype with increased level of Tf saturation, serum Ft, liver Hepc and an increase of Ft deposits in the liver and spleen at least, reduced iron recycling and demonstrate increased susceptibility to iron-deficiency anaemia (Bellelli *et al.*, 2016). Recently, an extra-hepatic function of NCOA4 was

demonstrated (Nai *et al.*, 2021). The increase of NCOA4 expression in erythroblasts (Ryu *et al.*, 2017) suggests a central role for ferritinophagy in hemoglobinization both *in vitro* (Ryu *et al.*, 2017) and *in vivo* models (Gao *et al.*, 2017).

In the context of neurodegenerative disorders (NDs) imbalance in iron metabolism and autophagy are described (Li *et al.*, 2019; Ndayisaba *et al.*, 2019). It could be possible that these events are connected to the pathogenesis of NDs by NCOA4-mediated ferritinophagy, although there is not yet direct evidence of data correlation.

Brain NCOA4 expression, functions and role is a field not yet fully explored. NCOA4 is expressed in the rats (Kollara and Brown, 2010) and the murine brain (Kollara and Brown, 2010; Mezzanotte *et al.*, 2021) (in revision) and the only study of NCOA4 function during aging demonstrated that, as a consequence of the increase in brain iron amount during physiological aging (Ward *et al.*, 2014), brain cells increased NCOA4. In turns, it could be responsible for a selective Ft-H degradation, favouring the formation of Ft-L rich heteropolymers more suitable for iron storage to prevent neuronal cell death (Mezzanotte *et al.*, 2021) (unpublished data).

Since a constitutive and systemic NCOA4 deletion in mice showed an iron overload phenotype (Bellelli *et al.*, 2016) we can hypothesize that NCOA4 overexpression could be associated, in terms of protection, with NDs. Clearly, additional studies are required to enlarge the understanding of the role of NCOA4 in the brain using murine models with NCOA4 targeted deletion in the brain cells.

Many NDs, including Alzheimer's Disease (AD), Parkinson's Disease (PD), Huntington's Disease (HD) are associated with increased iron levels, disruption iron homeostasis and ROS production that lead to ferroptosis an iron dependent form of cell death (Kim *et al.*, 2015; Ward *et al.*, 2014).

NDs model with genetic (Chen *et al.*, 2015b) or pharmacological inhibition (Skouta *et al.*, 2014) of ferroptosis shows that the block of ferroptosis decreases neuronal cells death.

1.4 Iron dependent cell death

1.4.1 Ferroptosis

The balance of physiological processes is finely maintained and regulated by programmed cell death, but its deregulation contributes to the onset of various disorders. The pioneer of controlled cell death was apoptosis followed by necrosis and autophagy (Doll and Conrad, 2017). A new kind of programmed cell death, ferroptosis, an iron dependent, non-apoptotic, oxidative cell death (a Greek word "ptosis", meaning "a fall", and Ferrum or iron), was first described in 2012 by Dixon (Dixon *et al.*, 2012). As the name suggests, iron is involved as a distinctive peculiarity of this phenomena of cell death (Dixon *et al.*, 2012). Ferroptosis gets involved in the onset and progression of lung, pancreas and gastrointestinal

tumors, nervous system diseases (including stroke and traumatic brain injury), ischemia-reperfusion in the liver, spleen and kidney injury (Li *et al.*, 2020) (Figure 9). Biochemically, lipid peroxides cannot be metabolized, due to reduction of glutathione peroxidase 4 (GPX4) activity and intracellular glutathione depletion (GSH). As a consequence, iron ($Fe2^+$) can oxidize lipids resulting in reactive oxygen species (ROS) accumulation triggering ferroptosis (Friedmann Angeli *et al.*, 2014; Yang and Stockwell, 2008) with a dysregulation of mitochondrial structure/function.
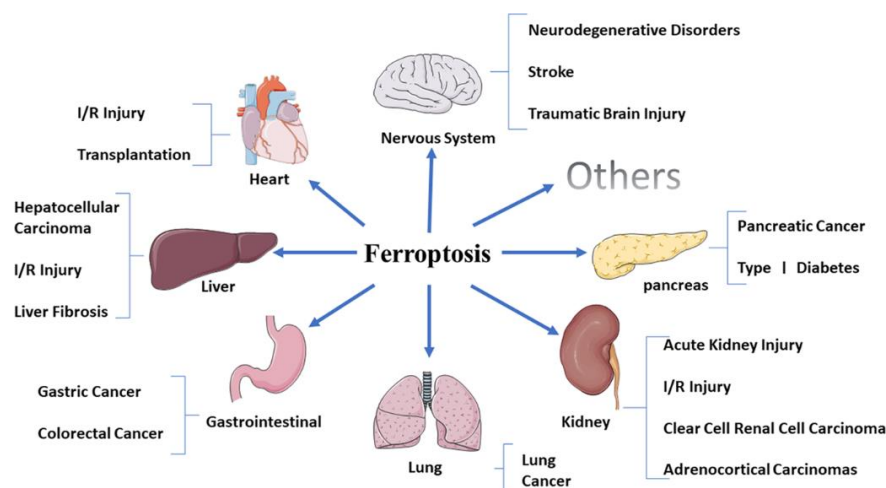

Figure 9: Ferroptosis involvement in different disease (Li *et al.*, 2020)

Indeed, morphologically, mitochondria appear smaller with increase membrane density and reduction of crista, but the cell membrane remains intact and normal size nucleus (Dixon *et al.*, 2012; Yang and Stockwell, 2008).

By Fenton reaction, the increase of iron in the cell supports lipid peroxidation and ROS production which triggers ferroptosis. The association between iron gene/metabolism and ferroptosis activation has been amply demonstrated. As matter of fact, TFRC silencing can inhibit erastin-induced ferroptosis, preventing labile iron pool (LIP) accumulation (Kwon *et al.*, 2015). Moreover, silencing of iron-responsive element-binding protein2 (IREB2) through shRNA causes the alteration of FT-H, FT-L and TFR1 expression, modifying iron intake and storage (Dixon *et al.*, 2012).

In the context of neurological diseases, ferroptosis covers an important role (Kenny *et al.*, 2019) in dopaminergic neurons in PD and other NDs (Do Van *et al.*, 2016).

Dopaminergic neurons are rich on iron that take part in dopamine metabolism (Moreau *et al.*, 2018) but iron imbalance causes dopamine oxidation and α-synuclein aggregation that induce dopaminergic neuron loss in PD (Guiney *et al.*, 2017). Moreover, genetic variants of iron-related genes, Transferrin

(TF) and TfR2 have a role in PD. Explorative findings shown that PD patients with genetic variation in TF gene decreased risk of PD (Rhodes *et al.,* 2014).

Moreover, TfR2 mutations limit iron absorption by explicating a protection mechanism in PD (Rhodes *et al.,* 2014). As ferroptosis is iron-dependent, in neurons iron accumulation could reduce GPX4 activity, which, in turn, leads to GSH depletion subsequently ROS accumulation membrane oxidation (Imai *et al.,* 2017).

To a greater extent damage attributable to ferroptosis are also found in the heart and liver: ferroptosis has been reported to play an essential role in the onset and development of cardiovascular (Huang *et al.*, 2021) and liver-related diseases mediated by an accumulation of lethal lipid hydroperoxides triggered by iron. Since hepatocytes are the major iron storage site, continually they tend to maintain iron homeostasis and ROS balance, known to induce hepatoxicity (Protchenko *et al.*, 2021). Recently, the substantial contribution of ferroptosis has been identified among the other types of cell death (Aizawa *et al.*, 2020). In the manuscript attached, we have explored the relevant literature to correlate common peculiarity between ferroptosis response in the heart and liver.

➕ *Publication: Iron Overload, Oxidative Stress, and Ferroptosis in the Failing Heart and Liver*

Review

Iron Overload, Oxidative Stress, and Ferroptosis in the Failing Heart and Liver

Daniele Mancardi *, **Mariarosa Mezzanotte, Elisa Arrigo, Alice Barinotti and Antonella Roetto**

Department of Clinical and Biological Sciences, University of Torino, 1043 Orbassano, Italy; mariarosa.mezzanotte@unito.it (M.M.); elisa.arrigo@unito.it (E.A.); alice.barinotti@unito.it (A.B.); antonella.roetto@unito.it (A.R.)
* Correspondence: daniele.mancardi@unito.it

Abstract: Iron accumulation is a key mediator of several cytotoxic mechanisms leading to the impairment of redox homeostasis and cellular death. Iron overload is often associated with haematological diseases which require regular blood transfusion/phlebotomy, and it represents a common complication in thalassaemic patients. Major damages predominantly occur in the liver and the heart, leading to a specific form of cell death recently named ferroptosis. Different from apoptosis, necrosis, and autophagy, ferroptosis is strictly dependent on iron and reactive oxygen species, with a dysregulation of mitochondrial structure/function. Susceptibility to ferroptosis is dependent on intracellular antioxidant capacity and varies according to the different cell types. Chemotherapy-induced cardiotoxicity has been proven to be mediated predominantly by iron accumulation and ferroptosis, whereas there is evidence about the role of ferritin in protecting cardiomyocytes from ferroptosis and consequent heart failure. Another paradigmatic organ for transfusion-associated complication due to iron overload is the liver, in which the role of ferroptosis is yet to be elucidated. Some studies report a role of ferroptosis in the initiation of hepatic inflammation processes while others provide evidence about an involvement in several pathologies including immune-related hepatitis and acute liver failure. In this manuscript, we aim to review the literature to address putative common features between the response to ferroptosis in the heart and liver. A better comprehension of (dys)similarities is pivotal for the development of future therapeutic strategies that can be designed to specifically target this type of cell death in an attempt to minimize iron-overload effects in specific organs.

Keywords: oxidative stress; heart failure; hepatic failure; iron; ferroptosis

1. Introduction

Iron is a pivotal element for cell metabolism and a key regulator of several cellular functions mainly through enzymatic activity modulation. The biological importance of iron is largely attributable to its chemical properties; as an element belonging to the transition metals, it promptly undertakes oxidation/reduction reactions between its ferric-reduced (Fe^{3+}) and ferrous-oxidized (Fe^{2+}) states. Iron is an essential component of haemoproteins such as myoglobin, haemoglobin, cytochrome p450, iron–sulphur proteins, and several other proteins that are involved in many aspects of cellular metabolism [1]. Under physiological conditions, there is no specific mechanism for iron excretion from the body, and iron metabolism is strictly influenced by its absorption through the diet (1–2 mg Fe/day), to compensate for nonspecific losses of the metal (mainly through cellular desquamation, menstrual bleeding, or other occasional blood loss) (Figure 1). Iron trafficking is a dynamic process: Transferrin mediates the transport among sites for absorption, recycling, storage, and utilization. Iron released by duodenal enterocytes and splenic macrophages is transferred to bone marrow where it is used to produce RBCs and to the liver where it is stored (Figure 1).
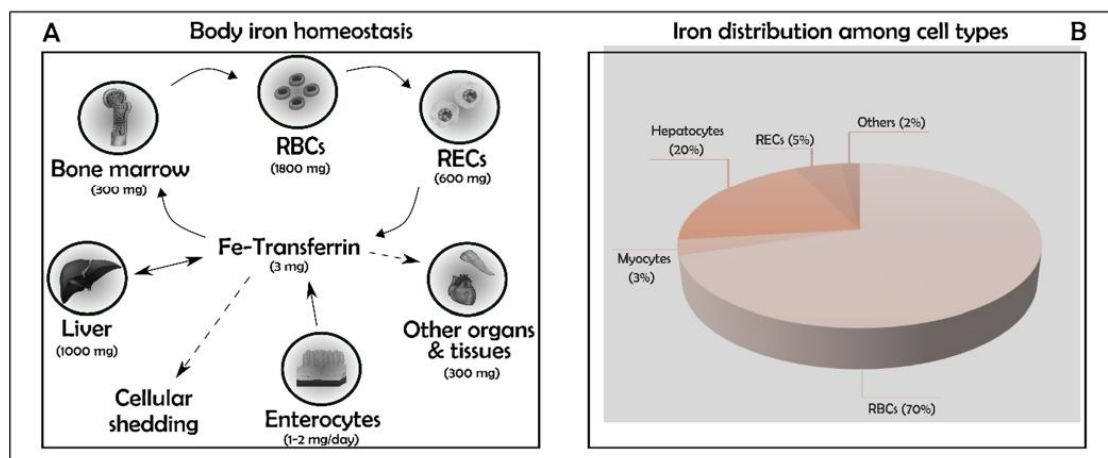
Figure 1. (**A**,**B**) Iron homeostasis and distribution. Summary of the main iron accumulation sites in the human body. In parenthesis the amount of the metal in each compartment. Iron trafficking is a dynamic process: transferrin is used to transport iron. Total iron together with myocytes (3%) and other minor types (2%) cover just one tenth of the total. Major contribution to iron storage capacity comes from Red Blood Cells (RBCs, 70%) and hepatocytes (20%). Macrophages remove senescent erythrocytes, clear haemoglobin-derived heme via hemeoxygenases (HO-1 and HO-2), and export the remaining Fe^{2+} to plasma via Ferroportin (Fpn1), the sole cellular iron exporter. Hepatocytes store excess of body iron within ferritin, the iron storage protein. RBCs: Red Blood Cells; RECs: Reticuloendothelial Cells.

Iron absorption is controlled via a negative feedback regulatory mechanism, that involves the iron-regulator Hepcidin (Hepc) [2]. In some organs, including the heart, liver, duodenum and bone marrow, iron metabolism is finely regulated.

2. Iron Balance

The adult human body content of iron is approximately 3–5 g, corresponding to ~55 mg/kg in males and ~44 mg/kg in females [3,4], differently distributed according to cell type (Figure 1B).

Nutritional iron is absorbed by two main sources: inorganic iron and heme iron, derived from red meat, this last having a higher bioavailability. The pathways involved in heme iron metabolism have been recently elucidated with a deeper understanding on the role of heme importers and exporters mediating the trafficking through the plasma membrane [5]. Similarly, the mechanism leading to inorganic iron absorption is quite well described [6], involving reduction of Fe^{3+} to Fe^{2+} by ferric reductases (such as Dcytb) or other reducing agents (such as ascorbate) in the small intestine lumen. Absorption is facilitated by transport across the apical membrane of enterocytes via the Divalent Metal Transporter 1 (DMT1). Internalized Fe^{2+} is subsequently transferred to the basolateral membrane by a rather unknown mechanism and exported to interstitial fluid and plasma via Ferroportin 1 (Fpn1). The externalization of Fe^{2+} is associated with its re-oxidation to Fe^{3+} by either the soluble or membrane-bound multicopper ferroxidases ceruloplasmin or hephaestin, respectively (Figure 2) [7].

The highest amount of iron is consumed by erythropoiesis although it is largely recycled from phagocytosis of senescent RBCs, mainly by splenic reticuloendothelial macrophages. The modulation of erythropoiesis is, in turn, adjusted by a pleiotropic regulator of iron metabolism, Hepcidin (Hepc, described below) together with Hepc newly described modulators (Gdf15, Twgs1, Erfe) although the precise mechanism of action has not yet been completely clarified [8].
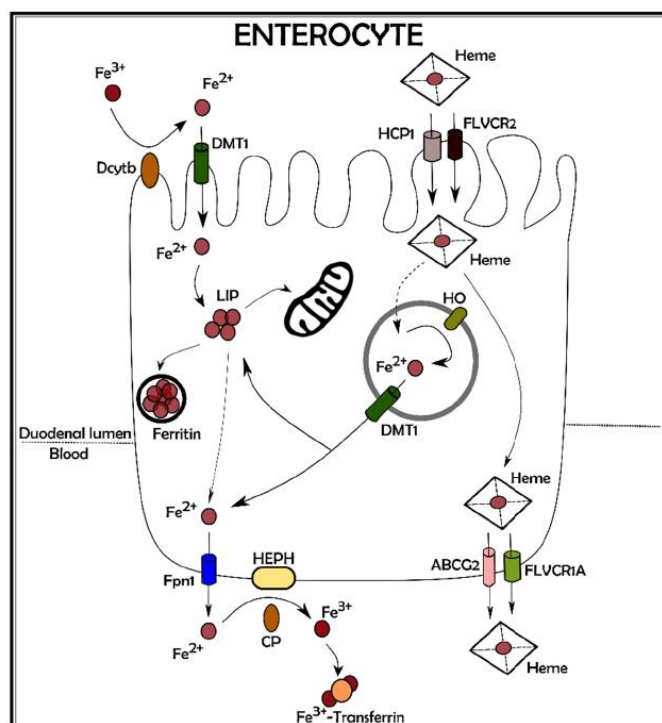
Figure 2. Dietary iron absorption. The iron ingested with the diet can be inorganic (ferric iron, Fe^{3+}) or incorporated in heme. Ferric iron is converted in its ferrous state (Fe^{2+}) by Dcytb, a ferric reductase enzyme on the brush border of the enterocytes. Fe^{2+} is then transported within the cell through DMT1, a transporter placed in the apical membrane of the enterocytes. Once inside the cell, the absorbed inorganic iron can be used for immediate biologic processes, stored in ferritin or released into circulation through Fpn1, the main iron exporter positioned in the basolateral membrane of enterocytes. To be bound to transferrin, Fe^{2+} must be re-oxidized in its ferric state by HEPH or CP. Intestinal heme is possibly incorporated through HCP1 or FLVCR2 transporters. Within the enterocyte, heme can be released unmodified into circulation or it can be degraded in endosomes/lysosomes by HO. The liberated iron follows the same fate of the absorbed inorganic iron. Dcytb: Duodenal cytochrome b; DMT1: Divalent Metal Transporter 1; LIP: Labile Iron Pool; Fpn1: Ferroportin 1; HEPH: Hephaestin; CP: Ceruloplasmin; ABCG2: ATP-Binding Cassette Subfamily G Member 2; FLVCR1A: Feline Leukaemia Virus subgroup C cellular Receptor 1A; HO: Heme Oxigenase; HCP1: Heme Carrier Protein 1; FLVCR2: Feline Leukaemia Virus subgroup C cellular Receptor 2.

Myocytes are the second major site of iron utilization, used to produce myoglobin [9] even though the mechanism of iron incorporation for myoglobin production is not well described. On the other hand, hepatocytes are the principal reservoirs for iron deposition and storage, but when the body content of iron is re-established, macrophages of the liver, spleen, and bone marrow also contribute to storing it. The iron amount in hepatocytes and macrophages can be mobilized to meet erythropoietic and cellular demands when body iron levels are low. An active mechanism for the excretion of iron is missing and only a very small amount is present each day in the urine or faeces [10]. Iron is also lost in females with blood during menstruation and childbirth, however iron loss from sweat and desquamated skin cells is negligible even during intense physical exercise [11,12]. As mentioned before, most of the iron in the human organism is retrieved from senescent red blood cells through the RECs of the spleen and the Kupffer cells of the liver.

3. Physiopathology Iron-Related in Heart and Liver

In several clinical scenarios, including primary hemochromatosis and secondary iron-overload, iron metabolism is chronically altered causing, in combination with confounding environmental factors, increased morbidity and mortality. Most interestingly, patients affected by iron-overload associated diseases (i.e., hemoglobinopathy and hemochromatosis) can manifest signs of organ dysfunction often degenerating in liver and heart failure. In iron-overload conditions, serum levels of iron are typically higher than the transferrin iron-binding capacity, leading to the increase of the content of iron non-transferrin-bound, which has a higher reactivity. It is well established that iron can enter the cells by two main mechanisms: either bound to the transporter protein Transferrin (Tf), through Transferrin/Transferrin receptor 1 (Tfr1) or, in form of non-transferrin-bound iron (NTBI), through Divalent Metal Ionic Transporter (DMT) which is associated with metallo-reductases Dcytb and the STEAP3 proteins [13]. Recently, new players have been shown to be involved in iron uptake, namely the neutral pH transporters ZIP8 and ZIP14 as well as a group of cytochrome-dependent oxido-reductases that shuttle reducing equivalents across the plasma membrane according to the plasma membrane electron transport (PMET) mechanism [13]. On the contrary, iron export from cells occurs through Fpn1, associated with different ferroxidases (ceruloplasmin, hephaestin, and zyclopen (HEPHL)) (Figure 3) [14]. Excessive NTBI uptake, along with ineffective iron excretory pathways, lead to a significant increase of the so-called labile intracellular iron pool (LIP), as well as the formation of highly reactive oxygen free radicals, augmenting detrimental peroxidation of membrane lipids and diffuse oxidative damage to cellular proteins [15]. Due to its potential toxicity (see above), intracellular iron is managed to allow a minimal amount of free iron within the cytoplasm. For this reason, it is essentially associated with the iron deposit protein, Ferritin (Ft) or utilized in cytoplasmic and mitochondrial iron requiring proteins. Mitochondria, in particular, use a consistent amount of cellular iron as a cofactor in several proteins involved in oxidation/reduction reactions of the respiratory chain [16].

Cellular iron homeostasis is regulated post transcriptionally by the so-called IRE/IRP system that involves the iron regulatory protein 1 (IRP1) and 2 (IRP2) (also known as ACO1 and IREB2, respectively) and two iron–sulphur (Fe–S) RNA-binding proteins that are able to bind to a *cis*-regulatory hairpin structures known as IRE (Iron Regulatory Element), located in the 5′ or 3′ untranslated regions (UTRs) of target mRNAs. In the condition of cellular iron deprivation, either of the two IRPs binds to the 5′ UTR IREs of target RNA, impeding the transcription initiation complex to exert its function and inhibiting the RNAs translation [17]. On the contrary, IRPs binding to the 3′ UTR IRE motif elements present in specific mRNAs prevent their endonucleolytic cleavage and subsequent degradation [18]. Consistently, other studies report the involvement of other elements of the IRE/IRP regulatory network including the human cell division cycle 14A mRNA [19] and human MRCKalpha [20] (See Table 1).

Table 1. List of the main genes submitted to IRE/IRP post-transcriptional regulation. Localization of the IRE element (5′ or 3′ untranslated regions (UTRs)) is reported for each gene mRNA; arrow down indicates the translation block caused by the IRPs binding to IRE sequence and diminished effect, arrow up indicates mRNA stabilization due to the IRPs binding to IRE sequence and augmented effect.

RNA	Protein	5′UTR	3′UTR	Translation	Effect	Refs.
FtH/L	Ferritin	√		↓	↓ iron storage protein	[17]
DMT1	Divalen Metal Transpoter		√	↑	↑ Iron import	[17]
TfR1	Transferrin Receptor		√	↑	↑ Iron import	[17]
Fpn1	Ferropotin 1	√		↓	↑ Iron export	[17]

Table 1. *Cont.*

RNA	Protein	5′UTR	3′UTR	Translation	Effect	Refs.
ACO2	Mitochondrial Aconitise 2	√		↓	↓ TCA cycle	[17]
HIF2α	Hypoxia-Inducible Factor 2α	√		↓	↓ Hypoxia reponse	[17]
ALAS2	△-Aminolevulinate Synthase 2	√		↓	↓ Heme biosynthesis	[17]
CDC14A	Cell cycle phosphatase var.1		√	↑	-	[18]
CDC42BPA	Myotonic dystrophy kinase-related Cdc42-binding kinase α		√	↑	↑ Tfr1	[19]
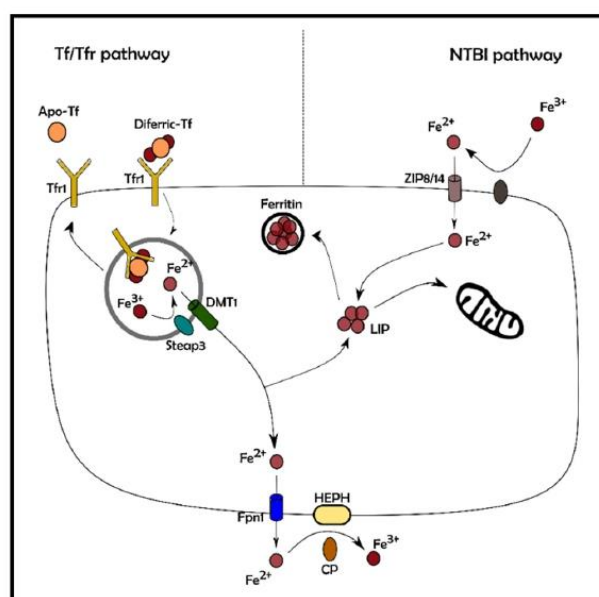
Figure 3. Non-heme iron absorption. Iron can be absorbed by the cells following two pathways: Transferrin/Transferrin Receptor 1 (Tf/Tfr1, on the left) or non-transferrin-bound iron (NTBI, on the right). The blood circulating diferric transferrin (diferric-Tf) binds to Tfr1, a membrane-bound receptor. The complex is transferred within the cells into endosomes; here, the acidic pH generated by proton pumps, results in the release of the ferric iron from the complex. Fe^{3+} is reduced in its ferrous state by Steap3 and released into the cytosol through DMT1. The Tf/Tfr1 complex is recycled, while the free cytosolic ferrous iron follows the same fate as mentioned in Figure 2. The uptake of the NTBI pool seizes on carriers such as DMT1 or the most recently studied zinc transporters ZIP8 and ZIP14. NTBI: Non-Transferrin-Bound Iron; Tf: Transferrin; Tfr1: Transferrin receptor 1; DMT1: Divalent Metal Transporter 1; LIP: Labile Iron Pool; Fpn1: Ferroportin 1; Steap3: Six-transmembrane epithelial antigen of prostate 3; HEPH: Hephaestin; CP: Ceruloplasmin; ZIP8: Zrt–Irt-like Protein 8; ZIP14: Zrt–Irt-like Protein 14, Apo-TF: iron-free Tf.

4. Iron Metabolism in the Heart

Cardiac myocytes are major oxygen consumers, and a commensurate intracellular iron pool is necessary to sustain this aerobic activity. The high metabolic demand of the heart and its dependency on iron is confirmed by the finding about the deletion of heart Tfr1 in a murine model which causes detrimental energetic failure in cardiac myocytes, even in the presence of normal systemic iron levels [21]. Normally, cardiomyocytes have relatively high levels of Hepc and Fpn1, although they have not been proved essential in controlling systemic iron accumulation and metabolism [22,23]. Most recently, the cardiac role of Hepc and Fpn1 has been investigated with animal models characterized by cardiomyocyte-specific downregulation of the Hepc/Fpn1 axis. Interestingly, cardiac specific deletion of Fpn1 encoding gene prompted mice to develop fatal dysfunction of the left ventricle by the third month of age. The dysfunction was associated with a threefold increase in iron levels within cardiac myocytes. It is worthy of note, that Tfr1 downregulation does not counteract ferroportin 1 deficiency to prevent iron overload in these hearts, indicating that iron release, mediated by ferroportin 1, is essential for iron homeostasis in the heart, along with other iron intake mechanism(s) [23]. In the same model of Fpn1 deficient heart, iron was predominantly stored in the cardiomyocytes, whilst in the hemochromatosis murine model, a major part of the iron was in the extracellular compartment, consistent with a significant increase in cardiomyocyte Fpn1. Therefore, ferroportin 1 is not only crucial for iron homeostasis in the heart, but it also responsible for deposition of iron in the heart in the conditions characterized by systemic iron overload. In fact, ferroportin 1 may be held responsible for the severity of cardiac dysfunction determined by iron deposition [23]. On the other side, specific deletion of Hepc in the heart of mice leads to a fatal dysfunction of the left ventricle between 3 and 6 months of age, even if systemic iron levels are maintained in a normal range. All these results together, suggest that the myocardial hepcidin/ferroportin 1 pathway is pivotal for the autonomous control of the intracellular iron stores which are required for physiological cardiomyocytes functions. The same cardiac hepcidin/ferroportin 1 axis has been also proven to be important to protect the myocardium from the consequences of systemic iron deficiency. Cardiac levels of Hepc protein were increased instead of decreased after dietary iron restriction in in vivo models and by iron chelation in in vitro experiments. Moreover, animal models with cardiac depletion of hepcidin have increased chances to develop hypertrophy in response to a sustained dietary iron restriction when compared to their littermate controls [22].

Although all cell types forming the heart are sensible to injury triggered by increased ROS production, cardiomyocytes have been shown to be particularly affected [23,24]. The high metabolic demand of the myocardium, in fact, is matched by a peculiar abundance in mitochondria with a consequent elevated oxygen consumption and a detrimental deficiency in antioxidant enzymes [25]. Unbalance of cardiomyocytes iron content is regulated by the expression of Tfr1 [26] and iron overload becomes critical when NTBI/LPI is exceeded due to the saturated binding capacity of Tf [27]. The exact mechanism for NTBI to enter cardiomyocytes is still largely undescribed although some studies report an involvement of L-type or T-type calcium channels in iron uptake under overload conditions and suggesting calcium channel blockers as a potential therapeutic tool to mitigate cardiac effects of iron overload [15]. This evidence is supported by ex vivo studies which demonstrated that L-type Ca^{2+} channels downregulation can reduce iron uptake under chronic overload condition [28]. In case of iron overload, therefore, L-type channels mediate the increased ferrous iron uptake which leads to an over production of ROS that triggers, among others, an excitation-contraction uncoupling with an impaired systolic and diastolic function, a typical sign of iron-overload cardiomyopathy [29]. Another iron carrier has been proposed to be potentially involved in the developing of heart failure, lipocalin-2 [30]. It has been reported that lipocalin-2 induces apoptosis in in vitro settings while the reported in vivo effects include acute inflammatory response and cardiac remodelling [31].

On the other hand, for the oxygen to react with intracellular molecules a catalyst is needed, one of the most potent being iron, and when LIP increases, oxidative stress

can pose a cytotoxic trigger mediated by accelerating the reaction between oxygen and biomolecules. Typically, the increased ferritin expression leads to a safe cytosolic stored iron as a part of the response to a pro-oxidative environment [32].

Most interestingly, oxidative stress in the heart plays a double role as a mediator of both protection and generation of the ischemia/reperfusion injury [33]. In addition, cardiac ferritin is enriched in H subunit [25], undergoing an iron-based mechanism in the ischemic preconditioning phenomenon [34]. In the regulation of intracellular iron, exporting excess could represent a way to counterbalance an exceeding entry of NTBI. Basal expression of H-ferritin cannot cope with iron overload and regulation of its expression is necessary for a rapid chelation of LIP to prevent oxidative stress [35] and these findings suggest a putative role for transcriptional regulation of iron transporters and ferritin subunits in the heart [36]. Paradoxically, Hepc levels can be decreased in β thalassemia-mediated cardiomyopathy as well as other iron overload-mediated conditions, where erythropoiesis-dependent downregulation of Hepc should prevail and these low levels of circulating Hepc are believed partially responsible for the ferroportin 1 expression and export activity, thereby concurring to limit iron accumulation in the heart [25].

5. Iron and Oxidative Stress in Cardiomyocytes and Hepatocytes

While it seems clear that iron externalization is almost solely regulated by ferroportin 1, the degree of internalization is synergistically determined by several transporters, some of which are tissue-specific and others are ubiquitous.

The estimated iron concentrations in the major cellular compartments (~6 μM cytosol [37], ~16 μM mitochondria [38], ~7 μM nuclei [39], and ~16 μM lysosomes [39]) are finely regulated by specific transporters. Under excessive extracellular iron, cardiac cells can uptake Fe^{3+} or Fe^{2+} through L-type and T-type Ca^{2+} channels [40], although in some models verapamil and amlodipine, but not efonidipine (all calcium-channel blockers), could mitigate iron uptake. In mitochondria, where iron is critical for several reasons, including the production of heme- and iron–sulphur-cluster proteins of the electron transport chain, a putative role has been shown for the calcium uniporter: blocking the activity of this specific transporter, leads to the preservation of mitochondrial structure and function after iron overload of cardiomyocytes [41]. On the other hand, two nuclear-encoded proteins, Mitoferrin1 (Mfrn1) and Mitoferrin2 (Mfrn2) have been shown to mediate internalization of iron [42] suggesting a multifactorial regulation of iron levels in mitochondria. Genetic deletion of Mfrn1 induces severe impairment of heme synthesis and is lethal during early embryonic development while its transcription, promoted by GATA1, is upregulated during erythropoiesis [43]. When Mfrn1 expression is experimentally blunted during adulthood, the phenotype is vital with defects in erythroid cells resulting in severe anaemia [44]. Most interestingly, mRNA for Mfrn1 is detectable in non-erythropoietic cell lines with lower levels compared to Mfrn2, which is ubiquitously expressed in virtually all tissues [43]; nevertheless, Mfrn1 absence is not shown to affect the development of heart, liver, or muscle [44]. With its ability to shift between two redox states, non-bound iron is highly reactive, leading to oxidative stress which is a pivotal trigger of tissue and organ failure [15]. The key step for the excessive production of radicals is the Fenton reaction, which has been demonstrated to play a fundamental role in the physiopathology of several diseases, including heart failure [45], liver failure [46], renal disease [47], and different types of neurodegeneration [48–50]. Cardiomyopathies related to iron-overload represent one of the major causes of mortality and comorbidity in patients with secondary and primary hemochromatosis, respectively [15,51–53]. Aside from direct ROS-mediated damage, iron overload has been shown to impair synthesis and function of respiratory subunits through mitochondrial DNA (mtDNA) alteration [54]. Full length mtDNA is accessed to verify the integrity of the mitochondrial genome and it is substantially reduced by 300 μm of extracellular iron [54].

6. Ferroptosis in Heart Failure

Numerous cardiovascular diseases are characterized by cardiac and vascular cell loss trough necrosis, apoptosis, and autophagy. As a novel type cell death, ferroptosis has been reported to play a pivotal role in the onset and development of various cardiovascular diseases mediated by an accumulation of lethal lipid hydroperoxides triggered by iron [55]. In the heart, several mechanisms are critical for the triggering of ferroptosis, including iron metabolism, glutamine metabolism, and lipid peroxidation, while recent studies suggest that myocardial dysfunction induced by ferroptosis can be inhibited by iron chelators and antioxidants [56]. In hemochromatosis patients, there is a significant deterioration of electro-mechanical coupling of cardiomyocytes mediated by ROS formation, while major cardiotoxic effects of doxorubicin have been proven to be ferroptosis-mediated [57]. Most interestingly, doxorubicin cytotoxicity on myocytes can be decreased through inhibition of ferroptosis induced by over expression of GPX4 and activation of Keap1 (Kelch-like ECH-associated protein 1)/Nrf2 signalling [57]. The involvement of ferroptosis in chemotherapy-induced cardiomyopathy, is confirmed by transgenic mouse models in which sequestration of Keap1 grants cardiac protection from doxorubicin-induced ferroptosis [58]. Consistently, other reports provide evidences about the role of Acyl-CoA thioesterase in preventing myocardial injury in doxorubicin-treated murine hearts [59].

Being characterized by the death of post-mitotic cardiomyocytes, heart failure (HF) is an irreversible condition for which an early prevention of cell loss is of paramount importance. Independently of the type of cell death to be targeted, retarding progression of heart failure is fundamental to preserve cardiac function as shown by a report describing a ferroptotic pathway in an animal model of HF induced by left ventricular pressure overload [60]. The interplay between HF and iron metabolism is complex and rich in negative feedback mechanisms leading to a general worsening of patient conditions. Anaemia, for instance, is often found in HF patients and prognosis is generally poorer according to blood haemoglobin content [61]. Among the pathogenic mechanisms linking anaemia and HF there is iron deficiency, although it is not clear which one may be held primarily responsible for the vicious loop [62] despite the abundance of reports describing iron-deficiency anaemia in patients with severe HF [63]. Some insights come from experimental models of HF in which a down-regulated duodenal iron transporter leads to iron deficiency and impaired liver expression of hepcidin [64]. In this study, the same outcomes in terms of iron-transporters and hepcidin expression, were achieved through an iron-deficient diet indicating that a diminished iron absorption is present in HF models [64]. Experimental data, therefore, suggest that iron supplementation may offer a clinical advantage in treating patients with HF and anaemia and three clinical trials have proven the beneficial outcomes in terms of exercise capacity in HF patients but failed to ameliorate HF-iron deficient patients [65]. The answer to these conflicting results may rely on the animal model, demonstrating a reduced absorption of iron in HF and the consequent inefficacy of oral supplementation. Consequently, a later large clinical trial investigated the effects of iron supplementation given intravenously but results and long-term safety for i.v. supplementation still need clarification [66].

There is evidence that Transferrin Receptor 2 (TfR2), a protein that plays a role in iron metabolism in different tissues [67], may be involved in erythroid iron trafficking through a mediation of lysosomes and a subsequent transfer to mitochondria [68]. Others suggest that the release of Fe^{2+} from lysosomes is mediated by Transient Receptor Potential Mucolipin 1 (TRPML1) and the mechanism can be considered, at least in part, responsible for haematological and degenerative symptoms in mucolipidosis type IV disease patients [69]. Once Fe^{2+} has reached the mitochondria, some sort of feedback is generated between the mitochondria and cytosol compartments although, when heme synthesis is impaired, iron continues to be incorporated by mitochondria probably due to poor uncoupling which leads to a positive feedback to restore heme synthesis [70].

A small mitochondrial protein, Frataxin (FXN) is involved in iron–sulphur clusters (Fe–S) formation essential for the mitochondrial respiratory chain complexes, aconitase and

other mitochondrial enzymes [71]. FXN is mostly expressed in organs with high metabolic demand as liver, kidney, neurons, and heart [72]. FXN functions can be diverse and act as: (i) iron chaperone during cellular heme production [73]; (ii) iron storage protein [74]; (iii) buffer of oxidative damage directed to aconitase Fe–S clusters; (iv) protective factor against oxidative damage [75]. FXN gene mutation has been shown to be responsible for the onset of an inherited autosomal recessive neurodegenerative disorder known as Friedreich's ataxia disease (FRDA) [76]. FRDA is characterized by mitochondrial dysfunction [77], iron accumulation in mitochondria, ROS accumulation and lipid peroxidation [78]. All these metabolic alterations draw a connection line between this disease and ferroptosis. The heart is the main organ affected by mitochondrial alteration [79] and is important to note that patients with this neurological syndrome develop a progressive hypertrophic cardiomyopathy [80]. Since the constitutive inactivation of frataxin causes embryonic lethality in mice [81] a specific striated muscle frataxin-deficient murine model and a neuron/cardiac muscle frataxin-deficient line were generated [82]. This model recapitulates the pathophysiological and biochemical peculiarity of the human disease.

7. The Role of Ferroptosis in Liver Failure

Several physiopathological pathways concur in the development of hepatocytes dysfunction and may lead, in the long term, to chronic liver failure. Being the second largest storage site in the body after RBCs (Figure 1), hepatocytes are constantly battling to maintain iron homeostasis and ROS balance [83]. While ROS overproduction is a well-established inducer of hepatotoxicity, only recently has the substantial contribution of ferroptosis been recognised among the other types of cell death. Indeed, most triggers commonly involved in liver failure are mediated by iron overload and consequent cell death [84]. In the drug-induced liver disease scenario, a recent study reports a prominent role of ferroptosis in a murine model of acute liver failure, induced with an overdose of acetaminophen (APAP), suggesting that this type of cell loss may represent a putative therapeutic target [85] whereas other authors disagree on the importance of the ferroptotic mechanism in this model [86]. There is consensus, however, regarding the involvement of the inhibition of ferroptosis in sorafenib resistance in the treatment of hepatocellular carcinoma [87] with a recognised role for ACSL4 (acyl-CoA synthetase long-chain family member 4), a known mediator of ferroptosis [88]. ACSL4 has been pharmacologically targeted in a mouse model of ferroptosis with a class of antidiabetics (thiazolidinediones), unveiling its role as inhibitor of ferroptosis, posing a potential therapeutic target [89]. Hepatic iron overload is often associated with hemochromatosis and intriguing results demonstrate that solute carrier family 7, member 11 (Slc7a11), an established ferroptosis-related gene, is up-regulated in iron-overloaded cells, again pointing at ferroptosis as a potential target for the treatment of hemochromatosis-induced tissue injury [90]. Moreover, in alcoholic liver steatosis and disease, ferroptosis has been proven to be increased through the deacetylase SIRT1 in mice with ethanol-induced liver injury [91] as well as in the progression of non-alcoholic steatohepatitis [92]. Non-alcoholic fatty liver disease, of which the aetiology remains largely unclear, is often associated with a high serum level of ferritin [93] and ROS-triggered ferroptosis which can be inhibited by the Keap1/Nrf2 signalling cascade [94].

Paradoxically, also when liver disease requires organ transplantation, ferroptosis must be taken into consideration, because of its role in the ischemia/reperfusion injury related to surgical procedures [95]. Not surprisingly, ACSL4 is also activated during intestinal ischemia/reperfusion and contributes to the development of ferroptosis-mediated cell loss [96] and similar mechanisms have been described in renal failure [97,98], cardiomyopathy [99], as well as in heart transplants [100].

Concluding, over the last decade it has become clearer how iron-induced toxicity is at the root of several physiopathological mechanisms and ferroptosis can, therefore, be considered a valid therapeutic target to mitigate liver failure. However, the precise molecular mediators have been identified in few cases, as for Glutathione Peroxidase 4

(GPX4) [101] and the cystine–glutamate antiporter system [102]. As a consequence, most of the data are from basic research studies whilst randomized clinical trials are still attempting to confirm results from in vivo and in vitro models.

8. What Is behind the Ferroptosis *Scenario*

According to recent findings, the main mechanism behind ferroptosis is ROS-dependent regulated cell death. Ferroptosis is triggered by intracellular iron accumulation, lipid peroxidation, and oxidation of polyunsaturated fatty acid-containing phospholipids (PUFA-PLs) [103]. The presence of iron in the cytosol causes the formation of ROS through the Fenton reaction, by which H_2O_2 is transformed in hydroxyl radicals that, in turn, cause lipid peroxidation to play an essential role in ferroptosis [103].

ROS increase can be modulated by the quenching action of GPX4, an enzyme converting reduced glutathione (GSH) into glutathione disulphide (GSSG) that utilizes hydrogen ions to reduce hydrogen peroxide as well as lipid peroxides [104]. GPX4 can be therefore considered a type of GSH peroxidase, representing the main intracellular antioxidant enzyme acting against ROS. In fact, it prevents iron dependent formation and accumulation of ROS, producing lipid alcohols (R–OH) from lipid hydroperoxide (R–OOH) with GSH as a cofactor. This metabolic process is cytoprotective against Fe^{2+}-dependent formation and accumulation of ROS [103,105].

Beside the central role of GPX4 in maintaining ROS low levels, a corollary of different pathways is necessary to support the efficiency of GPX antioxidant activity. First, the so-called System Xc^-, a heterodimeric antiport system that imports cystine and exports glutamate, formed by two subunits named SLC3A2 and SLC7A11 [106]. The imported cystine is further transformed in cysteine and then into GSH, in order to maintain redox homeostasis thus protecting cells from ferroptosis [107]. System Xc^- is the main mechanism supporting the efficiency of GPX antioxidant activity through the inhibition of a series of events triggering the reduction of GSH levels, lipid peroxidation, and consequent ferroptosis [103].

The second pathway that cooperates with GPX is composed of a protein complex involved in the enzymatic cascade that leads to the hydro peroxidation of lipid-polyunsaturated fatty acids (PL-PUFA-OOH), which represent the substrate for GPX4 to be oxidized and transformed into lipid-polyunsaturated fatty acids alcohols (PL-PUFA-OH). Several enzymes involved in the production of PL-PUFA-OOH are important in ferroptosis processes due to their regulation being associated with this particular type of cell death, namely ACSL4, LPCAT3, LOX [108].

In this particular case, ferroptosis depends on reduced detoxification of lipid peroxides through the action of the enzymatic activity of GPX4 [109] and, most recently, it was reported that its sensitivity can be also regulated by Nuclear Receptor Coactivator 4 (NCOA4) [110], a cargo protein involved in autophagic ferritin degradation [111]. Cytosolic ferritins work as iron storing molecules and are composed of 24 subunits of H (heavy) and L (light) chains that co-assemble in different proportion to form heteropolymers with a tissue specific distribution combined to functions: Ft heteropolymers present in organs designated to iron storage, as liver and spleen, are richer in L-subunits, while those present in heart and brain, that have a high ferroxidase activity, are richer in H-subunits [112]. The FtH subunit has enzymatic activity and oxidizes Fe^{2+} to Fe^{3+} to be incorporated into the protein shell. As a whole, Ft polymers are involved in iron detoxification, storage, and recycling [112]. The upregulation of ferritin can limit ferroptosis; the opposite effect occurs if the protein is downregulated [113]. The binding between NCOA4 and ferritin is FtH specific [114] and, as a consequence of it, FtH is carried into lysosomes, degraded, and iron is released to be used by the cells, modulating in this way the intracellular iron amount, in a process termed "ferritinophagy" [111,113]. Consistently, NCOA4 levels are regulated by intracellular iron status [115] and recent works showed that the amount of NCOA4 changes according to the interaction with an E3 ubiquitin protein ligase, HERC2 [115,116];

during iron overload condition, NCOA4 is degraded by HERC2, whose activation is in turn iron dependent (Figure 4) [113].
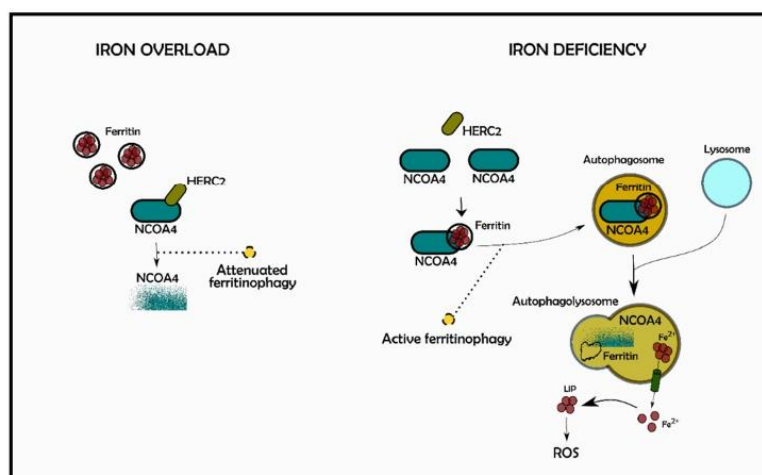

Figure 4. NCOA4-mediated *ferritinophagy*. Intracellular iron is regulated by a process known as ferritinophagy. In conditions of iron overload (on the **left**), NCOA4 is degraded by the binding with HERC2, an ubiquitin ligase protein, leading to the reduction in ferritin degradation. On the contrary, during iron deficiency (on the **right**), NCOA4 molecules stabilize being able to bind ferritin, thus activating ferritinophagy via lysosomal degradation. NCOA4: Nuclear Receptor Coactivator 4; HERC2: HECT and RLD domain Containing E3 Ubiquitin Protein Ligase 2; LIP: Labile Iron Pool.

Since intracellular iron regulation depends on NCOA4-mediated ferritinophagy, the lack of NCOA4 in a murine model induced systemic iron overload congruent to increased level of transferrin saturation, serum ferritin, liver hepcidin and ferritin deposits with decreased iron availability [117].

It is known that ferroptosis is a form of autophagic cell death [118]; autophagy promotes ferroptosis leading to ferritin degradation via ferritinophagy mediated by NCOA4 with an increase of labile iron pool (LIP), which promotes ROS accumulation, the main driver of the ferroptotic mechanism [118]. On the other hand, NCOA4 inhibition limits ferritin degradation and blocks the ferroptosis process; the opposite effect is triggered if NCAO4 is overexpressed [113].

The activation of cell defence mechanisms which enhance the detoxification of cells is also mediated by Nrf2 [119]. Nrf2 is a redox-sensitive transcription factor, whose activation results in cellular antioxidant responses modulating several stress-responsive proteins and phase II detoxification [119,120]. In normal conditions, Keap1 stimulates Nrf2 ubiquitination and its proteasomal degradation in order to keep its levels low; on the contrary under oxidative stress condition, Nrf2 disassociates from Keap1, translocates to the nucleus where it binds to antioxidant response element (ARE) located in the promoter region of target genes, and regulates/activates the transcription of heme oxygenase-1 (HO-1), NAD(P)H, quinone oxidoreductase (NQO1), glutathione S-transferase (GST), and glutathione peroxidase (GPx), favouring several cellular defence mechanisms and amplifying detoxification [119,121]. Nrf2 works as a ferroptosis suppressor since it promotes the expression of antioxidants or iron metabolism genes involved in iron import, as Transferrin receptor 1 (Tfr1) and iron storage protein ferritin [112,122]. The perturbation in iron metabolism during the process of import, export and storage of iron may influence the cell hypersensitivity to ferroptosis. Data has shown that pseudolaric acid B (PAB) treatment of glioma cells causes upregulation of Tfr1 and the resulting increased iron entry into the cells activates Nox4 leading to production of H_2O_2 and lipid peroxides, all signs of

ferroptotic process activation, [123]. Following the same rationale, using prominin2, a pentaspan protein involved in regulation of lipid metabolism, in mammary epithelial and breast carcinoma cells, improves ferroptosis resistance by promoting ferritin export [124].

It has been demonstrated that both the Nrf2 genetic inactivation in knockdown mouse Hepa1-6 and its pharmacological inhibition using erastin and sorafenib, trigger ferroptosis events in vivo [122]. This confirms that the loss of Nrf2 improves the ferroptosis process through the consequent reduction of the anti-ferroptosis gene transcription including FtH, HO-1, and NADPH quinone oxide-reductase, EC. 1.6.99.2 (NQO1) [122]. Furthermore, Nrf2 is able to upregulate a large number of other anti-ferroptotic genes such as glutamate–cysteine ligase catalytic subunit (GCLC), glutathione synthetase (GSS) and GPX4 to enhance GSH synthesis and function [125].

In this context, the chaperones protein HSB1 (Heat Shock protein Beta-1), protects cells against harmful stimuli [126]. It has also been demonstrated that, after erastin treatment, HSB1 is upregulated to inhibit ferroptosis by reducing cellular iron uptake through the inhibition of Tfr1 and lipid ROS production, in different cancer cells [127].

9. Conclusions

Similar to many other elements, iron is both detrimental and indispensable for life. The subtle balance between too low and too much iron, is regulated at the level of both the entire organism and the single cell. Moreover, iron continuously changing between the reduced and oxidised forms, adds complexity to its trafficking between the intra- and extracellular compartments because selective carriers are needed for its transport even inside cell organelles [128]. Perhaps the best model to study the mechanisms for iron import and export, are the enterocytes where iron assumed with the diet, is both internalised and externalised in the apical and basolateral membrane, respectively [129]. Nevertheless, it is important to unravel how every organ is able to manage and respond to iron variation to minimize the adverse effects that iron overload or deficiency could cause in that specific compartment. A typical example is represented by the central nervous system that, even in the condition of systemic anemia, maintains constant its own iron quantity [130]. As for iron overload, independent of the cause, it triggers detrimental processes within cells and the type of cell death induced by iron accumulation has been named ferroptosis [131]. While it is true that all cell types are affected by iron unbalance, two organs are paradigmatic in the ferroptosis scenario; the heart is one of the principal utilisers of iron while the liver is principally responsible for iron handling. Iron level alterations are detrimental in both directions as proved by the poor prognosis of heart failure patients with commonly associated iron deficiency [132]. Accordingly, iron mishandling has been proposed to be a major trigger for severe injury to cardiomyocytes and hepatocytes and therefore an important player in developing heart and liver failure [55,133]. On the other hand, while iron overload has been demonstrated as being associated with several cardiac diseases, its essential role in mediating ischemic preconditioning cardioprotection has been proposed [55]. These reports are in accordance with studies demonstrating the double role of ROS in mediating both injury and protection to the heart, ROS production being strictly related to iron activity inside the cell [134]. With the surge of results confirming the pivotal role of ferroptosis in developing heart and liver diseases, some recent studies have demonstrated how targeting the ferroptotic pathway can be beneficial in inhibiting cell death induced by iron overload. For instance, the use of both iron chelator and antioxidants have been proposed as therapeutic tools in the treatment of myocardial infarction and in preconditioning the hearts of patients undergoing reperfusion manoeuvres [135]. In liver, several physiopathological pathways can be affected by impaired iron homeostasis including alcohol-induced hepatotoxicity [136], acute liver failure [85], drug-induced liver injury [137], and hepatic fibrosis [138]. Thus, clarifying the subtle mechanisms that regulate iron balance within hepatocytes is of paramount importance in the attempt to mitigate the clinical outcome of the above-mentioned pathologies.

Although the main focus of this review is cardiac and hepatic ferroptosis, it is worth to briefly mention that ferroptosis emerged as a pivotal and broad mechanism responsible for cell death occurring in several other cell types. Consistently, ferroptotic cell death has been described as being implicated in a broad spectrum of disorders including, but not limited to, cancer, diabetes, acute kidney injuries and neurodegenerative disorders, and sometimes also associated with the progression of diseases like leukaemia, psoriasis, and haemolytic disorders [139].

Author Contributions: Conceptualization, D.M., A.R.; methodology, M.M.; software, E.A.; formal analysis, A.B.; resources, D.M.; writing—original draft preparation, D.M., A.R., M.M.; writing—review and editing, D.M., A.R., M.M.; visualization, E.A.; supervision, D.M. All authors have read and agreed to the published version of the manuscript.

Conflicts of Interest: The authors declare no conflict of interest.

References

1. Hentze, M.W.; Muckenthaler, M.U.; Andrews, N.C. Balancing acts: Molecular control of mammalian iron metabolism. *Cell* **2004**, *117*, 285–297. [CrossRef]
2. Hentze, M.W.; Muckenthaler, M.U.; Galy, B.; Camaschella, C. Two to Tango: Regulation of Mammalian Iron Metabolism. *Cell* **2010**, *142*, 24–38. [CrossRef]
3. Ganz, T. Systemic iron homeostasis. *Physiol. Rev.* **2013**, *93*, 1721–1741. [CrossRef] [PubMed]
4. Gkouvatsos, K.; Papanikolaou, G.; Pantopoulos, K. Regulation of iron transport and the role of transferrin. *Biochim. Biophys. Acta Gen. Subj.* **2012**, *1820*, 188–202. [CrossRef] [PubMed]
5. Chiabrando, D.; Vinchi, F.; Fiorito, V.; Mercurio, S.; Tolosano, E. Heme in pathophysiology: A matter of scavenging, metabolism and trafficking across cell membranes. *Front. Pharmacol.* **2014**, *5*, 61. [CrossRef] [PubMed]
6. Papanikolaou, G.; Pantopoulos, K. Systemic iron homeostasis and erythropoiesis. *IUBMB Life* **2017**, *69*, 399–413. [CrossRef]
7. Vashchenko, G.; MacGillivray, R.T.A. Multi-copper oxidases and human iron metabolism. *Nutrients* **2013**, *5*, 2289–2313. [CrossRef] [PubMed]
8. Camaschella, C.; Pagani, A.; Nai, A.; Silvestri, L. The mutual control of iron and erythropoiesis. *Int. J. Lab. Hematol.* **2016**, *38*, 20–26. [CrossRef]
9. Andrews, N.C. Iron metabolism: Iron deficiency and iron overload. *Annu. Rev. Genom. Hum. Genet.* **2000**, *1*, 75–98. [CrossRef]
10. Miret, S.; Simpson, R.J.; McKie, A.T. Physiology and molecular biology of dietary iron absorption. *Annu. Rev. Nutr.* **2003**, *23*, 283–301. [CrossRef]
11. DeRuisseau, K.C.; Cheuvront, S.N.; Haymes, E.M.; Sharp, R.G. Sweat iron and zinc losses during prolonged exercise. *Int. J. Sport Nutr. Exerc. Metab.* **2002**, *12*, 428–437. [CrossRef]
12. Brune, M.; Magnusson, B.; Persson, H.; Hallberg, L. Iron losses in sweat. *Am. J. Clin. Nutr.* **1986**, *43*, 438–443. [CrossRef] [PubMed]
13. Kosman, D.J. A holistic view of mammalian (vertebrate) cellular iron uptake. *Metallomics* **2020**, *12*, 1323–1334. [CrossRef]
14. Sharma, P.; Reichert, M.; Lu, Y.; Markello, T.C.; Adams, D.R.; Steinbach, P.J.; Fuqua, B.K.; Parisi, X.; Kaler, S.G.; Vulpe, C.D.; et al. Biallelic HEPHL1 variants impair ferroxidase activity and cause an abnormal hair phenotype. *PLoS Genet.* **2019**, *15*, e1008143. [CrossRef]
15. Murphy, C.J.; Oudit, G.Y. Iron-overload cardiomyopathy: Pathophysiology, diagnosis, and treatment. *J. Card. Fail.* **2010**, *16*, 888–900. [CrossRef] [PubMed]
16. Paul, B.T.; Manz, D.H.; Torti, F.M.; Torti, S.V. Mitochondria and Iron: Current questions. *Expert Rev. Hematol.* **2017**, *10*, 65–79. [CrossRef] [PubMed]
17. Chen, S.C.; Olsthoorn, R.C.L. Relevance of the iron-responsive element (IRE) pseudotriloop structure for IRP1/2 binding and validation of IRE-like structures using the yeast three-hybrid system. *Gene* **2019**, *710*, 399–405. [CrossRef]
18. Muckenthaler, M.U.; Galy, B.; Hentze, M.W. Systemic iron homeostasis and the iron-responsive element/iron-regulatory protein (IRE/IRP) regulatory network. *Annu. Rev. Nutr.* **2008**, *28*, 197–213. [CrossRef]
19. Sanchez, M.; Galy, B.; Dandekar, T.; Bengert, P.; Vainshtein, Y.; Stolte, J.; Muckenthaler, M.U.; Hentze, M.W. Iron regulation and the cell cycle: Identification of an iron-responsive element in the 3′-untranslated region of human cell division cycle 14A mRNA by a refined microarray-based screening strategy. *J. Biol. Chem.* **2006**, *281*, 22865–22874. [CrossRef]
20. Cmejla, R.; Petrak, J.; Cmejlova, J. A novel iron responsive element in the 3′UTR of human MRCKα. *Biochem. Biophys. Res. Commun.* **2006**, *341*, 158–166. [CrossRef]
21. Xu, W.; Barrientos, T.; Mao, L.; Rockman, H.A.; Sauve, A.A.; Andrews, N.C. Lethal Cardiomyopathy in Mice Lacking Transferrin Receptor in the Heart. *Cell Rep.* **2015**, *13*, 533–545. [CrossRef]

22. Lakhal-Littleton, S.; Wolna, M.; Chung, Y.J.; Christian, H.C.; Heather, L.C.; Brescia, M.; Ball, V.; Diaz, R.; Santos, A.; Biggs, D.; et al. An essential cell-autonomous role for hepcidin in cardiac iron homeostasis. *eLife* **2016**, *5*, e19804. [CrossRef] [PubMed]

23. Lakhal-Littleton, S.; Wolna, M.; Carr, C.A.; Miller, J.J.J.; Christian, H.C.; Ball, V.; Santos, A.; Diaz, R.; Biggs, D.; Stillion, R.; et al. Cardiac ferroportin regulates cellular iron homeostasis and is important for cardiac function. *Proc. Natl. Acad. Sci. USA* **2015**, *112*, 3164–3169. [CrossRef]

24. Chen, Y.R.; Zweier, J.L. Cardiac mitochondria and reactive oxygen species generation. *Circ. Res.* **2014**, *114*, 524–537. [CrossRef]

25. Gammella, E.; Recalcati, S.; Rybinska, I.; Buratti, P.; Cairo, G. Iron-induced damage in cardiomyopathy: Oxidative-dependent and independent mechanisms. *Oxid. Med. Cell. Longev.* **2015**, *2015*, 230182. [CrossRef] [PubMed]

26. Frazer, D.M.; Anderson, G.J. The regulation of iron transport. *BioFactors* **2014**, *40*, 206–214. [CrossRef] [PubMed]

27. Cabantchik, Z.I. Labile iron in cells and body fluids: Physiology, pathology, and pharmacology. *Front. Pharmacol.* **2014**, *5*, 45. [CrossRef] [PubMed]

28. Rose, R.A.; Sellan, M.; Simpson, J.A.; Izaddoustdar, F.; Cifelli, C.; Panama, B.K.; Davis, M.; Zhao, D.; Markhani, M.; Murphy, G.G.; et al. Iron overload decreases CaV1.3-dependent L-type Ca^{2+} currents leading to bradycardia, altered electrical conduction, and atrial fibrillation. *Circ. Arrhythmia Electrophysiol.* **2011**, *4*, 733–742. [CrossRef]

29. Cheng, C.F.; Lian, W.S. Prooxidant mechanisms in iron overload cardiomyopathy. *BioMed Res. Int.* **2013**, *2013*, 740573. [CrossRef]

30. Walsh, K. Adipokines, myokines and cardiovascular disease. *Circ. J.* **2009**, *73*, 13–18. [CrossRef]

31. Xu, G.; Ahn, J.H.; Chang, S.Y.; Eguchi, M.; Ogier, A.; Han, S.J.; Park, Y.S.; Shim, C.Y.; Jang, Y.S.; Yang, B.; et al. Lipocalin-2 induces cardiomyocyte apoptosis by increasing intracellular iron accumulation. *J. Biol. Chem.* **2012**, *287*, 4808–4817. [CrossRef] [PubMed]

32. Arosio, P.; Levi, S. Cytosolic and mitochondrial ferritins in the regulation of cellular iron homeostasis and oxidative damage. *Biochim. Biophys. Acta Gen. Subj.* **2010**, *1800*, 783–792. [CrossRef] [PubMed]

33. Penna, C.; Mancardi, D.; Raimondo, S.; Geuna, S.; Pagliaro, P. The paradigm of postconditioning to protect the heart: Molecular Medicine. *J. Cell. Mol. Med.* **2008**, *12*, 435–458. [CrossRef] [PubMed]

34. Chevion, M.; Leibowitz, S.; Aye, N.N.; Novogrodsky, O.; Singer, A.; Avizemer, O.; Bulvik, B.; Konijn, A.M.; Berenshtein, E. Heart protection by ischemic preconditioning: A novel pathway initiated by iron and mediated by ferritin. *J. Mol. Cell. Cardiol.* **2008**, *45*, 839–845. [CrossRef] [PubMed]

35. Ferreira, C.; Bucchini, D.; Martin, M.E.; Levi, S.; Arosio, P.; Grandchamp, B.; Beaumont, C. Early embryonic lethality of H ferritin gene deletion in mice. *J. Biol. Chem.* **2000**, *275*, 3021–3024. [CrossRef]

36. Brewer, C.J.; Wood, R.I.; Wood, J.C. mRNA regulation of cardiac iron transporters and ferritin subunits in a mouse model of iron overload. *Exp. Hematol.* **2014**, *42*, 1059–1067. [CrossRef] [PubMed]

37. Nakamura, T.; Naguro, I.; Ichijo, H. Iron homeostasis and iron-regulated ROS in cell death, senescence and human diseases. *Biochim. Biophys. Acta Gen. Subj.* **2019**, *1863*, 1398–1409. [CrossRef]

38. Rauen, U.; Springer, A.; Weisheit, D.; Petrat, F.; Korth, H.G.; De Groot, H.; Sustmann, R. Assessment of chelatable mitochondrial iron by using mitochondrion- selective fluorescent iron indicators with different iron-binding affinities. *ChemBioChem* **2007**, *8*, 341–352. [CrossRef]

39. Petrat, F.; De Groot, H.; Rauen, U. Subcellular distribution of chelatable iron: A laser scanning microscopic study in isolated hepatocytes and liver endothelial cells. *Biochem. J.* **2001**, *356*, 61–69. [CrossRef]

40. Chattipakorn, N. Calcium channels and iron uptake into the heart. *World J. Cardiol.* **2011**, *3*, 215–218. [CrossRef]

41. Sripetchwandee, J.; Sanit, J.; Chattipakorn, N.; Chattipakorn, S.C. Mitochondrial calcium uniporter blocker effectively prevents brain mitochondrial dysfunction caused by iron overload. *Life Sci.* **2013**, *92*, 298–304. [CrossRef] [PubMed]

42. Paradkar, P.N.; Zumbrennen, K.B.; Paw, B.H.; Ward, D.M.; Kaplan, J. Regulation of Mitochondrial Iron Import through Differential Turnover of Mitoferrin 1 and Mitoferrin 2. *Mol. Cell. Biol.* **2009**, *29*, 1007–1016. [CrossRef] [PubMed]

43. Shaw, G.C.; Cope, J.J.; Li, L.; Corson, K.; Hersey, C.; Ackermann, G.E.; Gwynn, B.; Lambert, A.J.; Wingert, R.A.; Traver, D.; et al. Mitoferrin is essential for erythroid iron assimilation. *Nature* **2006**, *440*, 96–100. [CrossRef] [PubMed]

44. Troadec, M.B.; Warner, D.; Wallace, J.; Thomas, K.; Spangrude, G.J.; Phillips, J.; Khalimonchuk, O.; Paw, B.H.; Ward, D.M.V.; Kaplan, J. Targeted deletion of the mouse Mitoferrin1 gene: From anemia to protoporphyria. *Blood* **2011**, *117*, 5494–5502. [CrossRef]

45. Münzel, T.; Gori, T.; Keaney, J.F.; Maack, C.; Daiber, A. Pathophysiological role of oxidative stress in systolic and diastolic heart failure and its therapeutic implications. *Eur. Heart J.* **2015**, *36*, 2555–2564. [CrossRef]

46. Wang, Y.; Chen, Q.; Shi, C.; Jiao, F.; Gong, Z. Mechanism of glycyrrhizin on ferroptosis during acute liver failure by inhibiting oxidative stress. *Mol. Med. Rep.* **2019**, *20*, 4081–4090. [CrossRef]

47. Ratliff, B.B.; Abdulmahdi, W.; Pawar, R.; Wolin, M.S. Oxidant mechanisms in renal injury and disease. *Antioxid. Redox Signal.* **2016**, *25*, 119–146. [CrossRef]

48. Konno, T.; Melo, E.P.; Chambers, J.E.; Avezov, E. Intracellular sources of ROS/H_2O_2 in health and neurodegeneration: Spotlight on endoplasmic reticulum. *Cells* **2021**, *10*, 233. [CrossRef]

49. Hemerková, P.; Vališ, M. Role of oxidative stress in the pathogenesis of amyotrophic lateral sclerosis: Antioxidant metalloenzymes and therapeutic strategies. *Biomolecules* **2021**, *11*, 437. [CrossRef]

50. Koziorowski, D.; Figura, M.; Milanowski, Ł.M.; Szlufik, S.; Alster, P.; Madetko, N.; Friedman, A. Mechanisms of neurodegeneration in various forms of parkinsonism—Similarities and differences. *Cells* **2021**, *10*, 656. [CrossRef]

51. Pennell, D.J.; Udelson, J.E.; Arai, A.E.; Bozkurt, B.; Cohen, A.R.; Galanello, R.; Hoffman, T.M.; Kiernan, M.S.; Lerakis, S.; Piga, A.; et al. Cardiovascular function and treatment in β-thalassemia major: A consensus statement from the american heart association. *Circulation* **2013**, *128*, 281–308. [CrossRef] [PubMed]

52. Allen, K.J.; Gurrin, L.C.; Constantine, C.C.; Osborne, N.J.; Delatycki, M.B.; Nicoll, A.J.; McLaren, C.E.; Bahlo, M.; Nisselle, A.E.; Vulpe, C.D.; et al. Iron-Overload–Related Disease in HFE Hereditary Hemochromatosis. *N. Engl. J. Med.* **2008**, *358*, 221–230. [CrossRef] [PubMed]

53. Olivieri, N. The beta-thalassemias. *N. Engl. J. Med.* **1999**, *341*, 99–109. [CrossRef] [PubMed]

54. Gao, X.; Campian, J.L.; Qian, M.; Sun, X.F.; Eaton, J.W. Mitochondrial DNA damage in iron overload. *J. Biol. Chem.* **2009**, *284*, 4767–4775. [CrossRef]

55. Huang, F.; Yang, R.; Xiao, Z.; Xie, Y.; Lin, X.; Zhu, P.; Zhou, P.; Lu, J.; Zheng, S. Targeting Ferroptosis to Treat Cardiovascular Diseases: A New Continent to Be Explored. *Front. Cell Dev. Biol.* **2021**, *9*, 737971. [CrossRef]

56. Baba, Y.; Higa, J.K.; Shimada, B.K.; Horiuchi, K.M.; Suhara, T.; Kobayashi, M.; Woo, J.D.; Aoyagi, H.; Marh, K.S.; Kitaoka, H.; et al. Protective effects of the mechanistic target of rapamycin against excess iron and ferroptosis in cardiomyocytes. *Am. J. Physiol. Heart Circ. Physiol.* **2018**, *314*, H659–H668. [CrossRef]

57. Luo, L.F.; Guan, P.; Qin, L.Y.; Wang, J.X.; Wang, N.; Ji, E.S. Astragaloside IV inhibits adriamycin-induced cardiac ferroptosis by enhancing Nrf2 signaling. *Mol. Cell. Biochem.* **2021**, *476*, 2603–2611. [CrossRef]

58. Hou, K.; Shen, J.; Yan, J.; Zhai, C.; Zhang, J.; Pan, J.A.; Zhang, Y.; Jiang, Y.; Wang, Y.; Lin, R.Z.; et al. Loss of TRIM21 alleviates cardiotoxicity by suppressing ferroptosis induced by the chemotherapeutic agent doxorubicin. *EBioMedicine* **2021**, *69*, 103456. [CrossRef]

59. Liu, Y.; Zeng, L.; Yang, Y.; Chen, C.; Wang, D.; Wang, H. Acyl-CoA thioesterase 1 prevents cardiomyocytes from Doxorubicin-induced ferroptosis via shaping the lipid composition. *Cell Death Dis.* **2020**, *11*, 756. [CrossRef]

60. Liu, B.; Zhao, C.; Li, H.; Chen, X.; Ding, Y.; Xu, S. Puerarin protects against heart failure induced by pressure overload through mitigation of ferroptosis. *Biochem. Biophys. Res. Commun.* **2018**, *497*, 233–240. [CrossRef]

61. Anand, I.; McMurray, J.J.V.; Whitmore, J.; Warren, M.; Pham, A.; McCamish, M.A.; Burton, P.B.J. Anemia and its relationship to clinical outcome in heart failure. *Circulation* **2004**, *110*, 149–154. [CrossRef] [PubMed]

62. Okonko, D.O.; Anker, S.D. Anemia in chronic heart failure: Pathogenetic mechanisms. *J. Card. Fail.* **2004**, *10*, S5–S9. [CrossRef]

63. Nanas, J.N.; Matsouka, C.; Karageorgopoulos, D.; Leonti, A.; Tsolakis, E.; Drakos, S.G.; Tsagalou, E.P.; Maroulidis, G.D.; Alexopoulos, G.P.; Kanakakis, J.E.; et al. Etiology of Anemia in Patients With Advanced Heart Failure. *J. Am. Coll. Cardiol.* **2006**, *48*, 2485–2489. [CrossRef] [PubMed]

64. Naito, Y.; Tsujino, T.; Fujimori, Y.; Sawada, H.; Akahori, H.; Hirotani, S.; Ohyanagi, M.; Masuyama, T. Impaired expression of duodenal iron transporters in Dahl salt-sensitive heart failure rats. *J. Hypertens.* **2011**, *29*, 741–748. [CrossRef] [PubMed]

65. Lewis, G.D.; Malhotra, R.; Hernandez, A.F.; McNulty, S.E.; Smith, A.; Michael Felker, G.; Wilson Tang, W.H.; LaRue, S.J.; Redfield, M.M.; Semigran, M.J.; et al. Effect of oral iron repletion on exercise capacity in patients with heart failure with reduced ejection fraction and iron deficiency the IRONOUT HF randomized clinical trial. *JAMA J. Am. Med. Assoc.* **2017**, *317*, 1958–1966. [CrossRef] [PubMed]

66. Tamargo, J.; Caballero, R.; Delpón, E. New drugs in preclinical and early stage clinical development in the treatment of heart failure. *Expert Opin. Investig. Drugs* **2019**, *28*, 51–71. [CrossRef]

67. Roetto, A.; Mezzanotte, M.; Pellegrino, R.M. The functional versatility of transferrin receptor 2 and its therapeutic value. *Pharmaceuticals* **2018**, *11*, 115. [CrossRef]

68. Khalil, S.; Holy, M.; Grado, S.; Fleming, R.; Kurita, R.; Nakamura, Y.; Goldfarb, A. A specialized pathway for erythroid iron delivery through lysosomal trafficking of transferrin receptor 2. *Blood Adv.* **2017**, *1*, 1181–1194. [CrossRef]

69. Dong, X.P.; Cheng, X.; Mills, E.; Delling, M.; Wang, F.; Kurz, T.; Xu, H. The type IV mucolipidosis-associated protein TRPML1 is an endolysosomal iron release channel. *Nature* **2008**, *455*, 992–996. [CrossRef]

70. Richardson, D.R.; Lane, D.J.R.; Becker, E.M.; Huang, M.L.H.; Whitnall, M.; Rahmanto, Y.S.; Sheftel, A.D.; Ponka, P. Mitochondrial iron trafficking and the integration of iron metabolism between the mitochondrion and cytosol. *Proc. Natl. Acad. Sci. USA* **2010**, *107*, 10775–10782. [CrossRef]

71. Maio, N.; Rouault, T.A. Iron-sulfur cluster biogenesis in mammalian cells: New insights into the molecular mechanisms of cluster delivery. *Biochim. Biophys. Acta Mol. Cell Res.* **2015**, *1853*, 1493–1512. [CrossRef] [PubMed]

72. Koutnikova, H.; Campuzano, V.; Foury, F.; Dollé, P.; Cazzalini, O.; Koenig, M. Studies of human, mouse and yeast homologues indicate a mitochondrial function for frataxin. *Nat. Genet.* **1997**, *16*, 345–351. [CrossRef] [PubMed]

73. Maliandi, M.V.; Busi, M.V.; Turowski, V.R.; Leaden, L.; Araya, A.; Gomez-Casati, D.F. The mitochondrial protein frataxin is essential for heme biosynthesis in plants. *FEBS J.* **2011**, *278*, 470–481. [CrossRef] [PubMed]

74. Bulteau, A.L.; O'Neill, H.A.; Kennedy, M.C.; Ikeda-Saito, M.; Isaya, G.; Szweda, L.I. Frataxin acts as an iron chaperone protein to modulate mitochondrial aconitase activity. *Science* **2004**, *305*, 242–245. [CrossRef]

75. Gakh, O.; Park, S.; Liu, G.; Macomber, L.; Imlay, J.A.; Ferreira, G.C.; Isaya, G. Mitochondrial iron detoxification is a primary function of frataxin that limits oxidative damage and preserves cell longevity. *Hum. Mol. Genet.* **2006**, *15*, 467–479. [CrossRef]

76. Campuzano, V.; Montermini, L.; Moltò, M.D.; Pianese, L.; Cossée, M.; Cavalcanti, F.; Monros, E.; Rodius, F.; Duclos, F.; Monticelli, A.; et al. Friedreich's ataxia: Autosomal recessive disease caused by an intronic GAA triplet repeat expansion. *Science* **1996**, *271*, 1423–1427. [CrossRef]

77. Abeti, R.; Parkinson, M.H.; Hargreaves, I.P.; Angelova, P.R.; Sandi, C.; Pook, M.A.; Giunti, P.; Abramov, A.Y. Mitochondrial energy imbalance and lipid peroxidation cause cell death in friedreich's ataxia. *Cell Death Dis.* **2016**, *7*, e2237. [CrossRef]

78. Lupoli, F.; Vannocci, T.; Longo, G.; Niccolai, N.; Pastore, A. The role of oxidative stress in Friedreich's ataxia. *FEBS Lett.* **2018**, *592*, 718–727. [CrossRef]

79. Koeppen, A.H.; Ramirez, R.L.; Becker, A.B.; Bjork, S.T.; Levi, S.; Santambrogio, P.; Parsons, P.J.; Kruger, P.C.; Yang, K.X.; Feustel, P.J.; et al. The pathogenesis of cardiomyopathy in Friedreich ataxia. *PLoS ONE* **2015**, *10*, e0116396. [CrossRef]

80. Weidemann, F.; Störk, S.; Liu, D.; Hu, K.; Herrmann, S.; Ertl, G.; Niemann, M. Cardiomyopathy of Friedreich ataxia. *J. Neurochem.* **2013**, *126*, 88–93. [CrossRef]

81. Cossée, M.; Puccio, H.; Gansmuller, A.; Koutnikova, H.; Dierich, A.; LeMeur, M.; Fischbeck, K.; Dollé, P.; Kœnig, M. Inactivation of the Friedreich ataxia mouse gene leads to early embryonic lethality without iron accumulation. *Hum. Mol. Genet.* **2000**, *9*, 1219–1226. [CrossRef]

82. Puccio, H.; Simon, D.; Cossée, M.; Criqui-Filipe, P.; Tiziano, F.; Melki, J.; Hindelang, C.; Matyas, R.; Rustin, P.; Koenig, M. Mouse models for Friedreich ataxia exhibit cardiomyopathy, sensory nerve defect and Fe-S enzyme deficiency followed by intramitochondrial iron deposits. *Nat. Genet.* **2001**, *27*, 181–186. [CrossRef]

83. Protchenko, O.; Baratz, E.; Jadhav, S.; Li, F.; Shakoury-Elizeh, M.; Gavrilova, O.; Ghosh, M.C.; Cox, J.E.; Maschek, J.A.; Tyurin, V.A.; et al. Iron Chaperone Poly rC Binding Protein 1 Protects Mouse Liver From Lipid Peroxidation and Steatosis. *Hepatology* **2021**, *73*, 1176–1193. [CrossRef] [PubMed]

84. Aizawa, S.; Brar, G.; Tsukamoto, H. Cell death and liver disease. *Gut Liver* **2020**, *14*, 20–29. [CrossRef]

85. Yamada, N.; Karasawa, T.; Kimura, H.; Watanabe, S.; Komada, T.; Kamata, R.; Sampilvanjil, A.; Ito, J.; Nakagawa, K.; Kuwata, H.; et al. Ferroptosis driven by radical oxidation of n-6 polyunsaturated fatty acids mediates acetaminophen-induced acute liver failure. *Cell Death Dis.* **2020**, *11*, 144. [CrossRef] [PubMed]

86. Jaeschke, H.; Ramachandran, A.; Chao, X.; Ding, W.X. Emerging and established modes of cell death during acetaminophen-induced liver injury. *Arch. Toxicol.* **2019**, *93*, 3491–3502. [CrossRef]

87. Sun, X.; Niu, X.; Chen, R.; He, W.; Chen, D.; Kang, R.; Tang, D. Metallothionein-1G facilitates sorafenib resistance through inhibition of ferroptosis. *Hepatology* **2016**, *64*, 488–500. [CrossRef] [PubMed]

88. Feng, J.; Lu, P.; Zhu, G.; Hooi, S.C.; Wu, Y.; Huang, X.; Dai, H.; Chen, P.; Li, Z.; Su, W.; et al. ACSL4 is a predictive biomarker of sorafenib sensitivity in hepatocellular carcinoma. *Acta Pharmacol. Sin.* **2021**, *42*, 160–170. [CrossRef] [PubMed]

89. Doll, S.; Proneth, B.; Tyurina, Y.Y.; Panzilius, E.; Kobayashi, S.; Ingold, I.; Irmler, M.; Beckers, J.; Aichler, M.; Walch, A.; et al. ACSL4 dictates ferroptosis sensitivity by shaping cellular lipid composition. *Nat. Chem. Biol.* **2017**, *13*, 91–98. [CrossRef]

90. Wang, H.; An, P.; Xie, E.; Wu, Q.; Fang, X.; Gao, H.; Zhang, Z.; Li, Y.; Wang, X.; Zhang, J.; et al. Characterization of ferroptosis in murine models of hemochromatosis. *Hepatology* **2017**, *66*, 449–465. [CrossRef]

91. Zhou, Z.; Ye, T.J.; DeCaro, E.; Buehler, B.; Stahl, Z.; Bonavita, G.; Daniels, M.; You, M. Intestinal SIRT1 Deficiency Protects Mice from Ethanol-Induced Liver Injury by Mitigating Ferroptosis. *Am. J. Pathol.* **2020**, *190*, 82–92. [CrossRef] [PubMed]

92. Qi, J.; Kim, J.W.; Zhou, Z.; Lim, C.W.; Kim, B. Ferroptosis Affects the Progression of Nonalcoholic Steatohepatitis via the Modulation of Lipid Peroxidation–Mediated Cell Death in Mice. *Am. J. Pathol.* **2020**, *190*, 68–81. [CrossRef]

93. Kowdley, K.V.; Belt, P.; Wilson, L.A.; Yeh, M.M.; Neuschwander-Tetri, B.A.; Chalasani, N.; Sanyal, A.J.; Nelson, J.E. Serum ferritin is an independent predictor of histologic severity and advanced fibrosis in patients with nonalcoholic fatty liver disease. *Hepatology* **2012**, *55*, 77–85. [CrossRef] [PubMed]

94. Gao, G.; Xie, Z.; Li, E.; Yuan, Y.; Fu, Y.; Wang, P.; Zhang, X.; Qiao, Y.; Xu, J.; Hölscher, C.; et al. Dehydroabietic acid improves nonalcoholic fatty liver disease through activating the Keap1/Nrf2-ARE signaling pathway to reduce ferroptosis. *J. Nat. Med.* **2021**, *75*, 540–552. [CrossRef] [PubMed]

95. Yamada, N.; Karasawa, T.; Wakiya, T.; Sadatomo, A.; Ito, H.; Kamata, R.; Watanabe, S.; Komada, T.; Kimura, H.; Sanada, Y.; et al. Iron overload as a risk factor for hepatic ischemia-reperfusion injury in liver transplantation: Potential role of ferroptosis. *Am. J. Transplant.* **2020**, *20*, 1606–1618. [CrossRef] [PubMed]

96. Li, Y.; Feng, D.; Wang, Z.; Zhao, Y.; Sun, R.; Tian, D.; Liu, D.; Zhang, F.; Ning, S.; Yao, J.; et al. Ischemia-induced ACSL4 activation contributes to ferroptosis-mediated tissue injury in intestinal ischemia/reperfusion. *Cell Death Differ.* **2019**, *26*, 2284–2299. [CrossRef]

97. Linkermann, A.; Skouta, R.; Himmerkus, N.; Mulay, S.R.; Dewitz, C.; De Zen, F.; Prokai, A.; Zuchtriegel, G.; Krombach, F.; Welz, P.S.; et al. Synchronized renal tubular cell death involves ferroptosis. *Proc. Natl. Acad. Sci. USA* **2014**, *111*, 16836–16841. [CrossRef]

98. Friedmann Angeli, J.P.; Schneider, M.; Proneth, B.; Tyurina, Y.Y.; Tyurin, V.A.; Hammond, V.J.; Herbach, N.; Aichler, M.; Walch, A.; Eggenhofer, E.; et al. Inactivation of the ferroptosis regulator Gpx4 triggers acute renal failure in mice. *Nat. Cell Biol.* **2014**, *16*, 1180–1191. [CrossRef]

99. Fang, X.; Wang, H.; Han, D.; Xie, E.; Yang, X.; Wei, J.; Gu, S.; Gao, F.; Zhu, N.; Yin, X.; et al. Ferroptosis as a target for protection against cardiomyopathy. *Proc. Natl. Acad. Sci. USA* **2019**, *116*, 2672–2680. [CrossRef]

100. Li, W.; Feng, G.; Gauthier, J.M.; Lokshina, I.; Higashikubo, R.; Evans, S.; Liu, X.; Hassan, A.; Tanaka, S.; Cicka, M.; et al. Ferroptotic cell death and TLR4/Trif signaling initiate neutrophil recruitment after heart transplantation. *J. Clin. Investig.* **2019**, *129*, 2293–2304. [CrossRef]

101. Hangauer, M.J.; Viswanathan, V.S.; Ryan, M.J.; Bole, D.; Eaton, J.K.; Matov, A.; Galeas, J.; Dhruv, H.D.; Berens, M.E.; Schreiber, S.L.; et al. Drug-tolerant persister cancer cells are vulnerable to GPX4 inhibition. *Nature* **2017**, *551*, 247–250. [CrossRef] [PubMed]

102. Dixon, S.J.; Patel, D.; Welsch, M.; Skouta, R.; Lee, E.; Hayano, M.; Thomas, A.G.; Gleason, C.; Tatonetti, N.; Slusher, B.S.; et al. Pharmacological inhibition of cystine-glutamate exchange induces endoplasmic reticulum stress and ferroptosis. *eLife* **2014**, *3*, e02523. [CrossRef] [PubMed]

103. Dixon, S.J.; Lemberg, K.M.; Lamprecht, M.R.; Skouta, R.; Zaitsev, E.M.; Gleason, C.E.; Patel, D.N.; Bauer, A.J.; Cantley, A.M.; Yang, W.S.; et al. Ferroptosis: An iron-dependent form of nonapoptotic cell death. *Cell* **2012**, *149*, 1060–1072. [CrossRef] [PubMed]

104. Forcina, G.C.; Dixon, S.J. GPX4 at the Crossroads of Lipid Homeostasis and Ferroptosis. *Proteomics* **2019**, *19*, e1800311. [CrossRef]

105. Conrad, M.; Friedmann Angeli, J.P. Glutathione peroxidase 4 (Gpx4) and ferroptosis: What's so special about it? *Mol. Cell. Oncol.* **2015**, *2*, 2. [CrossRef]

106. Lewerenz, J.; Hewett, S.J.; Huang, Y.; Lambros, M.; Gout, P.W.; Kalivas, P.W.; Massie, A.; Smolders, I.; Methner, A.; Pergande, M.; et al. The cystine/glutamate antiporter system xc- in health and disease: From molecular mechanisms to novel therapeutic opportunities. *Antioxid. Redox Signal.* **2013**, *18*, 522–555. [CrossRef]

107. Kim, D.H.; Kim, W.D.; Kim, S.K.; Moon, D.H.; Lee, S.J. TGF-β1-mediated repression of SLC7A11 drives vulnerability to GPX4 inhibition in hepatocellular carcinoma cells. *Cell Death Dis.* **2020**, *11*, 406. [CrossRef]

108. Magtanong, L.; Ko, P.J.; To, M.; Cao, J.Y.; Forcina, G.C.; Tarangelo, A.; Ward, C.C.; Cho, K.; Patti, G.J.; Nomura, D.K.; et al. Exogenous Monounsaturated Fatty Acids Promote a Ferroptosis-Resistant Cell State. *Cell Chem. Biol.* **2019**, *26*, 420–432.e9. [CrossRef] [PubMed]

109. Seiler, A.; Schneider, M.; Förster, H.; Roth, S.; Wirth, E.K.; Culmsee, C.; Plesnila, N.; Kremmer, E.; Rådmark, O.; Wurst, W.; et al. Glutathione Peroxidase 4 Senses and Translates Oxidative Stress into 12/15-Lipoxygenase Dependent- and AIF-Mediated Cell Death. *Cell Metab.* **2008**, *8*, 237–248. [CrossRef]

110. Hou, W.; Xie, Y.; Song, X.; Sun, X.; Lotze, M.T.; Zeh, H.J.; Kang, R.; Tang, D. Autophagy promotes ferroptosis by degradation of ferritin. *Autophagy* **2016**, *12*, 1425–1428. [CrossRef]

111. Santana-Codina, N.; Mancias, J.D. The role of NCOA4-mediated ferritinophagy in health and disease. *Pharmaceuticals* **2018**, *11*, 114. [CrossRef]

112. Harrison, P.M.; Arosio, P. The ferritins: Molecular properties, iron storage function and cellular regulation. *Biochim. Biophys. Acta Bioenerg.* **1996**, *1275*, 161–203. [CrossRef]

113. Latunde-Dada, G.O. Ferroptosis: Role of lipid peroxidation, iron and ferritinophagy. *Biochim. Biophys. Acta Gen. Subj.* **2017**, *1861*, 1893–1900. [CrossRef]

114. Mancias, J.D.; Wang, X.; Gygi, S.P.; Harper, J.W.; Kimmelman, A.C. Quantitative proteomics identifies NCOA4 as the cargo receptor mediating ferritinophagy. *Nature* **2014**, *508*, 105–109. [CrossRef] [PubMed]

115. Mancias, J.D.; Vaites, L.P.; Nissim, S.; Biancur, D.E.; Kim, A.J.; Wang, X.; Liu, Y.; Goessling, W.; Kimmelman, A.C.; Harper, J.W. Ferritinophagy via NCOA4 is required for erythropoiesis and is regulated by iron dependent HERC2-mediated proteolysis. *eLife* **2015**, *4*, e10308. [CrossRef] [PubMed]

116. Del Rey, M.Q.; Mancias, J.D. NCOA4-mediated ferritinophagy: A potential link to neurodegeneration. *Front. Neurosci.* **2019**, *13*, 238. [CrossRef] [PubMed]

117. Bellelli, R.; Federico, G.; Matte, A.; Colecchia, D.; Iolascon, A.; Chiariello, M.; Santoro, M.; De Franceschi, L.; Carlomagno, F. NCOA4 Deficiency Impairs Systemic Iron Homeostasis. *Cell Rep.* **2016**, *14*, 411–421. [CrossRef]

118. Gao, M.; Monian, P.; Pan, Q.; Zhang, W.; Xiang, J.; Jiang, X. Ferroptosis is an autophagic cell death process. *Cell Res.* **2016**, *26*, 1021–1032. [CrossRef]

119. Suzuki, T.; Motohashi, H.; Yamamoto, M. Toward clinical application of the Keap1-Nrf2 pathway. *Trends Pharmacol. Sci.* **2013**, *34*, 340–346. [CrossRef]

120. Keleku-Lukwete, N.; Suzuki, M.; Yamamoto, M. An Overview of the Advantages of KEAP1-NRF2 System Activation during Inflammatory Disease Treatment. *Antioxid. Redox Signal.* **2018**, *29*, 1746–1755. [CrossRef]

121. Silva-Islas, C.A.; Maldonado, P.D. Canonical and non-canonical mechanisms of Nrf2 activation. *Pharmacol. Res.* **2018**, *134*, 92–99. [CrossRef]

122. Sun, X.; Ou, Z.; Chen, R.; Niu, X.; Chen, D.; Kang, R.; Tang, D. Activation of the p62-Keap1-NRF2 pathway protects against ferroptosis in hepatocellular carcinoma cells. *Hepatology* **2016**, *63*, 173–184. [CrossRef]

123. Wang, Z.; Ding, Y.; Wang, X.; Lu, S.; Wang, C.; He, C.; Wang, L.; Piao, M.; Chi, G.; Luo, Y.; et al. Pseudolaric acid B triggers ferroptosis in glioma cells via activation of Nox4 and inhibition of xCT. *Cancer Lett.* **2018**, *428*, 21–33. [CrossRef] [PubMed]

124. Brown, C.W.; Amante, J.J.; Chhoy, P.; Elaimy, A.L.; Liu, H.; Zhu, L.J.; Baer, C.E.; Dixon, S.J.; Mercurio, A.M. Prominin2 Drives Ferroptosis Resistance by Stimulating Iron Export. *Dev. Cell* **2019**, *51*, 575–586.e4. [CrossRef] [PubMed]

125. Sasaki, H.; Sato, H.; Kuriyama-Matsumura, K.; Sato, K.; Maebara, K.; Wang, H.; Tamba, M.; Itoh, K.; Yamamoto, M.; Bannai, S. Electrophile response element-mediated induction of the cystine/glutamate exchange transporter gene expression. *J. Biol. Chem.* **2002**, *277*, 44765–44771. [CrossRef]

126. Georgopoulos, C.; Welch, W.J. Role of the major heat shock proteins as molecular chaperones. *Annu. Rev. Cell Biol.* **1993**, *9*, 601–634. [CrossRef] [PubMed]

127. Sun, X.; Ou, Z.; Xie, M.; Kang, R.; Fan, Y.; Niu, X.; Wang, H.; Cao, L.; Tang, D. HSPB1 as a novel regulator of ferroptotic cancer cell death. *Oncogene* **2015**, *34*, 5617–5625. [CrossRef] [PubMed]
128. Wang, D.; Ye, P.; Kong, C.; Chao, Y.; Yu, W.; Jiang, X.; Luo, J.; Gu, Y.; Chen, S.L. Mitoferrin 2 deficiency prevents mitochondrial iron overload-induced endothelial injury and alleviates atherosclerosis. *Exp. Cell Res.* **2021**, *402*. [CrossRef]
129. Vogt, A.C.S.; Arsiwala, T.; Mohsen, M.; Vogel, M.; Manolova, V.; Bachmann, M.F. On iron metabolism and its regulation. *Int. J. Mol. Sci.* **2021**, *22*, 4591. [CrossRef] [PubMed]
130. Pellegrino, R.M.; Boda, E.; Montarolo, F.; Boero, M.; Mezzanotte, M.; Saglio, G.; Buffo, A.; Roetto, A. Transferrin receptor 2 dependent alterations of brain iron metabolism affect anxiety circuits in the mouse. *Sci. Rep.* **2016**, *6*, 30725. [CrossRef] [PubMed]
131. Chen, X.; Kang, R.; Kroemer, G.; Tang, D. Ferroptosis in infection, inflammation, and immunity. *J. Exp. Med.* **2021**, *218*, 218. [CrossRef]
132. Paterek, A.; Kępska, M.; Sochanowicz, B.; Chajduk, E.; Kołodziejczyk, J.; Polkowska-Motrenko, H.; Kruszewski, M.; Leszek, P.; Mackiewicz, U.; Mączewski, M. Beneficial effects of intravenous iron therapy in a rat model of heart failure with preserved systemic iron status but depleted intracellular cardiac stores. *Sci. Rep.* **2018**, *8*, 15758. [CrossRef] [PubMed]
133. Kim, K.M.; Cho, S.S.; Ki, S.H. Emerging roles of ferroptosis in liver pathophysiology. *Arch. Pharm. Res.* **2020**, *43*, 985–996. [CrossRef] [PubMed]
134. Penna, C.; Mancardi, D.; Rastaldo, R.; Pagliaro, P. Cardioprotection: A radical view. Free radicals in pre and postconditioning. *Biochim. Biophys. Acta Bioenerg.* **2009**, *1787*, 781–793. [CrossRef] [PubMed]
135. Hwang, J.W.; Park, J.H.; Park, B.W.; Kim, H.; Kim, J.J.; Sim, W.S.; Mishchenko, N.P.; Fedoreyev, S.A.; Vasileva, E.A.; Ban, K.; et al. Histochrome attenuates myocardial ischemia-reperfusion injury by inhibiting ferroptosis-induced cardiomyocyte death. *Antioxidants* **2021**, *10*, 1624. [CrossRef] [PubMed]
136. Liu, C.Y.; Wang, M.; Yu, H.M.; Han, F.X.; Wu, Q.S.; Cai, X.J.; Kurihara, H.; Chen, Y.X.; Li, Y.F.; He, R.R. Ferroptosis is involved in alcohol-induced cell death in vivo and in vitro. *Biosci. Biotechnol. Biochem.* **2020**, *84*, 1621–1628. [CrossRef]
137. Iorga, A.; Dara, L. Cell death in drug-induced liver injury. In *Advances in Pharmacology*; Elsevier: Amsterdam, The Netherlands, 2019; Volume 85, pp. 31–74, ISBN 9780128167595.
138. Pan, Q.; Luo, Y.; Xia, Q.; He, K. Ferroptosis and liver fibrosis. *Int. J. Med. Sci.* **2021**, *18*, 3361–3366. [CrossRef] [PubMed]
139. Li, J.; Cao, F.; Yin, H.; Huang, Z.; Lin, Z.; Mao, N.; Sun, B.; Wang, G. Ferroptosis: Past, present and future. *Cell Death Dis.* **2020**, *11*, 88. [CrossRef] [PubMed]

1.5 Brain iron regulation

Brain presents several peculiarities that make it a unique organ regarding iron metabolism. Brain iron is involved in a variety of neurological processes: myelination of axons, neuronal cells division and dopaminergic neurotransmitters synthesis in particular synthesis and signaling of dopamine, noradrenaline, adrenaline and serotonin. It acts as a cofactor for proteins such as phenylalanine hydroxylase, tyrosine hy-droxylase, and tryptophan hydroxylase (Hare *et al.,* 2013). Iron is present in different brain cells types and regions: neurons, astrocytes, oligodendrocytes, in the interstitial space, in the soma and in the processes of nerve cells (Rouault, 2013). As in peripheral organs, increased iron levels in the brain work as a potent neurotoxin (Halliwell, 1987); iron produces toxic radicals which cause damage both at cellular and tissue levels (Nandar *et al.*, 2013) that leads to Neurodegenerative Diseases (NDs) (Rouault, 2013). The brain, and in general the Central Nervous System (CNS), is susceptible to free radicals for two mains reasons: i) the brain is not particularly rich in compounds or enzymes with antioxidant activity; ii) it uses high oxygen levels and it contains a high concentration of oxidizable polyunsaturated fatty acids (Yu *et al.*, 2011). Although the high iron concentration inside the brain, its reactivity is low, probably because of the efficient systems for its absorption, transport and storage. Iron enters into the brain crossing the blood-brain barrier (BBB) that it is also the principal protective physical barrier to avoid iron overload (Mills *et al.*, 2010).

Brain iron up-take occurs through Transferrin Receptor 1 (TfR1) that is expressed on the luminal side of brain capillaries. TfR1 binds circulating Tf-Fe$_2$ to promote iron uptake into brain microvascular endothelial cells (BMVECs) through TfR1-mediated endocytosis mechanism (Mills *et al.*, 2010). Iron is released into the cytoplasmic space and exported at the abluminal membrane level by unknown pathways that could involve Fpn1 (Donovan *et al.*, 2000).

Several other genes that regulate iron homeostasis are expressed in the murine CNS, including Iron Regulatory Protein (IRPs) (Leibold *et al.*, 2001), Ferritin (Ft) (MacKenzie *et al.*, 2008) Neogenin (Rodriguez *et al.*, 2007) and Hepcidin (Hepc) (Zechel *et al.*, 2006).

Iron enters into neurons, microglial and choroid plexus' cells bound to TfR1 and it has been shown that Hepc is present in the brain, in mature astrocytes, oligodendrocyte (Vela, 2018) and neurons both in human (Hänninen *et al.*, 2009) and in mouse (Zechel *et al.*, 2006), where it plays a role in iron amount control as well as the other iron regulatory proteins (Ward *et al.*, 2014). It is not clear yet whether Hepc is directly produced by the brain or whether the Hepc that acts on the brain-derived Fpn1 comes from liver (Vela, 2018).

Although the peptide size (Raha-Chowdhury *et al.*, 2015) and its amphipathic cationic chemical structure (Bulet *et al.*, 2004) would allow it to pass BBB, it has been shown that there is an endogenous cerebral Hepc expression and that it is regulated by the organ iron state (Pellegrino *et al.*, 2016). Similar to other Hepc regulatory proteins, Transferrin receptor 2 (TfR2) is expressed in total brain (Kawabata *et al.*, 1999), in specific cerebral compartments, in brain tumour cell lines (Hänninen *et al.*, 2009) or in specific neuronal subtypes (Rouault, 2013). Furthermore, Tf/TfR2-mediated iron transport pathway in the mitochondria of dopaminergic neurons has been studied. This Tf/TfR2 pathway deliver Tf-Fe to mitochondria and to the respiratory complex I. Alteration of this Tf/TfR2-dependent mechanism has been associated with Parkinson's Disease (PD), highlighting the role of iron accumulation in this disorder (Mastroberardino *et al.*, 2009). This hypothesis has been validated in a mouse models of PD with TfR2 deletion specifically in dopaminergic neurons. Authours found that TfR2 deletion carries out a neuroprotective mechanic against dopaminergic degeneration, against PD and aging related iron overload in a gender-dependent manner (Milanese *et al.*, 2021).

1.6 Brain iron accumulation during aging

Brain iron balance should be carefully maintained in order to avoid neurotoxicity. However, several conditions which are typical of aging such as inflammation and BBB damage (Almutairi *et al.*, 2016), cause iron redistribution and unbalance into the brain (Conde and Streit, 2006; Farrall and Wardlaw, 2009).

The physiological process of aging is a suitable model to study iron metabolism alteration found in neurodegenerative diseases (Hou *et al.*, 2019; Wyss-Coray, 2016). Indeed, aged-dependent brain iron accumulation could be due to a change in iron proteins that impair its homeostasis. In this context, various researchers have confirmed that iron levels, Transferrin and Ferritin levels are altered during aging in human astrocytes and in oligodendrocytes (Connor et al., 1990). They found that there is a quite high level of heavy chain (H) ferritin compared to light chain (L) ferritin in younger individuals andferritins heteropolymers increase with age in the frontal cortex, caudate, putamen, substantia nigra and globus pallidus (Connor et al., 1995). The same results were obtained in rats' brains (Roskams and Connor, 1994). Moreover, in the substantia nigra and locus coeruleus it was found that neuromelanin increases during aging acting as an iron chelator compound (Zecca *et al.*, 2002; Zecca *et al.*, 2004a; Zucca *et al.*, 2017). Besides these quite dated papers, few data are available about the

mechanism of age-related iron accumulation. The brain vulnerability to iron increase during aging could explain why iron accumulation is a peculiarity of several neurodegenerative diseases.

2 Aim of the study

The main focus of my thesis was to unravel what are the mechanisms involved in iron handling in *the* Central Nervous System (CNS) in a murine model of Tfr2 germinal silencing and in a Wild-Type (WT) mice during aging. My PhD work has developed into two different but interconnected studies.

In the first study focused on brain iron metabolism, we aimed to clarify TfR2 functions in the brain using TfR2-KO mouse model (Roetto et al., 2010). We demonstrated that TfR2 is produced in a specific brain region, hippocampus, amygdala, hypothalamic paraventricular nucleus, and thalamic paraventricular nucleus, involved in the circuits of anxiety and stress. Our data show that TfR2 silencing causes a blunting of brain Hepc response to the systemic iron increase, with altered iron mobilization and/or cellular distribution in the nervous tissue. Moreover, TfR2-KO mice present a selective over-activation of neurons in the limbic circuit and the emergence of an anxious-like behavior demonstrated by Elevated Plus Maze (EPM) test. The anxious behaviour was partially recovered in TfR2 KO mice treated with an iron-deficient diet (IDD) but it was absent in Wild Type (WT) mice treated with an iron-enriched diet (IED). We concluded that this altered demenor in TfR2 KO mice is due to the increased iron amount caused by the blunting of Hepc response. Accordingly, we deduced that TfR2 is a key regulator of brain iron homeostasis and it is involved in anxiety regulation, an important behavioural feature in many neurodegenerative disorders.

Likewise, in regions more vulnerable to age-dependent neurodegeneration, such as the Cerebral cortex (Ctx) and the Hippocampus (Hip), iron deposits were evidenced during the process of physiological aging, but the underlying mechanism it is not yet known.

The aim of my second study was to investigate brain iron management in WT mice brain during aging.

The obtained results give evidence that there is a progressive neuroinflammatory and oxidative states in the brain of WT mice during aging. These factors are involved in iron misregulation, together with a decrease of BBB integrity. In conditions of brain iron overload and inflammation, we demonstrated

for the first time, that the iron regulatory Hepcidin/Ferroportin1 pathway is activated even in the brain during physiologic aging. Moreover, we revealed that a new protein demonstrated to be involved in intracellular iron management in the liver, Nuclear receptor coactivator 4 (NCOA4), carries out its function in CNS as well. Lastly, we highlighted that iron handling in the brain is cell-specific, at least in the Ctx and Hip. This iron availability imbalance could cause oxidative damage, stress, and neurodegeneration. Altogether our data represent a starting point to clarify the mechanisms of brain iron dyshomeostasis in the elderly and in neurodegenerative disorders, these last representing important health and social problems.

These two studies gave me the opportunity to publish one paper in 2016 and a second one uploaded to bioRxiv that is currently under editor's decision for publication in Scientific Reports journal after revision.

Publication: Transferrin Receptor 2 Dependent Alteration of Brain Iron Metabolism Affect Anxiety Circuits in the Mouse

Publication: Activation of the Hepcidin-Ferroportin1 pathway in the brain and astrocytic-neuronal crosstalk to counteract iron dyshomeostasis during aging

OPEN

Transferrin Receptor 2 Dependent Alterations of Brain Iron Metabolism Affect Anxiety Circuits in the Mouse

Rosa Maria Pellegrino[1,2,*], Enrica Boda[3,4,*], Francesca Montarolo[4], Martina Boero[1,2], Mariarosa Mezzanotte[1,2], Giuseppe Saglio[1,2], Annalisa Buffo[3,4,†] & Antonella Roetto[1,2,†]

The Transferrin Receptor 2 (Tfr2) modulates systemic iron metabolism through the regulation of iron regulator Hepcidin (Hepc) and *Tfr2* inactivation causes systemic iron overload. Based on data demonstrating *Tfr2* expression in brain, we analysed *Tfr2*-KO mice in order to examine the molecular, histological and behavioural consequences of *Tfr2* silencing in this tissue. *Tfr2* abrogation caused an accumulation of iron in specific districts in the nervous tissue that was not accompanied by a brain Hepc response. Moreover, *Tfr2*-KO mice presented a selective overactivation of neurons in the limbic circuit and the emergence of an anxious-like behaviour. Furthermore, microglial cells showed a particular sensitivity to iron perturbation. We conclude that Tfr2 is a key regulator of brain iron homeostasis and propose a role for Tfr2 alpha in the regulation of anxiety circuits.

Body iron amount and availability is finely regulated by Hepcidin (Hepc), a peptide produced mainly by the liver, that acts on the cellular iron exporter Ferroportin 1 (Fpn1), causing its degradation and decreasing *de facto* the amount of serum iron[1]. A complex protein network is involved in hepatic Hepc regulation according to the body iron needs, causing Hepc decrease in iron demand conditions (anaemia, hypoxia, ineffective erythropoiesis) and, on the contrary, a Hepc increase when a sufficient iron amount is present in the body or during inflammatory processes[2]. Dysfunction of most Hepc regulatory proteins is responsible of hereditary disorders of iron metabolism[3,4]. Among these regulators, Transferrin receptor 2 (Tfr2) is codified by a gene whose mutations are responsible for a rare form of hereditary haemochromatosis named HFE3[5,6]. The *TFR2* gene is transcribed in two main isoforms, Tfr2 alpha and Tfr2 beta. Tfr2 alpha is highly produced in the liver and works as an iron sensor that regulates serum Hepc level. Accordingly, *Tfr2* targeted animals show iron overload due to an inappropriately low level of Hepc[7–9]. The Tfr2 beta isoform, instead, appears to play a specific role in the regulation of iron export from reticulo-endothelial cells[9].

In the central nervous system (CNS), iron levels need to be tightly controlled to appropriately regulate key functions such as neurotransmission and myelination as well as neural cell division[10]. Iron overload in defined CNS areas associates with neurodegeneration in Parkinson's and Alzheimer's diseases[11–13], suggesting a role for iron overload in circuit malfunctioning and damage. Furthermore, studies in animal models in which iron amount was experimentally increased show an alteration of the main iron-related proteins Ferritin (Ft) and Transferrin Receptor 1 (Tfr1) in the brain[14–16], revealing perturbation of iron brain homeostasis.

It is generally accepted that iron enters neurons[10], microglial[17,18] and choroid plexi cells[19] bound to Tfr1 and it has been shown that the iron hormone Hepc is expressed in the brain[20–23], similar to other Hepc regulatory proteins[10]. Yet, it is still unclear how iron levels and localization are regulated in cerebral compartments. Similarly, it remains to be fully understood whether the iron protein regulatory network in the CNS is the same operating in the rest of the body and how systemic and cerebral iron regulation are interconnected.

[1]Department of Clinical and Biological Sciences, University of Torino, Turin, Italy. [2]AOU San Luigi Regione Gonzole 10043 Orbassano Turin, Italy. [3]Department of Neuroscience Rita Levi-Montalcini, University of Torino, Turin, Italy. [4]Neuroscience Institute Cavalieri Ottolenghi Regione Gonzole 10043 Orbassano Turin, Italy. *These authors contributed equally to this work. †These authors jointly supervised this work. Correspondence and requests for materials should be addressed to A.R. (email: antonella.roetto@unito.it)

Similar to other Hepc regulatory proteins, *Tfr2* gene expression has been shown in total brain extracts[23], in defined cellular compartments of specific neuronal subtypes[24] and in brain tumor cell lines[23,25]. Furthermore, a transcriptome study on *Tfr2* null mice revealed that several genes involved in the control of neuronal functions are abnormally transcribed[16].

In this study we aimed to clarify *Tfr2* functions in the brain by examining a mouse model in which both *Tfr2* isoforms are inactivated (*Tfr2*-KO)[9]. To distinguish the effects of *Tfr2* abrogation from those due to *Tfr2*-independent iron load modifications, we also examined WT sib pairs subjected to an iron enriched diet (IED) and WT or Tfr2-KO mice upon an iron deficient diet (IDD).

Results show that *Tfr2* silencing determines an increased brain iron availability that associates with anxious-like behaviours.

Materials and Methods

Animals. Ten weeks old *Tfr2*-KO male mice[9] maintained on 129 X 1/svJ strain were analyzed and compared to wild type (WT) sex and age matched sib pairs. Animal housing and all the experimental procedures were performed in accordance with European (Official Journal of the European Union L276 del 20/10/2010, Vol. 53, p. 33–80) and National Legislation (Gazzetta Ufficiale n° 61 del 14/03/2014, p. 2–68) for the protection of animals used for scientific purposes. Groups of 4–5 mice were housed in transparent conventional polycarbonate cages (Tecnoplast, Buggirate, Italy) provided with sawdust bedding, boxes/tunnels hideout as environmental enrichment and striped paper as nesting material. Food and water were provided ad libitum; environmental conditions were 12 h/12 h light/dark cycle, room temperature 21 °C ± 1 °C and room humidity 55% ± 5%. Experimental procedure was preventively approved by the Ethical Committee of the University of Turin.

Experimental conditions. *Tfr2*-KO mice were fed with a standard diet (SD) (GLOBAL DIET 2018, Mucedola SrL, Italy, 0, 2 g iron/Kg food). Age and sex matched animals in SD were used as WT controls. Subgroups of mice were further kept on:

a) iron deficient diet (IDD) to induce anaemia in WT mice and to decrease iron amount in Tfr2-KO mice, by feeding mice with a purified diet without added iron (Mucedola SrL, Italy) starting from weaning until sacrifice (8 weeks of treatment);

b) iron enriched diet (IED) to trigger secondary iron overload in WT animals by feeding them with a 2% iron enriched standard diet from weaning until sacrifice (8 weeks of treatment).

IED was preferred to parenteral iron injection because it resembles iron overload occurring in chronic haemochromatosis. Furthermore, since it has been demonstrated that an iron enriched diet for a short period of time does not cause changes in iron regulating proteins[26], we decided to submit animals to 8 weeks of IED. On the other hand, IDD treatment was chosen to avoid the side-effects of acute iron deprivation obtained by extensive phlebotomies that, by causing inflammation, influence the Hepc pathway[27,28].

At the end of the experiments, mice were given an anaesthetic overdose (see below) and sacrificed. Blood, brain and liver were collected for subsequent analysis.

For behavioural analyses, 8 WT and 9 *Tfr2*-KO naïve mice in SD were tested in the *Morris water maze* and elevated plus maze *(EPM) tests*. Subsequently, 19 WT and 13 *Tfr2*-KO naïve mice in SD, 12 WT and 17 *Tfr2*-KO naïve mice in IDD and 5 WT naïve mice in IED were tested in EPM.

A subset of *Tfr2*-KO and WT mice was transcardially perfused with 0.12 M phosphate buffer (PB) pH 7.2–7.4 (50 ml, 15 min) to remove blood from brain tissue before Western Blot analysis and the measurement of brain iron content (see below). Perfusions were carried out under deep general anaesthesia (ketamine, 100 mg/kg; Ketavet, Bayern, Leverkusen, Germany; xylazine, 5 mg/kg; Rompun; Bayer, Milan, Italy).

Molecular biology analyses. Frozen dissected regions or total brains from WT mice were utilized for quantitative PCR while only total brain of Tfr2-KO and WT animals was used for Western Blot analysis.

Real time quantitative PCR analysis. For reverse transcription, 1 μg of total RNA, 25 μM random hexamers, and 100 U of reverse transcriptase (Applied Biosystems) were used. Gene expression levels were measured by real-time quantitative PCR in a CFX96 Real-Time System (BIO-RAD). For Tfr2 alpha, Tfr2 beta and BDNF, SYBR Green PCR technology (EVAGreen, BIO-RAD, Italy) was used utilising specific primers whose sequences are reported in Supplemental Informations. *Gus* (β-glucuronidase) gene was utilized as housekeeping control[9,29]. The results were analysed using the $\Delta\Delta_{Ct}$ method[30]. All analyses were carried out in triplicate; results showing a discrepancy greater than one cycle threshold in one of the wells were excluded.

Western Blot analysis. WB experiments were done with at least 6 animals for each experimental group. Fifty μg of total brain lysates were separated on an 8–15% SDS polyacrylamide gel and immunoblotted according to standard protocols. Antibodies against the following proteins were used: Transferrin (Tf) (F-8), Tfr1 (CD71 H-300), Divalent Metal Transporter1 (DMT1) (H-108), Fpn1 (G-16) and β-Actin (C-4) (*Santa Cruz Biotechnology*); Tfr2 alpha and Hepc (Alpha Diagnostic International). Antibodies against the two Ferritins (Ft-H and Ft-L) were kindly provided by Sonia Levi, University of Vita Salute, Milan, Italy. Data from WB quantification (Image Lab Software, BIO-RAD, Italy) were normalized on levels of β-Actin bands and expressed as fold increase relative to the mean value obtained from WT mice.

Liver and brain iron content. Iron concentration on livers (Liver Iron Content, LIC) and brains (Brain Iron Content, BIC) freshly dissected was assessed according to standard procedures[9] using at least 20 mg of dried total tissue. For histological assessment of non-heme iron deposition, brain slices of perfused animals were stained with DAB-enhanced Prussian blue Perls' staining[31].

61

Histological and immunofluorescence procedures. For histological analyses experimental animals were perfused with 4% paraformaldehyde in PB. Brains were removed and post-fixed for 24 h at 4 °C, cryoprotected in 30% sucrose in 0.12 M phosphate buffer and processed according to standard protocols[32]. Brains were cut in 30 μm thick coronal sections collected in PBS and then stained to detect the expression of different antigens: Glial fibrillary acidic protein (GFAP) (1:1000, Dakopatts); Iba1 (1:1000, Wako); cFos (1:1000, Santa Cruz Biotechnology); Zif-268 (1:1000, Santa Cruz Biotechnology); vGlut1 (1:1500, Synaptic System); vGlut2 (1:1500, Synaptic System); Tfr2 alpha (1:500, Alpha Diagnostics); hepcidin/pro-hepcidin (1:1000 with amplification with tyramide kit, see below, Alpha Diagnostics). Incubation with primary antibodies was made overnight at 4 °C in PBS with 0.5% Triton-X 100. The sections were then exposed for 2 h at room temperature (RT) to secondary Cy3- (Jackson ImmunoResearch Laboratories, West Grove, PA) and Alexafluor- (Molecular Probes Inc, Eugene Oregon) conjugated antibodies[33]. 4,6-diamidino-2-phenylindole (DAPI, Fluka, Milan, Italy) was used to counterstain cell nuclei. After processing, sections were mounted on microscope slides with Tris-glycerol supplemented with 10% Mowiol (Calbiochem, LaJolla, CA). For colabelling of primary antibodies developed in the same species, the high sensitivity tyramide signal amplification kit (Perkin Elmer, Monza, Italy) was utilized according to the manufacturer's instruction[33]. Myelin Gallyas staining was performed as documented[34].

Image Processing and Data Analysis. Histological specimens were examined using an E-800 Nikon microscope (Nikon, Melville, NY) connected to a colour CCD Camera and a Leica TCS SP5 (Leica Microsystems, Wetzlar, Germany) confocal microscope. Adobe Photoshop 6.0 (Adobe Systems, San Jose, CA) was used to adjust image contrast and assemble the final plates. Quantitative evaluations (densitometry of staining intensities, cell densities) were performed on confocal images followed by Neurolucida- (MicroBrightfield, Colchester, VT) and ImageJ- (Research Service Branch, National Institutes of Health, Bethesda, MD; available at: http://rsb.info.nih.gov/ij/) based analyses. For the analysis of microglia in the cerebral cortex, we routinely scanned the entire cortical grey matter included in slices from Bregma 1.10 mm to Bregma-2.00 mm. Analyses were performed on slices from Bregma-1.50 mm to Bregma-2.00 mm for the dorsal hippocampus; from Bregma-2.50 mm to Bregma-3.00 mm for the ventral hippocampus; from Bregma1.50 mm to Bregma 2.20 mm for the medial prefrontal cortex (mPFC); from Bregma-1.20 mm to Bregma-1.60 mm for the basolateral and central amygdala (BLA and CeA); from Bregma-0.70 mm to Bregma-1.00 mm for the hypothalamic periventricular nucleus (PVN). When the high density of cFos/Zif-268-positive cells impaired the easy recognition of individual nuclei (i.e., in *Cornu Ammonis* 1, CA1 and medial prefrontal Cortex, mPFC), the mean cFos/Zif-268 staining intensity (with background subtraction) over the whole area of the region of interest was evaluated. Measurements derived from at least 3 sections per animal. At least three animals were analysed for each experimental condition.

Behavioural tests. The *Morris water maze*[35] and EPM[36] tests were performed to evaluate learning and anxious-like behaviours, respectively. Data were recorded automatically from the digitized image by using a computerized video tracking software. Details about the procedures can be found in Supplemental Information.

Serum Collection and Analysis. Blood samples were collected, centrifuged, and serum was frozen at −20 °C until analysis. Serum was assayed for corticosterone levels by using commercially available kits (Corticosterone 3H RIA, MP Biomedicals, Italy). All the blood samples were collected at the same time in the morning to minimize the physiological variations.

Statistical analysis. Statistical analyses were carried out by GraphPad Prism (San Diego California, USA) or SPSS software packages (Bangalore, India, www.spss.co.in). In most cases we used Unpaired t-test or one-way ANOVA followed by Bonferroni's post hoc analysis. As regards behavioural data, repeated-measures two-way ANOVA followed by Bonferroni's post hoc analysis was performed to evaluate *Morris water maze* performances during days. Mann-Whitney U test was assessed to evaluate the statistical significance for Accuracy Ratio (AR) and path length in *Morris water maze* test. One-way ANOVA followed by Bonferroni's post hoc analysis was used to evaluate the EPM performances. In all instances, $P < 0.05$ was considered as statistically significant. Data were expressed as averages ± standard error of the mean. Only statistically significant results vs WT and vs *Tfr2*-KO were shown in the figures while all statistically significant P and F values as well as outputs of post hoc analyses were included in Table 1S. Statistically not-significant results were omitted.

Results

Tfr2 alpha expression in anxiety and stress-related circuits.
A transcriptional analysis on WT mice major brain compartments revealed that Tfr2 alpha mRNA is expressed, although less than in the liver, in all analysed areas, and reaches the highest level in the hippocampus (Fig. 1A).

Conversely, real time analysis, performed with primers of similar efficiency, showed a low and homogeneous level of Tfr2 beta mRNA expression in the same brain areas that, also in this case, was lower compared to the liver (Fig. 1A). Based on these data, we concluded that Tfr2 alpha is the main Tfr2 isoform in the brain and consequently we focused on Tfr2 alpha for the next experiments.

Tfr2 alpha protein in total brain extracts showed a trend to decrease in WT IDD mice compared to WT mice, while it did not vary in WT IED animals (Fig. 1B). These data are in line with the role of Tfr2 as an iron sensor contributing to iron homeostasis and with previous data demonstrating that Tfr2 protein is stabilized on plasma membranes by iron loaded Transferrin (Fe-Tf)[37].

Immunofluorescence labelling with an anti-Tfr2 alpha specific antibody showed elongated thin structures occurring either as tightly associated fascicles or isolated fibers (Fig. 1C,G). In grey matter nuclei, a dense punctate staining was occasionally seen (Fig. 1E,F,H). Both patterns are consistent with labelling of neurites or fiber tracts. Interestingly, anti-Tfr2 alpha labelling was prominent in brain circuits controlling anxiety and stress[38,39] including the hippocampus (where Mossy fibers, Mf; were strongly stained, Fig. 1C,D), the amygdala (namely
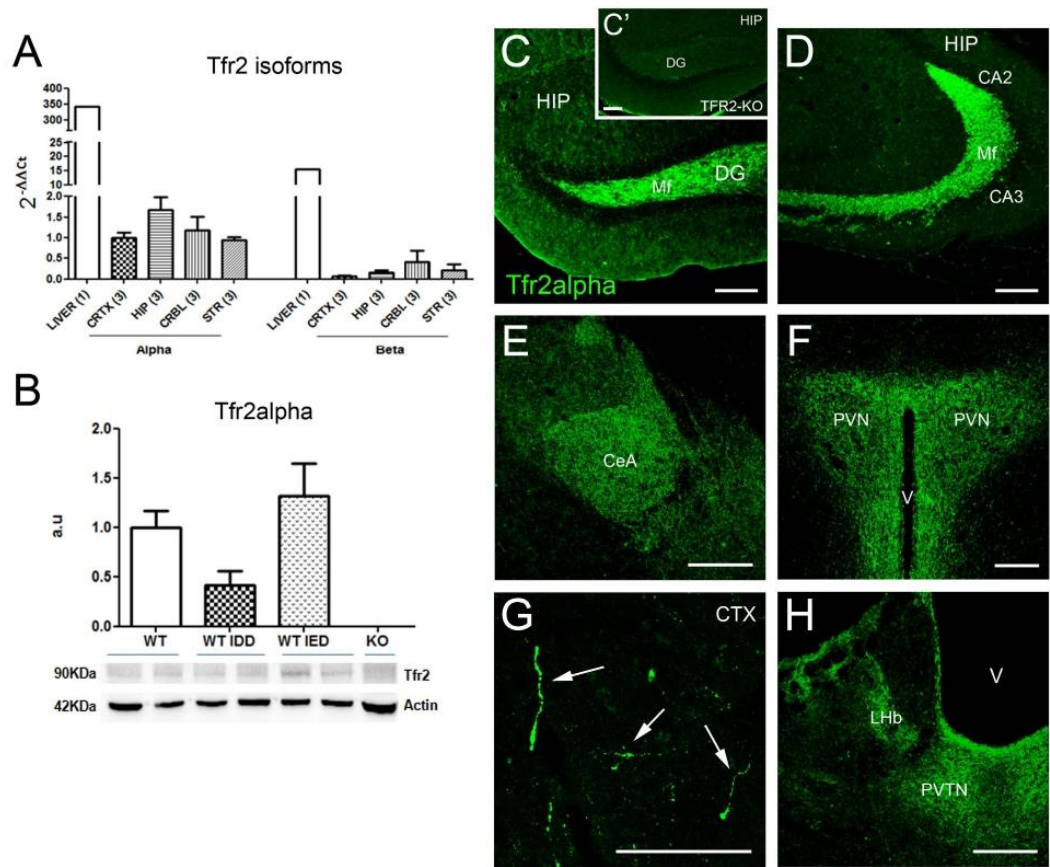
Figure 1. Tfr2 alpha expression in the adult telencephalon. (**A**) Tfr2 alpha and beta isoforms transcription pattern in major brain compartments of WT SD mice. CRTX, cortex; HIP, hippocampus; CRBL, cerebellum; STR, striatum; transcription amount of both Tfr2 isoforms in the liver was used as comparison. Number in parenthesis under each column indicates the number of animals compartments analysed. The expression level of the two Tfr2 isoforms was normalized to levels of GUS housekeeping gene as described in the MM section. In order to perform a double comparison of the same genes in different brain compartments and of the two Tfr2 isoforms in the same compartment we normalized all data on the value of Tfr2 alpha in the cerebral cortex (CRTX). (**B**) Western blot analysis and quantification of brain Tfr2 alpha protein. Results are shown as averages ± standard error of the mean of 3 independent experiments. All the statistically significant results are reported in Table 1S. a.u. arbitrary unit; SD standard diet, IDD iron deficient diet; IED iron enriched diet. (**C–H**) Immunofluorescence localization of Tfr2 alpha in brain. In WT brains Tfr2 alpha positivity is found in fibers of the dentate gyrus of the hippocampus and their terminal region in the CA3/CA2 areas (**D**). A dense dotted staining is also detected in the CeA (**E**), PVN (**F**), LHb (**H**) and PVN (**H**) grey matter nuclei. Sparse axon fibers are labelled for Tfr2 alpha in the cerebral cortex (**G**). Absence of staining in *Tfr2*-KO mice confirms the antibody specificity (C'). Scale bars: 100 μm. DG, dentate gyrus; CA, Cornus Ammonis; CeA, central nucleus of the amygdala; PVN, paraventricular nucleus of hypothalamus; CTX, neocortex (primary M1 motor cortex); LHb, lateral habenula; PVTN, paraventricular nucleus of thalamus; Mf, mossy fibers; V, ventricle.

the central nucleus, CeA; Fig. 1E) and the hypothalamic paraventricular nucleus (PVN; Fig. 1F). Scattered Tfr2 alpha-positive (+) fiber-like structures were also found in the in the cerebral cortex (Fig. 1G) and in thalamic par-aventricular and habenular nuclei (Fig. 1H). Absence of labelling in *Tfr2*-KO mouse brain testified the specificity of anti-Tfr2 alpha staining (Fig. 1C').

Increased iron amount in Tfr2-KO brain. All mice were examined at 10 weeks of age, when tissue alter-ations have been observed in other mouse models of iron loading[40,41]. *Tfr2*-KO showed a significant increase in total brain iron amount compared to WT mice (Table 1). However, this increase was attributable to circulating iron, since brains of Tfr2-KO mice in which blood was removed though tissue perfusion, have a BIC (Brain Iron Content) similar to WT (Table 1). Interestingly, aged-matched WT IED mice, despite being iron overloaded in

63

Genotype Diet	WT SD	WT IDD	WT IED	*Tfr2*-KO SD	*Tfr2*-KO IDD
BIC ($\mu g/g$ *dry tissue*)	237.3 ± 30.8	189.8 ± 17.4°°°	240.2 ± 30.5°	317.8 ± 81.9**	175.7 ± 25.3*·°°°
BIC^ ($\mu g/g$ *dry tissue*)	154.5 ± 18.3	ND	ND	178.1 ± 21.7	ND
LIC ($\mu g/g$ *dry tissue*)	480.2 ± 116.7	246.1 ± 34.5°°°	1099.2 ± 87.2°	1839.3 ± 448.9***	326.2 ± 105.4°°°
hepatic Hepc ($\Delta\Delta Ct$ *mean*)	1 ± 0.152°°	0.003 ± 0.001***	2.78 ± 0.360***·°°°	0.424 ± 0.174**	0.002 ± 0.003***

Table 1. Brain and liver iron amount and hepatic Hepc transcription. WT, wild type; SD, standard diet; IDD, iron deficient diet; IED, iron enriched diet; ND, not determined; ^, perfused brain. * significance vs WT; ° significance vs *Tfr2*-KO. Only statistically significant results vs WT and Tfr2 KO are shown. All the other statistically significant results are reported in Table 1S.

the liver (Table 1) and in the serum (Transferrin saturation: $49,8 \pm 4.45\%$ vs $26 \pm 4.95\%$ $P < 0,05$), did not display evidence of global iron increase in the brain. In both *Tfr2*-KO and WT mice in IDD, BIC decreased below controls levels (Table 1).

To assess possible localised changes in iron levels or distribution, we performed histochemical analysis in PFA perfused brains by DAB-enhanced Prussian blue Perls' staining. *Tfr2*-KO brains sections showed an increased number of brown positive precipitates compared to control mice (Fig. 2) in defined parenchymal regions such as the hippocampal CA1 and CA3 regions (Fig. 2C–F), the PVN (Fig. 2I–J') and the striatal white matter (Fig. 2G,H). We also observed DAB-positive small cells, mostly resembling microglia (insets in 2G and H), that were more frequently detected in *Tfr2*-KO brains (Fig. 2A,B,I–J'). Increased iron was also highlighted by intense staining of both choroid plexi and ependyma in mutant mice (Fig. 2A,B,I,J). These results show that iron accumulates in the nervous tissue when Tfr2 is abrogated.

Brain Hepc levels in iron overloaded Tfr2-KO mice.
Since Tfr2 is a regulator of Hepc production[2] in the liver, we asked whether its deletion also affected Hepc amount in the brain. In agreement with its role of negative regulator of iron availability, in liver and brain of WT mice Hepc production changed according to the different systemic iron amount: it decreased in animals on IDD and increased in animals on IED (Table 1, Fig. 3A). On the contrary, in Tfr2-KO mice, despite increased systemic and circulating iron, cerebral Hepc was significantly lower than in WT mice (Fig. 3A). Furthermore, while liver Hepc transcription significantly decreased in *Tfr2*-KO IDD mice (Table 1) brain Hepc transcription increased in consequence of IDD, reaching WT IDD levels (Fig. 3A) and suggesting a deregulated expression of Hepc in the KO brain. In order to distinguish the contribution of the circulating protein to the Hepc level found in *Tfr2*-KO brain, Hepc quantification was repeated in brains of perfused animals. Despite iron accumulation in KO brains, there is no obvious dysregulation of brain-derived Hepc. These data are consistent with lack of overexpression of Hepc in perfused *Tfr2*-KO brain (Fig. 1S).

To further corroborate these data with an independent approach, we examined anti-Hepc immunostaining on brain slices. Consistently with previous data[42], Hepc positive cells in the cerebral cortex and hippocampus mainly displayed neuronal morphologies (Fig. 3B,C,F,G). In these areas no relevant differences were observed in the Hepc expression pattern or in the densities of positive cells of WT and *Tfr2*-KO mice, although the latter seems to have a slight decrease in overall staining. Conversely, and in line with systemic Hepc regulation[2], WT IED mice had a marked increase in the number of Hepc + cells in the cortex and in the hippocampal dentate gyrus (DG) (Fig. 3E–I). Surprisingly, and on the contrary to what occurs in the liver, where Hepc transcription significantly decreases (Table 1), the pattern and the density of brain Hepc + cells in *Tfr2*-KO IDD mice remains comparable to WT (Fig. 3B–D,F–H), confirming the result of WB analysis.

Brain iron regulatory proteins are altered in Tfr2-KO mice.
Transcriptional analysis of main Hepc regulatory genes, *Hfe* and *Hjv*[2] did not reveal significant variations in the brain of *Tfr2*-KO mice compared to WT animals (not shown). Total brain production of the Hepc target protein Fpn1[43], resulted to be modulated in the different WT experimental groups with an opposite trend compared to cerebral Hepc amount, even if results did not reach statistical significance (Fig. 3L). Inverse relationship between the two proteins in WT animals is further evidenced by a very good fitting in regression analysis, while an apparent opposite trend, despite not statistically different from the WT pattern, could be observed in *Tfr2*-KO mice (Fig. 2S).

To molecularly analyse the increased amount of intracellular iron in the brain parenchyma, we evaluated the three main iron proteins responsible of cellular iron storage (Ft subunits H and L) and transport (Tf). They all resulted modulated. While in *Tfr2*-KO mice brain both Ft-H and Ft-L were higher, in WT IED mice only Ft-L was significantly increased (Fig. 3M,N). Iron transport protein Tf was incremented in IDD mice, as expected on the basis of its capability to supply with iron tissues in which iron amount is decreased[44,45] (Table 1). Surprisingly, also *Tfr2*-KO mice presented an overall higher Tf amount, while this was not true for WT IED mice (Fig. 3O).

Again to verify that these proteins amount was not due to blood presence in non-perfused brains, Fts and Tf were analysed in brain of perfused animals. Blood removal in *Tfr2*-KO brains seems to cause a decrease of the three proteins amount. While an overall increase for Fts was confirmed, Tf displayed levels similar to WT brains, indicating a major role of circulating Tf in measurements in non-perfused brains (Fig. 1S).

As regards the main proteins responsible of cellular iron import, no significant variations were found for Tfr1 levels in all the experimental groups (Fig. 3P). A lower amount of DMT1 protein was instead observed in *Tfr2*-KO brains compared to WT controls (Fig. 3Q). This result supports the hypothesis that the higher iron amount in *Tfr2*-KO mouse brains triggers a decrease in DMT1 protein according to the IRE/IRP pathway[45]. The same
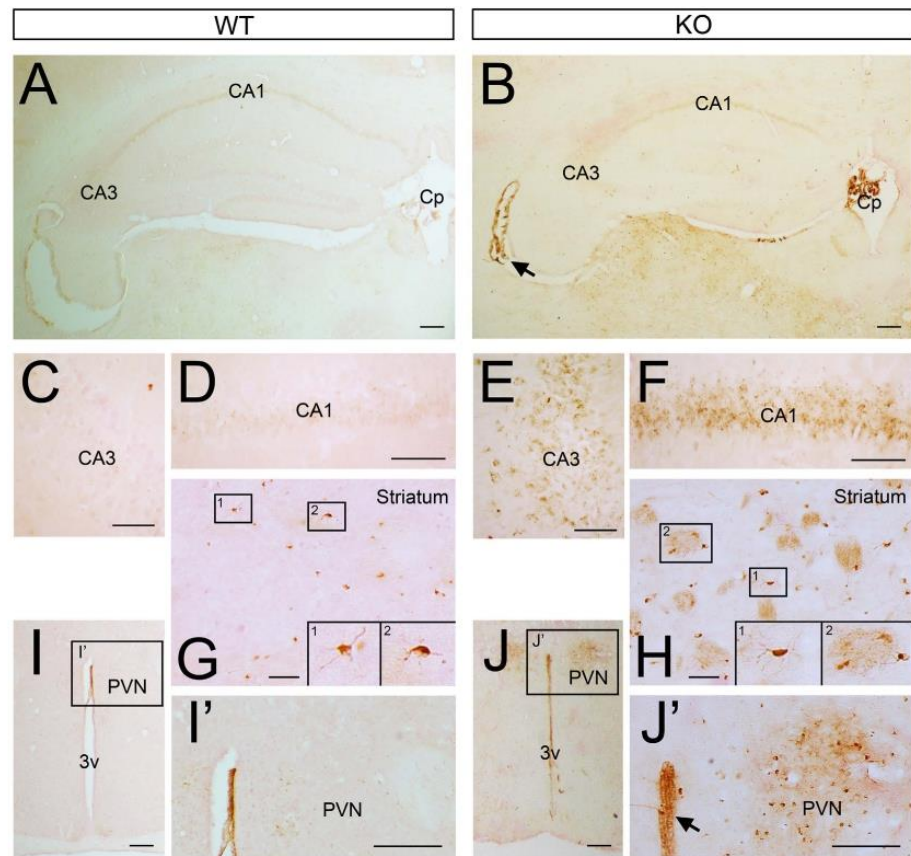
Figure 2. Iron accumulation in *Tfr2*-KO mouse brain. Iron in sections of the brain of WT and *Tfr2*-KO mice (**A,B**) DAB-enhanced Prussian Blue staining revealed iron accumulation in the choroid plexi (Cp) and ependyma (arrows) of *Tfr2*-KO mice (**B,J'**) compared to WT controls (**A,I'**). Higher magnification analysis also showed increased density of brown precipitates in the CA1 and CA3 of the mutant hippocampus (**E,F**), striatum (**H**) and periventricular nucleus (**J,J'**) compared to WT tissues (**C–I'**). (**G,H,I',J'**). Iron labelling also decorates small glial cells that appeared more frequent in *Tfr2*-KO mice. This pattern was confirmed on 3 *Tfr2*-KO and WT mice. Scale bars: (**A,B,I–J'**): 100 um; (**B–G**): 50 um. CA1, Cornus Ammonis 1, CA3, Cornus Ammonis 3, Cp, choroid plexus, PVN, paraventricular nucleus, 3v, third ventricle.

regulatory mechanism accounts for DMT1 increase in WT IDD mice compared to WT, as well as in *Tfr2*-KO IDD animals compared to *Tfr2*-KO (Fig. 3Q).

In conclusion, Tfr2 silencing associates with changes in both CNS iron import and storage proteins, in line with an altered cellular distribution and availability of the metal in the brain of these mice.

Tfr2-KO mice exhibit increased anxiety. Based on high expression of Tfr2 in the hippocampus and limbic circuits, we examined learning abilities and anxiety in the *Tfr2*-KO mice by behavioural tests. In the Morris water maze test no differences were found between WT and *Tfr2*-KO mice in the initial performance (day 1) (Fig. 4A). Furthermore, both WT and *Tfr2*-KO mice were able to improve their performance across days without differences (Fig. 4A). In the probe trial, the mean accuracy ratio (AR) did not show any significant difference between WT and *Tfr2*-KO mice, although *Tfr2*-KO mice spent about 2 fold more time in the target quadrant compared to wild type mice (Fig. 4B). Also in swim velocity and distance there were no differences between WT and *Tfr2*-KO mice (mean velocity $\pm$ SE, WT $= 23.1 \pm 1.4$ cm/s, *Tfr2*-KO $= 26.4 \pm 0.8$ cm/s; mean travelled distance $\pm$ SE, WT $= 1380 \pm 83.9$ cm, Tfr2-KO $= 1582 \pm 48.4$ cm; Mann-Whitney U; P > 0.05). Thus, *Tfr2*-KO mice do not show impairments of hippocampal-related spatial memory tasks. However, the trend for a stronger preference for the probe quadrant in *Tfr2*-KO mice (Fig. 4B) led us to measure the path length after mice reached the target zone. An increased path length outside the target zone, after reaching the original location of the platform, would suggest increased flexibility in an attempt to look for a new location of the platform. On the contrary, longer path length in the target zone would suggest persistency possibly related to increased anxiety[35]. *Tfr2*-KO
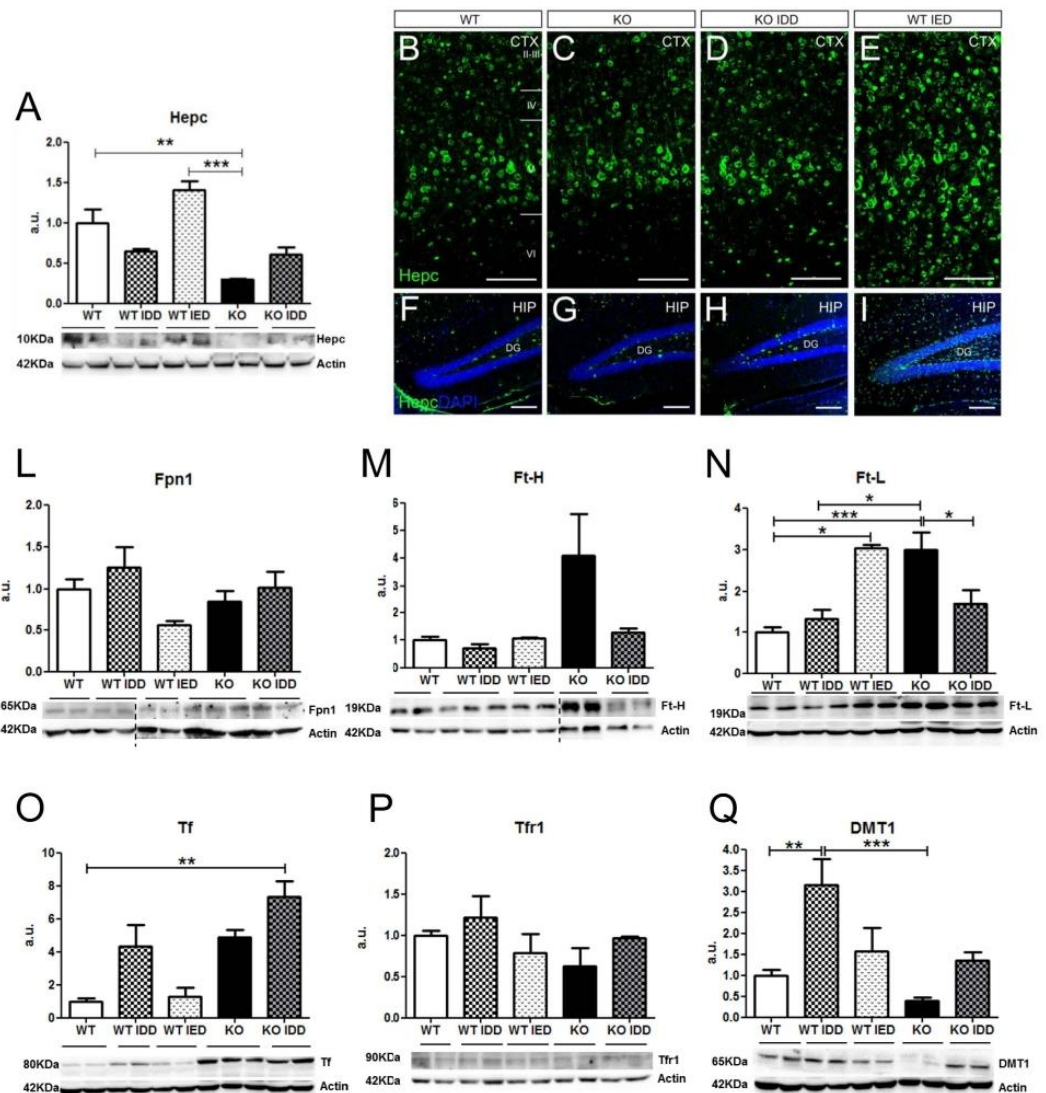
65

Figure 3. Hepcidin production and iron transport/storage proteins quantification in the brain. (A) Western blot analysis and quantification of Hepcidin (Hepc) production changes. (**B–I**) Immunofluorescence with Anti-Hepc antibody in the neocortex. Scale bars: 100 μm. Western blot analysis and quantification of (**L**) Ferroportin (Fpn1) (**M**) Ferritin H (Ft-H) (**N**) Ferritin L (Ft-L) (**O**) Transferrin (Tf) (**P**) Transferrin receptor 1 (Tfr1) (**Q**) DMT1. Results are shown as averages ± standard error of the mean. Symbols refer to a statistically significant difference: *$P < 0.05$, **$P < 0.01$, ***$P < 0.001$. For reasons of clarity, only statistically significant results vs WT and Tfr2 KO are shown in the figure. All the other statistically significant results are reported in Table 1S. Vertical dotted lines indicate images taken from different gels. WT, wild type; KO, *Tfr2*-KO; IDD, iron deficient diet; IED, iron enriched diet; a.u., arbitrary unit; DG, dentate gyrus; HIP, hippocampus; CTX, neocortex (primary M1 motor cortex).

mice displayed a significantly longer path length in the target zone after reaching the original position occupied by the platform compared with their WT sib pairs (Fig. 4C,D).

Furthermore, to avoid confounding effects due to changes in mutants of innate preference for swimming in defined areas of the maze[46], we calculated the distance travelled and the time spent in the centre zone of the pool versus the periphery region on the first trial of the first day, when the spatial location of the platform was completely unknown to the mice. WT and *Tfr2*-KO mice did not show significant differences in the percentages of travelled distances and time spent in the centre of the pool (mean percentage of distance travelled in centre ± SE,
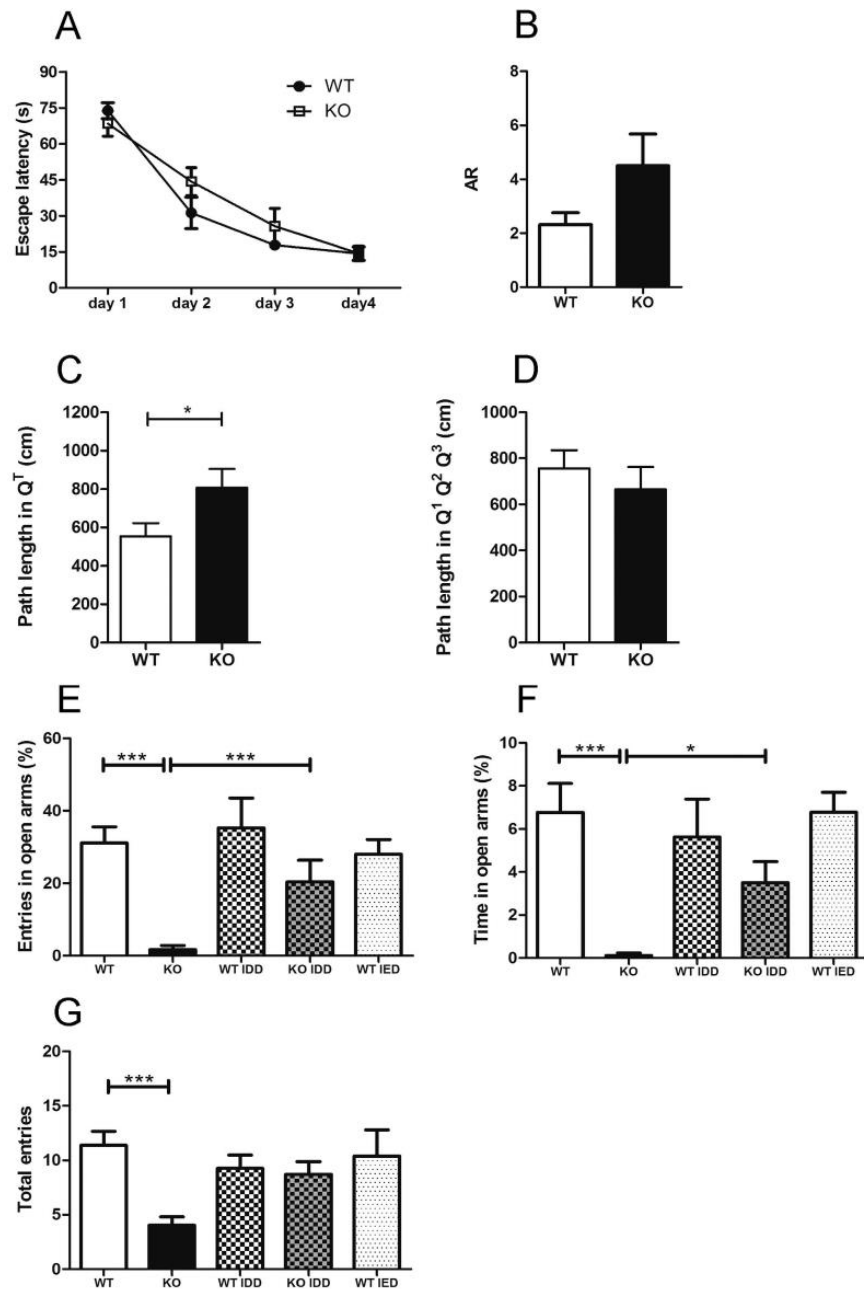
Figure 4. Overt anxiety-like behaviour in Tfr2-KO mice. (A,B) Performance in Morris water maze test. Both WT (n = 8) and Tfr2-KO (n = 9) mice improve their performance across days and during the probe trial without differences between genotypes. **(C,D)** Path length in Morris water maze test. Measures of the total distance (cm) covered by WT mice and Tfr2-KO mice after they reached the target zone in the probe trial. **(C)** Tfr2-KO mice showed longer path length in the target quadrant (Q^t) compared to WT mice. No differences are found in quadrants outside the target zone (Q^1, Q^2, Q^3). **(E–G)** Performance in EPM test. Tfr2-KO (n = 22) mice reveal anxiety levels higher than WT SD mice (n = 27). In IDD, Tfr2-KO mice (n = 17) show a rescue in anxious behaviors and perform similarly to WT mice (n = 12). AR, accuracy ratio; EPM, elevated plus maze; SD, standard diet, IDD; iron deficient diet, IED, iron enriched diet; Q_T target quadrant; error bars, standard error of the mean. Asterisks refer to statistically significant differences: *$P < 0.05$, **$P < 0.01$, ***$P < 0.001$. Statistically significant results are reported in Table 1S.

WT $= 7.1 \pm 3.4$, *Tfr2*-KO $= 7.1 \pm 2.2$; mean percentage of time spent in centre $\pm$ SE, WT $= 5.4 \pm 2.5$ cm, *Tfr2*-KO $= 5.8 \pm 2.0$ Mann-Whitney U; P > 0.05) thus showing that both WT and *Tfr2*-KO mice have the same innate preference for swimming in distinct areas of the maze.

Finally, we further assessed anxiety in the EPM. Notably, *Tfr2*-KO mice showed increased anxiety as expressed by a dramatically low frequency of entries in the open arms of the EPM (Fig. 4E). Consistently, they spent a little time in the open arms of the EPM (Fig. 4F) compared with WT siblings. Also, the total number of entries was reduced in *Tfr2*-KO mice (Fig. 4G). Then, we asked whether such anxious-like behaviour depends on iron levels by examining mice subjected to IDD and IED. Reductions in the frequency and time spent in open arms and in total entries were reverted to control values by IDD in *Tfr2*-KO mice (Fig. 4E,F,G). Notably, neither IDD nor IED affected the anxious behaviour of WT mice (Fig. 4E,F). Altogether, these data show that loss of Tfr2 associated with iron overload promotes the occurrence of anxious behaviours.

Higher levels of activation of the anxiety circuitry in Tfr2-KO mice.

The marked anxious behaviour in *Tfr2*-KO mice suggests that *Tfr2* deletion in combination with iron overload might cause an abnormal activation of the anxiety system. We therefore investigated the expression pattern of cFos and Zif-268, the immediate early genes frequently used as markers for neuronal activity[47], in brain nuclei belonging to the anxiety circuitry, including the hippocampus, the medial prefrontal cortex (mPFC), the basolateral (BLA), and central (CeA) amygdala and the hypothalamic paraventricular nuclei (PVN). Interestingly, in the hippocampus of *Tfr2*-KO mice the two activity markers were highly upregulated in CA3 (Fig. 5A,B,L,P) and CA1 neurons (Fig. 5A,B,F,G,I,J,M,Q), while their expression in the dentate gyrus (DG) did not differ from that of WT mice (Fig. 3SB and not shown). Of note, in *Tfr2*-KO mice fed with IDD anti-cFos and Zif-268 staining decreased to the levels of the WT mice in both CA3 and CA1 subregions (Fig. 5C,H,K,L,M,P,Q). The medial prefrontal cortex (mPFC) is one of the main targets of the hippocampal neurons and contributes to the anxiety control and stress responses by projecting to the BLA and, indirectly, to the PVN[39]. The levels of both cFos and Zif-268 increased significantly in this area of *Tfr2*-KO mice compared to WT or *Tfr2*-KO IDD mice (Fig. 5N,R). Consistently, both transcription factors appeared significantly upregulated in the BLA of the *Tfr2*-KO mice (Fig. 5O,S). Furthermore, anti-cFos/Zif-268 immunostainings did not reveal differences in activity levels of neurons included either in the PVN (Fig. 5D,E) and CeA (or in other areas unrelated to anxiety control) (not shown). In line with the maintenance of WT activation levels in the CeA and PVN, the corticotropin-releasing factor (CRF) immunostaining in the PVN of *Tfr2*-KO mice did not differ from that of WT mice (Fig. 4SA,B), showing that, despite being associated with a pronounced anxious behaviour, *Tfr2* deletion does not alter CRF release into the hypothalamo-hypophyseal portal system[38]. Accordingly, we did not find differences in corticosterone levels in *Tfr2*-KO serum compared to WT (Fig. 4SC). We further tested whether the altered activity pattern of *Tfr2*-KO was associated with changes in levels of BDNF, a key-regulator of synaptic plasticity and hippocampal activity, whose alterations were associated with iron changes and anxiety[48]. However, we did not find changes of BDNF mRNA levels in hippocampus of *Tfr2*-KO mice compared to WT animals (Fig. 4SD). Of note, IED in WT animals also triggered a response that promoted a diffuse and aspecific upregulation of cFos throughout most brain areas (Fig. 3S). Thus, iron alterations due to Tfr2 deficiency positively and specifically modulate neuronal activation in the CA3-CA1-mPFC-BLA circuitry, while they do not alter the neuroendocrine compartment implicated in anxiety regulation.

Given the high levels of expression of Tfr2 alpha in the Mossy fiber pathway, we further hypothesized that the activation of the anxiety circuitry were triggered by altered signals conveyed by Mf to CA3 neurons. Therefore, we investigated possible changes in the density of glutamatergic vGlut1/2+ terminals in CA3. While no difference was observed in the number of VGlut1+ puncta, the density of anti-VGlut2 positivity significantly increased at this site, suggesting incremented excitation and terminal remodelling (Fig. 5T,U,V). Collectively, these data are consistent with a role of Tfr2 alpha in the regulation of both the Mf output and the activity of the anxiety system.

Increased microglia reactivity, dystrophic changes and death in Tfr2-KO mice.

Recent findings indicate that microglia alterations are frequently associated with increased stress and anxiety[49]. Although immunohistological analyses did not reveal alterations of the gross anatomy of the *Tfr2*-KO mouse brain (Fig. 5S), in *Tfr2*-KO we found a decrease in the density of microglial cells identified by labelling for the ionized calcium-binding adaptor molecule 1 (Iba1), (Fig. 6A,B). This decrease occurred throughout the brain and was quantified in *Tfr2*-KO mouse cerebral cortex (Fig. 6A,B,F) and hippocampus (Fig. 6G,H).

Here, the density of both reactive (i.e showing hypertrophy and very little short processes Fig. 6C) or degenerating (i.e. bearing fragmented or dystrophic processes and a pyknotic nucleus; Fig. 6D–E') Iba1+ cells appeared significantly increased compared to WT mice (Fig. 6G,H), suggesting that reactive and degenerative events occur in parallel and that the latter changes dominate, thereby resulting in the reduction of the microglial pool in the *Tfr2*-KO mice.

In order to understand the correlation of the *Tfr2*-KO microglial phenotype with iron overload and/or anxiety, we looked at microglia in *Tfr2-KO* IDD and WT IED mice. Despite recovering a physiological density of Iba1+ cells in the cerebral cortex, (Fig. 6F), KO IDD mice still displayed some microglia activation and degeneration in the examined areas (Fig. 6G,H). Low iron levels in these mice (Table 1) indicated that such microglial alterations might not be due to iron overload *per se*. Yet, the decrease in microglial density could be a factor participating in the behavioural abnormalities found in *Tfr2*-KO mice. However, in WT IED animals microglia are also diminished in the absence of anxiety signs (Fig. 6F). Moreover, microglial reactivity and degeneration occurred in both *Tfr2*-KO IDD (Fig. 5) and WT IED mice (Fig. 6S) in the absence of an anxious phenotype, indicating that these features are also not directly linked to anxiety. Interestingly, we found signs of ongoing inflammation (as monitored by levels of the Serum Amyloid A1 (SAA1) acute phase protein[50]; Fig. 7S) in the brain of WT IED mice but not in those of *Tfr2*-KO animals, suggesting that Tfr2 may be implicated in the regulation of the inflammatory
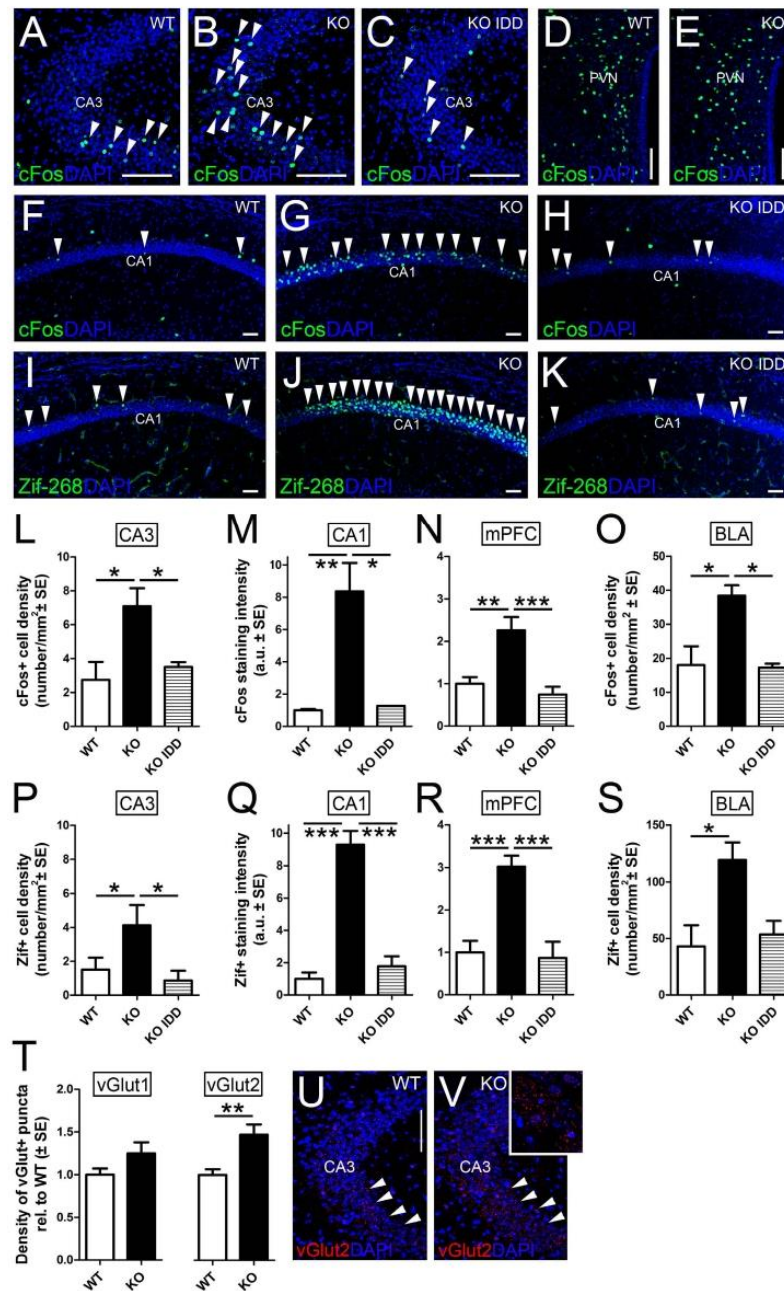
68

Figure 5. Activity-related immediate early genes in anxiety circuits. The immediate early genes cFos (**A–H**) and Zif-268 (**I–K**) are upregulated in neurons of the CA1 (**F,G**) and CA3 (**A,B**) areas of *Tfr2*-KO mice compared to WT brains, while no increase in positive cells occurs in the PVN (**D,E**). Quantifications of the number of positive nuclei over the area of the corresponding layers show that cFos+ or Zif-268+ cells significantly increased in mutant mice in standard conditions while they return to control levels in mutant fed with IDD diet (**H,K,L,M,P,Q**). This very same trend is found in the mPFC and BLA (**N,O,R,S**). (**T–V**) Quantifications of glutamatergic terminals in CA3 (red in (**U,V**)) show that vGlut2+ puncta are higher in number in *Tfr2*-KO mice, while vGlut1+ ones do not differ from WT. Asterisks refer to statistically significant differences: *$P < 0.05$, **$P < 0.01$, ***$P < 0.001$. Scale bars: 100 μm, IDD, iron deficient diet; IED, iron enriched diet; PVN, periventricular hypothalamic nucleus; mPFC, medial prefrontal cortex; BLA, basolateral amygdala; error bars, standard error of the mean. Statistically significant results are reported in Table 1S.
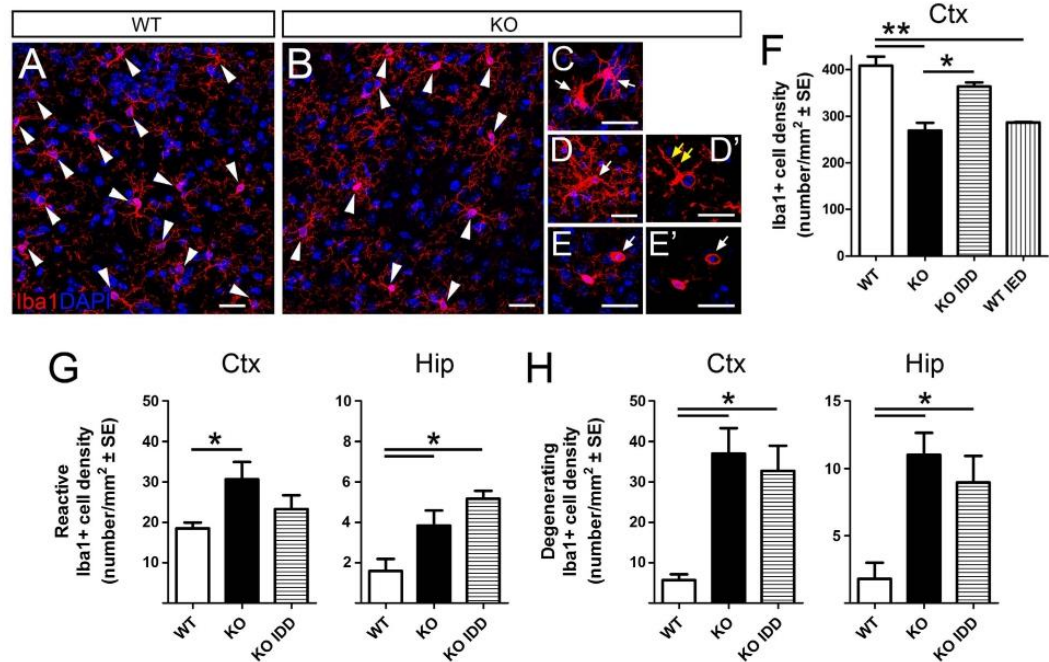
69

Figure 6. Microglial phenotypes in Tfr2-KO and WT mice. Immunofluorescence (**A**–E') and quantification (**F**) of microglial cells using Iba1 marker in total brain. Quantification of reactive (**G**) and degenerating (**H**) cells in cortex (Ctx) and hippocampus (Hip). Arrowheads indicate Iba1+ microglia density (**A,B**). Arrows indicate reactive morphologies (**C**), signs of degeneration (yellow arrows, D') and pyknosis (arrows in (**E**), E'). Asterisks refer to statistically significant differences: *P < 0.05, **P < 0.01. Statistically significant results are reported in Table 1S. CTX, neocortex (primary M1 motor cortex); HIP, hippocampus; IDD, iron deficient diet; IED, iron enriched diet; error bars, standard error of the mean. D', E', single optical slices. Scale bars: 20 μm.

profile of these cells. Thus, microglia appear to strongly respond to alteration of iron metabolism but they do not play a specific role in the behavioural alterations of *Tfr2*-KO.

Discussion

In this work we show that *Tfr2* germinal silencing affects brain iron homeostasis. Furthermore, we reveal that Tfr2 alpha is highly expressed in neurites of brain circuits of anxiety and stress disorders. This pattern, together with the prominent anxious behaviour of *Tfr2*-KO mice, strongly suggests a role for Tfr2 alpha in the regulation of anxiety circuits. Finally, our results further highlight a particular sensitivity of microglia to perturbations of iron metabolism, even when peripheral iron accumulation is moderate and does not associate with behavioural alterations.

Tfr2 alpha is the mainly transcribed isoform of the *TFR2* gene, whose mutations are responsible of a form of hereditary hemochromatosis named HFE3[6]. Hereditary haemochromatosis is a genetically heterogeneous disease due to functional impairment of the iron hormone Hepc and of several Hepc regulating proteins[3].

Tfr2 alpha is a key iron sensor that, in liver, triggers a signal transduction cascade that activates the expression of Hepc, a small protein that reduces iron efflux from cells and leads to its intracellular accumulation[2]. Tfr2 beta isoform is instead known to exert a role in iron efflux in spleen reticuloendothelial cells[9]. So far, several papers reported a Tfr2 alpha expression in the nervous tissue[23–25] that was proposed to be restricted to specific brain regions[23,24]. Our transcriptional and immunohistological analyses validated in *Tfr2*-KO mice, showed relevant Tfr2 alpha expression in the nervous tissue and revealed Tfr2 alpha protein distribution in the neurite compartment of limbic areas implicated in anxiety and stress response. This expression pattern is not fully consistent with those previously reported in human tissues[23], that described Tfr2 expression only in the cerebellum. While this discrepancy may be due to species-specific factors, open access transcriptome data published on GEO Profiles indicate that in both humans and rodents Tfr2 is not exclusively expressed in the cerebellum and is detected in hippocampus, cerebral cortex, basal ganglia and amygdala (Profile: GDS2678/40311_at/, Brain regions of humans and chimpanzees; Profile: GDS1406/160674_at/Tfr2, Brain regions of various inbred strains). Further, a low and ubiquitous Tfr2 alpha expression in mouse neural cells and brain endothelium below the sensitivity of the detection approach applied in this study may occur. Indeed, the diffuse upregulation of Hepc in WT IED brains supports the presence of a more widespread Tfr2 alpha expression.

Based on the key role of Tfr2 in regulating liver iron load, one obvious expectation was to find an increased iron amount in the parenchymal nervous tissue upon Tfr2 deletion. Indeed, in total brain extracts of *Tfr2*-KO including circulating blood, BIC was significantly higher than that of both WT and WT IED, underscoring that in these animals brain parenchyma is exposed to a higher iron amount. Moreover, Perls' staining on brains from *Tfr2*-KO perfused mice revealed that iron accumulates in some of the brain regions where we found relevant Tfr2 expression (hippocampal CA1 and CA3, PVN) as well as in compartments, such as the choroid plexi, which are sites of iron trafficking between systemic circulation and the brain environment[51].

Yet, despite iron deposition, no changes in Hepc protein levels were observed in the nervous tissue, as detected by WB and immunofluorescence. Thus, the strong Hepc reduction in samples containing circulating blood reflects essentially peripheral/systemic Hepc blunting in the absence of Tfr2.

In line with an increased iron amount in *Tfr2*-KO brain, levels of the iron storage protein ferritin globally increase. Ferritin H subunit in particular, is specifically increased in *Tfr2*-KO mice. This induction may reflect the need to counteract the deleterious effects of an enhanced iron-based Fenton reaction, which produces damaging hydroxyl radicals[52]. Tf protein is overexpressed in both WT IDD and *Tfr2*-KO IDD brain, as expected in condition of iron deprivation[44,45]. Unexpectedly Tf displays an increase, although not statistically significant, also in *Tfr2*-KO brains from non-perfused mice, while it is comparable to WT levels in brains from perfused animals. These results are consistent with the additional presence of blood Tf in non-perfused brains.

There is a tendency to decrease for the iron importer DMT1 in *Tfr2*-KO brains, in agreement with a higher iron content, at least in defined cell type(s) of the brain tissue. Moreover, its increase both in *Tfr2*-KO IDD and in WT IDD mice brain is a correct response to iron deprivation based on the activation of the intracellular iron regulatory IRE/IRP response system[45]. Overall these alterations are consistent with a Tfr2 alpha-dependent dysfunctional iron handling in the brain, even though we cannot exclude that over time an exacerbation of the iron burden in WT IED animals could eventually lead to a phenotype overlapping that of *Tfr2*-KO mice.

From the behavioural point of view, iron increase in *Tfr2*-KO mice was accompanied by anxious-like behaviour as assessed by the EPM, where *Tfr2*-KO SD mice spent proportionally less time in the anxiogenic arm compared to other genotypes and conditions. Anxiety-like behaviours were dependent on iron increase, because they were reverted by IDD in *Tfr2*-KO mice. Despite in this study we cannot definitively dissect the contribution of systemic vs. parenchymal iron overload to the anxious phenotype, lack of anxiety signs in WT IED mice that are systemically overloaded but with normal brain iron content - as notably detected without perfusion to wash away the contaminating blood-, suggests that increased parenchymal iron deposits play a prominent role in promoting behavioural alterations. However, the lower systemic iron load in WT IED mice compared to *Tfr2*-KO mice may take part in the absence of the phenotype. In former studies both iron deficiency and iron overload during critical developmental windows or at adult ages have been shown to affect emotional behaviour in rodents[53]. However, the biological mechanisms mediating the effect of iron level alterations at early or mature stages are likely to be distinct. While precocious actions are plausible to rely on abnormal circuit formation, here we find changes of circuit activity, possibly accompanied by some degree of remodelling (see below). In line with our findings, a former study on the effects of experimental brain iron overload (i.p. injections of 3 mg/kg of ferrous sulphate for 5 consecutive days) also reported anxiety in rats, though in association with defects in spatial learning[54]. Moreover, iron-deficiency was also shown to lead to anxiety in mutant mice, likely due to the iron requirement in the synthesis of serotonin and noradrenaline[48]. Since WT IDD mice in this study did not show a brain-specific iron decrease, they are not expected to show behavioural alterations associated with brain iron deficiency. Finally, no data are known about brain iron metabolism in the few HFE3 iron overloaded patients available and no sign of neurological alterations has been evidenced so far. Nevertheless, it must be taken into account that these patients nowadays undergo early diagnosis and efficient phlebotomy until serum iron parameters normalization.

Consistent with behavioural data, in *Tfr2*-KO mice we found a specific and selective overactivation of the limbic circuits controlling anxiety and stress responses, as demonstrated by increased expression of cFos and Zif-268 (Fig. 8S). Surprisingly, also IED in WT mice promoted cFos/Zif-268 upregulation in the brain, but that was far more broad and intense compared to *Tfr2*-KO animals, suggesting that distinct mechanisms account for the induction in the two experimental models. These data provide in-depth explanation to former hints indicating that alterations of iron homeostasis affect expression of neurotransmitters and trophic factors[15,16,26,48,53]. Importantly, in *Tfr2*-KO cFos/Zif-268 upregulation declined in IDD, thereby showing dependence on iron levels. Notably, in *Tfr2*-KO mice all the limbic stations displayed enhanced activity, with the exception of areas belonging to the neuroendocrine stress axis, whose functioning appears unaffected as shown by absence of alterations in PVN CRF and blood corticosterone (Fig. 4S). Moreover, we report an increased V-Glut2 positivity compared to control levels in the CA3 Mf terminal field suggesting that Tfr2 deletion may affect the final output of the Mf pathway by inducing terminal remodeling or promoting immature traits in these fibers, in line with restriction of V-Glut2 during immature developmental stages[55]. Several studies have shown a positive correlation between Mf sprouting and increased anxiety-like behaviour in rodents[56–59], suggesting that the Mf system may contribute to modulation of anxiety-like responses. Thus, collectively data are consistent with a model where Tfr2-dependent alterations in iron homeostasis affect the activity of the main brain areas responsible for the neural control of emotional behaviour, and promote anxiety. Further, high Tfr2 alpha expression along Mf and in nuclei of the limbic circuit suggests a specific role for this isoform in the regulation of the anxiety circuits.

It is interesting to note that activity alterations and behavioural abnormalities in *Tfr2*-KO mice are not due to degenerative events in neurons or astrocytes. We found degeneration only in microglia, that also display increased iron storage in KO mice, as detected by Perls' staining. This suggests that iron-mediated challenge may be compensated in other neural cells. Yet, microglial loss and alterations were also found in WT IED brains that did not show behavioural alterations, ruling out their role in the detected anxious-like traits. Nevertheless, microglial cells were clearly affected in the *Tfr2*-KO mice and displayed reactivity, dystrophic changes and death. These findings are in line with their known action as buffering elements that counteract disturbances in iron regulation[60].

However, in our study, microglial alterations are detected not only in *Tfr2*-KO SD but also in WT IED mice, thereby excluding their specific dependence on Tfr2 abrogation and supporting the hypothesis that either the altered or increased iron processing is responsible for the observed dystrophic modifications and degeneration in microglia.

Taken together, these data add to the growing body of evidence that alterations of systemic iron loading affect brain homeostasis and functioning, and reveal a specific role for *Tfr2*-dependent iron overload in the control of iron regulatory network in the brain tissue as well as in the control of anxious behaviours.

References

1. Ganz, T. Systemic iron homeostasis. *Physiol Rev.* **93**, 1721–1741 (2013).
2. Hentze, M. W., Muckenthaler, M. U., Galy, B. & Camaschella, C. Two to tango: regulation of Mammalian iron metabolism. *Cell.* **142**, 24–38 (2010).
3. Roetto, A. & Camaschella, C. New insights into iron homeostasis through the study of non-HFE hereditary haemochromatosis. *Best Pract Res Clin Haematol.* **18**, 235–250 (2005).
4. Finberg, K. E. Iron-refractory iron deficiency anemia. *Semin Hematol.* **46**, 378–386 (2009).
5. Kawabata, H. *et al.* Molecular cloning of transferrin receptor 2. A new member of the transferrin receptor-like family. *J Biol Chem.* **274**, 20826–20832 (1999).
6. Camaschella, C. *et al.* The gene TFR2 is mutated in a new type of haemochromatosis mapping to 7q22. *Nat Genet.* **25**, 14–15 (2000).
7. Fleming, R. E. *et al.* Targeted mutagenesis of the murine transferrin receptor-2 gene produces hemochromatosis. *Proc Natl Acad Sci USA* **99**, 10653–10658 (2002).
8. Wallace, D. F., Summerville, L., Lusby, P. E. & Subramaniam, V. N. First phenotypic description of transferrin receptor 2 knockout mouse, and the role of hepcidin. *Gut.* **54**, 980–986 (2005).
9. Roetto, A. *et al.* Comparison of 3 Tfr2-deficient murine models suggests distinct functions for Tfr2-alpha and Tfr2-beta isoforms in different tissues. *Blood.* **115**, 3382–3389 (2010).
10. Moos, T., Rosengren Nielsen, T., Skjørringe, T. & Morgan, E. H. Iron trafficking inside the brain. *J Neurochem* **103**, 1730–1740 (2007).
11. Rouault, T. A. Iron metabolism in the CNS: implications for neurodegenerative diseases. *Nat Rev Neurosci.* **14**, 551–564 (2013).
12. Crespo, Â. C. *et al.* Genetic and biochemical markers in patients with Alzheimer's disease support a concerted systemic iron homeostasis dysregulation. *Neurobiol Aging.* **35**, 777–785 (2013).
13. Ayton, S. & Lei, P. Nigral iron elevation is an invariable feature of Parkinson's disease and is a sufficient cause of neurodegeneration. *Biomed Res Int.* **581256** (2014) http://dx.doi.org/10.1155/2014/581256.
14. Yu, S., Feng, Y., Shen, Z. & Li, M. Diet supplementation with iron augments brain oxidative stress status in a rat model of psychological stress. *Nutrition.* **27**, 1048–1052 (2011).
15. Johnstone, D. *et al.* Brain transcriptome perturbations in the Hfe(−/−) mouse model of genetic iron loading. *Brain Res.* 1448–1452 (2012).
16. Acikyol, B. *et al.* Brain transcriptome perturbations in the transferrin receptor 2 mutant mouse support the case for brain changes in iron loading disorders, including effects relating to long-term depression and long-term potentiation. *Neuroscience.* **235**, 119–128 (2013).
17. Kaur, C. & Ling, E. A. Transient expression of transferrin receptors and localisation of iron in amoeboid microglia in postnatal rats. *J Anat.* **186**, 165–173 (1995).
18. Kaur, C. & Ling, E. A. Increased expression of transferrin receptors and iron in amoeboid microglial cells in postnatal rats following an exposure to hypoxia. *Neurosci Lett.* **262**, 183–186 (1999).
19. Aldred, A. R., Dickson, P. W., Marley, P. D. & Schreiber G. Distribution of transferrin synthesis in brain and other tissues in the rat. *J Biol Chem.* **11**, 5293–5297 (1987).
20. Zechel, S., Huber-Wittmer, K. & von Bohlen und Halbach, O. Distribution of the iron-regulating protein hepcidin in the murine central nervous system. *J Neurosci Res.* **84**, 790–800 (2006).
21. Clardy, S. L. *et al.* Is ferroportin-hepcidin signaling altered in restless legs syndrome? *J Neurol Sci.* **247**, 173–179 (2006).
22. Wang, Q. *et al.* Lipopolysaccharide induces a significant increase in expression of iron regulatory hormone hepcidin in the cortex and substantia nigra in rat brain. *Endocrinology.* **149**, 3920–3925 (2008).
23. Hänninen, M. M. *et al.* Expression of iron-related genes in human brain and brain tumors. *BMC Neurosci.* **10**, 36 (2009).
24. Mastroberardino, P. G. *et al.* A novel transferrin/TfR2-mediated mitochondrial iron transport system is disrupted in Parkinson's disease. *Neurobiol Dis.* **34**, 417–431 (2009).
25. Calzolari, A. *et al.* Transferrin receptor 2 is frequently and highly expressed in glioblastomas. *Transl Oncol.* **3**, 123–134 (2010).
26. Johnstone, D. & Milward, E. A. Genome-wide microarray analysis of brain gene expression in mice on a short-term high iron diet. *Neurochem Int.* **56**, 856–863 (2010).
27. Bondi, A. *et al.* Hepatic expression of hemochromatosis genes in two mouse strains after phlebotomy and iron overload. *Haematologica.* **90**, 1161–1167 (2005).
28. Nicolas, G. *et al.* The gene encoding the iron regulatory peptide hepcidin is regulated by anemia, hypoxia, and inflammation. *J Clin Invest.* **110**, 1037–1044 (2002).
29. Boda, E., Pini, A., Hoxha, E., Parolisi, R. & Tempia, F. Selection of reference genes for quantitative real-time RT-PCR studies in mouse brain. *J Mol Neurosci.* **37**, 238–253 (2009).
30. Livak, K. J. & Schmittgen, T. D. Analysis of relative gene expression data using real-time quantitative PCR and the 2(-Delta Delta C(T)) Method. *Methods.* **25**, 402–408 (2001).
31. Meguro, R., Asano, Y., Odagiri, S., Li, C., Iwatsuki, H. & Shoumura, K. Nonheme-iron histochemistry for light and electron microscopy: a historical, theoretical and technical review. *Arch Histol Cytol.* **70**, 1–19 (2007).
32. Buffo, A. *et al.* Expression pattern of the transcription factor Olig2 in response to brain injuries: implications for neuronal repair. *Proc Natl Acad Sci USA* **102**, 18183–18188 (2005).
33. Boda, E. *et al.* The GPR17 receptor in NG2 expressing cells: focus on *in vivo* cell maturation and participation in acute trauma and chronic damage. *Glia.* **59**, 1958–1973 (2011).
34. Pistorio, A. L., Hendry, S. H. & Wang, X. A modified technique for high-resolution staining of myelin. *J Neurosci Methods.* **153**, 135–146 (2006).
35. Vorhees, C. V. & Williams, M. T. Morris water maze: Procedures for assessing spatial and related forms of learning and memory. *Nat Protoc.* **1**, 848–858 (2006).
36. Longo, A. *et al.* Conditional inactivation of neuropeptide Y Y1 receptors unravels the role of Y1 and Y5 receptors coexpressing neurons in anxiety. *Biol Psychiatry.* **76**, 840–849 (2014).
37. Johnson, M. B., Chen, J., Murchison, N., Green, F. A. & Enns, C. A. Transferrin receptor 2: evidence for ligand-induced stabilization and redirection to a recycling pathway. *Mol Biol Cell.* **18**, 743–754 (2007).
38. Ulrich-Lai, Y. M. & Herman, J. P. Neural regulation of endocrine and autonomic stress responses. *Nat Rev Neurosci.* **10**, 397–409 (2009).

72

39. Adhikari, A. Distributed circuits underlying anxiety. *Front Behav Neurosci.* **8,** 112 (2014).
40. Omara, F. O., Blakley, B. R. & Wanjala, L. S. Hepatotoxicity associated with dietary iron overload in mice. *Hum Exp Toxicol.* **12,** 463–467 (1993).
41. Boero, M. *et al.* A comparative study of myocardial molecular phenotypes of two tfr2 null mice: Role in ischemia/reperfusion. *Biofactors.* **41,** 360–371 (2015).
42. Ding, H. *et al.* Hepcidin is involved in iron regulation in the ischemic brain. *PLoS One.* **6,** e25324 (2011).
43. Nemeth, E. *et al.* Hepcidin regulates cellular iron efflux by binding to ferroportin and inducing its internalization. *Science.* **306,** 2090–2093 (2004).
44. Zakin, M. M. Regulation of transferrin gene expression. *FASEB J.* **6,** 3253–3258 (1992).
45. Muckenthaler, M. U., Galy, B. & Hentze, M. W. Systemic iron homeostasis and the iron-responsive element/iron-regulatory protein (IRE/IRP) regulatory network. *Annu Rev Nutr.* **28,** 197–213 (2008).
46. Pritchett, D. *et al.* Searching for cognitive enhancement in the Morris water maze: Better and worse performance in D-amino acid oxidase knockout (Dao-/-) mice. *Eur J Neurosci.*, doi: 10.1111/ejn.13192 (2016).
47. Sheng, M. & Greenberg, M. E. The regulation and function of c-fos and other immediate early genes in the nervous system. *Neuron.* **4,** 477–485 (1990).
48. Texel, S. J. *et al.* Ceruloplasmin deficiency results in an anxiety phenotype involving deficits in hippocampal iron, serotonin, and BDNF. *J Neurochem.* **120,** 125–134 (2012).
49. Kreisel, T. *et al.* Dynamic microglial alterations underlie stress-induced depressive-like behavior and suppressed neurogenesis. *Mol Psychiatry.* **19,** 699–709 (2014).
50. Uhlar, C. M. & Whitehead, A. S. Serum amyloid A, the major vertebrate acute-phase reactant. *Eur J Biochem.* **265,** 501–523 (1999).
51. Rouault, T. A., Zhang, D. L. & Jeong, S. Y. Brain iron homeostasis, the choroid plexus, and localization of iron transport proteins. *Metab Brain Dis.* **24,** 673–684 (2009).
52. Chelikani, P., Fita, I. & Loewen, P. C. Diversity of structures and properties among catalases. *Cell Mol Life Sci.* **6,** 192–208 (2004).
53. Kim, J. & Wessling-Resnick, M. Iron and mechanisms of emotional behavior. *J Nutr Biochem.* **25,** 1101–1107 (2014).
54. Maaroufi, K. *et al.* Impairment of emotional behavior and spatial learning in adult Wistar rats by ferrous sulfate. *Physiol Behav.* **96,** 343–349 (2009)
55. Herzog, E., Takamori, S., Jahn, R., Brose, N. & Wojcik, S. M. Synaptic and vesicular co-localization of the glutamate transporters VGLUT1 and VGLUT2 in the mouse hippocampus. *J Neurochem.* **99,** 1011–1018 (2006).
56. Prior, H., Schwegler, H. & Dücker, G. Dissociation of spatial reference memory, spatial working memory, and hippocampal mossy fiber distribution in two rat strains differing in emotionality. *Behav Brain Res.* **87,** 183–194 (1997).
57. de Oliveira, D. L. *et al.* Effects of early-life LiCl-pilocarpine-induced status epilepticus on memory and anxiety in adult rats are associated with mossy fiber sprouting and elevated CSF S100B protein. *Epilepsia.* **49,** 842–852 (2008).
58. Oztan, O., Aydin, C. & Isgor, C. Chronic variable physical stress during the peripubertal-juvenile period causes differential depressive and anxiogenic effects in the novelty-seeking phenotype: functional implications for hippocampal and amygdalar brain-derived neurotrophic factor and the mossy fibre plasticity. *Neuroscience.* **192,** 334–344 (2011).
59. Aydin, C., Oztan, O. & Isgor, C. Hippocampal Y2 receptor-mediated mossy fiber plasticity is implicated in nicotine abstinence-related social anxiety-like behavior in an outbred rat model of the novelty-seeking phenotype. *Pharmacol Biochem Behav.* **125,** 48–54 (2014).
60. Simmons, D. A., Casale, M., Alcon, B., Pham, N., Narayan, N. & Lynch, G. Ferritin accumulation in dystrophic microglia is an early event in the development of Huntington's disease. *Glia.* **55,** 1074–1084 (2007).

Acknowledgements

Author Contributions

R.M.P. and E.B. performed molecular biology and immunohistochemical experiments, respectively, analysed and discussed data and wrote the manuscript; M.B. and M.M. performed iron dosage experiments and analysis; F.M. performed behavioural experiments and analysed results; G.S. contributed to data interpretation. A.B. and A.R. conceived experiments, interpreted the data and wrote the manuscript. All authors reviewed and approved the final manuscript.

Additional Information

Supplementary information accompanies this paper at http://www.nature.com/srep

Competing financial interests: The authors declare no competing financial interests.

How to cite this article: Pellegrino, R. M. *et al.* Transferrin Receptor 2 Dependent Alterations of Brain Iron Metabolism Affect Anxiety Circuits in the Mouse. *Sci. Rep.* **6,** 30725; doi: 10.1038/srep30725 (2016).

Activation of the Hepcidin-Ferroportin1 pathway in the brain and astrocytic-neuronal crosstalk to counteract iron dyshomeostasis during aging

Mariarosa Mezzanotte[1], Giorgia Ammirata[1,3], Marina Boido[2], Serena Stanga[2,†,*] and Antonella Roetto[1,†,*]

[1]Department of Clinical and Biological Sciences, University of Turin, 10126 Italy
[2]Department of Neuroscience Rita Levi Montalcini, Neuroscience Institute Cavalieri Ottolenghi, University of Turin, 10126 Turin, Italy
[3] Current affiliation: Molecular Biotechnology Center, University of Turin, Turin, Italy
[†]These authors contributed equally to this study

*Correspondence: Serena Stanga serena.stanga@unito.it and Antonella Roetto antonella.roetto@unito.it

ABSTRACT

During physiological aging, iron accumulates in the brain with a preferential distribution in regions that are more vulnerable to age-dependent neurodegeneration such as the cerebral cortex and hippocampus. In the brain of aged wild-type mice, alteration of the Brain Blood Barrier integrity, together with a marked inflammatory and oxidative state lead to increased permeability and deregulation of brain-iron homeostasis. In this context, we found that iron accumulation drives Hepcidin upregulation in the brain and the inhibition of the iron exporter Ferroportin1. We observed a NCOA4-dependent ferritinophagy of ferritin heavy-chain isoform which determines the increase of light-chain enriched ferritin heteropolymers, more efficient as iron chelators. Interestingly, in cerebral cortex and hippocampus, Ferroportin1 is mainly expressed by astrocytes, while the iron storage protein ferritin light-chain by neurons. This differential distribution suggests that astrocytes mediate iron shuttling in the nervous tissue and that neurons are unable to metabolize it. Our findings highlight for the first time that Hepcidin/Ferroportin1 axis and NCOA4 are directly involved in iron metabolism in mice brain during physiological aging as a response to a higher brain iron influx.

Keywords: Aging / Blood Brain Barrier / Hepc / Iron / Neurodegeneration

Introduction

Iron is essential in many cellular and biological processes but it can also generate Reactive Oxidative Species (ROS) by Fenton reaction, contributing to the pathophysiology of many diseases [1]. Iron homeostasis is guaranteed by the action of proteins involved in iron import: Transferrin (Tf), Transferrin Receptors (TfR1), and Divalent Metal Transporter 1 (DMT1); iron export: Ferroportin 1 (Fpn1) [2] and iron storage: cytosolic ferritin (Ft) heteropolymer, composed of 24 subunits of ferritin heavy (Ft-H) and light (Ft-L) chains [3]. However, the regulator of iron content and availability in the body is Hepcidin (Hepc), a peptide mainly produced by hepatocytes, that regulates iron levels by interacting with Fpn1. When body iron increases, Hepc rises as well and this causes Fpn1 degradation and, consequently, iron retention by the cells. So, Hepc lowers the amount of iron in the serum [1], controlling intestinal iron uptake and release from splenic macrophages [4], according to the body's needs. The opposite situation occurs in iron deficiency conditions (i.e. anemia, hypoxia, ineffective erythropoiesis) [4,5].

A new protein involved in iron metabolism is the Nuclear Receptor Coactivator 4 (NCOA4), a cargo protein able to promote selective autophagic ferritin degradation [6]. After NCOA4 binding to Ft-H, ferritin is carried to the lysosome and degraded and iron is released in the cytoplasm, modulating intracellular iron regulation, via "ferritinophagy" [7]. NCOA4 levels are in turn regulated by intracellular iron status [7] and by the interaction with HERC2, an E3 ubiquitin-protein ligase [7,8]. In a NCOA4 knockout mouse model, it has been shown an iron phenotype with increased levels of Tf saturation, serum Ft and liver Hepc and an increase of Ft deposits in the liver and spleen [9]. Recently, an extra-hepatic function of NCOA4 was demonstrated [10]. However, up to now, no data are available on brain NCOA4 and Hepc/Fpn1 expression and function during aging or neurodegeneration.

In the brain, iron regulates important functions such as neurotransmission, myelination and division of neuronal cells [11]. Iron reaches the brain crossing the Blood Brain Barrier (BBB) [12]. Iron up-take is then mediated by TfR1 expressed on the luminal side of brain capillaries [13]. Once inside the cell, iron is released into the cytoplasmic space and exported through the abluminal membrane by unknown mechanisms in which Fpn1 and other transporters may be involved [14].

It has been shown that Hepc is present in the brain, in mature astrocytes and oligodendrocytes [15], where it plays a role in the control of iron amount together with its own iron regulatory proteins [14]. However, it is not yet clear whether the Hepc acting on Fpn1 in the brain is the one produced in the liver or not [15]. Although the peptide size and its amphipathic cationic structure [16] would allow hepatic Hepc to pass the BBB, it has been shown that there is an endogenous cerebral Hepc expression [17] and that it responds to brain iron state [18].

Several conditions which are typical of aging such as inflammation, BBB damage due to the release of inflammatory mediators, free radicals and vascular endothelial growth factor [19] cause iron redistribution and unbalance in the brain [20].

With age, iron accumulates in the cerebral cortex (Ctx) and in the hippocampus (Hip), regions which are involved in neurodegenerative disorders [12], but the underlying mechanism it is not yet known. Here we demonstrated that NCOA4, Hepc and Fpn1 are activated in WT mice brain during physiological aging as a consequence of iron accumulation and that they participate to brain response to increased iron entry. Furthermore, we assessed the astrocytic-neuronal crosstalk and we found that the iron exporter Fpn1 co-localizes with astrocytes, while neurons are enriched in the iron deposit Ft-L heteropolymers, both in the Ctx and Hip. These data suggest that, while glial cells enhance iron export in the nervous tissue, neurons accumulate it, triggering neurodegenerative processes.

2

Results

Iron amount and distribution in the brain during aging correlates to the level of BBB permeability. Brain Iron Content (BIC) increases during aging at each experimental time point (Fig. 1**A**) in different brain areas as shown by histochemical analysis with DAB-enhanced Prussian blue Perls' staining (Fig. 1**B**). WT O mice show an increased number of brown precipitates compared to WT A mice in specific parenchymal region such as Ctx, Hip CA regions, third ventricle (3V) and striatum. Similarly, we also observed an age-dependent increase in the levels of iron in liver and in serum of old mice indicating a general perturbation of iron metabolism with physiological aging (Suppl. Fig. 1S). Since progressive BBB damage is occurring not only in neurodegeneration [21] but also during aging, we analysed ZO-1 protein, whose role is to maintain the compactness of BBB acting as a bridge connecting Claudin and Occludin proteins to the actin cytoskeleton in order to stabilize the tight junction (TJ) structure [22]. ZO-1 levels significantly decrease during aging (Fig. 1**C**), therefore, we can hypothesize that age-dependent BBB altered permeability, could contribute, together with age-dependent metal dyshomeostasis, to iron accumulation in specific areas of the brain during physiological aging.

Increased inflammatory and oxidative stress state during brain aging. The two main markers of neuroinflammation and oxidative stress, SAA1 [23] and Nrf2 [24], are overexpressed in aged brains. SAA1 expression levels is more than 20 times higher in WT O animals compared to WT A (Fig. 2**A**) and Nrf2 expression levels are constantly increasing during aging (Fig. 2**B**).

Moreover, we performed immunohistochemistry to selectively label reactive intermediate filament protein (GFAP)-positive astrocytes. In fact, GFAP is an indicator of neuroinflammation in the CNS [25] and it is also involved in the progression of neurodegeneration in ischemia, AD, MS, Amyotrophic Lateral Sclerosis (ALS) and PD [26-28]. In addition, we also checked the expression of IBA-1, a microglia/macrophage-specific calcium-binding protein which is also a key molecule in proinflammatory processes [29]. We identified high astrocytes activation and an increased expression of microglia in both parenchymal regions of WT O mice where iron accumulated, Ctx and Hip, compared to those of WT A (Fig. 2**C** and **D**).

These data show that iron accumulation in the brain is accompanied by the neuroinflammatory and antioxidative stress response.

Hepc/Fpn1 activation and ferritins response to iron accumulation during brain aging via ferritinophagy. In order to evaluate if the Hepc/Fpn1 axis has a role during brain physiologic aging, we measured both Hepc and Fpn1 in the whole brain of aged mice. Interestingly, we observed that Hepc gene expression significantly increases in WT M-A and WT O mice brain (Fig. 3**A**), while Fpn1 protein decreases (Fig. 3**B**). To investigate how neuronal cells responded to the increase of iron amount, we analysed in the total brain also the iron deposit protein ferritins (Ft) and separately evaluating the two polymers: ferritin light-chains (Ft-L) and ferritin heavy-chains (Ft-H). As expected, we observed a significant increase in Ft-L amount (Fig. 3**C**), but a 40% reduction of Ft-H in WT O animals' brains compared to the WT A (Fig. 3**D**). To verify if these differences could be caused by the action of the ferritinophagy inductor NCOA4, we checked for its levels of transcription and translation in the brain. NCOA4 gene results to be highly transcribed in the brain and its expression is comparable to that of the liver (Ct values 25±1 and 24±1.5 respectively) (Fig. 3**E** and [9]).

3

76

Furthermore, NCOA4 protein amount is also significantly increased in WT O mice brain compared to WT A (Fig. 3**F**).

Altogether, these results demonstrate that in old mice brain iron accumulation together with the inflammatory condition (Fig. 2**A-C** and **D**) induces Hepcidin expression and, consequently, Fpn1 degradation; therefore, activation of the Hepc/Fpn1 pathway in the brain promotes cellular iron retention. Furthermore, our results show for the first time that NCOA4 is transcribed in the brain during aging in response to iron accumulation and suggest that NCOA4 can promote the formation of Ft-L heteropolymers, more suitable to iron storage, acting specifically on Ft-H degradation.

Cellular distribution of iron deposits and export proteins in Ctx and Hip. Due to the presence of important deposits of iron in the Ctx and Hip (Fig. 1**B**), we decided to analyse Fpn1 expression in that specific brain compartments. Even tough, we observed a decrease of global Fpn1 levels after Hepc induction in the total homogenates, immunofluorescence experiments revealed a localized increase of the protein specifically in WT M-A and WT O mice Ctx and Hip compared to the same WT A mice areas (Fig. 4**A**). We hypothesized that the Fpn1 reversal distribution could be due to a differential expression and activity of Hepc/Fpn1 at the cellular level. Therefore, we co-labelled Fpn1 with a specific astrocytic and neuronal marker, GLAST and VGLUT1, respectively. We found that Fpn1 increases with aging and co-localizes with astrocytes in the Ctx and Hip, while it remains constant in neurons compared to WT A mice areas (Fig. 4**B**).

Additionally, to discriminate if the accumulation of iron occurred specifically inside neurons and/or astrocytes, we co-stained Ft-L and Ft-H with MAP-2 and GFAP, respectively. Compared to WT A, in WT O mice brains we observed a specific and marked increase of Ft-L deposits in cortical and hippocampal neurons but not in astrocytes (Fig. 4**C**). Ft-H isoform was also identified in the soma of cortical and hippocampal neurons (Fig. 4**D**), and resulted to be less abundant than Ft-L isoform in these cells. These results demonstrate that there is an "iron cross-talk" between astrocytes and neurons but they are participating differently in the process of iron distribution and metabolism/accumulation.

Discussion

During aging and in neurodegenerative diseases with old age onset such as PD and AD, an increase in iron content was observed in multiple brain regions [30,31]. In pathological conditions, it was demonstrated to be the cause of motor deterioration [12] and of proteins aggregation [32] leading to cellular stress [33]. Parallel to deposition of iron in the brain, in the periphery, systemic iron levels decrease and old subjects are subjected to anemia [34].

Systemic iron regulation is based on a complex protein regulatory system in which the hepatic Hepcidin (Hepc) plays a major role. Indeed, the iron dependent modulation of Hepc expression determines *de facto* iron availability in the body [35]. In the brain, iron homeostasis is regulated by the same proteins network that acts at the systemic level [30] and the Hepc regulatory system is active also in the CNS [31]. Indeed, Hepc is expressed by glial cells and neurons from different brain regions and, under brain iron accumulation, it is activated and it induces Fpn1 decrease [36,37]. However, it is not clear yet whether this rely on brain or hepatic Hepc [15]. Moreover, it is not known how this regulatory system respond to intracerebral iron increase during aging. Intrigued by this question, we studied the brain expression of proteins involved in systemic iron homeostasis in wild type (WT) mice during aging.

We characterized the state of the brain at different ages by studying BBB integrity, brain inflammation and oxidative state, all key features related to the process of aging and that influence

4

iron homeostasis (Figures 1 and 2). It is known that BBB mitigates iron entry from the blood to the brain through highly regulated and selective systems: iron crosses the BBB bound to Tf through TfR-mediated endocytosis [38] and brain vascular endothelial cells (BVECs) export intracellular iron using Fpn1, whose activity is conditioned by the iron ferroxidases ceruloplasmin and hephaestin [31]. Finally, iron is acquired by nervous cells through iron transporter proteins, as DMT1, and released from these cells through Fpn1 [31].

It is also known that iron accumulation in the brain, triggers the release of pro-inflammatory cytokines, determining an environment prone to neurodegeneration [39].

Indeed, we demonstrated the progressive accumulation of iron during physiological aging in the Ctx, Hip, third ventricle and striatum and the parallel decrease of the BBB integrity. As a consequence of iron accumulation, the transcription of SAA-1, a protein related to acute inflammation and marker of neuroinflammation, [40,41] described also in AD as able to stimulate the release of cytokines and chemokines [23,41], increases up to 1000 times in old mice brain. Moreover, the transcription of Nrf2, a redox-sensitive transcription factor [24], is also increased, supporting the evidence of a stressful condition in WT O mice brain.

During aging, a consistent activation of astrocytes and a generalized neuroinflammation are evident [42]. In line with these findings, in both Ctx and Hip of WT O mice we observed high astrocytic and microglial activation.

Interestingly, in this context of increased iron deposition and inflammation in the brain, we found the activation of the Hepc/Fpn1 pathway: brain Hepc transcription increases and brain Fpn1 amount gradually decreases during aging. These observations are in line with what Sato and colleagues observed in the cerebral cortex and in mitochondria isolated from the brain of aged mice [43]. To better decipher the mechanism of the regulation of iron content in neuronal tissue during physiological aging, we also analyzed the iron deposit protein Ft and a newly characterized protein, NCOA4 since it is involved in Ft degradation and its inactivation in mice causes iron accumulation in the liver [9]. Specifically, NCOA4 promotes autophagic ferritin degradation through its binding to Ft-H subunit [7,44]. Ferritin levels are enhanced in a cellular model (HeLa cells) in which NCOA4 is silenced, suggesting that ferritin is constantly degraded by an NCOA4-dependent pathway [45]. Surprisingly, in old mice's brains we found an increased amount of NCOA4, contrary to what happens in the liver [9]. Furthermore, specifically evaluating the ferritin polymers, we observed an increase of Ft-L and a decrease of Ft-H chains in the aged mice brains. These data demonstrated that a differential Ft chains degradation occurs in both cortical and hippocampal neurons of old animals. We can suppose that Ft-L enriched heteropolymers are more efficient in iron chelation [3] and are also more abundant in cortical and hippocampal neurons since Ft-H is selectively degraded by NCOA4.

Interestingly, when we analysed by immunofluorescence the specific areas in which there is the highest iron amount, Ctx and Hip, we found that Fpn1 is increased in old mice contrary to what happens in the total brain homogenates. This could be due to i) a differential and local regulation of brain iron, ii) a dilution of Ctx and Hip region in the total brain homogenate or iii) a misregulation of Hepc and/or Fpn1 transcription and translation due to abnormal iron amount in the cells of these regions. Indeed, we showed that Fpn1 amount in old mice brain is cell specific.

Since it increases in cortical and hippocampal astrocytes and remains unchanged in neurons, all this regardless of the relevant Hepc increase (30x) in total brain. This could be due to: i) a different detoxifying mechanism carried out by neurons and astrocytes, aimed to store or remove iron excess, respectively; ii) an impairment of the Hepc/Fpn1 physiologic metabolism of cortical and hippocampal

5

neurons and astrocytes due to the selective increase of iron amount in these regions; iii) the fact that Fpn1 expressed in these cells could be one of the different and already characterized isoforms, which is not responsive to Hepc or modulated through different mechanisms [46]. On the contrary, Ft-L increase and Ft H decrease were evident in cortical and hippocampal neurons close to the soma, but not in astrocytes.

On the whole, this data revealed that aging dependent brain iron accumulation compromises the cells specific response: astrocytes, which are less susceptible than neurons to iron deposits-related toxicity [47] and which play a protective role towards neurons [42], have an increased iron export, while, neurons increase the metal storage in Ft-L rich heteropolymers. These deposits could trigger the neuronal death in Ctx and Hip evidenced during aging and even more during neurodegeneration [30].

Furthermore, we showed that brain cells respond to higher intracellular iron amount by increasing NCOA4, that could be responsible for a selective degradation of Ft-H, promoting in turn the formation of Ft-L rich heteropolymers, more effective for iron storage.

In conclusion, we demonstrated that even during physiologic aging, iron accumulates in the brain and that its accumulation, selectively localized in the Ctx and Hip, triggers neuroinflammation and the modification of the Hepc/Fpn1 pathway, all this enhancing iron availability imbalance and oxidative stress that could lead to neurodegeneration (Fig. 5).

In perspective, since NDs are characterized by inappropriate Hepc production [48], a therapeutic approach aimed at modifying the Hepc response could be taken in consideration. Different strategies could be used, such as mini-Hepc and Hepc agonists [49,50] by the stimulation/inhibition of Hepc production by targeting its regulators [35,48,51-53]. Additional research studies in animal models of NDs are required to clarify the CNS response to the increased iron aimed to exploit the results for the prevention and clinical management of patients with these diseases.

Methods

Animals. C57BL/6J mice (WT) used for the study were purchased from the Jackson Laboratory and subdivided for age according to its classification (https://www.jax.org): until 2 months of age mice are considered Young (WT Y n=5); from 2 to 6 months of age Adult (WT A n=7); from 6 to 12 months of age Middle-aged (WT M-A n=5) and from12 months of age (between 18-24 months of age) Old (WT O n=5) (Table 1S). Since from a pilot analysis on potential gender-related issues, no gender bias was observed (Suppl. Fig. 2S), both male and female mice were analysed and grouped according to their age. Mice were housed in polycarbonate cages (Tecnoplast, Buggirate, Italy) provided with sawdust bedding, boxes/tunnels hideout as environmental enrichment. Food and water were provided ad libitum; environmental conditions were 12 h/12 h light/dark cycle, room temperature 24 °C ± 1 °C and room humidity 55% ± 5%. Each group of mice was fed with a Standard Diet (SD) (VRF1, Special Diets Services, Essex, United Kingdom). Mice were anaesthetized (ketamine, 100 mg/kg; Ketavet, Bayern, Leverkusen, Germany; xylazine, 5 mg/kg; Rompun; Bayer, Milan, Italy) and sacrificed by cervical dislocation. To performed histological analysis, a subset of at least n=5 WT A and WT O mice were transcardially perfused with 4% paraformaldehyde (PFA) in phosphate buffered saline (PBS). Animals housing and all the experimental procedures were performed in accordance with European (Official Journal of the European Union L276 del 20/10/2010, Vol. 53, p. 33–80) and National Legislation (Gazzetta Ufficiale n° 61 del 14/03/2014, p. 2–68) for the protection of animals used for scientific purposes and the experimental procedure was

6

approved by the Ethical Committee of the University of Turin and conducted according the ARRIVE guidelines.

Real-time quantitative PCR. Total RNA from whole brain was extracted with TRIzol reagent. For reverse transcription, 2 μg of total RNA, 25 μM random hexamers and 100 U of reverse transcriptase (Applied Biosystems, California, USA) were used. Gene expression levels were measured using Real-time quantitative PCR in a CFX96 Real-time System (Bio-Rad, California, USA). For Nuclear factor erythroid 2-related factor 2 (Nfr2) and NCOA4 gene analysis, SYBR Green PCR technology (EVAGreen, Bio-Rad, California, USA) was used with specific primers (Suppl. Table 2S). For Hepc and Serum Amyloid A1 (SAA1) genes analysis, Taqman PCR method was used (Assays-on-Demand, Gene Expression Products, Applied Biosystems, California, USA). β-glucuronidase (Gus-β) was used as housekeeping control. Real-time quantitative PCR of the animals' transcripts was carried out making duplicates of each n (n per group= min 3). The results were analyzed using the ΔΔCt method [54].

Immunoblotting. The Fpn1, Ft-H, Ft-L, NCOA4 and Zonula occludens-1 (ZO-1) proteins' amount in the whole brain homogenates was evaluated by Western Blotting using specific antibodies. 50 μg of total brain lysates were separated on 6–12% SDS polyacrylamide gel and immunoblotted [55]. Primary antibodies Fpn1 (G-16), β-Actin (C-4), NCOA4 or ARA 70 (H-300) (Santa Cruz Biotechnology, Dallas, Texas, USA), ZO-1 (GeneTex, California, USA) and Vinculin (Invitrogen, Massachusetts, USA) were used. Antibodies used to detect Ft-H and Ft-L were provided by Sonia Levi, University of Vita Salute, Milan, Italy. Data were normalized on β-Actin or Vinculin amount in the same samples (Image Lab 4.0.1 Software, Bio-Rad, California, USA) [56]. Complete reference to all the antibodies is reported in Suppl. List 1.

Immunofluorescence. Animals were perfused, brains were removed, post-fixed in PFA for 24h at 4°C and cryoprotected in 30% sucrose in 0.12 M phosphate buffer [57]. Brains were cut in 30 μm thick coronal sections collected in PBS and then stained to detect: Fpn1 (G-16, Santa Cruz Biotechnology, Dallas, Texas, USA), Ft-L, Ft-H (S. Levi, University of Vita Salute, Milan), Glial Fibrillary Acidic Protein (GFAP) (Dako, California, United States), Microtubule-Associated Protein 2 (MAP-2) (Merck Millipore Burlington, Massachusetts, United States), Vesicular Glutamate Transporter 1 (VGLUT1) (Merck Millipore Burlington, Massachusetts, United States), Glutamate Transporter (GLAST) (Thermo Fischer Scientific Waltham, Massachusetts, United States) and Ionized calcium-binding adaptor molecule 1 (IBA-1) (Abcam, Cambridge, United Kingdom). After overnight incubation at 4°C in PBS with 2% normal donkey serum (NDS) [58], sections were exposed to Cy2-, Cy3- (Jackson ImmunoResearch Laboratories, West Grove, PA) and 647 Alexa Fluor-conjugated secondary antibodies (Molecular Probes Inc, Eugene Oregon) for 1 h at room temperature. DAPI (4,6-diamidino-2-phenylindole, Fluka, Italy) was used to counterstain cell nuclei. After processing, sections were mounted with Tris-glycerol supplemented with 10% Mowiol (Calbiochem, LaJolla, CA). The samples were examined by a Leica TCS SP5 confocal laser scanning microscope (Leica, Mannheim); z-stacks images were taken at 40X and 63X magnification.

Iron parameters. Brain nonheme iron content (BIC) was evaluated using 20 mg of dissected and dried murine whole brains [59]. Perfused brains were stained for nonheme ferrous iron by Prussian blue Perl's using a commercial kit (Bio-Optica, Milan, Italy). To improve the sensitivity, an intensification step with DAB (3-3'-diaminobenzidine tetrahydrochloride) [60] was performed. Images were taken at

7

10X magnification using a Leica DM4000B automated microscope with IM50 program for acquisition (Leica Microsystems, Wetzlar, Germany).

Statistical analysis. One-way ANOVA followed by Bonferroni's post hoc analysis or two-tailed Student's t-test were applied according to the experimental group's number. P values of <0.05 were considered as statistically significant. Analyses were performed with Image Lab 4.0.1 and GraphPad Prism 7.00. Data were expressed as average $\pm$ SD of the mean. Significance was defined as $*P< 0.05$, $**P<0.01$ and $***P<0.001$. WT adult (A) mice were used as normalizer. The number of samples in each experimental condition is indicated in the figure legends. In each Western Blotting experiment, we reported 3 samples per group.

References

1   Ganz, T. Systemic iron homeostasis. *Physiol Rev* **93**, 1721-1741, doi:10.1152/physrev.00008.2013 (2013).

2   Ginzburg, Y. Z. Hepcidin-ferroportin axis in health and disease. *Vitamins and hormones* **110**, 17-45, doi:10.1016/bs.vh.2019.01.002 (2019).

3   Arosio, P., Ingrassia, R. & Cavadini, P. Ferritins: a family of molecules for iron storage, antioxidation and more. *Biochimica et biophysica acta* **1790**, 589-599, doi:10.1016/j.bbagen.2008.09.004 (2009).

4   Sangkhae, V. & Nemeth, E. Regulation of the Iron Homeostatic Hormone Hepcidin. *Advances in nutrition (Bethesda, Md.)* **8**, 126-136, doi:10.3945/an.116.013961 (2017).

5   Roetto, A., Mezzanotte, M. & Pellegrino, R. M. The Functional Versatility of Transferrin Receptor 2 and Its Therapeutic Value. *Pharmaceuticals (Basel)* **11**, doi:10.3390/ph11040115 (2018).

6   Mancias, J. D., Wang, X., Gygi, S. P., Harper, J. W. & Kimmelman, A. C. Quantitative proteomics identifies NCOA4 as the cargo receptor mediating ferritinophagy. *Nature* **509**, 105-109, doi:10.1038/nature13148 (2014).

7   Mancias, J. D. *et al.* Ferritinophagy via NCOA4 is required for erythropoiesis and is regulated by iron dependent HERC2-mediated proteolysis. *Elife* **4**, doi:10.7554/eLife.10308 (2015).

8   Quiles Del Rey, M. & Mancias, J. D. NCOA4-Mediated Ferritinophagy: A Potential Link to Neurodegeneration. *Frontiers in neuroscience* **13**, 238, doi:10.3389/fnins.2019.00238 (2019).

9   Bellelli, R. *et al.* NCOA4 Deficiency Impairs Systemic Iron Homeostasis. *Cell Rep* **14**, 411-421, doi:10.1016/j.celrep.2015.12.065 (2016).

10   Nai, A. *et al.* NCOA4-mediated ferritinophagy in macrophages is crucial to sustain erythropoiesis in mice. *Haematologica* **106**, 795-805, doi:10.3324/haematol.2019.241232 (2021).

11   Moos, T., Rosengren Nielsen, T., Skjorringe, T. & Morgan, E. H. Iron trafficking inside the brain. *J Neurochem* **103**, 1730-1740, doi:10.1111/j.1471-4159.2007.04976.x (2007).

12   Mills, E., Dong, X. P., Wang, F. & Xu, H. Mechanisms of brain iron transport: insight into neurodegeneration and CNS disorders. *Future Med Chem* **2**, 51-64, doi:10.4155/fmc.09.140 (2010).

13   Bien-Ly, N. *et al.* Transferrin receptor (TfR) trafficking determines brain uptake of TfR antibody affinity variants. *J Exp Med* **211**, 233-244, doi:10.1084/jem.20131660 (2014).

14   Ward, R. J., Zucca, F. A., Duyn, J. H., Crichton, R. R. & Zecca, L. The role of iron in brain ageing and neurodegenerative disorders. *The Lancet. Neurology* **13**, 1045-1060, doi:10.1016/s1474-4422(14)70117-6 (2014).

15   Vela, D. Hepcidin, an emerging and important player in brain iron homeostasis. *Journal of translational medicine* **16**, 25, doi:10.1186/s12967-018-1399-5 (2018).

16   Bulet, P., Stocklin, R. & Menin, L. Anti-microbial peptides: from invertebrates to vertebrates. *Immunol Rev* **198**, 169-184, doi:10.1111/j.0105-2896.2004.0124.x (2004).

17   Zechel, S., Huber-Wittmer, K. & von Bohlen und Halbach, O. Distribution of the iron-regulating protein hepcidin in the murine central nervous system. *Journal of neuroscience research* **84**, 790-800, doi:10.1002/jnr.20991 (2006).

8

18   Pellegrino, R. M. *et al.* Transferrin Receptor 2 Dependent Alterations of Brain Iron Metabolism Affect Anxiety Circuits in the Mouse. *Sci Rep* **6**, 30725, doi:10.1038/srep30725 (2016).

19   Almutairi, M. M., Gong, C., Xu, Y. G., Chang, Y. & Shi, H. Factors controlling permeability of the blood-brain barrier. *Cell Mol Life Sci* **73**, 57-77, doi:10.1007/s00018-015-2050-8 (2016).

20   Farrall, A. J. & Wardlaw, J. M. Blood-brain barrier: ageing and microvascular disease--systematic review and meta-analysis. *Neurobiol Aging* **30**, 337-352, doi:10.1016/j.neurobiolaging.2007.07.015 (2009).

21   Salmina, A. B. *et al.* Blood-Brain Barrier Breakdown in Stress and Neurodegeneration: Biochemical Mechanisms and New Models for Translational Research. *Biochemistry. Biokhimiia* **86**, 746-760, doi:10.1134/s0006297921060122 (2021).

22   Maiuolo, J. *et al.* The "Frail" Brain Blood Barrier in Neurodegenerative Diseases: Role of Early Disruption of Endothelial Cell-to-Cell Connections. *Int J Mol Sci* **19**, doi:10.3390/ijms19092693 (2018).

23   Jang, S. *et al.* Serum amyloid A1 is involved in amyloid plaque aggregation and memory decline in amyloid beta abundant condition. *Transgenic Res* **28**, 499-508, doi:10.1007/s11248-019-00166-x (2019).

24   Jiang, Z., Wang, J., Liu, C., Wang, X. & Pan, J. Hyperoside alleviated N-acetyl-para-amino-phenol-induced acute hepatic injury via Nrf2 activation. *Int J Clin Exp Pathol* **12**, 64-76 (2019).

25   O'Callaghan, J. P. & Sriram, K. Glial fibrillary acidic protein and related glial proteins as biomarkers of neurotoxicity. *Expert Opin Drug Saf* **4**, 433-442, doi:10.1517/14740338.4.3.433 (2005).

26   Block, M. L. & Hong, J. S. Microglia and inflammation-mediated neurodegeneration: multiple triggers with a common mechanism. *Prog Neurobiol* **76**, 77-98, doi:10.1016/j.pneurobio.2005.06.004 (2005).

27   Glass, C. K., Saijo, K., Winner, B., Marchetto, M. C. & Gage, F. H. Mechanisms underlying inflammation in neurodegeneration. *Cell* **140**, 918-934, doi:10.1016/j.cell.2010.02.016 (2010).

28   Hirsch, E. C. & Hunot, S. Neuroinflammation in Parkinson's disease: a target for neuroprotection? *The Lancet. Neurology* **8**, 382-397, doi:10.1016/S1474-4422(09)70062-6 (2009).

29   Lier, J. *et al.* Loss of IBA1-Expression in brains from individuals with obesity and hepatic dysfunction. *Brain research* **1710**, 220-229, doi:10.1016/j.brainres.2019.01.006 (2019).

30   Zecca, L., Youdim, M. B., Riederer, P., Connor, J. R. & Crichton, R. R. Iron, brain ageing and neurodegenerative disorders. *Nat Rev Neurosci* **5**, 863-873, doi:10.1038/nrn1537 (2004).

31   Rouault, T. A. Iron metabolism in the CNS: implications for neurodegenerative diseases. *Nat Rev Neurosci* **14**, 551-564, doi:10.1038/nrn3453 (2013).

32   Yamamoto, A. *et al.* Iron (III) induces aggregation of hyperphosphorylated tau and its reduction to iron (II) reverses the aggregation: implications in the formation of neurofibrillary tangles of Alzheimer's disease. *J Neurochem* **82**, 1137-1147, doi:10.1046/j.1471-4159.2002.t01-1-01061.x (2002).

33   Liu, Y. & Connor, J. R. Iron and ER stress in neurodegenerative disease. *Biometals* **25**, 837-845, doi:10.1007/s10534-012-9544-8 (2012).

34   Hong, C. H. *et al.* Anemia and risk of dementia in older adults: findings from the Health ABC study. *Neurology* **81**, 528-533, doi:10.1212/WNL.0b013e31829e701d (2013).

35   Muckenthaler, M. U., Rivella, S., Hentze, M. W. & Galy, B. A Red Carpet for Iron Metabolism. *Cell* **168**, 344-361, doi:10.1016/j.cell.2016.12.034 (2017).

36   Du, F., Qian, Z. M., Luo, Q., Yung, W. H. & Ke, Y. Hepcidin Suppresses Brain Iron Accumulation by Downregulating Iron Transport Proteins in Iron-Overloaded Rats. *Mol Neurobiol* **52**, 101-114, doi:10.1007/s12035-014-8847-x (2015).

37   Moos, T. & Morgan, E. H. The metabolism of neuronal iron and its pathogenic role in neurological disease: review. *Annals of the New York Academy of Sciences* **1012**, 14-26, doi:10.1196/annals.1306.002 (2004).

38   Leitner, D. F. & Connor, J. R. Functional roles of transferrin in the brain. *Biochimica et biophysica acta* **1820**, 393-402, doi:10.1016/j.bbagen.2011.10.016 (2012).

39   Ndayisaba, A., Kaindlstorfer, C. & Wenning, G. K. Iron in Neurodegeneration - Cause or Consequence? *Frontiers in neuroscience* **13**, 180, doi:10.3389/fnins.2019.00180 (2019).

9

40   Yu, M. H. *et al.* SAA1 increases NOX4/ROS production to promote LPS-induced inflammation in vascular smooth muscle cells through activating p38MAPK/NF-κB pathway. *BMC molecular and cell biology* **20**, 15, doi:10.1186/s12860-019-0197-0 (2019).

41   Erdembileg, A. *et al.* Attenuated age-impact on systemic inflammatory markers in the presence of a metabolic burden. *PloS one* **10**, e0121947, doi:10.1371/journal.pone.0121947 (2015).

42   Ke, Z. J. & Gibson, G. E. Selective response of various brain cell types during neurodegeneration induced by mild impairment of oxidative metabolism. *Neurochemistry international* **45**, 361-369, doi:10.1016/j.neuint.2003.09.008 (2004).

43   Sato, T., Shapiro, J. S., Chang, H. C., Miller, R. A. & Ardehali, H. Aging is associated with increased brain iron through cortex-derived hepcidin expression. *Elife* **11**, doi:10.7554/eLife.73456 (2022).

44   Dowdle, W. E. *et al.* Selective VPS34 inhibitor blocks autophagy and uncovers a role for NCOA4 in ferritin degradation and iron homeostasis in vivo. *Nat Cell Biol* **16**, 1069-1079, doi:10.1038/ncb3053 (2014).

45   Fujimaki, M. *et al.* Iron Supply via NCOA4-Mediated Ferritin Degradation Maintains Mitochondrial Functions. *Molecular and cellular biology* **39**, doi:10.1128/mcb.00010-19 (2019).

46   Drakesmith, H., Nemeth, E. & Ganz, T. Ironing out Ferroportin. *Cell metabolism* **22**, 777-787, doi:10.1016/j.cmet.2015.09.006 (2015).

47   Kress, G. J., Dineley, K. E. & Reynolds, I. J. The relationship between intracellular free iron and cell injury in cultured neurons, astrocytes, and oligodendrocytes. *The Journal of neuroscience : the official journal of the Society for Neuroscience* **22**, 5848-5855, doi:10.1523/jneurosci.22-14-05848.2002 (2002).

48   Qian, Z. M. & Ke, Y. Hepcidin and its therapeutic potential in neurodegenerative disorders. *Med Res Rev* **40**, 633-653, doi:10.1002/med.21631 (2020).

49   Kautz, L. *et al.* Identification of erythroferrone as an erythroid regulator of iron metabolism. *Nat Genet* **46**, 678-684, doi:10.1038/ng.2996 (2014).

50   Casu, C. *et al.* Minihepcidins improve ineffective erythropoiesis and splenomegaly in a new mouse model of adult β-thalassemia major. *Haematologica* **105**, 1835-1844, doi:10.3324/haematol.2018.212589 (2020).

51   Blanchette, N. L., Manz, D. H., Torti, F. M. & Torti, S. V. Modulation of hepcidin to treat iron deregulation: potential clinical applications. *Expert Rev Hematol* **9**, 169-186, doi:10.1586/17474086.2016.1124757 (2016).

52   Huang, S. N., Ruan, H. Z., Chen, M. Y., Zhou, G. & Qian, Z. M. Aspirin increases ferroportin 1 expression by inhibiting hepcidin via the JAK/STAT3 pathway in interleukin 6-treated PC-12 cells. *Neurosci Lett* **662**, 1-5, doi:10.1016/j.neulet.2017.10.001 (2018).

53   Zhao, Y. *et al.* Nano-liposomes of lycopene reduces ischemic brain damage in rodents by regulating iron metabolism. *Free Radic Biol Med* **124**, 1-11, doi:10.1016/j.freeradbiomed.2018.05.082 (2018).

54   Livak, K. J. & Schmittgen, T. D. Analysis of relative gene expression data using real-time quantitative PCR and the 2(-Delta Delta C(T)) Method. *Methods* **25**, 402-408, doi:10.1006/meth.2001.1262 (2001).

55   Boero, M. *et al.* A comparative study of myocardial molecular phenotypes of two tfr2beta null mice: role in ischemia/reperfusion. *Biofactors* **41**, 360-371, doi:10.1002/biof.1237 (2015).

56   Hage, S. *et al.* Gamma-secretase inhibitor activity of a Pterocarpus erinaceus extract. *Neuro-degenerative diseases* **14**, 39-51, doi:10.1159/000355557 (2014).

57   Stanga, S. *et al.* APP-dependent glial cell line-derived neurotrophic factor gene expression drives neuromuscular junction formation. *FASEB journal : official publication of the Federation of American Societies for Experimental Biology* **30**, 1696-1711, doi:10.1096/fj.15-278739 (2016).

58   d'Errico, P. *et al.* Selective vulnerability of spinal and cortical motor neuron subpopulations in delta7 SMA mice. *PloS one* **8**, e82654, doi:10.1371/journal.pone.0082654 (2013).

59   Roetto, A. *et al.* Comparison of 3 Tfr2-deficient murine models suggests distinct functions for Tfr2-alpha and Tfr2-beta isoforms in different tissues. *Blood* **115**, 3382-3389, doi:10.1182/blood-2009-09-240960 (2010).

60   Meguro, R. *et al.* Nonheme-iron histochemistry for light and electron microscopy: a historical, theoretical and technical review. *Archives of histology and cytology* **70**, 1-19, doi:10.1679/aohc.70.1 (2007).

Conflicts of Interest

The authors declare that the research was conducted in the absence of any commercial or financial relationships that could be construed as a potential conflict of interest.

Author Contributions

MM performed research, analyzed data and wrote the paper. GA and MB performed research and analyzed data. SS and AR designed and performed research, analyzed data and wrote the paper. MM and SS performed revision. All the authors contributed to the article and approved the submitted version.

Data availability statement

The data regarding reference genes for Nrf2, NCOA4 and Gus-B primers are openly available in the repository "Nucleotide" at https://www.ncbi.nlm.nih.gov/nuccore, reference numbers NM_010902.4, NM_019744.4 and NM_010368.2.

Figure Legends

Figure 1. Iron accumulation in WT mice brain and impaired permeability of blood brain barrier (BBB).
(**A**) Brain Iron Content (BIC) from mice total brain at different ages. (**B**) Sections of mice brain stained with DAB-enhanced Prussian Blue staining in cerebral cortex (Ctx), hippocampus (Hip), third ventricle (3v) and Striatum during aging. Scale bars:10X. Results on Liver Iron Content (LIC), Prussian Blue staining and serum iron are shown in Suppl. Fig. 1S. (**C**) Western blotting analysis and quantification of Zonula occludens-1 (ZO-1). Vertical black lines indicate image taken from different gels. Full length ZO-1 blot with a positive control (HeLa cells) is shown in Suppl. Fig. 3S.
*Statistically significant vs WT A control group *P <0.05; **P <0.01 ***P <0.001 using two-tailed Student's t-test. Number of analyzed mice: WT Y n=5, WT A n=7, WT M-A n=5 and WT O n=5.

Figure 2. Iron-dependent inflammatory response and oxidative stress during aging.
(**A**) Real-time PCR of Serum amyloid A1 (SAA1) in total brain from all genotypes. (**B**) Nuclear factor erythroid 2-related factor 2 (Nrf2) mRNA expression levels in total brain. The expression levels of

11

the two genes were normalized to levels of β-glucuronidase (Gus-β) housekeeping gene (material and methods section). (**C**) Immunofluorescence anti-GFAP (green) and anti-IBA1 (pink) antibodies in cerebral cortex (Ctx) and hippocampus (Hip); 4,6 diamidino-2-phenylindole (DAPI) (blue) was used to counterstain cell nuclei. Scale bars:40X. *Statistically significant vs WT A control group *P <0.05; **P <0.01 ***P <0.001 using OneWay ANOVA followed by Bonferroni's post hoc analysis. Number of analyzed mice: Fig. A-B: WT Y n=5, WT A n=7, WT M-A n=5 and WT O n=5; Fig. C-D: WT A n=5 and WT O n=5.

Figure 3. Hepcidin expression and iron transport/storage proteins quantification in mice brain.
(**A**) Hepcidin (Hepc) transcription pattern. (**B**) Western blotting analysis and quantification of Ferroportin (Fpn1). (**C**) Ferritin-L (Ft-L) and (**D**) Ferritin-H (Ft-H). in mice total brain. (**E**) Real-time PCR of Nuclear receptor coactivator 4 (NCOA4) in total brain. The expression levels of NCOA4 were normalized to the levels of β-Glucuronidase (Gus-β) housekeeping gene (material and methods section) and (**F**) Western blotting analysis and quantification of NCOA4. Vertical black lines in blots images indicate that they are taken from different gels. Full length blots are presented in Suppl. Fig.4S. The full length blot with a positive control (liver) for Fpn1 is presented in Suppl. Fig. 5S. *Statistically significant vs WT A control group *P <0.05; **P <0.01 ***P <0.001 using OneWay ANOVA followed by Bonferroni's post hoc analysis or two-tailed Student's t-test. Number of analyzed mice: WT Y n=5, WT A n=7, WT M-A n=5 and WT O n=5.

Figure 4. Ferroportin 1, Ferritin L and H chain protein cellular allocation in Ctx and Hip.
(**A**) Immunofluorescence anti-Fpn1 antibody (red) in cerebral cortex (Ctx) and hippocampus (Hip). Arrows indicate Fpn1 expression and localization. (**B**) Immunofluorescence of neuronal and astrocytic cells using anti-GLUT1 (green), anti-GLAST (red) and anti-Fpn1 antibodies in cerebral cortex (Ctx) and hippocampus (Hip). (**C-D**) Immunofluorescence of astrocytic and neuronal cells using anti-GFAP (green), anti-MAP2 (red), anti-Ft-L and anti-Ft-H antibodies in cerebral cortex (Ctx) and hippocampus (Hip). 4,6-diamidino-2-phenylindole (DAPI) (blue) was used to counterstain cell nuclei. Scale bars: 63X. Number of analyzed mice: WT Y n=5, WT A n=5, WT M-A n=5 and WT O n=5. Specifically, neuronal (MAP2) and Ferritins (Ft-L and Ft-H) localization are shown in Suppl. Fig. 6S.

Figure 5. Iron regulation in the brain during aging.
Schematic representation illustrating iron metabolism in old mice brains vs adults (see text for details). Fe: iron; Hepc: Hepcidin; Fpn 1: Ferroportin 1; Ft-L: Ferritin-L; Ctx: cerebral cortex; Hip: hippocampus.

12

Fig. 1 Iron amount and distribution in the brain during aging correlates to the level of BBB permeability
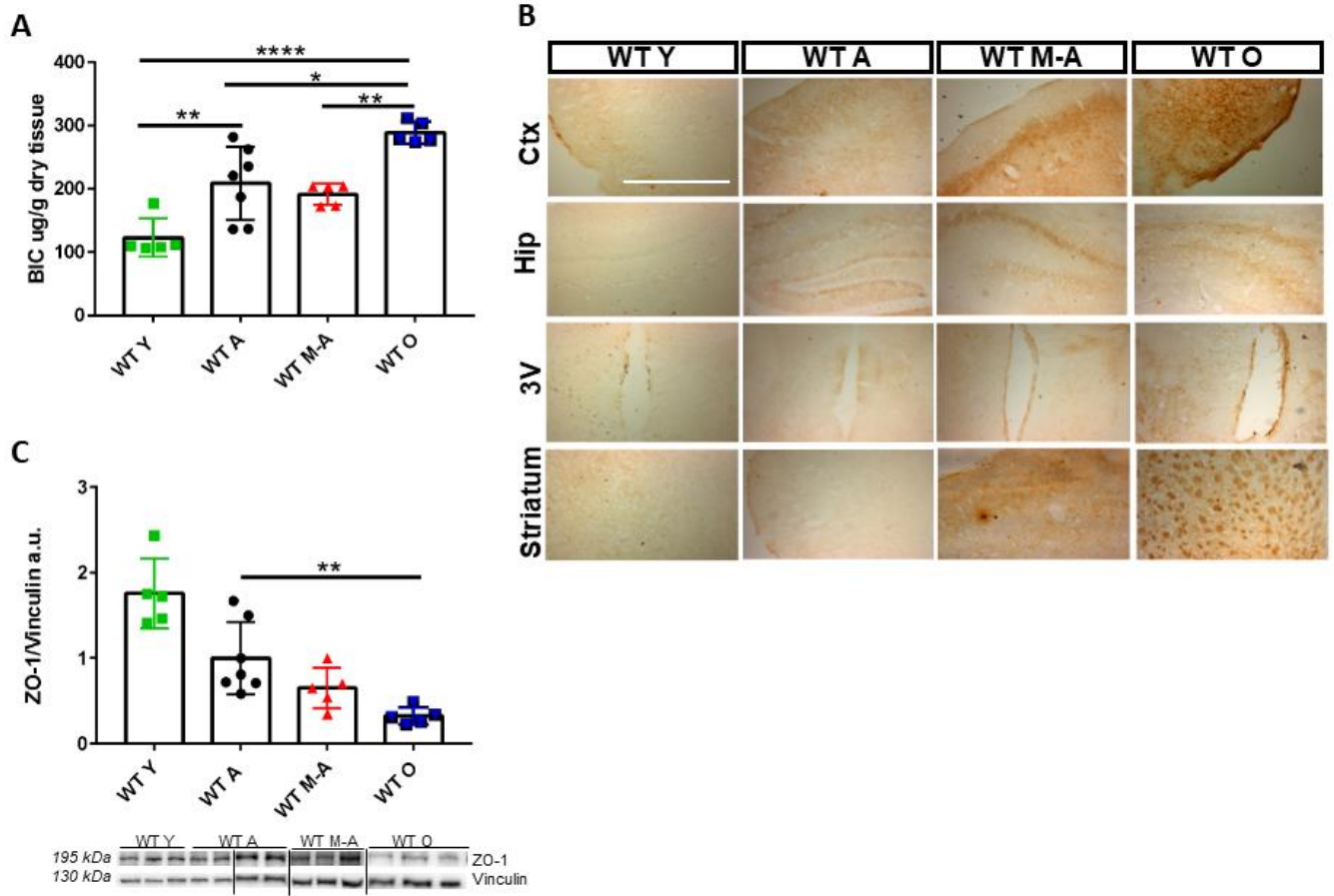
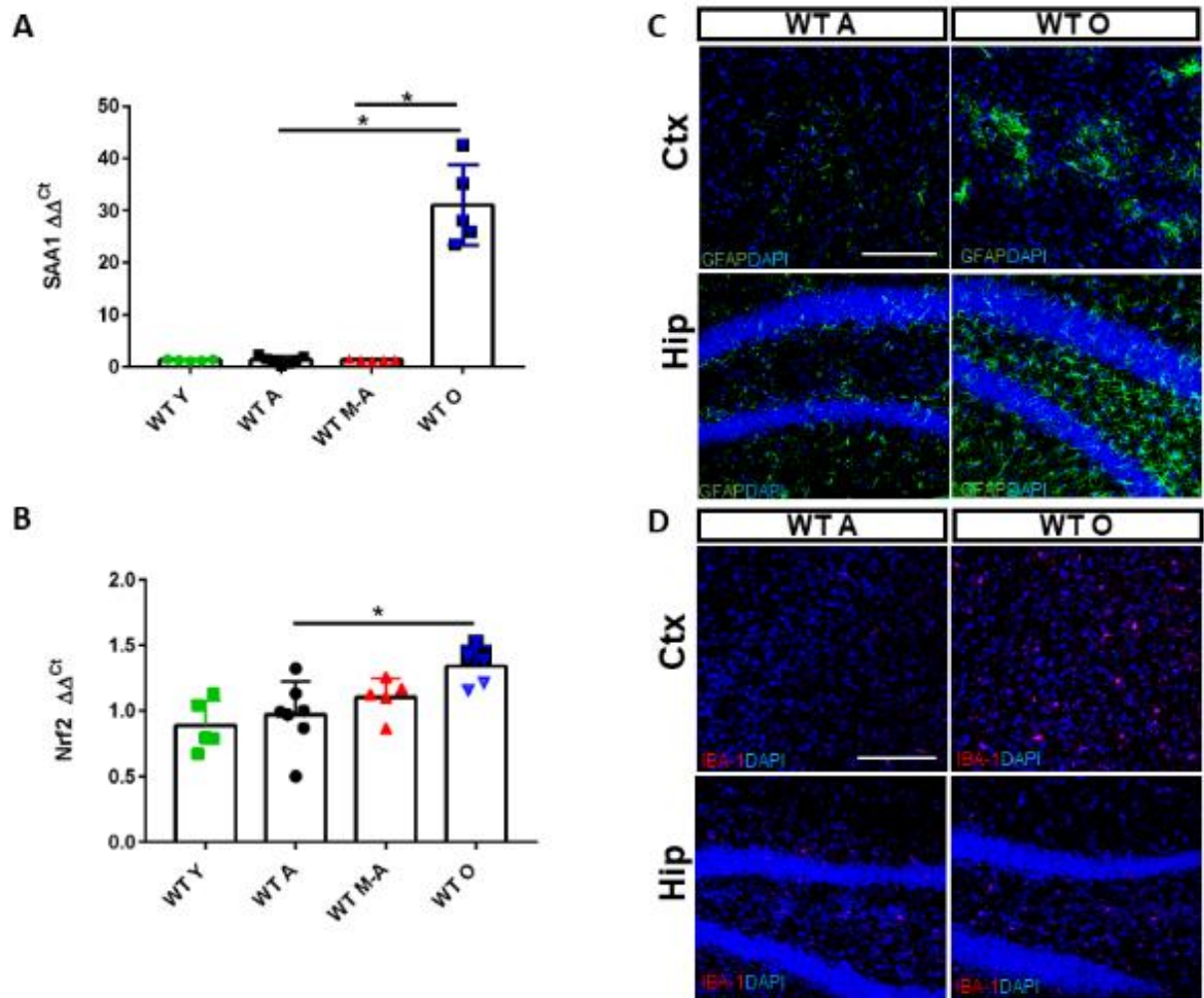**Fig. 2 Increased inflammatory and oxidative stress state during brain aging**

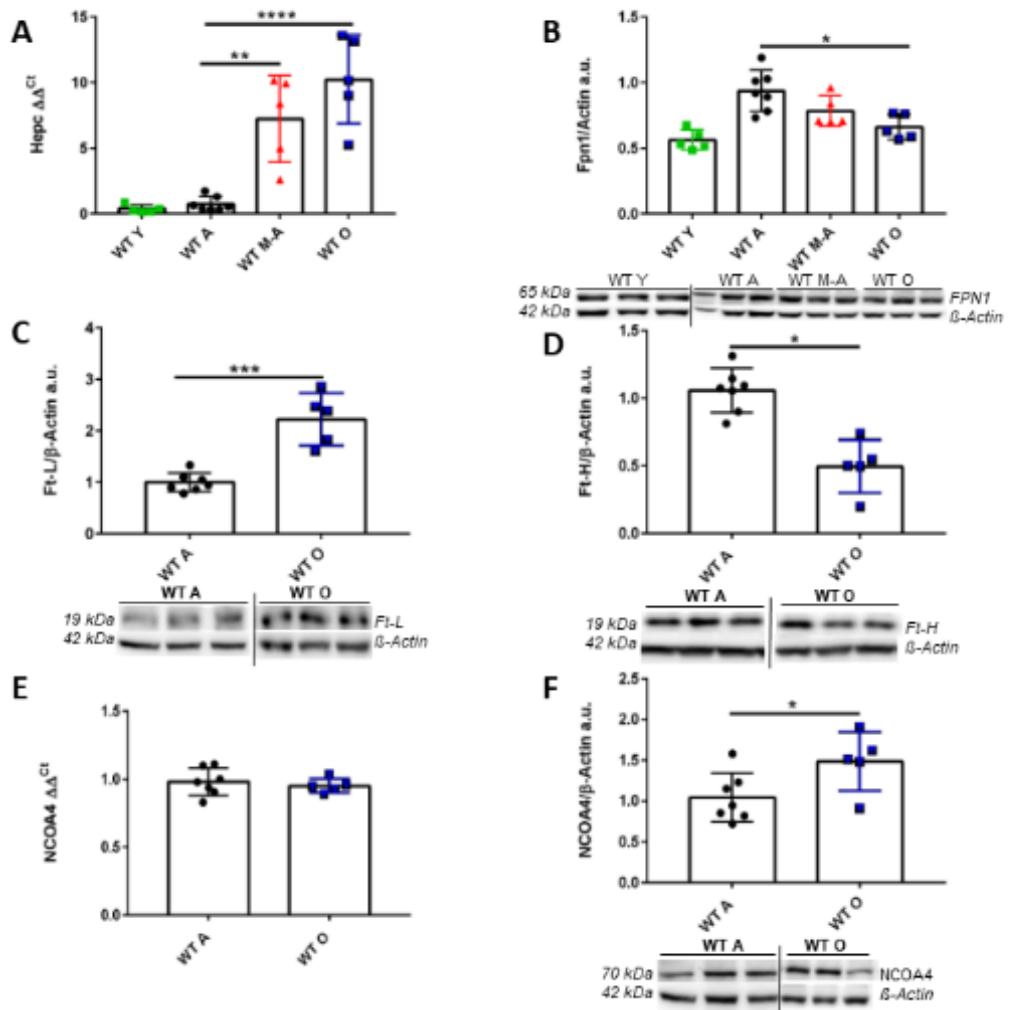**Fig. 3 Hepc/Fpn1 activation and ferritins response to iron overload during brain aging via ferritinophagy**

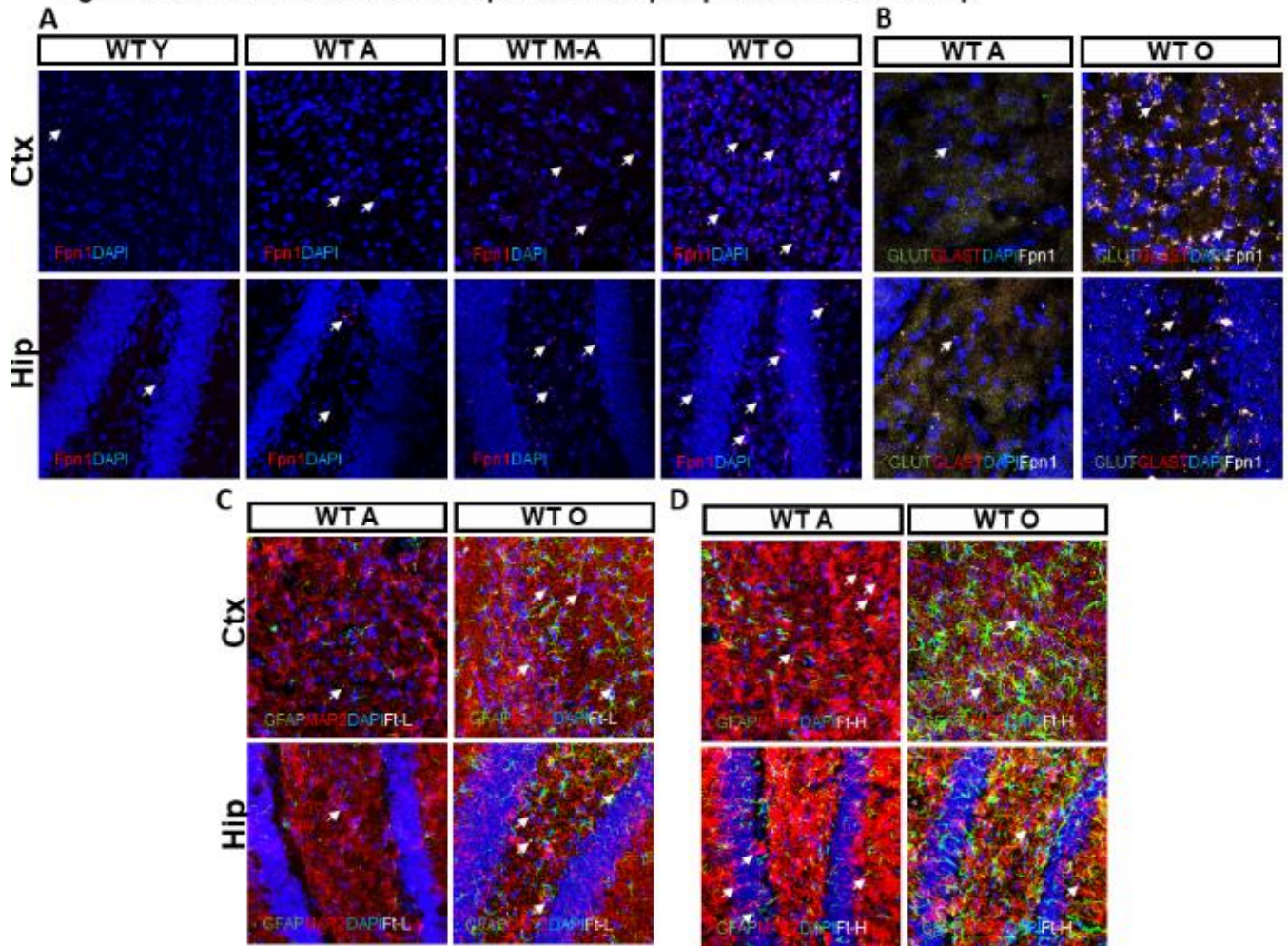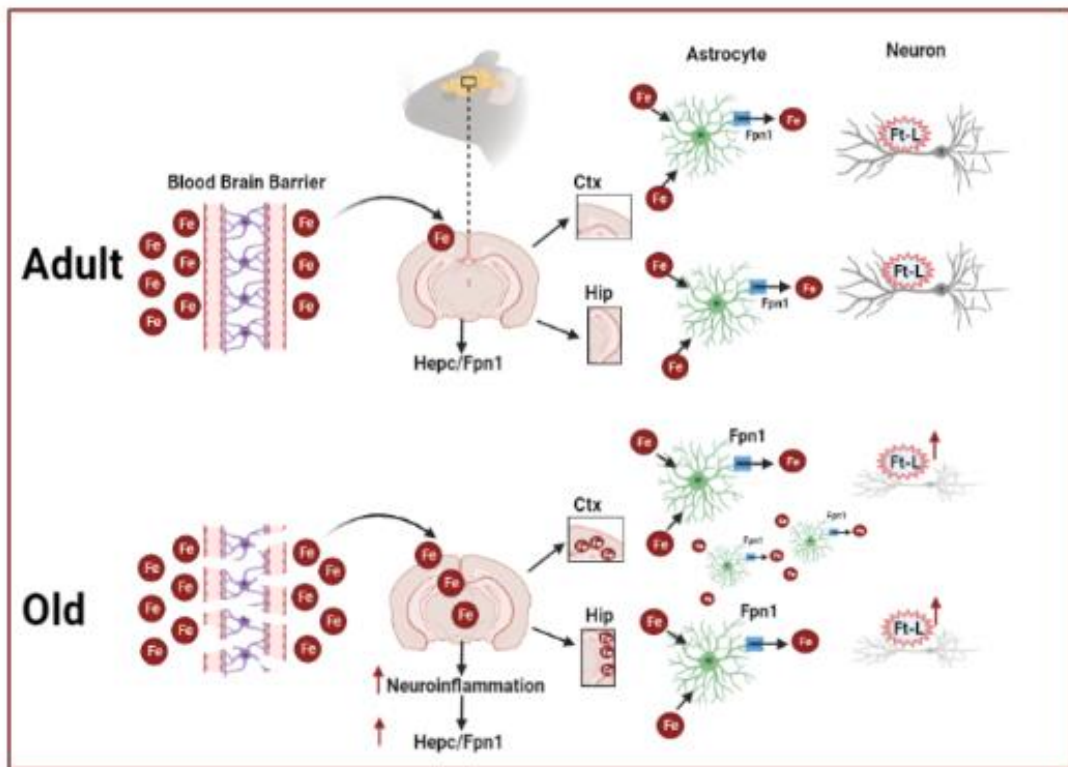# Fig. 4 Cellular distribution of iron deposits and export proteins in Ctx and Hip

Fig. 5 Schematic representation of iron regulation in brain aged

3 Other collaborations

During the last year of my PhD School I was involved in a work, in collaboration with the Prof. Porporato group, aimed to study iron metabolism in the skeletal muscle both in cancer cachectic patients and in mice where cancer cachexia has been induced. Our results further strengthen the hypothesis that iron is a key element in a multitude of pathological situation including cancer associated cachexia. Indeed, we demonstrated that cancer drivers iron dyshomeostasis, in terms of iron deficiency, in cachectic muscle. Iron levels directly effect on functional alterations of the mitochondria, on myotube size *in vitro* and muscle mass in cachectic mice but iron supplementation allows muscle mass restoration via mitochondrial metabolism normalization. This work, attached below, was recently published in EMBO Reports.

Publication: Iron supplementation is sufficient to rescue cancer-induced muscle wasting and function.

Iron supplementation is sufficient to rescue skeletal muscle mass and function in cancer cachexia

Elisabeth Wyart[1,†] , Myriam Y Hsu[1,†] , Roberta Sartori[2] , Erica Mina[1], Valentina Rausch[1], Elisa S Pierobon[3] , Mariarosa Mezzanotte[4], Camilla Pezzini[2], Laure B Bindels[5] , Andrea Lauria[6], Fabio Penna[4], Emilio Hirsch[1], Miriam Martini[1], Massimiliano Mazzone[1,7,8] , Antonella Roetto[4], Simonetta Geninatti Crich[1], Hans Prenen[9,10] , Marco Sandri[2], Alessio Menga[1,‡] & Paolo E Porporato[1,*,‡]

Abstract

Cachexia is a wasting syndrome characterized by devastating skeletal muscle atrophy that dramatically increases mortality in various diseases, most notably in cancer patients with a penetrance of up to 80%. Knowledge regarding the mechanism of cancer-induced cachexia remains very scarce, making cachexia an unmet medical need. In this study, we discovered strong alterations of iron metabolism in the skeletal muscle of both cancer patients and tumor-bearing mice, characterized by decreased iron availability in mitochondria. We found that modulation of iron levels directly influences myotube size *in vitro* and muscle mass in otherwise healthy mice. Furthermore, iron supplementation was sufficient to preserve both muscle function and mass, prolong survival in tumor-bearing mice, and even rescues strength in human subjects within an unexpectedly short time frame. Importantly, iron supplementation refuels mitochondrial oxidative metabolism and energy production. Overall, our findings provide new mechanistic insights in cancer-induced skeletal muscle wasting, and support targeting iron metabolism as a potential therapeutic option for muscle wasting diseases.

Introduction

In healthy humans, skeletal muscle makes up to 40% of the total body mass (Janssen *et al*, 2000), of which 20% are constituted by proteins. Massive skeletal muscle atrophy is the hallmark of a multi-organ wasting disorder known as cachexia, which causes severe asthenia and intolerance to therapies in patients with chronic diseases such as cardiac failure, COPD, and notably cancer, leading to poor clinical outcomes (Fearon *et al*, 2011; Porporato, 2016). Indeed, the prevalence of cachexia reaches 80% in advanced-stage cancer patients and has been estimated to directly cause at least 20% of all cancer-related deaths (Tisdale, 2002).

In cancer cachexia, systemic alterations contribute to the uncontrollable decrease in quality of life, insulin resistance, liver dysfunction, chronic inflammation, and even altered gut microbiota and nutrient absorption (Porporato, 2016). Remarkably, iron deficiency is diagnosed in more than half of patients afflicted with colorectal, lung, and pancreatic cancers, which are also associated with high prevalence of cachexia (Ludwig *et al*, 2013). Chronic inflammation hampers iron absorption from the diet and causes iron retention in reticuloendothelial cells, which results in insufficient iron availability to meet the body's needs. Iron is indeed a versatile cofactor essential to a multitude of vital metabolic processes including oxygen supply, DNA synthesis, redox homeostasis, or energy metabolism. Energy production directly depends on the availability of iron. It is indispensable for the activity of several mitochondrial enzymes involved in the TCA cycle and the electron transport chain, where iron is found under the form of heme or iron–sulfur cluster (ISC).

1 Department of Molecular Biotechnology and Health Sciences, Molecular Biotechnology Center, University of Torino, Turin, Italy
2 Department of Biomedical Sciences, University of Padova, Padova, Italy
3 Department of Surgical, Oncological and Gastroenterological Sciences, Padova University Hospital, Padova, Italy
4 Department of Clinical and Biological Sciences, University of Torino, Turin, Italy
5 Metabolism and Nutrition Research Group, Louvain Drug Research Institute, Université catholique de Louvain (UCLouvain), Brussels, Belgium
6 Department of Life Sciences and System Biology, University of Torino, Turin, Italy
7 Laboratory of Tumor Inflammation and Angiogenesis, Center for Cancer Biology (CCB), Vlaams Instituut voor Biotechnologie (VIB), Leuven, Belgium
8 Laboratory of Tumor Inflammation and Angiogenesis, Department of Oncology, Katholieke Universiteit Leuven (KUL), Leuven, Belgium
9 Department of Medical Oncology, University Hospital Antwerp, Edegem, Belgium
10 Center for Oncological Research (CORE), Integrated Personalized and Precision Oncology Network (IPPON), University of Antwerp, Antwerp, Belgium
*Corresponding author. Tel: +39 0116706422; E-mail: paolo.porporato@unito.it
†These authors contributed equally to this work as first authors
‡These authors contributed equally to this work as senior authors

Moreover, iron has been shown to directly regulate mitochondrial biogenesis, highlighting the sensitivity of these organelles to iron availability (Rensvold *et al*, 2016). Notably, both iron accumulation and iron deficiency are detrimental to mitochondrial function. Cellular iron homeostasis is thus a tightly regulated process involving a broad variety of proteins responsible for its transport (transferrin), uptake (transferrin receptor/TFR1), storage (ferritin/FT), and export (ferroportin/FPN1). The fine tuning of intracellular iron metabolism is made possible by the Iron Responsive Element/Iron Responsive Protein (IRE/IRP) system exerting a major control on the translation of several key iron-related proteins.

In the skeletal muscle, iron is particularly needed to support the high metabolic activity required for ATP generation, a requisite for contraction and movement. While mitochondrial dysfunction (in particular, decreased oxidative capacity, inefficient energy production, and altered mitochondrial dynamics) has been proven to promote skeletal muscle wasting in cachexia (Boengler *et al*, 2017; Abrigo *et al*, 2019), little is known about the consequence of altered iron levels on skeletal muscle function and mass. Importantly, iron deficiency is present in the vast majority of cancer patients and has been associated to advanced stage and poor prognosis (Ludwig *et al*, 2013). Hence, we decided to investigate the role of iron metabolism in cancer cachexia-related muscle wasting.

Results

Iron deficiency induces skeletal muscle atrophy

Iron deficiency is highly prevalent in cancer patients and has been associated to advanced stage and poor prognosis (Ludwig *et al*, 2013). To assess the effects of cancer-induced iron deficiency on skeletal muscle metabolism, we analyzed the transcript levels of the main cellular iron importer, transferrin receptor 1 (TFR1) in a cohort of cancer patients presenting body weight loss and anemia (Fig 1A and B). During iron deficiency, cells normally increase iron import through TFR1 to maintain homeostasis (Camaschella *et al*, 2020). Surprisingly, the patients displayed decreased TFR1 (Fig 1C). To

simulate the condition of iron-deficient anemia typical of cancer patients, we induced severe anemia in mice by combined phlebotomy and iron-free diet (Fig EV1A). This treatment resulted in muscle atrophy (Figs 1D and EV1B), supporting the hypothesis of an involvement of iron homeostasis in the onset of cancer-associated muscle wasting. As expected, iron deficiency promoted TFR1 upregulation in liver (Fig 1E), presumably to ensure the necessary supply of iron to the organ (Camaschella *et al*, 2020). However, TFR1 was downregulated in skeletal muscle of iron-deficient mice (Figs 1F and EV1C), suggesting a different response of this tissue to iron deprivation. To study the role of TFR1 expression on muscle mass, we transfected TFR1-silencing or TFR1-overexpressing plasmid by electroporating the tibialis anterior of healthy mice. TFR1 silencing was sufficient to induce fiber atrophy (Figs 1G and EV1D), while TFR1 overexpression triggered hypertrophy in the positive fibers (Fig 1H). Coherently, inhibition of iron import by silencing TFR1 induced significant myotube atrophy *in vitro* and decrease of the labile iron pool (Figs 1I and EV1E and F). Similarly, blocking intracellular iron mobilization by silencing NCOA4 (a cytoplasmic protein that mediates autophagic degradation of ferritin (Bellelli *et al*, 2016)), also caused significant myotube atrophy (Figs 1J and EV1G). Furthermore, to assess the direct impact of iron deficiency on muscle, we evaluated the effect of iron chelation on murine and human myotubes. Treatment with different iron chelators, namely deferoxamine (DFO), bathophenanthroline disulfonic acid (BPS), and apotransferrin (Apo-Tf), which is known to decrease transferrin saturation, led to a reduction in C2C12 myotube diameter and labile iron pool (Figs 1K and EV1H). Consistently, iron chelation by DFO exerted the same atrophic effect on human myotubes (Figs 1L). In summary, we found that cachectic cancer patients have decreased muscular TFR1 expression, and decreased iron availability is sufficient to induce skeletal muscle atrophy *in vivo* and myotube diameter reduction *in vitro*.

Altered iron metabolism in the skeletal muscle is a feature of cancer-induced cachexia

To confirm the link between cancer cachexia and iron metabolism in the skeletal muscle, we recreated cancer cachexia in mice using

---

Figure 1. Iron deficiency induces skeletal muscle atrophy.

A, B Hemoglobin (A) and hematocrit (B) levels of healthy subjects and cachectic cancer patients presenting a body weight loss superior to 10% of initial body weight (19 healthy subjects, 17 cachectic patients).

C   TFR1 mRNA levels in muscle biopsies from cancer patients of late stage cachexia with at least 10% total body weight loss (19 healthy subjects, 17 cachectic patients).

D   Gastrocnemius weight in mice subjected to iron deprivation by feeding with an iron-deficient diet (IDD) combined to a phlebotomy (PHL) (*n* = 5–6).

E   TFR1 mRNA levels in the liver of mice subjected to iron deprivation by feeding with an iron-deficient diet (IDD) combined to a phlebotomy (PHL) (*n* = 5–6).

F   TFR1 mRNA levels in the gastrocnemius of mice subjected to iron deprivation by feeding with an iron- deficient diet (IDD) combined to a phlebotomy (PHL) (*n* = 5–6).

G   Cross-sectional area of skeletal muscle fibers transfected with shSCR (scramble) and shTFR1 (*n* = 3–4) and representative picture of shTFR1 transfected fibers. Scale bar = 50 μm.

H   Cross-sectional area of skeletal muscle fibers transfected with TFR-pHuji (*n* = 4) and representative picture of TFR-pHuji transfected fibers. Scale bar = 50 μm.

I, J Diameter of TFR1 (I) or NCOA4 (J) knocked down C2C12 myotubes at day 3 post-transfection (*n* = 7 and *n* = 3 respectively).

K   Diameter of C2C12 myotubes after 48 h treatment with Deferoxamine (DFO), bathophenanthroline disulfonate (BPS), or apo-transferrin (Apo-Tf).

L   Representative pictures and diameter measurements of human myoblast-derived myotubes after 48 h treatment with DFO (*n* = 3). Scale bar = 50 μm.

Data information: For all data, *n* represents the number of biological replicates. Statistical significance was calculated by unpaired, two-tailed Student's *t*-test. Data are mean ± SEM. *P < 0.05, **P < 0.01, ***P < 0.001.
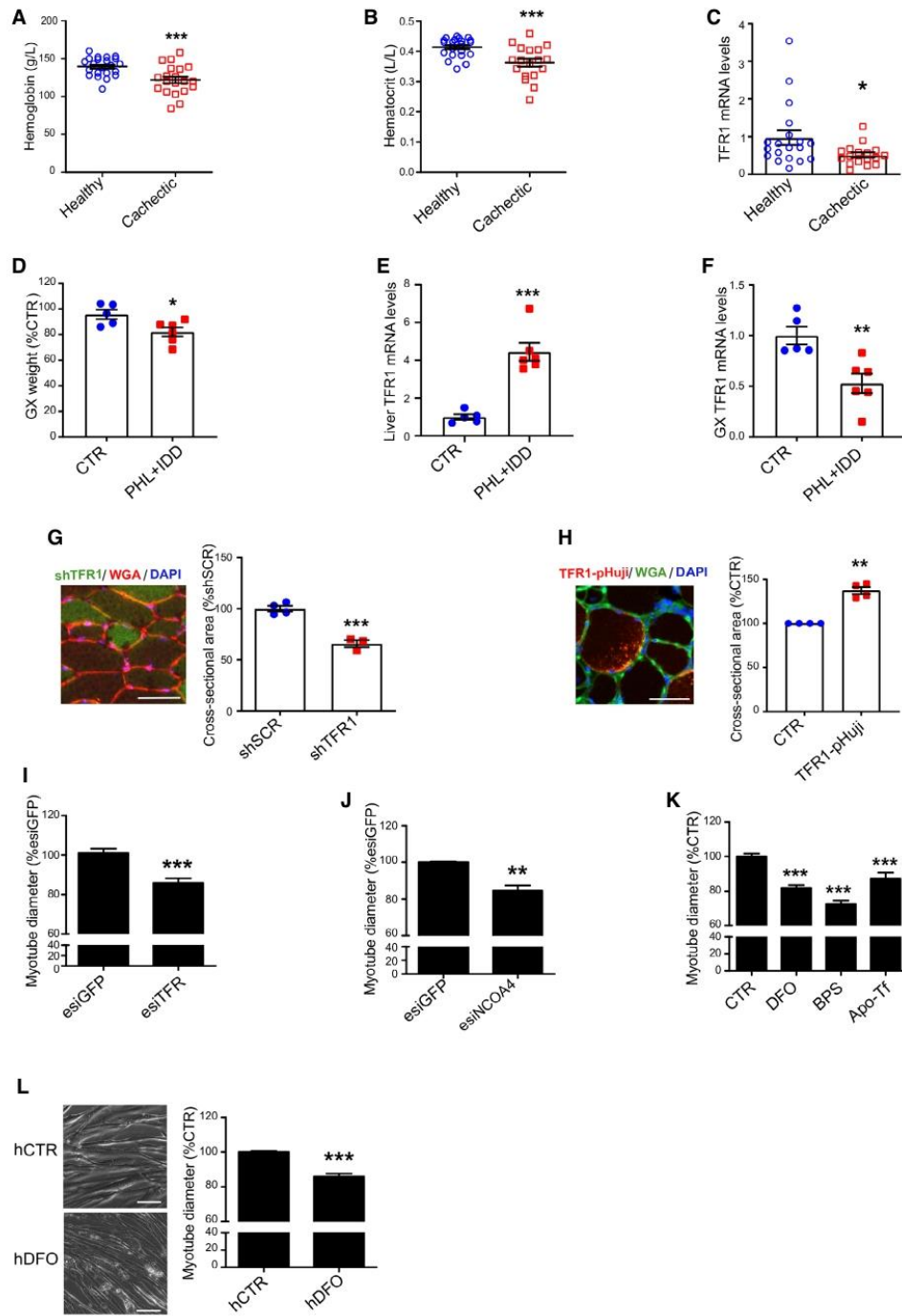Source data are available online for this figure.

Figure 1.

94

the C26-colon cancer model in Balb/C mice, which led to significant hematocrit reduction, total body weight loss, and muscle mass reduction (Figs 2A and EV2A–C). In line with the human data, cachectic mice showed a drastic reduction of TFR1 in the skeletal muscle (Fig 2B and C) despite no change in liver TFR1 or hepatic iron content (Fig EV2D and E), suggesting that the regulation of iron metabolism is organ-specific. Muscle TFR1 downregulation was

further confirmed in two different murine cachexia models, namely, LLC (Lewis Lung Carcinoma) and BaF3 (murine interleukin 3-dependent pro-B cell line) (Fig EV2F–K). Moreover, we assessed iron-sensing RNA-binding proteins mediating post-transcriptional regulation of iron metabolism in mammalian cells (Meyron-Holtz *et al*, 2004; Wang *et al*, 2020). We observed a decrease in cytosolic aconitase activity (hence a switch to iron-regulatory protein/IRP1)
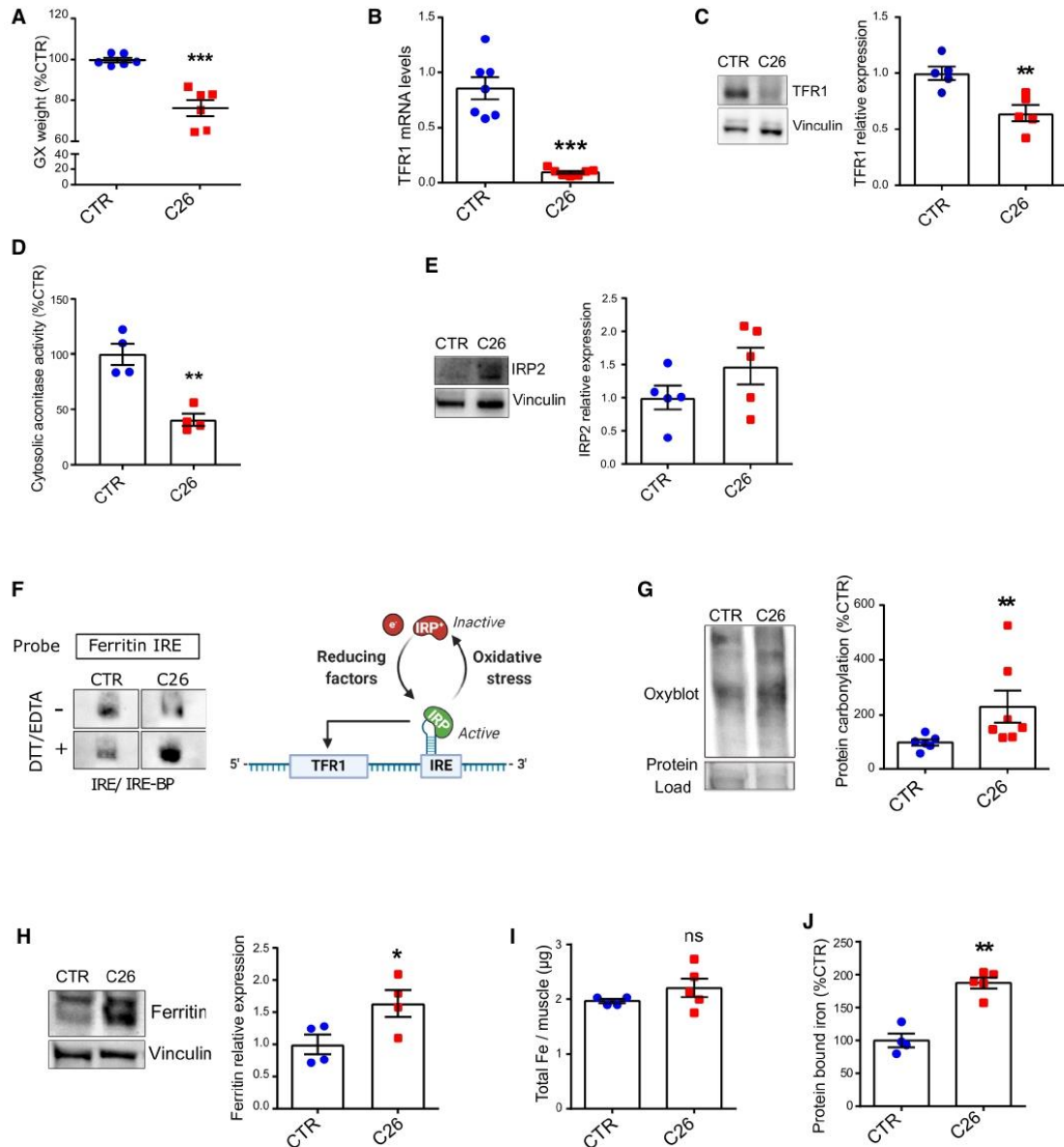

Figure 2.

Figure 2. Altered iron metabolism in the skeletal muscle is a feature of cancer-induced cachexia.

A   Gastrocnemius weight normalized to tibial length in C26 tumor-bearing mice on day 12 post C26-injection ($n = 6$–7).
B   TFR1 mRNA levels normalized to 18s ($n = 6$–7).
C   TFR1 protein expression and densitometric quantification in mouse gastrocnemius ($n = 5$).
D   Cytosolic aconitase activity in mouse quadriceps ($n = 4$) measured following subcellular fractionation ($n = 4$).
E   Representative Western blot of IRP2 in mouse gastrocnemius and densitometric quantification ($n = 5$).
F   Binding of IRE-BPs to the ferritin IRE. The biotin-labeled IRE probe was incubated with cytosolic gastrocnemius extracts from mice, in native or reducing conditions (with EDTA and DTT) ($n = 3$).
G   Representative protein carbonylation blot and densitometric quantification in mouse quadriceps ($n = 6$–7).
H   Representative Western blot of ferritin in mouse gastrocnemius and densitometric quantification ($n = 4$).
I, J   ICP-MS quantification of total (I) and protein-bound (J) iron in mouse quadriceps ($n = 4$–5).

Data information: For all data, n represents the number of biological replicates. Statistical significance was calculated by unpaired, two-tailed Student's *t*-test. Data are mean ± SEM. *$P < 0.05$, **$P < 0.01$, ***$P < 0.001$.
Source data are available online for this figure.

(Fig 2D), and an upregulation of iron-regulatory protein 2 (IRP2) (Fig 2E), indicating an iron-deficient state in the skeletal muscle of tumor-bearing mice. As IRP activity should drive TFR1 expression via iron-responsive element (IRE), we measured the activity of the IRE-IRP system in cachectic muscles by RNA electrophoretic mobility shift assay (REMSA). Despite the decreased aconitase function of IRP1 and the overexpression of IRP2, we observed a lower RNA-binding activity to the IRE site of ferritin (FT) in cachectic samples compared to control in native conditions (Figs 2F and EV2L). The phenotype appeared to be linked to protein oxidation. Indeed, by performing the assay in reducing condition, we evidenced the opposite pattern, with cachectic samples presenting a higher IRE-binding, suggesting an oxidative damage, which is known to negatively regulate IRP2 activity (Gehring *et al*, 1999). The oxidative stress in skeletal muscle of C26 tumor-bearing mice was further confirmed by upregulated protein carbonylation (Fig 2G). In addition, we observed an overexpression of FT (Fig 2H), which is in line with impaired IRP activity (Cairo *et al*, 1996). Coherently, cachectic muscles showed significantly increased protein-chelated iron despite no change in total iron content (Fig 2I and J).

Cachectic muscles are characterized by mitochondrial iron deficiency and impaired oxidative metabolism

In most cells, a major amount of iron is taken up by mitochondria for the production of ISCs and heme. In the skeletal muscle of C26 tumor-bearing mice, we found a significant reduction of mitochondrial iron and total heme content (Fig 3A and B), as well as upregulated levels of mitochondrial iron importer mitoferrin 2 (MFRN2) and of the rate-limiting enzyme of heme synthesis aminolevulinic acid synthase 2 (ALAS2) (Fig 3C and D) (Barman-Aksozen *et al*, 2019). Given that iron is essential for several enzymes involved in the TCA cycle and mitochondrial oxidative metabolism (OXPHOS) (Xu *et al*, 2013), we assessed the enzymatic activity of two iron–sulfur proteins, aconitase (ACO) and succinate dehydrogenase (SDH), and found a 50% reduction in the activity of both enzymes in cachectic muscles (Fig 3E and F). Along with these alterations, we observed a drop in mitochondrial ATP (Fig 3G) and increased AMPK phosphorylation, denoting mitochondrial dysfunction in cachectic muscles (Zhao *et al*, 2016) (Fig 3H). In summary, tumor-bearing mice display remarkable alterations in muscle iron metabolism coupled with mitochondrial dysfunction, which has been linked to muscle atrophy.

Iron supplementation prevents mitochondrial dysfunction and atrophy *in vitro*

In line with the *in vivo* data, we found considerably decreased mitochondrial DNA and proteins in myotubes treated with C26 conditioned medium (CM) (Fig 4A and B). To verify the hypothesis that cancer-associated iron shortage could cause mitochondrial dysfunction, a known feature of muscle atrophy (Liu *et al*, 2016), we supplemented atrophic C2C12-myotubes with iron. Iron supplementation fully rescued the C26 CM-induced reduction of the oxygen consumption rate (OCR) (Fig 4C–F), while showing no effect on control myotubes (Fig EV3A). Moreover, microscopic analysis confirmed that iron supplementation prevents C26-induced diameter decreased in both murine and human myotubes *in vitro* (Fig 4G and H). Noteworthy, although iron substantially increases the diameter of C26-treated myotubes over time, we observed no change in the fusion index, excluding a potential effect on myogenesis (Fig EV3B and C). Consistently with the C26 model, iron supplementation prevented other cancer CM- and activin A (ActA)-induced atrophy (Zhou *et al*, 2020) in murine myotubes (Fig EV3D and E). Similarly, normalization of iron levels using the iron–ionophore hinokitiol (Grillo *et al*, 2017) also rescued myotube atrophy induced by TFR1-silencing or C26 CM (Fig EV3F and G). Importantly, low-dose rotenone (complex 1 inhibitor) caused a mild atrophy that cannot be rescued by iron, indicating that the protective effects of iron are mediated by mitochondrial function (Fig 4I). Altogether, these data demonstrate that C26 CM treatment recapitulates the mitochondrial dysfunction observed *in vivo* (Fig 3), which can be fully rescued *in vitro* by iron supplementation.

Iron supplementation rescues skeletal muscle mass and mitochondrial function

To assess if iron supplementation could prevent cancer-induced muscle atrophy *in vivo*, C26 tumor-bearing mice were *i.v.* treated with ferric carboxymaltose (FeCM) every 5 days post C26 injection. Remarkably, intravenous injections of iron resulted in healthier (smooth fur, no orbital discharge, no humpback) and more physically active mice that survived far beyond the usually fatal 2 weeks (Fig 5A and B). Of note, iron improved notably the grip strength within 24 h (Fig EV4A) and the protection was preserved until the end-point of the experiment (Fig 5C), without affecting hematocrit (Fig EV4B). In addition, the loss of body weight and muscle mass occurring at day 12 after C26 injection was prevented in FeCM-
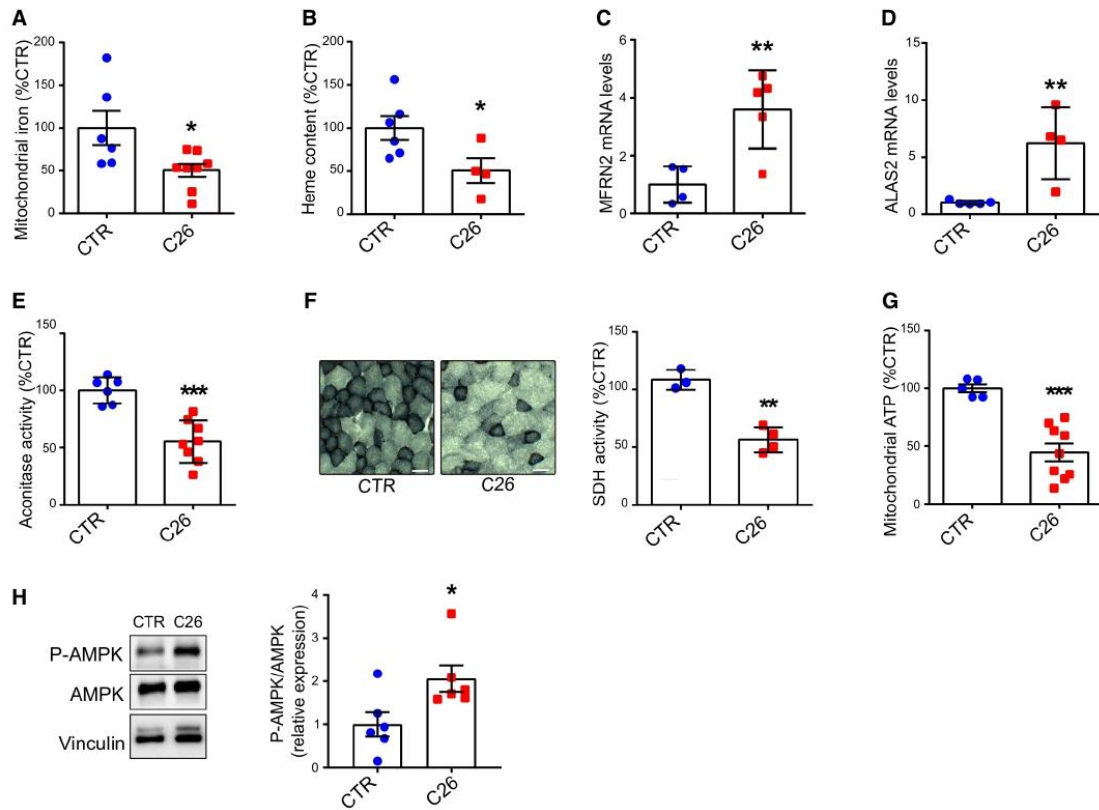
Figure 3. Cachectic muscles are characterized by mitochondrial iron deficiency and impaired oxidative metabolism.

A   ICP-MS quantification of mitochondrial iron in mouse quadriceps (n = 6–8).

B   Gastrocnemius heme content quantified by fluorescent heme assay (n = 4–6).

C, D   mRNA levels of mitochondrial iron importer MFRN2 (C) and the rate limiting enzyme of heme synthesis ALAS2 (D) normalized to 18s in mouse gastrocnemius (n = 4–5).

E   Aconitase activity in mouse quadriceps lysates normalized to protein content (n = 6–8).

F   Succinate Dehydrogenase activity staining in transversal sections of mouse gastrocnemius and corresponding intensity quantification (n = 3–4). Scale bar = 50 μm.

G   Mitochondrial ATP content in mouse quadriceps (n = 5–9).

H   Representative Western blot and densitometric quantification of phospho-AMPK and total AMPK in mouse gastrocnemius (n = 6).

Data information: For all data, n represents the number of biological replicates. Statistical significance was calculated by unpaired, two-tailed Student's t-test. Data are mean ± SEM. *P < 0.05, **P < 0.01, ***P < 0.001.

Source data are available online for this figure.

treated mice (Figs 5D–F and EV4C). Noteworthy, iron supplementation downregulated TFR1 in the tumor without affecting tumor growth (Figs 5E and EV4F). Consistently, immunostaining for myosin heavy chain revealed larger muscle fibers in the gastrocnemius of FeCM-treated mice, especially in the fast-twitch fibers, the most susceptible to atrophy (Fig 5G, in green). The protection from atrophy was further confirmed by the cross-sectional area (CSA) distribution, showing a shift toward bigger areas in FeCM-treated mice compared to C26 tumor-bearing, untreated animals, and the average CSA (Figs 5G and H, and EV4D and E). These findings were further

reinforced by a significant drop of FBXO32 (ATRO1), TRIM63 (MURF1), and DDIT4 (REDD1) mRNA levels, which are indicators of skeletal muscle atrophy (Fig 5I–K).

Iron supplementation refuels mitochondrial oxidative metabolism and energy generation

Since our findings *in vitro* indicate that iron can refuel mitochondrial metabolism and maintain myotube mass, we sought to validate our hypothesis *in vivo*. After verifying the replenishment of mitochondrial
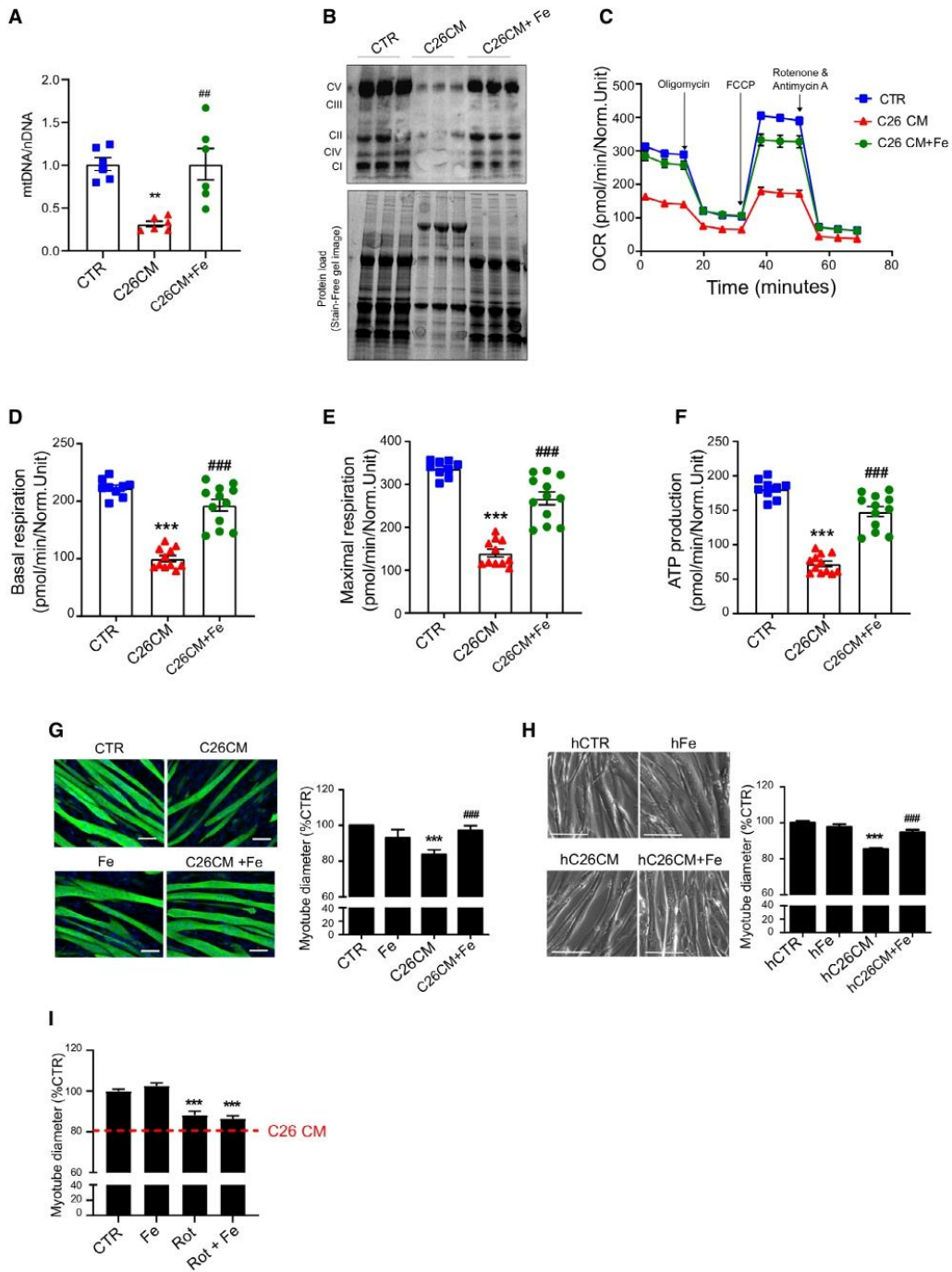
Figure 4.

98

iron in skeletal muscle (Fig 6A), we measured the activity of aconitase and succinate dehydrogenase and observed a significant recovery of enzymatic functionality following iron injection (Figs 6B and C, and EV4G). In agreement with these findings in mice showing restored mitochondrial metabolism upon iron treatment, we also found a significant increase in mitochondrial ATP content (Fig 6D) and coherently a drop in AMPK phosphorylation (Fig 6E). As AMPK drives fatty acid oxidation (FAO), which has been functionally linked to the cachectic process (Fukawa *et al*, 2016), we next evaluated the effect of iron injection on FAO. Consistently, iron supplementation reduced the C26-induced upregulation of FAO genes (Fig 6F–H). Altogether, these data indicate that iron supplementation of tumor-bearing mice mitigates energetic stress and catabolic pathways, which mediate the increase in muscle functionality and mass.

Iron supplementation improves muscle strength in cancer patients

Based on the results obtained in the pre-clinical model of cancer-associated muscle wasting, we measured the handgrip force in cancer patients with severe anemia, who reported muscle weakness, before and after FeCM injection (Table EV1). Improved strength was observed in the dominant hand of all patients, while more than half showed also increased force in the non-dominant hand (Fig 7A and B) as short as 3 days after the injection. Together with our data reporting TFR1 downregulation in the skeletal muscle of cachectic patients (Fig 1C), these findings indicate that altered iron metabolism may contribute to muscle weakness in cachectic patients. Consequently, these results highlight the contribution of iron on both muscle mass and functionality and suggest a new promising therapeutic strategy to counteract cancer-induced skeletal muscle wasting. Altogether, our findings show that iron supplementation prevents cancer-induced cachexia through a recovery of mitochondrial function (Fig 7C).

Discussion

Our study indicates iron as a key element of skeletal muscle mass homeostasis through the maintenance of mitochondrial function. In particular, we evidenced that cancer causes striking iron dysregulation in cachectic muscle, and that muscle wasting is reversible by iron supplementation. Despite being the biggest tissue in the human body, the involvement of skeletal muscle in systemic iron homeostasis has been generally neglected. Nevertheless, skeletal muscle holds a substantial pool of iron that can be mobilized, as demonstrated by its ability to support erythropoiesis in healthy humans during high-altitude hypoxia (Robach *et al*, 2007). Since iron deficiency and anemia are common in cancer patients (Ludwig *et al*, 2013) and are associated with several features of cachexia, such as impaired physical function, weakness, and fatigue, we hypothesized a link between altered iron metabolism and muscle wasting. We found that iron deficiency, either cancer-induced or obtained with iron chelators, disrupts iron homeostasis in the skeletal muscle and leads to muscle atrophy in different murine models. Surprisingly, atrophic muscle paradoxically downregulate the iron importer TFR1 despite the lack of iron, highlighting the role of skeletal muscle as an expendable body compartment. Similarly, we found a consistent decrease of TFR1 in late-stage anemic cancer cachexia patients while it has also been reported that chemotherapy negatively affects TFR1 levels in the skeletal muscle (Hulmi *et al*, 2018). TFR1 emerges as a direct player in muscle mass homeostasis, as we show that its expression is sufficient *per se* to regulate myofiber size *in vivo*. These data are also supported by previous work on muscle-specific TFR1 KO mice which displayed severe systemic metabolic dysfunction (Barrientos *et al*, 2015). Intriguingly, skeletal muscle from C26 tumor-bearing mice combine typical hallmarks of iron deficiency (*i.e.*, IRP2 upregulation, decrease in both cytosolic and mitochondrial aconitase activity, and mitochondrial iron) with the ones of iron overload (*i.e.*, TFR1 downregulation, increase in ferritin, and in protein-bound iron). Such discrepancy can be explained by the impaired IRE-IRP system, due to a significant oxidative damage, which can be reversed by reducing conditions *ex vivo* (Cairo *et al*, 1998; Mikhael *et al*, 2006). Consequently, cachectic muscles sequestrate intracellular iron, downregulate its import despite the need for iron. This phenotype matches the observations reported in several IRP2 knockout models (Meyron-Holtz *et al*, 2004; Galy *et al*, 2010; Li *et al*, 2018). To understand whether the resulting inadequate levels of iron impact muscle fitness, we focused on the *in vitro* myotube model (both murine and human). Importantly, iron deprivation in myotubes, induced by TFR1 or NCOA4 knockdown, apotransferrin, DFO, or BPS treatment was sufficient to trigger atrophy, whereas iron replenishment proved to be protective against conditioned medium-induced atrophy. Thus, we speculated that iron availability directly influences muscle mass. To this aim, we used ferric carboxymaltose (FeCM), a clinically approved supplement (Scott, 2018) known to enter in cells regardless of TFR1 expression (Marone *et al*, 1986). Surprisingly, intravenous

administrations of FeCM rescued body mass, muscle mass and function, and even increased the viability of tumor-bearing mice, in accordance with a previous study demonstrating that preventing

muscle loss in cachexia resulted in longer survival (Zhou *et al*, 2010). From the mechanistic standpoint, our *in vitro* data shows that iron supplementation refuels mitochondrial function. The
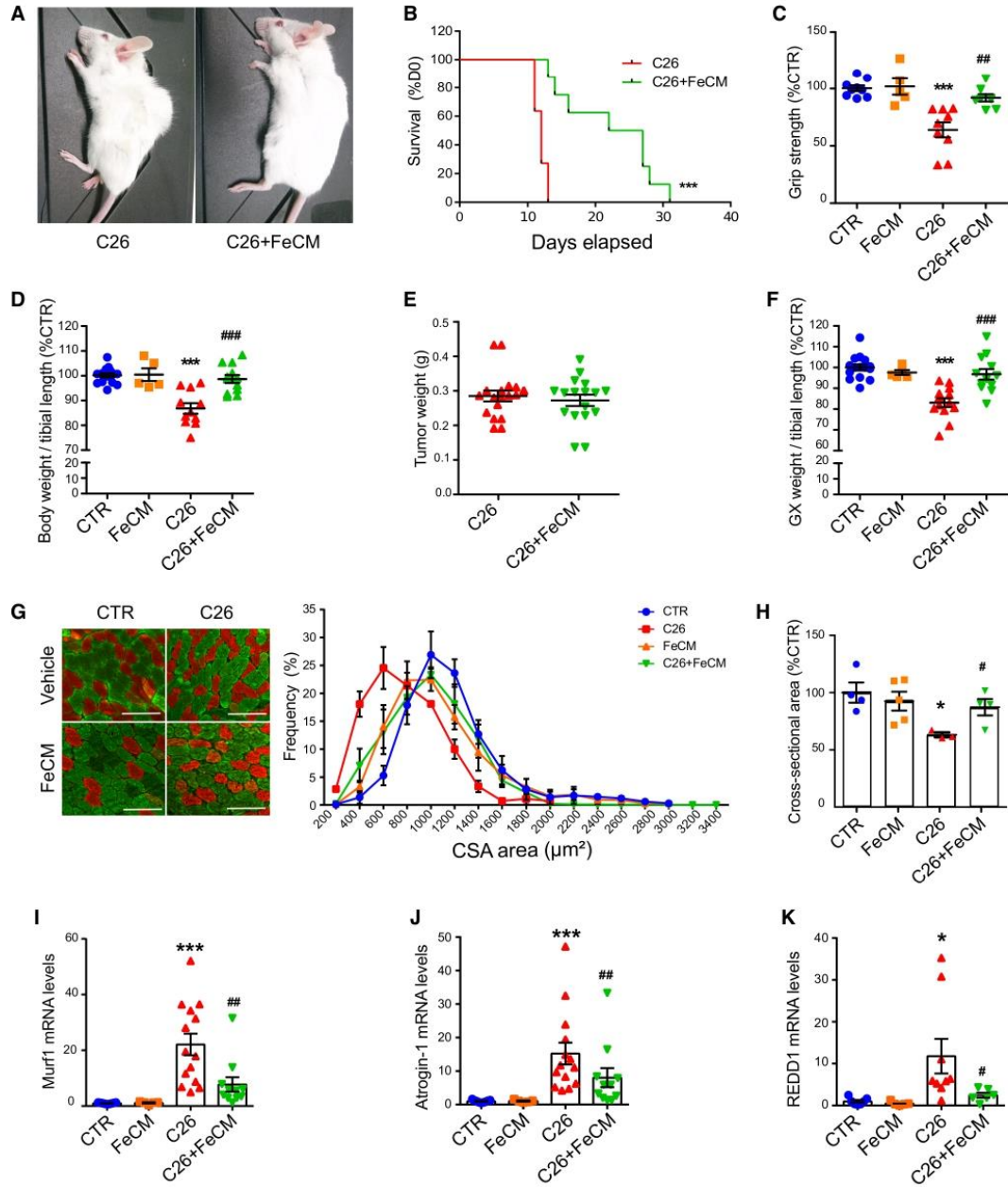

Figure 5.

100

Figure 5. Iron supplementation prevents cancer-induced cachexia.

A   Representative images of C26 tumor-bearing mice receiving saline solution (left) or FeCM 15 mg/kg I.V. injection (right) taken at day 12 after C26 injection.
B   Kaplan–Meier depicting the survival of C26 tumor-bearing mice after I.V. injection of saline or iron every 5 days post C26-injection (3-month-old Balb/C, *n* = 8–11).
C   Grip strength of mice measured at day 12 post C26 injection, normalized to average strength of the control group (*n* = 5–9).
D   Final body weight of C26 tumor-bearing mice after iron supplementation at day 12 post C26 injection (*n* = 5–12).
E   Final weight of total tumor mass extracted from mice after sacrifice (*n* = 17).
F   Gastrocnemius weight normalized to tibial length of C26 tumor-bearing mice after iron supplementation at day 12 post C26 injection (*n* = 5–12).
G, H   Immunofluorescent staining of myosin heavy chain fast (green) and slow (red) of transversal sections of gastrocnemius (midbelly) with corresponding frequency distribution (G) and average cross-sectional areas (H) (*n* = 3–5). Scale bar = 100 μm.
I–K   mRNA levels of Murf 1 (I), Atrogin 1 (J), and REDD1 (K) normalized to GAPDH in gastrocnemius (*n* = 5–14).

Data information: For all data, *n* represents the number of biological replicates. Statistical significance was calculated by one-way Anova with Bonferroni's correction, or chi-square test for the survival curves (B). Data are mean ± SEM. *$P < 0.05$ and ***$P < 0.001$ compared to control and #$P < 0.05$, ##$P < 0.01$, ###$P < 0.001$ compared to C26-untreated group.
Source data are available online for this figure.

upregulation of MFRN2 and ALAS2 could be interpreted as a compensatory response of the skeletal muscle to mitochondrial iron deficiency. In particular, ALAS2 overexpression has been associated to muscle weakness and atrophy in transgenic mice (Peng *et al*, 2021). Indeed, mitochondrial dysfunction has been functionally linked to wasting, both in pathological conditions (Romanello *et al*, 2010) and aging (Tezze *et al*, 2017; Palla *et al*, 2021), while an increasing pool of data associates declined oxidative metabolism with muscle myopathies (Dziegala, 2018). Notably, cardiac iron concentration inversely correlated with disease severity in non-ischemic heart failure patients (Hirsch *et al*, 2020). Of note, iron is essential for mitochondrial function (Levi & Rovida, 2009) as it catalyzes several bioenergetic processes and its deprivation causes impaired mitochondrial biogenesis, enhanced mitophagy as well as metabolic dysfunction (Allen *et al*, 2013; Rensvold *et al*, 2013; Bastian *et al*, 2019).

We specifically found in cachectic mice that reduced mitochondrial iron content impairs mitochondrial activity and promotes AMPK phosphorylation, reflecting increased catabolism. The oxidative stress generated by dysfunctional mitochondria might reinforce iron dysregulation via IRPs inhibition, creating a vicious cycle. Furthermore, mitochondrial dysfunction is known to trigger catabolic pathways, notably FAO (Romanello & Sandri, 2015) that has been widely associated with skeletal muscle wasting (Brown *et al*, 2017; Abrigo *et al*, 2019). Our results pointed at two major ISC proteins of the TCA cycle and electron transport chain that have strongly reduced enzymatic activities, aconitase, and SDH, corroborating with the decreased oxidative capacities and energetic inefficiency as features of cachexia (Argiles *et al*, 2014; Neyroud *et al*, 2019). This confirms and extends studies showing that iron deficiency decreases ISC proteins, cytochrome content, and total oxidative capacity in cancer cachexia (Maguire *et al*, 1982; Oexle *et al*, 1999; Leermakers *et al*, 2020). Our data indicate that adequate iron supply restores mitochondrial function, as reflected by ATP production increase, AMPK deactivation, and FAO reduction.

Noteworthy, iron-induced muscle protection was independent from tumor growth, as iron supplementation did not alter tumor volume. This observation is in line with the fact that C26 tumors do not show iron addiction and respond to iron supplementation by downregulating the iron-import machinery.

Of note, consistent with the *in vitro* data of rapid mitochondrial metabolism rescue, the beneficial effects of iron injection *in vivo* were unexpectedly fast as muscle strength was improved within 24 h. The rescue is therefore unlikely due to muscle stem cell differentiation/regeneration or erythropoiesis. In line with this hypothesis, anemia remained after iron supplementation in C26 tumor-bearing mice.

Although we found that iron supplementation can restore muscle mass homeostasis, both *in vitro* and *in vivo*, we do not exclude other systemic effects of iron repletion, for example liver (Klempa *et al*, 1989) and adipose tissue function (Gao *et al*, 2015), or immune system modulation (Serra *et al*, 2020), which might contribute to the increased survival but require further studies. However, our *in vivo* electroporation data show that TFR1 levels can directly influence myofiber size in healthy mice, without confounding systemic factors such as inflammation. Coherently, our preliminary data from iron-deficient patients demonstrated an improvement of handgrip strength within a few days after iron treatment, excluding the potential involvement of erythropoiesis, while previous data on cardiac failure patients showed beneficial effects after long-term treatment (Jankowska *et al*, 2016). Nevertheless, this is a very preliminary study on a limited number of patients who required iron supplementation because of iron-deficiency anemia; hence they lack a placebo group. Further studies will be essential to better define the impact of short-term iron treatment on patients, including a control group, as well as the impact on blood parameters a few days following supplementation.

Our findings corroborate with the assumption that iron deficiency causes metabolic dysfunction and energy insufficiency in skeletal muscle (Dziegala *et al*, 2018). Indeed, both iron deficiency (Leermakers *et al*, 2020) (Higashida *et al*, 2020) and iron overload (Alves *et al*, 2021) are detrimental to muscle physiology. Previous work suggested that excessive iron could underlie muscle loss in sarcopenic gastric cancer patients (Zhou *et al*, 2020). However, our study indicates that the distribution of iron rather than its total amount influences muscle homeostasis. Notably, we show that the total amount of iron is not changed in cachectic muscle compared to healthy controls in our C26 model, but it is mostly sequestered in the cytosol and lacking in the mitochondria. While we confirmed the phenotype of altered iron metabolism in several wasting models (related to cancer or not), the beneficial effects of iron supplementation remain to be validated in other cancer models given that some cancer types would rely more on iron than others (Hsu *et al*, 2020).
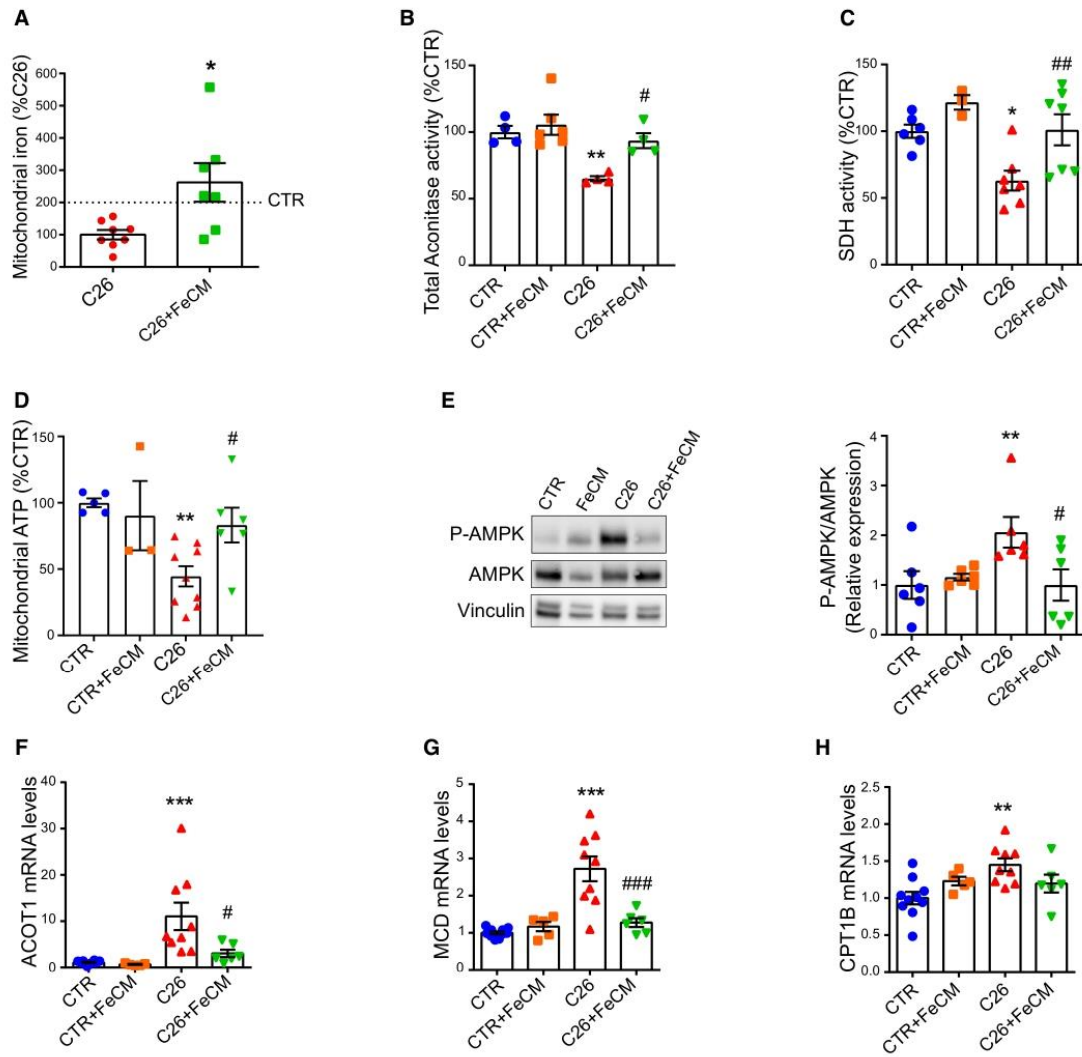
Figure 6. Iron supplementation rescues mitochondrial function.

A   Mitochondrial iron quantified by ICP-MS in quadriceps of C26 tumor-bearing mice after FeCM supplementation ($n = 7$–8).
B   Aconitase activity of quadriceps lysates normalized to protein content ($n = 3$–7).
C   Succinate Dehydrogenase activity staining of gastrocnemius transversal sections and resulting intensity quantification ($n = 3$–7).
D   Mitochondrial ATP content determined by luminescence assay in quadriceps ($n = 3$–9).
E   Representative Western blot and densitometric quantification of phospho-AMPK and total AMPK (stripped and re-blotted) in the gastrocnemius of C26 tumor-bearing mice after iron carboxymaltose supplementation ($n = 6$).
F–H   mRNA levels of ACOT 1 (F), MCD (G), and CPT1B (H) normalized to GAPDH in gastrocnemius ($n = 5$–10).

Data information: For all data, *n* represents the number of biological replicates. Statistical significance was calculated by unpaired, two-tailed Student's *t*-test. Data are mean ± SEM. *$P < 0.05$, **$P < 0.01$, ***$P < 0.001$ compared to control and #$P < 0.05$, ##$P < 0.01$, ###$P < 0.001$ compared to C26-untreated group.
Source data are available online for this figure.

Figure 7. Iron supplementation improves muscle function in iron deficient cancer patients.

A, B Grip force of dominant or non-dominant arm in iron-deficient cancer patients, expressed in percentage of baseline force (A) and absolute values normalized to height (B) before/after single dose of iron carboxymaltose (15 mg/kg, 7 subjects).

C Working model: C26 tumor-bearing mice present alterations of key iron metabolism proteins such as the downregulation of TFR1 and the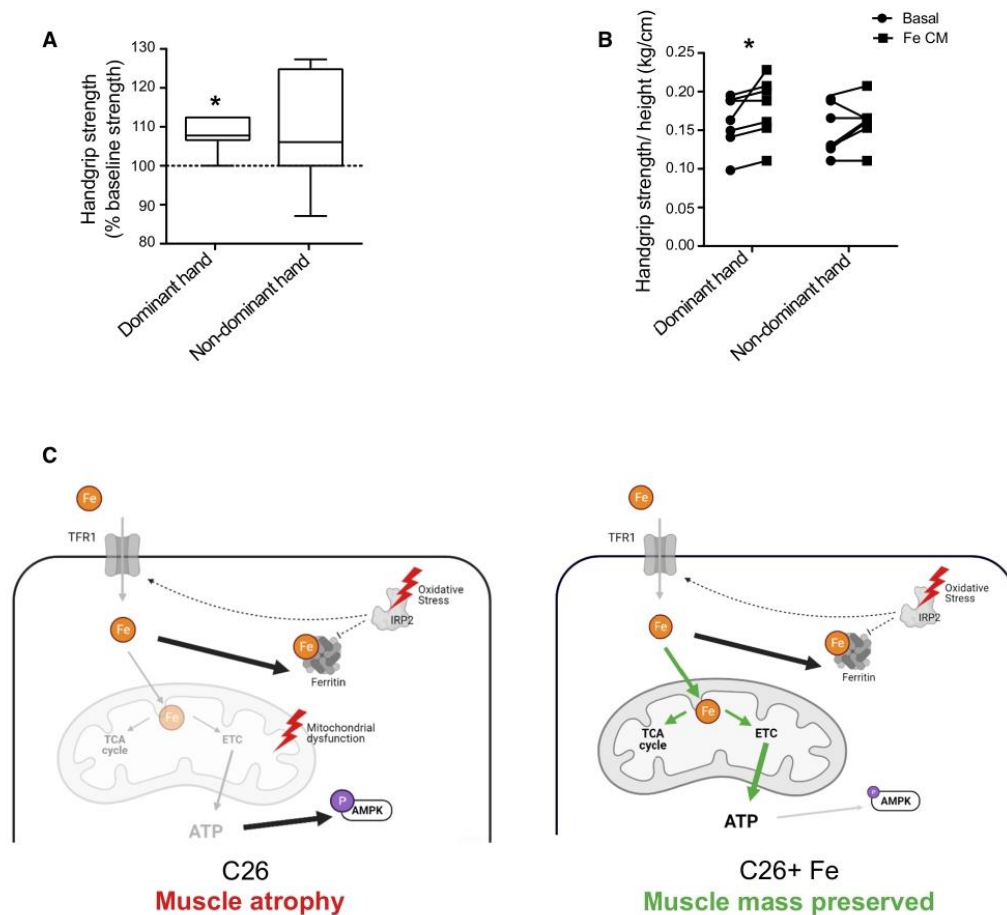 upregulation FT in the skeletal muscle. Decreased cytosolic aconitase activity and the stabilization of IRP2 indicate a low iron status. However, IRP activity is hampered by oxidative stress and is no longer able to regulate TFR and FT (indicated by dashed lines). As a consequence, mitochondrial iron loading is low, and the decrease activity of iron-dependent enzymes negatively affect the TCA cycle and the electron transport chain, resulting in decreased ATP production, AMPK activation, and muscle atrophy. Iron supplementation replenishes the mitochondrial iron pool and prevents mitochondrial dysfunction. Notably, it restores TCA cycle and electron transport chain activity resulting in higher ATP production, deactivation of AMPK, and preserved muscle mass.

Data information: For all data, *n* represents the number of biological replicates. Statistical significance was calculated by paired, one-tailed Student's *t*-test. Data are mean ± SEM. *$P < 0.05$. In graph (A), the boxes represent the range of values with the median value being the central band and whiskers the SEM.

In conclusion, our findings establish a direct role of iron availability in the control of skeletal muscle mass. Therefore, iron supplementation restores skeletal muscle homeostasis via mitochondrial metabolism normalization, paving the way for a new therapeutic strategy to fight muscle atrophy in cachectic patients, but also in non-cancer conditions presenting iron deficiency as co-morbidity, such as COPD and chronic cardiac failure.

Materials and Methods

Human skeletal muscle biopsies

The study enrolled patients (age > 18 years) with pancreatic cancer surgically treated at the 3rd Surgical Clinic of Padova University Hospital. Cancer patients were classified as severely

103

cachectic in cases of > 10% weight loss in the 6 months preceding surgery.

The study also enrolled control, healthy donors undergoing elective surgery for non-neoplastic and non-inflammatory diseases. Patients with signs of infection were excluded. All patients joined the protocol according to the guidelines of the Declaration of Helsinki and the research project has been approved by Ethical Committee for Clinical Experimentation of Provincia di Padova (protocol number 3674/AO/15). Written informed consent was obtained from participants. From all patients a blood sample was retrieved prior to any surgical manipulation and the biopsies were performed during elective surgery within 30 min of the start of the surgery by cold section of a rectus abdominal fragment of about 0.5–1 cm. The fragment was immediately frozen and conserved in liquid nitrogen for gene expression analysis.

Human handgrip strength

Participants with either an absolute iron deficiency (AID) or a functional iron deficiency (FID) were included in the clinical study. AID is defined by an iron-saturation of transferrin (TSAT) < 20% and serum ferritin level < 30 ng/ml. FID is defined by a TSAT < 20% and serum ferritin levels above 30 ng/ml. Patients were treated with a single infusion of 1,000 mg of iron intravenously (ferric carboxymaltose).

The participants were asked to perform two handgrip tests to measure their strength using a hand dynamometer. The first handgrip test (HG1) was conducted prior to iron administration. The second handgrip test (HG2) was conducted within 2–12 days after the iron IV administration.

The hand dynamometer was calibrated and the measurements have an accuracy of +/− 5%. The test–retest reliability is good ($r > 0.80$) and the inter-rater reliability is excellent ($r = 0.98$).

The handgrip test required the participants to be seated, positioning their forearm of their hand in a 90° angle with their body. The arm should not be pressed to the body or supported by an armrest and the shoulders should be relaxed. The grip of the hand dynamometer was adjusted to the hand size of the participant. The hand dynamometer was placed in the dominant hand and the participant was asked to squeeze the hand dynamometer as hard as possible until the strength indicator was stabilized (this took approximately 3–5 s). This was repeated three times, in between each measurement the participant was given 30 s to relax the arm and hand muscles.

All participants gave written informed consent to participate in the study and the study was approved by the Antwerp University Hospital ethical committee in accordance with the ethical standards established by the 1964 Declaration of Helsinki.

Animal experimentation

All animal experiments were authorized by the Italian Ministry of Health and carried out according to the European Community guiding principles in the care and use of animals. The BaF experiments performed in Belgium were approved by and performed in accordance with the guidelines of the local ethics committee from the UCLouvain, Belgium. Housing conditions were as specified by the Belgian Law of 29 May 2013, regarding the protection of laboratory animals. In all experiments, female littermates of 8–10 weeks were assigned randomly to experimental groups. Cancer cell lines (C26 colon murine adenocarcinoma and LLC Lewis lung carcinoma, 1×10^6 cells/mouse) were injected subcutaneously in the flank of 8-weeks-old female mice (BALB/C for C26, C57 BL/6 for LLC). Baf3 cachexia was induced as previously reported (Bindels *et al*, 2012), injecting Bcr-Abl-transfected Baf3 intravenously in 6-weeks-old Balb/C mice. LLC (Lewis Lung Carcinoma) tumor-bearing mice were necropsied at day 24. For C26, to compare the various treatment all mice were necropsied at day 12, except for the survival experiment. Electroporation experiments were performed as previously described (Sartori *et al*, 2021) on tibialis anterior muscle with pHuji-TFR1 plasmid (Addgene 61505) or shTFR-GFP plasmid using BLOCK-iT PolII miR RNAi expression kit (Thermo Fisher K493600).

Ferric carboxymaltose (Ferrinject 15 mg/kg, Vifor Pharma) or saline solution (NaCl 0.9%) was injected in the tail vein every 5 days starting from day 5 post-C26 inoculation. Blood was collected by cardiac puncture, and perfusion with PBS after anesthesia was performed to obtain samples for iron quantification. For the phlebotomy experiment, retroorbital bleeding (400 μl of blood) was performed under anesthesia, and mice were fed with iron-deprived diet (Mucedola) for 11 days before sacrifice. To measure strength, mice were held by the middle part of the tail and allowed to grab the metal grid of a dynamometer (2Biol) in a parallel position before being gently pulled backward. The maximal force generated by the grip was recorded, and the measure was repeated six times. To quantify muscle wasting, gastrocnemii and quadriceps were freshly isolated, weighted, and normalized to the respective tibial length.

Cell culture and *in vitro* treatments

C2C12 myoblasts were purchased from ATCC and cultured in DMEM with 10% fetal bovine serum (FBS). After reaching full confluency, differentiation was induced by switching to 2% horse serum (HS) DMEM for 4 days. Human myoblast cell line, originated from the quadriceps of a 38-year-old male donor. The cells were cultured in Skeletal Muscle Cell Basal Medium (PromoCell, Heidelberg, Germany) containing 5% FBS and supplemented with hbFGF, hEGF, fetuin, insulin, and dexamethasone. Differentiation was induced by switching to DMEM containing 10 μg/ml insulin, gentamicin 1% (Gibco) for 7 days.

Conditioned medium (CM) was prepared as previously described (Wyart *et al*, 2018). Briefly, cancer cells were grown to high confluency, then conditioned in serum-free DMEM for 24 h, medium was harvested and centrifuged at 500 *g* for 10 min. Supernatant was collected and used as CM at 10% final concentration. Deferoxamine (DFO, Sigma D9533) and bathophenanthroline disulfonic acid (BPS, Sigma 146617) were used at 100 μM. Apotransferrin (Sigma T0178), Hinokitiol (HNK, Sigma 469521), and ferric citrate (Sigma F3388) were used at 400 μg/ml, 5 μM, and 250 nM, respectively. Activin A (RnD Sytem 338-AC) and Dexamethasone (DEXA, Sigma D4902) were used at 1 nM and 1 μM, respectively. Rotenone was used at 20 nM. Myotubes were treated for 48 h for all compounds. For cell transfection, C2C12 myoblasts were differentiated for 3 days prior to transfection with esiTFR1, esiNCOA4, or esiGFP (250 ng/ml) using Lipofectamine 2000 (Invitrogen 11668019). Myotubes were photographed and lysed at 72 h post-transfection. For myotube diameter quantification, pictures of

myotubes were taken with phase contrast microscopy (Zeiss) at 20× magnification, and myotube diameter was measured using the software JMicroVision as previously described (Murata et al, 2018).

Western Blotting

Frozen gastrocnemius samples were lysed in RIPA lysis buffer (150 mM of NaCl, 50 mM of Tris-HCl, 0.5% sodium deoxycholate, 1% Triton X-100, 0.1% SDS, and 1 mM of EDTA) supplemented with protease and phosphatase inhibitor cocktail (Roche). Protein concentration was determined using BCA assay (Thermo Fisher Scientific). Fifteen or thirty micrograms of protein from cell or gastrocnemius lysates, respectively, were loaded per well on Mini-Protean TGX Stain-Free precast polyacrylamide gels (Bio-rad) for SDS-PAGE. Stain-Free imaging was performed using Chemidoc MP imager in order to visualize total protein patterns. Proteins were then transferred onto PVDF membranes prior to immunoblotting analysis. Blots were probed with the following primary antibodies: P-Thr172-AMPK (Cell Signaling 2535), Total-AMPK (Cell Signaling 2532), Ferritin (Sigma F5012), IRP2(PA-116544), Transferrin Receptor 1 (Santa Cruz sc65882), NCOA4 (Santa Cruz C-4), OxPhos cocktail (Thermofisher 8199), Ferroportin (Novus NBP1-21502), Vinculin (Cell Signaling 4650). Protein carbonylation was assessed by measuring the levels of carbonyl groups using the OxyBlot protein oxidation detection kit (Sigma-Aldrich S7150). Quantification analysis of blots was performed with Image Lab software (BioRad).

Iron quantification and Heme assay

Iron content in skeletal muscle was quantified by ICP-MS (Element-2; Thermo-Finnigan, Rodano, Italy) using medium mass resolution (M/ΔM ~4,000). Fifty to hundred milligrams of freshly excised and snap-frozen quadriceps were submitted to overnight dialysis. Samples were collected before and after dialysis to assess total and protein-bound iron, respectively. Additionally, iron content was also measured in isolated mitochondria from quadriceps. All samples were digested overnight in 0.5 ml of concentrated HNO_3 (70%) and mineralized by microwave heating for 6 min at 150°C (Milestone, Ethos Up Microwave Digestion System). A natural abundance iron standard solution was analyzed in parallel in order to check for changes in the systematic bias. The calibration curve was obtained using four iron standard solutions (Sigma-Aldrich) in the range of 0.2–0.005 μg/ml. For liver and spleen iron, samples were heated at 180°C overnight and mineralized in 10 ml of HCl 3 M/ 10% trichloroacetic acid per gram of dry tissue overnight at 65°C with gentle shaking. 10 μl of supernatants were mixed with a solution of 1.7% of thioglycolic acid (TGA), 84.7% of sodium acetate acetic acid pH 4.5, 13.6% of BPS (Sigma 146617). After 1 h of incubation at 37°C, absorbance was measured at 535 nm. Iron content was determined using a standard curve of ferrous ammonium sulfate. Heme concentration was determined by fluorescence assay as previously described (Sinclair et al, 2001). Saturated oxalic acid solution was added to 40 μg of proteins from gastrocnemius lysates prior to heating at 95°C for 30 min. Samples were loaded in triplicates and fluorescence was measured at 400 nm excitation and 662 nm emission wavelengths.

Intracellular labile iron pool was measured as previously described with modifications (Schoenfeld et al, 2017). Briefly, C2C12 cells were treated with 500 nM Calcein AM (Sigma 56496) for 15 min and fluorescence intensity was measured using a microplate reader. Cells were then incubated for 15 min with 100 μm of 2′,2′-Bipyridyl (BIP) prior to the second measurement of fluorescence. The LIP was calculated as following : LIP (A.U) = MFI after BIP − MFI before BIP. The obtained value were normalized on DAPI fluorescence intensity.

Mitochondria isolation and metabolic assays

Mitochondria were isolated from snap-frozen quadriceps by Mitocheck Mitochondrial Isolation kit (Cayman chemical 701010). ATP content was quantified in 20 μg of fresh isolated mitochondria by CellTiter-Glo® Luminescent Cell Viability Assay (Promega G7570). Aconitase activity was measured in quadriceps homogenates by enzymatic assay (Cayman Chemical 705502). Oxygen Consumption Rate (OCR) measurements were conducted using a Seahorse XFe96 analyzer according to manufacturer's protocol. C2C12 cells were directly differentiated in XFe96 cell culture plates and treated with 10% C26 CM, ferric citrate 250 nM, or the combination of both for 48 h and incubated in 5% CO_2 at 37°C. One hour prior to analysis, growth medium was replaced with assay medium (DMEM without phenol red and sodium bicarbonate (Corning 90-013-PB) that was supplemented with 1 mM of pyruvate, 2 mM of L-glutamine, and 10 mM of glucose, pH 7.4) and incubated in a non-CO_2 incubator. During assay, 1 μM of oligomycin (Sigma 495455), 1 μM of FCCP (Sigma C2920), and 0.5 μM of rotenone/antimycin A (Sigma R8875 and A8674) were sequentially injected into each well in accordance with standard protocols. Absolute rates (p moles/min) were normalized to μg of protein determined by Bradford Assay (BioRad 5000006).

Histology

Extracted gastrocnemii were immediately frozen in isopentane cooled in liquid nitrogen and stored at −80°C. Transversal sections of 5 μm thickness were cut at the midbelly with a cryostat. Sections were fixed for 10 min in PFA 4%, then blocked with 0.1% triton x-100, 1% BSA in PBS before incubating with primary antibodies against fast/slow isoforms of myosin heavy chain and laminin (Abcam 91506, Abcam M8421, Santa Cruz 59854), followed by incubation with the corresponding secondary antibodies (Alexa-488, Alexa-568). For the electroporation of tibialis anterior with reporter plasmids, 8 μm cryosections were stained with AlexaFluor 555-conjugated Wheat Germ Agglutinin (WGA, Thermo Fisher Scientific W32464) and DAPI. Pictures were taken with a fluorescent microscope and fiber areas were measured with ImageJ software (more than 500 fibers were analyzed per animal). The enzymatic activity of succinate dehydrogenase (SDH) was assessed on cryosections using the Succinic Dehydrogenase Stain (Bio-Optica, 30–30114LY) according to manufacturer's instructions.

RNA isolation and quantitative PCR

Total RNA was isolated from snap-frozen tissue samples using TRIzol reagent (Invitrogen 15596026) according to the manufacturer's guidelines. 1 μg of total RNA was reverse-transcribed using the High Capacity cDNA Reverse Transcriptase kit (Applied Biosystems 4374966). cDNA was analyzed by Real Time Quantitative PCR

(ABI PRISM 7900HT FAST Real-Time PCR system, Applied Biosystems) using the Luna Universal Probe qPCR master mix (NEB M3004) and the Universal Probe Library system (Roche Applied Science), or with SYBR Green master mix (Applied Biosystems A25741). Relative mRNA levels were calculated using the 2-ΔΔCT method and normalized to GAPDH or 18s mRNA (Eukaryotic 18s rRNA Endogenous Control, Thermo Fisher 4310893E), respectively. For human skeletal muscle biopsies, 500 ng of RNA was reverse transcribed using SuperScript IV Reverse Transcriptase (Thermo Fisher 18090010). Human data were all normalized to Actb gene expression. The following primers were used:

Gene	Forward sequence (5′–3′)	Reverse sequence (5′–3′)
Human TFR1	aggaaccgagtctccagtga	atcaactatgatcaccgagt
Human ACTB	gggaaatcgtgcgtgaca	ggactccatgcccagga
mTFR1	tcctttccttgcatattctgg	ccaaataaggatagtctgcatcc
mMFRN2	tgtgtggcgacattacttcat	gcatcctctgcttgacgact
mALAS2	ctcaccgtctttggttcgtc	ggacaggaccgtagcaacat
mATRO1	agtgaggaccggctactgtg	gatcaaacgcttgcgaatct
mMURF1	tgacatctacaagcaggagtgc	tcgtcttcgtgttccttgc
mREDD1	ccagagaagagggccttga	ccatccaggtatgaggagtctt
mCPT1B	aagagaccccgtagccatcat	gacccaaaacagtatcccaatca
mACOT1	caactacgatgacctcccca	gagccattgatgaccacagc
mMCD	gcacgtccgggaaatgaac	gcctcacactcgctgatctt
mGAPDH	aggtcggtgtgaacggatttg	tgtagaccatgtagttgaggtca

RNA electrophoretic mobility shift assay (REMSA)

The fractionation method described by Rothermel *et al* (2000) was adopted with minor modification to extract the cytosolic protein fractions from gastrocnemius muscle. Briefly, after removal of connective tissues, muscle samples were homogenized for 1 min in ice-cold lysis buffer (25 mM of Hepes pH 8, 5 mM of KCl, 0.5 mM of $MgCl_2$, 1% NP-40, 1× protease inhibitors) using a tight-fitting Teflon pestle attached to a Potter S homogenizer (Sartorius Stedium) set to 1,000 rpm. Following centrifugation at 800 *g* for 15 min at 4°C to pellet the nuclei and cell debris, the supernatants were collected, subjected to further centrifugation three times at 500 *g* for 15 min at 4°C to remove residual nuclei and used for the REMSA as nuclei-free total cytosolic protein fractions. The IRP-IRE interactions were performed using the LightShift Chemiluminescent RNA Electrophoretic mobility shift assay kit (REMSA, Thermo Fisher 20148). Briefly, 20 μl of reaction containing nuclease-free water, 5×REMSA Binding Buffer (50 mM of Tris-HCl pH 8.0, 750 mM of KCl, 0.5% Triton-X 100, 62.5% glycerol), tRNA (Thermo Fisher 20158), 6 μg of muscle cytosolic extracts, biotinylated and unlabeled ferritin probe 5′–UCCUGCUUCAACAGUGCUUGGACGGAAC–3′ and where indicated, 0.5 mM of EDTA and 1 mM of DTT, were incubated for 30 min at room temperature. Afterward, the samples were carefully mixed with 5 μl of 5×REMSA Loading Buffer and resolved on 6% polyacrylamide gel and transferred on to nylon membrane (Roche Diagnostics, Indianapolis, IN). After the membrane was cross linked with UV-light, the IRP-IRE complexes were visualized by the chemiluminescent nucleic acid detection module (Thermo Fisher 20158).

mtDNA copy number analysis

Briefly, DNA was isolated from C2C12 myotubes using phenol–chloroform method as reported in (Quiros *et al*, 2017). Approximately 50 ng total DNA was used for quantitative analysis of mtDNA level by qPCR using SYBR Green master mix. The relative copy number of mtDNA was determined using mitochondrial-specific primers for ND1 and 16S and nuclear specific Hexokinase 2 (HK2):

Gene	Forward sequence (5′–3′)	Reverse sequence (3′–5′)
16S rRNA	CCGCAAGGGAAAGATGAAAGAC	TCGTTTGGTTTCGGGGTTTC
ND1	CTAGCAGAAACAAACCGGGC	CCGGCTGCGTATTCTACGTT
HK2	GCCAGCCTCTCCTGATTTTAGTGT	GGGAACACAAAAGACCTCTTCTGG

Quantitative analysis was carried out using the following reaction conditions; the pre-amplification step was carried out at 95°C for 3 min, followed by 40 cycles at 95°C for 10 s, annealing was performed at 58°C for 30 s and final extension was carried out at 72°C for 30 s. After obtaining the Ct values, the mtDNA copy number was calculated using the following formula: ΔCt = Ct(mtDNA gene)−Ct(nDNA gene).

Fusion index

After 48 h treatment with C26CM and FeCM as described previously, cells were fixed in 4% PFA, permeabilized and stained for Myosin Heavy Chain (Sigma M4276) and nuclei were stained with DAPI. The fusion index was determined as followed : (fusion %) = (number of nuclei per myotube)/(total number of nuclei in the field. At least 6 random fields (10× magnification) were analyzed per condition using the ImageJ Software.

Quantification and statistical analysis

All graphs show mean ± SEM. N represents the total number of independent experiments. Statistical significance was tested as indicated in figure legends with GraphPad Prism (version 6.0, GraphPad Software). Statistical significance was tested using two-tailed Student's *t*-test for comparisons of two groups, one-way Anova followed by Bonferroni correction for comparisons of multiple groups with one variable, or two-way Anova followed by Tukey's multiple comparison test. Significance of survival rate difference was determined by Chi-square test. Non-parametric Mann–Whitney test was used for human grip strength data. Significance was defined as $*P < 0.05$, $**P < 0.01$, and $***P < 0.001$.

Data availability

No data requiring public database deposition have been generated.

Expanded View for this article is available online.

Author contributions

Elisabeth Wyart: Conceptualization; Data curation; Investigation; Writing – original draft. **Myriam Hsu:** Investigation; Methodology equal); Writing – original draft; Writing – review & editing. **Roberta Sartori:** Methodology. **Erica Mina:** Investigation. **Valentina Rausch:** Methodology. **Elisa Sefora Pierobon:** Resources. **Mariarosa Mezzanotte:** Methodology. **Camilla Pezzini:** Methodology. **Laure Bindels:** Resources; Formal analysis. **Andrea Lauria:** Software. **Fabio Penna:** Investigation. **Emilio Hirsch:** Formal analysis. **Miriam Martini:** Data curation; Formal analysis; Writing – review & editing. **Massimiliano Mazzone:** Conceptualization equal). **Antonella Roetto:** Investigation; Methodology. **Simonetta Geninatti Crich:** Investigation; Methodology. **Hans Prenen:** Conceptualization; Formal analysis. **Marco Sandri:** Data curation; Visualization. **Alessio Menga:** Project administration; Writing – review & editing. **Paolo Ettore Porporato:** Conceptualization; Supervision; Funding acquisition; Investigation; Writing – original draft; Project administration; Writing – review & editing.

Disclosure and competing interests statement

The authors declare that they have no conflict of interest.

References

Abrigo J, Simon F, Cabrera D, Vilos C, Cabello-Verrugio C (2019) Mitochondrial dysfunction in skeletal muscle pathologies. *Curr Protein Pept Sci* 20: 536–546

Allen GF, Toth R, James J, Ganley IG (2013) Loss of iron triggers PINK1/Parkin-independent mitophagy. *EMBO Rep* 14: 1127–1135

Alves FM, Kysenius K, Caldow MK, Hardee JP, Crouch PJ, Ayton S, Bush AI, Lynch GS, Koopman R (2021) Iron accumulation in skeletal muscles of old mice is associated with impaired regeneration after ischaemia-reperfusion damage. *J Cachexia Sarcopenia Muscle* 12: 476–492

Argiles JM, Fontes-Oliveira CC, Toledo M, Lopez-Soriano FJ, Busquets S (2014) Cachexia: a problem of energetic inefficiency. *J Cachexia Sarcopenia Muscle* 5: 279–286

Barman-Aksozen J, Halloy F, Iyer PS, Schumperli D, Minder AE, Hall J, Minder EI, Schneider-Yin X (2019) Delta-aminolevulinic acid synthase 2 expression in combination with iron as modifiers of disease severity in erythropoietic protoporphyria. *Mol Genet Metab* 128: 304–308

Barrientos T, Laothamatas I, Koves TR, Soderblom EJ, Bryan M, Moseley MA, Muoio DM, Andrews NC (2015) Metabolic catastrophe in mice lacking transferrin receptor in muscle. *EBioMedicine* 2: 1705–1717

Bastian TW, von Hohenberg WC, Georgieff MK, Lanier LM (2019) Chronic energy depletion due to iron deficiency impairs dendritic mitochondrial motility during hippocampal neuron development. *J Neurosci* 39: 802–813

Bellelli R, Federico G, Matte A, Colecchia D, Iolascon A, Chiariello M, Santoro M, De Franceschi L, Carlomagno F (2016) NCOA4 deficiency impairs systemic iron homeostasis. *Cell Rep* 14: 411–421

Bindels LB, Beck R, Schakman O, Martin JC, De Backer F, Sohet FM, Dewulf EM, Pachikian BD, Neyrinck AM, Thissen J-P *et al* (2012) Restoring specific lactobacilli levels decreases inflammation and muscle atrophy markers in an acute leukemia mouse model. *PLoS One* 7: e37971

Boengler K, Kosiol M, Mayr M, Schulz R, Rohrbach S (2017) Mitochondria and ageing: role in heart, skeletal muscle and adipose tissue. *J Cachexia Sarcopenia Muscle* 8: 349–369

Brown JL, Rosa-Caldwell ME, Lee DE, Blackwell TA, Brown LA, Perry RA, Haynie WS, Hardee JP, Carson JA, Wiggs MP *et al* (2017) Mitochondrial degeneration precedes the development of muscle atrophy in progression of cancer cachexia in tumour-bearing mice. *J Cachexia Sarcopenia Muscle* 8: 926–938

Cairo G, Castrusini E, Minotti G, Bernelli-Zazzera A (1996) Superoxide and hydrogen peroxide-dependent inhibition of iron regulatory protein activity: a protective stratagem against oxidative injury. *FASEB J* 10: 1326–1335

Cairo G, Tacchini L, Recalcati S, Azzimonti B, Minotti G, Bernelli-Zazzera A (1998) Effect of reactive oxygen species on iron regulatory protein activity. *Ann N Y Acad Sci* 851: 179–186

Camaschella C, Nai A, Silvestri L (2020) Iron metabolism and iron disorders revisited in the hepcidin era. *Haematologica* 105: 260–272

Dziegala M, Josiak K, Kasztura M, Kobak K, von Haehling S, Banasiak W, Anker SD, Ponikowski P, Jankowska E (2018) Iron deficiency as energetic insult to skeletal muscle in chronic diseases. *J Cachexia Sarcopenia Muscle* 9: 802–815

Fearon K, Strasser F, Anker SD, Bosaeus I, Bruera E, Fainsinger RL, Jatoi A, Loprinzi C, MacDonald N, Mantovani G *et al* (2011) Definition and classification of cancer cachexia: an international consensus. *Lancet Oncol* 12: 489–495

Fukawa T, Yan-Jiang BC, Min-Wen JC, Jun-Hao ET, Huang D, Qian C-N, Ong P, Li Z, Chen S, Mak SY *et al* (2016) Excessive fatty acid oxidation induces muscle atrophy in cancer cachexia. *Nat Med* 22: 666–671

Galy B, Ferring-Appel D, Sauer SW, Kaden S, Lyoumi S, Puy H, Kolker S, Grone HJ, Hentze MW (2010) Iron regulatory proteins secure mitochondrial iron sufficiency and function. *Cell Metab* 12: 194–201

Gao Y, Li Z, Gabrielsen JS, Simcox JA, Lee SH, Jones D, Cooksey B, Stoddard G, Cefalu WT, McClain DA (2015) Adipocyte iron regulates leptin and food intake. *J Clin Invest* 125: 3681–3691

Gehring NH, Hentze MW, Pantopoulos K (1999) Inactivation of both RNA binding and aconitase activities of iron regulatory protein-1 by quinone-induced oxidative stress. *J Biol Chem* 274: 6219–6225

Grillo AS, SantaMaria AM, Kafina MD, Cioffi AG, Huston NC, Han M, Seo YA, Yien YY, Nardone C, Menon AV *et al* (2017) Restored iron transport by a small molecule promotes absorption and hemoglobinization in animals. *Science* 356: 608–616

Higashida K, Inoue S, Nakai N (2020) Iron deficiency attenuates protein synthesis stimulated by branched-chain amino acids and insulin in myotubes. *Biochem Biophys Res Commun* 531: 112–117

Hirsch VG, Tongers J, Bode J, Berliner D, Widder JD, Escher F, Mutsenko V, Chung B, Rostami F, Guba-Quint A *et al* (2020) Cardiac iron concentration in relation to systemic iron status and disease severity in non-ischaemic heart failure with reduced ejection fraction. *Eur J Heart Fail* 22: 2038–2046

Hsu MY, Mina E, Roetto A, Porporato PE (2020) Iron: an essential element of cancer metabolism. *Cells* 9: 2591

Hulmi JJ, Nissinen TA, Rasanen M, Degerman J, Lautaoja JH, Hemanthakumar KA, Backman JT, Ritvos O, Silvennoinen M, Kivela R (2018) Prevention of chemotherapy-induced cachexia by ACVR2B ligand blocking has different effects on heart and skeletal muscle. *J Cachexia Sarcopenia Muscle* 9: 417–432

Jankowska EA, Tkaczyszyn M, Suchocki T, Drozd M, von Haehling S, Doehner W, Banasiak W, Filippatos G, Anker SD, Ponikowski P (2016) Effects of intravenous iron therapy in iron-deficient patients with systolic heart failure: a meta-analysis of randomized controlled trials. *Eur J Heart Fail* 18: 786−795

Janssen I, Heymsfield SB, Wang ZiMian, Ross R (2000) Skeletal muscle mass and distribution in 468 men and women aged 18−88 yr. *J Appl Physiol* 89: 81−88

Klempa KL, Willis WT, Chengson R, Dallman PR, Brooks GA (1989) Iron deficiency decreases gluconeogenesis in isolated rat hepatocytes. *J Appl Physiol* 67: 1868−1872

Leermakers PA, Remels AHV, Zonneveld MI, Rouschop KMA, Schols A, Gosker HR (2020) Iron deficiency-induced loss of skeletal muscle mitochondrial proteins and respiratory capacity; the role of mitophagy and secretion of mitochondria-containing vesicles. *FASEB J* 34: 6703−6717

Levi S, Rovida E (2009) The role of iron in mitochondrial function. *Biochim Biophys Acta* 1790: 629−636

Li H, Zhao H, Hao S, Shang L, Wu J, Song C, Meyron-Holtz EG, Qiao T, Li K (2018) Iron regulatory protein deficiency compromises mitochondrial function in murine embryonic fibroblasts. *Sci Rep* 8: 5118

Liu J, Peng Y, Wang X, Fan Y, Qin C, Shi LE, Tang Y, Cao KE, Li H, Long J et al (2016) Mitochondrial dysfunction launches dexamethasone-induced skeletal muscle atrophy via AMPK/FOXO3 signaling. *Mol Pharm* 13: 73−84

Ludwig H, Muldur E, Endler G, Hubl W (2013) Prevalence of iron deficiency across different tumors and its association with poor performance status, disease status and anemia. *Ann Oncol* 24: 1886−1892

Maguire JJ, Davies KJ, Dallman PR, Packer L (1982) Effects of dietary iron deficiency of iron-sulfur proteins and bioenergetic functions of skeletal muscle mitochondria. *Biochim Biophys Acta* 679: 210−220

Marone G, Poto S, Giugliano R, Celestino D, Bonini S (1986) Control mechanisms of human basophil releasability. *J Allergy Clin Immunol* 78: 974−980

Meyron-Holtz EG, Ghosh MC, Iwai K, LaVaute T, Brazzolotto X, Berger UV, Land W, Ollivierre-Wilson H, Grinberg A, Love P et al (2004) Genetic ablations of iron regulatory proteins 1 and 2 reveal why iron regulatory protein 2 dominates iron homeostasis. *EMBO J* 23: 386−395

Mikhael M, Kim SF, Schranzhofer M, Soe-Lin S, Sheftel AD, Mullner EW, Ponka P (2006) Iron regulatory protein-independent regulation of ferritin synthesis by nitrogen monoxide. *FEBS J* 273: 3828−3836

Murata A, Amaya K, Mochizuki K, Sotokawa M, Otaka S, Tani K, Nakagaki S, Ueda T (2018) Superior mesenteric artery-pancreaticoduodenal arcade bypass grafting for repair of inferior pancreaticoduodenal artery aneurysm with celiac axis occlusion. *Ann Vasc Dis* 11: 153−157

Neyroud D, Nosacka RL, Judge AR, Hepple RT (2019) Colon 26 adenocarcinoma (C26)-induced cancer cachexia impairs skeletal muscle mitochondrial function and content. *J Muscle Res Cell Motil* 40: 59−65

Oexle H, Gnaiger E, Weiss G (1999) Iron-dependent changes in cellular energy metabolism: influence on citric acid cycle and oxidative phosphorylation. *Biochim Biophys Acta* 1413: 99−107

Palla AR, Ravichandran M, Wang YX, Alexandrova L, Yang AV, Kraft P, Holbrook CA, Schurch CM, Ho ATV, Blau HM (2021) Inhibition of prostaglandin-degrading enzyme 15-PGDH rejuvenates aged muscle mass and strength. *Science* 371: 8059

Peng Y, Li J, Luo D, Zhang S, Li S, Wang D, Wang X, Zhang Z, Wang X, Sun C et al (2021) Muscle atrophy induced by overexpression of ALAS2 is related to muscle mitochondrial dysfunction. *Skelet Muscle* 11: 9

Porporato PE (2016) Understanding cachexia as a cancer metabolism syndrome. *Oncogenesis* 5: e200

Quiros PM, Goyal A, Jha P, Auwerx J (2017) Analysis of mtDNA/nDNA ratio in mice. *Curr Protoc Mouse Biol* 7: 47−54

Rensvold JW, Krautkramer KA, Dowell JA, Denu JM, Pagliarini DJ (2016) Iron Deprivation induces transcriptional regulation of mitochondrial biogenesis. *J Biol Chem* 291: 20827−20837

Rensvold JW, Ong SE, Jeevananthan A, Carr SA, Mootha VK, Pagliarini DJ (2013) Complementary RNA and protein profiling identifies iron as a key regulator of mitochondrial biogenesis. *Cell Rep* 3: 237−245

Robach P, Cairo G, Gelfi C, Bernuzzi F, Pilegaard H, Viganò A, Santambrogio P, Cerretelli P, Calbet JAL, Moutereau S et al (2007) Strong iron demand during hypoxia-induced erythropoiesis is associated with down-regulation of iron-related proteins and myoglobin in human skeletal muscle. *Blood* 109: 4724−4731

Romanello V, Guadagnin E, Gomes L, Roder I, Sandri C, Petersen Y, Milan G, Masiero E, Del Piccolo P, Foretz M et al (2010) Mitochondrial fission and remodelling contributes to muscle atrophy. *EMBO J* 29: 1774−1785

Romanello V, Sandri M (2015) Mitochondrial quality control and muscle mass maintenance. *Front Physiol* 6: 422

Rothermel B, Vega RB, Yang J, Wu H, Bassel-Duby R, Williams RS (2000) A protein encoded within the Down syndrome critical region is enriched in striated muscles and inhibits calcineurin signaling. *J Biol Chem* 275: 8719−8725

Sartori R, Hagg A, Zampieri S, Armani A, Winbanks CE, Viana LR, Haidar M, Watt KI, Qian H, Pezzini C et al (2021) Perturbed BMP signaling and denervation promote muscle wasting in cancer cachexia. *Sci Transl Med* 13: 9592

Schoenfeld JD, Sibenaller ZA, Mapuskar KA, Wagner BA, Cramer-Morales KL, Furqan M, Sandhu S, Carlisle TL, Smith MC, Abu Hejleh T et al (2017) O2(-) and H2O2-mediated disruption of Fe metabolism causes the differential susceptibility of NSCLC and GBM cancer cells to pharmacological ascorbate. *Cancer Cell* 32: 487−500 e488

Scott LJ (2018) Ferric carboxymaltose: a review in iron deficiency. *Drugs* 78: 479−493

Serra M, Columbano A, Ammarah U, Mazzone M, Menga A (2020) Understanding metal dynamics between cancer cells and macrophages: competition or synergism? *Front Oncol* 10: 646

Sinclair PR, Gorman N, Jacobs JM (2001) Measurement of heme concentration. *Curr Protoc Toxicol* Chapter 8: Unit 8 3

Tezze C, Romanello V, Desbats MA, Fadini GP, Albiero M, Favaro G, Ciciliot S, Soriano ME, Morbidoni V, Cerqua C et al (2017) Age-associated loss of OPA1 in muscle impacts muscle mass, metabolic homeostasis, systemic inflammation, and epithelial senescence. *Cell Metab* 25 1374−1389 e1376

Tisdale MJ (2002) Cachexia in cancer patients. *Nat Rev Cancer* 2: 862−871

Wang H, Shi H, Rajan M, Canarie ER, Hong S, Simoneschi D, Pagano M, Bush MF, Stoll S, Leibold EA et al (2020) FBXL5 regulates IRP2 stability in iron homeostasis via an oxygen-responsive [2Fe2S] cluster. *Mol Cell* 78: 31−41 e35

Wyart E, Reano S, Hsu MY, Longo DL, Li M, Hirsch E, Filigheddu N, Ghigo A, Riganti C, Porporato PE (2018) Metabolic alterations in a slow-paced model of pancreatic cancer-induced wasting. *Oxid Med Cell Longev* 2018: 6419805

Xu W, Barrientos T, Andrews NC (2013) Iron and copper in mitochondrial diseases. *Cell Metab* 17: 319−328

Zhao B, Qiang L, Joseph J, Kalyanaraman B, Viollet B, He YY (2016) Mitochondrial dysfunction activates the AMPK signaling and autophagy to promote cell survival. *Genes Dis* 3: 82–87

Zhou D, Zhang Y, Mamtawla G, Wan S, Gao X, Zhang L, Li G, Wang X (2020) Iron overload is related to muscle wasting in patients with cachexia of gastric cancer: using quantitative proteome analysis. *Med Oncol* 37: 113

Zhou X, Wang JL, Lu J, Song Y, Kwak KS, Jiao Q, Rosenfeld R, Chen Q, Boone T, Simonet WS *et al* (2010) Reversal of cancer cachexia and muscle

wasting by ActRIIB antagonism leads to prolonged survival. *Cell* 142: 531–543

109

4 Discussion

It is well known that if on the one hand iron is essential for life, on the other hand, if badly managed, it can be harmful to organs, tissues and cells. This is partly due to its occurrence of interconversion between the reduced and oxidized state. The ability of each organ to manage and actively respond to iron variations ensures that the damage caused by overload and/or its deficiency are minimized but exogenous, endogenous and aging-related factors can alter this equilibrium.

This equilibrium, in fact, is compromised in several genetic diseases (*i.e* hereditary hemochromatosis) leading to excessive iron deposition in the liver and, subsequently, to other parenchymal cells compromising organ functionality and, if not treated, patient's life expectancies.

During my PhD School, I have mainly focused my study on the Central Nervous System (CNS), that exhibits peculiar characteristics regarding brain iron management

Systemic iron regulation is based on a complex protein regulatory system in which the hepatic Hepcidin (Hepc) plays a central role. Hepc is a small protein that reduced iron efflux from cells and leads to its intracellular accumulation (Hentze *et al.*, 2010). Indeed, the modulation of Hepc expression by low or high iron availability determines *de facto* iron availability in the body (Muckenthaler *et al.*, 2017). In the brain, iron homeostasis is regulated by the same proteins network that acts at the systemic level (Zecca *et al.*, 2004b) and the Hepc regulatory system is active also in the CNS (Rouault, 2013). Indeed, Hepc is expressed by glial cells and neurons from different brain regions and, it is activated and it induces Fpn1 decrease under brain iron overload condition (Ding *et al.*, 2011; Du *et al.*, 2015; Moos and Morgan, 2004), even if it is not clear yet whether this rely on brain or hepatic Hepc or both (Vela, 2018). Interestingly, iron overload selective localized in specific regions of the CNS has also been associated with and aging (Lozoff and Georgieff, 2006; Zecca *et al.*, 2004a) and neurodegenerative diseases, such as Parkinson's Disease (PD) and Alzheimer's Diseases (AD), (Rouault, 2013).

As known, Hepc expression is regulated by Transferrin receptor 2 (TfR2), in particular by the α-isoform, the mainly transcribed isoform of the TFR2 gene, and the one that is expressed in the brain (Hänninen *et al.*, 2009; Kawabata *et al.*, 1999). Mutation on TFR2 gene are responsible of hereditary hemochromatosis type 3 (HFE3), which is characterized by systemic iron overload (Roetto *et al.*, 2018).

During my PhD, I worked on a project aimed to the molecular characterization of iron metabolism in mice brain in i) a murine model in which TfR2 has been systemically silenced and in ii) an aged Wild-type (WT) model.

In the TfR2 KO mouse model (Pellegrino *et al.*, 2016) we demonstrated that TfR2-α is expressed in the neurite compartment of limbic areas involved in anxiety and stress response and its silencing causes an increase of iron circulating in specific brain regions due to the lack of response of neuronal hepcidin. In line with a high iron amount in TfR2 KO mouse, a global increase of the iron storage protein Ferritin (in particular Ferritin-H isoform) was found. This induction may reflect the need to counteract the deleterious effects of an enhanced iron-based Fenton reaction, which produces damaging hydroxyl radicals (Chelikani *et al.*, 2004).

It is interesting to note that the increase of iron in TfR2 KO mice brain, provokes behavioural changes associated with an anxious phenotype as demonstrated by the results of the Elevated Plus Maze test (EPM).

According to behavioural results, TfR2 KO mice showed ad increased expression of markers of neuronal activity, cFos and Zif-268, (Sheng and Greenberg, 1990), proof of which limbic circuits controlling anxiety and stress responses were overactivated. Alterations and behavioural changes in TfR2 KO mice are accompanied with degenerative events in microglia, where the iron storage is increased.

In conclusion, the control of anxious behaviours and the regulation of iron in the brain depends on Tfr2-dependent iron overload.

The main focus of my PhD was to investigate how Hepc regulatory system respond to intracerebral iron increase during physiological aging. For this reason, we decided to study proteins expression involved in iron metabolism in WT mice during aging.

We characterized the state of the brain at different ages in relation to brain iron content, BBB integrity, brain inflammation and oxidative state.

We demonstrated that during healthy aging in physiological conditions, iron overload occurred in the brain that is selectively localized in the Cerebral cortex, Hippocampus, third ventricle and striatum.

The increase of iron in the brain combined to a BBB altered permeability, demonstrated by a decrease of the protein levels of Zonula occludents 1 protein, marker of BBB integrity (Maiuolo *et al.*, 2018). Although iron and inflammation are both regulators of Hepcidin expression, to investigate if the accumulation of iron in the brain could trigger an inflammatory process and if it could cause oxidative

stress, we respectively analysed, the two main markers of these biological processes: Serum amyloid A1 (SAA1) and Nuclear factor erythroid 2-related factor 2, (Nrf2).

SAA1 is an acute-phase protein and it's considered an accurate and sensitive indicator of inflammation (Erdembileg *et al.*, 2015). We showed that its expression levels are significantly increased from M-A (6-12 months of age) and became more than 20 times higher in old animals compared to adults' mice.

The nuclear factor-erythroid 2 (NF-E2)-related factor 2 (Nrf2) is a redox-sensitive transcription factor, whose activation results in cellular antioxidant responses via modulation of several stress-responsive proteins (Jiang *et al.*, 2019). As we expected, Nrf2 expression levels appeared to be in a gradual but constant and significant increase in WT old mice brain. It has been demonstrated that, during aging neuroinflammation and astrocytes activation are evident (Ke and Gibson, 2004).

Indeed, we also identified high astrocytes activation and an increased expression of microglia in both parenchymal regions of WT O mice, Ctx, and Hip, where iron accumulated.

Since the cornerstone of iron metabolism regulation is Hepc/Fpn1 pathway activation, we demonstrated that in the context of increased iron amount and inflammation in the brain of WT old mice, Hepc gene expression significantly increased; while Fpn1 decreases.

To better understand iron regulation in brain tissue, we also analysed iron deposits Ferritin (Ft) and Nuclear receptor coactivator 4 (NCOA4) protein, involved in ferritinophagy (Mancias *et al.*, 2015). In particular, NCOA4 promotes autophagic ferritin degradation binding Ft-H isoform. We observed an increased amount of NCOA4 combined to an increase of Ft-L and a decrease of Ft-H isoform in the aged mice brains.

These data demonstrated that in old mice brain inflammation, due to iron accumulation, induces Hepc expression and consequently Fpn1 degradation. The activation of the Hepc/Fpn1 pathway in the nervous tissue promotes iron retention; in turn, cells respond with an increase on NCOA4 levels that could be responsible for a selective Ft-H degradation, promoting in this way the formation of Ft-L rich ferritin heteropolymers, more effective for iron storage.

Moreover, when we looked for Fpn1, Ft-L and Ft-H localization, we found that Fpn1 not only is increased in old mice Ctx and Hip of WT old mice, but also that its distribution is cell specific since it increases in cortical and hippocampal astrocytes and remains constant in neurons. On the contrary, Ft-L increase and Ft-H decrease were evident in cortical and hippocampal neurons but not in astrocytes.

These data revealed that aging-related brain iron accumulation is accompanied by neuroinflammation and Hepc/Fpn1 pathway activation. As a consequence, astrocytic activation occurs and Fpn1 amount increases, implying a higher iron export from these cells.

As a protective mechanism, cortical and hippocampal neurons increase the amount of Ft-L isoform leading to the production of Ft-L enriched ferritins heteropolymers, more suitable to chelate free iron. Taken together, these data highlight an involvement of Hepc/Fpn1 axis in brain iron metabolism during aging as a response to a higher iron flux in CNS due to a BBB alteration. This, enhancing iron availability imbalance, could cause oxidative damage, stress and neurodegeneration.

Additional studies could be conducted in order to understand if the response to the increased amount of iron in the brain during aging could be helpful for the understanding of mechanisms underlying neurodegenerative diseases

5 Conclusion

In conclusion, our work contributes to the understanding of the molecular mechanisms underlying brain iron overload.

We could hypothesize then to perform iron chelation as a strategy to prevent neurotoxicity caused by free iron in the disorders associated with brain iron imbalance.

However, iron chelation is a complex process: a chelator should be able to pass the BBB and to trap iron specifically in the regions where iron overload occurs, without depleting transferrin bound iron from the plasma and to transfer it to other proteins such as circulating transferrin.

Three iron chelators have been approved by Federal Drug Administration (FDA) to symptomatic treatment in NDs: deferoxamine, deferasirox and deferiprone. But, while deferoxamine and deferasirox do not easily pass through the BBB and bind iron in a dose dependent manner, the molecular structure of deferiprone allow to pass BBB and it is the drug of choice in the majority of clinical trials for neurodegenerative disorders (Jiang *et al.*, 2006; Martin-Bastida *et al.*, 2017; Sripetchwandee *et al.*, 2016).

Analyzing the three drugs more closely, the therapeutic effects of deferoxamine are promising in the treatment of AD; indeed *in vivo* study using APP/PS1 transgenic mice fed with iron-rich diet showed that after deferoxamine injection, *tau* phosphorylation iron-dependent is inhibited through the CDK5 and GSK-3β pathways (Guo *et al.*, 2013a). Moreover, deferoxamine injection in AD transgenic mice not only inhibits the formation of amyloid precursor protein (APP), but it can improve memory deficits (Guo *et al.*, 2013b).

However, although deferoxamine has been approved by FDA, the clinical application is still tricky due to: *i)* its poor bioavailability; *ii)* low ability to cross the BBB; *iii)* ant its methods of administration through injection. It was proven that deferoxamine, as well as deferiprone, ameliorate BBB integrity, reducing brain iron overload and brain mitochondrial alteration (Sripetchwandee *et al.*, 2016).

Is iron overload in neurodegenerative disorders directly involved in the pathogenesis or is it a secondary effect of the disease? More fundamental research on models of neurodegeneration related also to the restoration of brain iron homeostasis is necessary to try to find mechanisms and new targets to cure neurodegenerative disorders that increasingly afflict the population, and represent not only a health but also a social problem.

6 References

Aizawa, S., Brar, G., Tsukamoto, H., 2020. Cell Death and Liver Disease. *Gut and liver* 14**,** 20-29.

Almutairi, M.M., Gong, C., Xu, Y.G., Chang, Y., Shi, H., 2016. Factors controlling permeability of the blood-brain barrier. *Cell Mol Life Sci* 73**,** 57-77.

Andrews, N.C., 1999. The iron transporter DMT1. *The international journal of biochemistry & cell biology* 31**,** 991-994.

Arosio, P., Ingrassia, R., Cavadini, P., 2009. Ferritins: a family of molecules for iron storage, antioxidation and more. *Biochimica et biophysica acta* 1790**,** 589-599.

Babitt, J.L., Huang, F.W., Wrighting, D.M., Xia, Y., Sidis, Y., Samad, T.A., Campagna, J.A., Chung, R.T., Schneyer, A.L., Woolf, C.J., Andrews, N.C., Lin, H.Y., 2006. Bone morphogenetic protein signaling by hemojuvelin regulates hepcidin expression. *Nature genetics* 38**,** 531-539.

Bellelli, R., Castellone, M.D., Guida, T., Limongello, R., Dathan, N.A., Merolla, F., Cirafici, A.M., Affuso, A., Masai, H., Costanzo, V., Grieco, D., Fusco, A., Santoro, M., Carlomagno, F., 2014. NCOA4 transcriptional coactivator inhibits activation of DNA replication origins. *Molecular cell* 55**,** 123-137.

Bellelli, R., Federico, G., Matte, A., Colecchia, D., Iolascon, A., Chiariello, M., Santoro, M., De Franceschi, L., Carlomagno, F., 2016. NCOA4 Deficiency Impairs Systemic Iron Homeostasis. *Cell reports* 14**,** 411-421.

Boero, M., Pagliaro, P., Tullio, F., Pellegrino, R.M., Palmieri, A., Ferbo, L., Saglio, G., De Gobbi, M., Penna, C., Roetto, A., 2015. A comparative study of myocardial molecular phenotypes of two tfr2β null mice: role in ischemia/reperfusion. *BioFactors (Oxford, England)* 41**,** 360-371.

Bulet, P., Stöcklin, R., Menin, L., 2004. Anti-microbial peptides: from invertebrates to vertebrates. *Immunological reviews* 198**,** 169-184.

Camaschella, C., Nai, A., Silvestri, L., 2020. Iron metabolism and iron disorders revisited in the hepcidin era. *Haematologica* 105**,** 260-272.

Camaschella, C., Pagani, A., Nai, A., Silvestri, L., 2016. The mutual control of iron and erythropoiesis. *International journal of laboratory hematology* 38 Suppl 1**,** 20-26.

Camaschella, C., Roetto, A., Calì, A., De Gobbi, M., Garozzo, G., Carella, M., Majorano, N., Totaro, A., Gasparini, P., 2000. The gene TFR2 is mutated in a new type of haemochromatosis mapping to 7q22. *Nature genetics* 25**,** 14-15.

Chelikani, P., Fita, I., Loewen, P.C., 2004. Diversity of structures and properties among catalases. *Cellular and molecular life sciences : CMLS* 61**,** 192-208.

Chen, A.C., Donovan, A., Ned-Sykes, R., Andrews, N.C., 2015a. Noncanonical role of transferrin receptor 1 is essential for intestinal homeostasis. *Proceedings of the National Academy of Sciences of the United States of America* 112**,** 11714-11719.

Chen, L., Hambright, W.S., Na, R., Ran, Q., 2015b. Ablation of the Ferroptosis Inhibitor Glutathione Peroxidase 4 in Neurons Results in Rapid Motor Neuron Degeneration and Paralysis. *The Journal of biological chemistry* 290**,** 28097-28106.

Chiabrando, D., Vinchi, F., Fiorito, V., Mercurio, S., Tolosano, E., 2014. Heme in pathophysiology: a matter of scavenging, metabolism and trafficking across cell membranes. *Frontiers in pharmacology* 5**,** 61.

Chifman, J., Laubenbacher, R., Torti, S.V., 2014. A systems biology approach to iron metabolism. *Advances in experimental medicine and biology* 844**,** 201-225.

Cohen, L.A., Gutierrez, L., Weiss, A., Leichtmann-Bardoogo, Y., Zhang, D.L., Crooks, D.R., Sougrat, R., Morgenstern, A., Galy, B., Hentze, M.W., Lazaro, F.J., Rouault, T.A., Meyron-Holtz, E.G., 2010. Serum ferritin is derived primarily from macrophages through a nonclassical secretory pathway. *Blood* 116**,** 1574-1584.

Conde, J.R., Streit, W.J., 2006. Microglia in the aging brain. *J Neuropathol Exp Neurol* 65**,** 199-203.

Connor, J.R., Menzies, S.L., St Martin, S.M., Mufson, E.J., 1990. Cellular distribution of transferrin, ferritin, and iron in normal and aged human brains. *Journal of neuroscience research* 27**,** 595-611.

Connor, J.R., Snyder, B.S., Arosio, P., Loeffler, D.A., LeWitt, P., 1995. A quantitative analysis of isoferritins in select regions of aged, parkinsonian, and Alzheimer's diseased brains. *Journal of neurochemistry* 65**,** 717-724.

Core, A.B., Canali, S., Babitt, J.L., 2014. Hemojuvelin and bone morphogenetic protein (BMP) signaling in iron homeostasis. *Frontiers in pharmacology* 5**,** 104.

Corradini, E., Meynard, D., Wu, Q., Chen, S., Ventura, P., Pietrangelo, A., Babitt, J.L., 2011. Serum and liver iron differently regulate the bone morphogenetic protein 6 (BMP6)-SMAD signaling pathway in mice. *Hepatology (Baltimore, Md.)* 54**,** 273-284.

Costain, G., Ghosh, M.C., Maio, N., Carnevale, A., Si, Y.C., Rouault, T.A., Yoon, G., 2019. Absence of iron-responsive element-binding protein 2 causes a novel neurodegenerative syndrome. *Brain : a journal of neurology* 142**,** 1195-1202.

Daher, R., Karim, Z., 2017. Iron metabolism: State of the art. *Transfusion clinique et biologique : journal de la Societe francaise de transfusion sanguine* 24**,** 115-119.

Daru, J., Colman, K., Stanworth, S.J., De La Salle, B., Wood, E.M., Pasricha, S.R., 2017. Serum ferritin as an indicator of iron status: what do we need to know? *The American journal of clinical nutrition* 106**,** 1634s-1639s.

De Domenico, I., Vaughn, M.B., Li, L., Bagley, D., Musci, G., Ward, D.M., Kaplan, J., 2006. Ferroportin-mediated mobilization of ferritin iron precedes ferritin degradation by the proteasome. *The EMBO journal* 25**,** 5396-5404.

De Domenico, I., Ward, D.M., Kaplan, J., 2009. Specific iron chelators determine the route of ferritin degradation. *Blood* 114**,** 4546-4551.

Dev, S., Babitt, J.L., 2017. Overview of iron metabolism in health and disease. *Hemodialysis international. International Symposium on Home Hemodialysis* 21 Suppl 1**,** S6-s20.

Ding, H., Yan, C.Z., Shi, H., Zhao, Y.S., Chang, S.Y., Yu, P., Wu, W.S., Zhao, C.Y., Chang, Y.Z., Duan, X.L., 2011. Hepcidin is involved in iron regulation in the ischemic brain. *PloS one* 6**,** e25324.

Dixon, S.J., Lemberg, K.M., Lamprecht, M.R., Skouta, R., Zaitsev, E.M., Gleason, C.E., Patel, D.N., Bauer, A.J., Cantley, A.M., Yang, W.S., Morrison, B., 3rd, Stockwell, B.R., 2012. Ferroptosis: an iron-dependent form of nonapoptotic cell death. *Cell* 149**,** 1060-1072.

Do Van, B., Gouel, F., Jonneaux, A., Timmerman, K., Gelé, P., Pétrault, M., Bastide, M., Laloux, C., Moreau, C., Bordet, R., Devos, D., Devedjian, J.C., 2016. Ferroptosis, a newly characterized form of cell death in Parkinson's disease that is regulated by PKC. *Neurobiology of disease* 94**,** 169-178.

Doll, S., Conrad, M., 2017. Iron and ferroptosis: A still ill-defined liaison. *IUBMB life* 69**,** 423-434.

Donovan, A., Brownlie, A., Zhou, Y., Shepard, J., Pratt, S.J., Moynihan, J., Paw, B.H., Drejer, A., Barut, B., Zapata, A., Law, T.C., Brugnara, C., Lux, S.E., Pinkus, G.S., Pinkus, J.L., Kingsley, P.D., Palis, J., Fleming, M.D., Andrews, N.C., Zon, L.I., 2000. Positional cloning of zebrafish ferroportin1 identifies a conserved vertebrate iron exporter. *Nature* 403**,** 776-781.

Dowdle, W.E., Nyfeler, B., Nagel, J., Elling, R.A., Liu, S., Triantafellow, E., Menon, S., Wang, Z., Honda, A., Pardee, G., Cantwell, J., Luu, C., Cornella-Taracido, I., Harrington, E., Fekkes, P., Lei, H., Fang, Q., Digan, M.E., Burdick, D., Powers, A.F., Helliwell, S.B., D'Aquin, S., Bastien, J., Wang, H., Wiederschain, D., Kuerth, J., Bergman, P., Schwalb, D., Thomas, J., Ugwonali, S., Harbinski, F., Tallarico, J., Wilson, C.J., Myer, V.E., Porter, J.A., Bussiere, D.E., Finan, P.M., Labow, M.A., Mao, X., Hamann, L.G., Manning, B.D., Valdez, R.A., Nicholson, T., Schirle, M., Knapp, M.S., Keaney, E.P., Murphy, L.O., 2014. Selective VPS34 inhibitor blocks autophagy and uncovers a role for NCOA4 in ferritin degradation and iron homeostasis in vivo. *Nature cell biology* 16**,** 1069-1079.

Du, F., Qian, Z.M., Luo, Q., Yung, W.H., Ke, Y., 2015. Hepcidin Suppresses Brain Iron Accumulation by Downregulating Iron Transport Proteins in Iron-Overloaded Rats. *Molecular neurobiology* 52**,** 101-114.

Du, X., She, E., Gelbart, T., Truksa, J., Lee, P., Xia, Y., Khovananth, K., Mudd, S., Mann, N., Moresco, E.M., Beutler, E., Beutler, B., 2008. The serine protease TMPRSS6 is required to sense iron deficiency. *Science (New York, N.Y.)* 320**,** 1088-1092.

Erdembileg, A., Mirsoian, A., Enkhmaa, B., Zhang, W., Beckett, L.A., Murphy, W.J., Berglund, L.F., 2015. Attenuated age-impact on systemic inflammatory markers in the presence of a metabolic burden. *PloS one* 10**,** e0121947.

Farrall, A.J., Wardlaw, J.M., 2009. Blood-brain barrier: ageing and microvascular disease--systematic review and meta-analysis. *Neurobiol Aging* 30**,** 337-352.

Fillebeen, C., Charlebois, E., Wagner, J., Katsarou, A., Mui, J., Vali, H., Garcia-Santos, D., Ponka, P., Presley, J., Pantopoulos, K., 2019. Transferrin receptor 1 controls systemic iron homeostasis by fine-tuning hepcidin expression to hepatocellular iron load. *Blood* 133**,** 344-355.

Fleming, R.E., Ahmann, J.R., Migas, M.C., Waheed, A., Koeffler, H.P., Kawabata, H., Britton, R.S., Bacon, B.R., Sly, W.S., 2002. Targeted mutagenesis of the murine transferrin receptor-2 gene produces hemochromatosis. *Proceedings of the National Academy of Sciences of the United States of America* 99**,** 10653-10658.

Forejtnikovà, H., Vieillevoye, M., Zermati, Y., Lambert, M., Pellegrino, R.M., Guihard, S., Gaudry, M., Camaschella, C., Lacombe, C., Roetto, A., Mayeux, P., Verdier, F., 2010. Transferrin receptor 2 is a component of the erythropoietin receptor complex and is required for efficient erythropoiesis. *Blood* 116**,** 5357-5367.

Friedmann Angeli, J.P., Schneider, M., Proneth, B., Tyurina, Y.Y., Tyurin, V.A., Hammond, V.J., Herbach, N., Aichler, M., Walch, A., Eggenhofer, E., Basavarajappa, D., Rådmark, O., Kobayashi, S., Seibt, T., Beck, H., Neff, F., Esposito, I., Wanke, R., Förster, H., Yefremova, O., Heinrichmeyer, M., Bornkamm, G.W., Geissler, E.K., Thomas, S.B., Stockwell, B.R., O'Donnell, V.B., Kagan, V.E., Schick, J.A., Conrad, M., 2014. Inactivation of the ferroptosis regulator Gpx4 triggers acute renal failure in mice. *Nature cell biology* 16**,** 1180-1191.

Fuqua, B.K., Vulpe, C.D., Anderson, G.J., 2012. Intestinal iron absorption. *Journal of trace elements in medicine and biology : organ of the Society for Minerals and Trace Elements (GMS)* 26**,** 115-119.

Gammella, E., Recalcati, S., Cairo, G., 2016. Dual Role of ROS as Signal and Stress Agents: Iron Tips the Balance in favor of Toxic Effects. *Oxidative medicine and cellular longevity* 2016**,** 8629024.

Ganz, T., 2013. Systemic iron homeostasis. *Physiological reviews* 93**,** 1721-1741.

Gao, X., Lee, H.Y., Li, W., Platt, R.J., Barrasa, M.I., Ma, Q., Elmes, R.R., Rosenfeld, M.G., Lodish, H.F., 2017. Thyroid hormone receptor beta and NCOA4 regulate terminal erythrocyte differentiation. *Proceedings of the National Academy of Sciences of the United States of America* 114**,** 10107-10112.

Goswami, T., Andrews, N.C., 2006. Hereditary hemochromatosis protein, HFE, interaction with transferrin receptor 2 suggests a molecular mechanism for mammalian iron sensing. *The Journal of biological chemistry* 281**,** 28494-28498.

Guiney, S.J., Adlard, P.A., Bush, A.I., Finkelstein, D.I., Ayton, S., 2017. Ferroptosis and cell death mechanisms in Parkinson's disease. *Neurochemistry international* 104**,** 34-48.

Gunshin, H., Mackenzie, B., Berger, U.V., Gunshin, Y., Romero, M.F., Boron, W.F., Nussberger, S., Gollan, J.L., Hediger, M.A., 1997. Cloning and characterization of a mammalian proton-coupled metal-ion transporter. *Nature* 388**,** 482-488.

Gunshin, H., Starr, C.N., Direnzo, C., Fleming, M.D., Jin, J., Greer, E.L., Sellers, V.M., Galica, S.M., Andrews, N.C., 2005. Cybrd1 (duodenal cytochrome b) is not necessary for dietary iron absorption in mice. *Blood* 106**,** 2879-2883.

Guo, C., Wang, P., Zhong, M.L., Wang, T., Huang, X.S., Li, J.Y., Wang, Z.Y., 2013a. Deferoxamine inhibits iron induced hippocampal tau phosphorylation in the Alzheimer transgenic mouse brain. *Neurochemistry international* 62**,** 165-172.

Guo, C., Wang, T., Zheng, W., Shan, Z.Y., Teng, W.P., Wang, Z.Y., 2013b. Intranasal deferoxamine reverses iron-induced memory deficits and inhibits amyloidogenic APP processing in a transgenic mouse model of Alzheimer's disease. *Neurobiology of aging* 34, 562-575.

Halliwell, B., 1987. Oxidants and human disease: some new concepts. *FASEB journal : official publication of the Federation of American Societies for Experimental Biology* 1, 358-364.

Hänninen, M.M., Haapasalo, J., Haapasalo, H., Fleming, R.E., Britton, R.S., Bacon, B.R., Parkkila, S., 2009. Expression of iron-related genes in human brain and brain tumors. *BMC neuroscience* 10, 36.

Hare, D., Ayton, S., Bush, A., Lei, P., 2013. A delicate balance: Iron metabolism and diseases of the brain. *Frontiers in aging neuroscience* 5, 34.

Harrison, P.M., Arosio, P., 1996. The ferritins: molecular properties, iron storage function and cellular regulation. *Biochimica et biophysica acta* 1275, 161-203.

Hentze, M.W., Muckenthaler, M.U., Galy, B., Camaschella, C., 2010. Two to tango: regulation of Mammalian iron metabolism. *Cell* 142, 24-38.

Hou, Y., Dan, X., Babbar, M., Wei, Y., Hasselbalch, S.G., Croteau, D.L., Bohr, V.A., 2019. Ageing as a risk factor for neurodegenerative disease. *Nature reviews. Neurology* 15, 565-581.

Huang, F., Yang, R., Xiao, Z., Xie, Y., Lin, X., Zhu, P., Zhou, P., Lu, J., Zheng, S., 2021. Targeting Ferroptosis to Treat Cardiovascular Diseases: A New Continent to Be Explored. *Frontiers in cell and developmental biology* 9, 737971.

Imai, H., Matsuoka, M., Kumagai, T., Sakamoto, T., Koumura, T., 2017. Lipid Peroxidation-Dependent Cell Death Regulated by GPx4 and Ferroptosis. *Current topics in microbiology and immunology* 403, 143-170.

Jiang, H., Luan, Z., Wang, J., Xie, J., 2006. Neuroprotective effects of iron chelator Desferal on dopaminergic neurons in the substantia nigra of rats with iron-overload. *Neurochemistry international* 49, 605-609.

Jiang, Z., Wang, J., Liu, C., Wang, X., Pan, J., 2019. Hyperoside alleviated N-acetyl-para-amino-phenol-induced acute hepatic injury via Nrf2 activation. *International journal of clinical and experimental pathology* 12, 64-76.

Kawabata, H., Yang, R., Hirama, T., Vuong, P.T., Kawano, S., Gombart, A.F., Koeffler, H.P., 1999. Molecular cloning of transferrin receptor 2. A new member of the transferrin receptor-like family. *The Journal of biological chemistry* 274, 20826-20832.

Ke, Z.J., Gibson, G.E., 2004. Selective response of various brain cell types during neurodegeneration induced by mild impairment of oxidative metabolism. *Neurochemistry international* 45, 361-369.

Kenny, E.M., Fidan, E., Yang, Q., Anthonymuthu, T.S., New, L.A., Meyer, E.A., Wang, H., Kochanek, P.M., Dixon, C.E., Kagan, V.E., Bayir, H., 2019. Ferroptosis Contributes to Neuronal Death and Functional Outcome After Traumatic Brain Injury. *Critical care medicine* 47, 410-418.

Kim, G.H., Kim, J.E., Rhie, S.J., Yoon, S., 2015. The Role of Oxidative Stress in Neurodegenerative Diseases. *Experimental neurobiology* 24, 325-340.

Kollara, A., Brown, T.J., 2010. Variable expression of nuclear receptor coactivator 4 (NcoA4) during mouse embryonic development. *The journal of histochemistry and cytochemistry : official journal of the Histochemistry Society* 58, 595-609.

Kwon, M.Y., Park, E., Lee, S.J., Chung, S.W., 2015. Heme oxygenase-1 accelerates erastin-induced ferroptotic cell death. *Oncotarget* 6, 24393-24403.

Latour, C., Besson-Fournier, C., Meynard, D., Silvestri, L., Gourbeyre, O., Aguilar-Martinez, P., Schmidt, P.J., Fleming, M.D., Roth, M.P., Coppin, H., 2016. Differing impact of the deletion of hemochromatosis-associated molecules HFE and transferrin receptor-2 on the iron phenotype of mice lacking bone morphogenetic protein 6 or hemojuvelin. *Hepatology (Baltimore, Md.)* 63, 126-137.

Leibold, E.A., Gahring, L.C., Rogers, S.W., 2001. Immunolocalization of iron regulatory protein expression in the murine central nervous system. *Histochemistry and cell biology* 115, 195-203.

Li, J., Cao, F., Yin, H.L., Huang, Z.J., Lin, Z.T., Mao, N., Sun, B., Wang, G., 2020. Ferroptosis: past, present and future. *Cell death & disease* 11**,** 88.

Li, Y., Zhou, D., Ren, Y., Zhang, Z., Guo, X., Ma, M., Xue, Z., Lv, J., Liu, H., Xi, Q., Jia, L., Zhang, L., Liu, Y., Zhang, Q., Yan, J., Da, Y., Gao, F., Yue, J., Yao, Z., Zhang, R., 2019. Mir223 restrains autophagy and promotes CNS inflammation by targeting ATG16L1. *Autophagy* 15**,** 478-492.

Lozoff, B., Georgieff, M.K., 2006. Iron deficiency and brain development. *Seminars in pediatric neurology* 13**,** 158-165.

MacKenzie, E.L., Iwasaki, K., Tsuji, Y., 2008. Intracellular iron transport and storage: from molecular mechanisms to health implications. *Antioxidants & redox signaling* 10**,** 997-1030.

Maiuolo, J., Gliozzi, M., Musolino, V., Scicchitano, M., Carresi, C., Scarano, F., Bosco, F., Nucera, S., Ruga, S., Zito, M.C., Mollace, R., Palma, E., Fini, M., Muscoli, C., Mollace, V., 2018. The "Frail" Brain Blood Barrier in Neurodegenerative Diseases: Role of Early Disruption of Endothelial Cell-to-Cell Connections. *International journal of molecular sciences* 19.

Mancardi, D., Mezzanotte, M., Arrigo, E., Barinotti, A., Roetto, A., 2021. Iron Overload, Oxidative Stress, and Ferroptosis in the Failing Heart and Liver. *Antioxidants (Basel, Switzerland)* 10.

Mancias, J.D., Pontano Vaites, L., Nissim, S., Biancur, D.E., Kim, A.J., Wang, X., Liu, Y., Goessling, W., Kimmelman, A.C., Harper, J.W., 2015. Ferritinophagy via NCOA4 is required for erythropoiesis and is regulated by iron dependent HERC2-mediated proteolysis. *eLife* 4.

Mancias, J.D., Wang, X., Gygi, S.P., Harper, J.W., Kimmelman, A.C., 2014. Quantitative proteomics identifies NCOA4 as the cargo receptor mediating ferritinophagy. *Nature* 509**,** 105-109.

Martin-Bastida, A., Ward, R.J., Newbould, R., Piccini, P., Sharp, D., Kabba, C., Patel, M.C., Spino, M., Connelly, J., Tricta, F., Crichton, R.R., Dexter, D.T., 2017. Brain iron chelation by deferiprone in a phase 2 randomised double-blinded placebo controlled clinical trial in Parkinson's disease. *Scientific reports* 7**,** 1398.

Mastroberardino, P.G., Hoffman, E.K., Horowitz, M.P., Betarbet, R., Taylor, G., Cheng, D., Na, H.M., Gutekunst, C.A., Gearing, M., Trojanowski, J.Q., Anderson, M., Chu, C.T., Peng, J., Greenamyre, J.T., 2009. A novel transferrin/TfR2-mediated mitochondrial iron transport system is disrupted in Parkinson's disease. *Neurobiology of disease* 34**,** 417-431.

McKie, A.T., 2008. The role of Dcytb in iron metabolism: an update. *Biochemical Society transactions* 36**,** 1239-1241.

McKie, A.T., Marciani, P., Rolfs, A., Brennan, K., Wehr, K., Barrow, D., Miret, S., Bomford, A., Peters, T.J., Farzaneh, F., Hediger, M.A., Hentze, M.W., Simpson, R.J., 2000. A novel duodenal iron-regulated transporter, IREG1, implicated in the basolateral transfer of iron to the circulation. *Molecular cell* 5**,** 299-309.

Mezzanotte, M., Ammirata, G., Boido, M., Stanga, S., Roetto, A., 2021. BBB damage in aging causes brain iron deposits via astrocyte-neuron crosstalk and Hepc/Fpn1 pathway. 2021.2007.2001.450665.

Milanese, C., Gabriels, S., Barnhoorn, S., Cerri, S., Ulusoy, A., Gornati, S.V., Wallace, D.F., Blandini, F., Di Monte, D.A., Subramaniam, V.N., Mastroberardino, P.G., 2021. Gender biased neuroprotective effect of Transferrin Receptor 2 deletion in multiple models of Parkinson's disease. *Cell death and differentiation* 28**,** 1720-1732.

Mills, E., Dong, X.P., Wang, F., Xu, H., 2010. Mechanisms of brain iron transport: insight into neurodegeneration and CNS disorders. *Future medicinal chemistry* 2**,** 51-64.

Moos, T., Morgan, E.H., 2004. The metabolism of neuronal iron and its pathogenic role in neurological disease: review. *Annals of the New York Academy of Sciences* 1012**,** 14-26.

Moreau, C., Duce, J.A., Rascol, O., Devedjian, J.C., Berg, D., Dexter, D., Cabantchik, Z.I., Bush, A.I., Devos, D., 2018. Iron as a therapeutic target for Parkinson's disease. *Movement disorders : official journal of the Movement Disorder Society* 33**,** 568-574.

Muckenthaler, M.U., Galy, B., Hentze, M.W., 2008. Systemic iron homeostasis and the iron-responsive element/iron-regulatory protein (IRE/IRP) regulatory network. *Annual review of nutrition* 28**,** 197-213.

Muckenthaler, M.U., Rivella, S., Hentze, M.W., Galy, B., 2017. A Red Carpet for Iron Metabolism. *Cell* 168**,** 344-361.

Nai, A., Lidonnici, M.R., Federico, G., Pettinato, M., Olivari, V., Carrillo, F., Geninatti Crich, S., Ferrari, G., Camaschella, C., Silvestri, L., Carlomagno, F., 2021. NCOA4-mediated ferritinophagy in macrophages is crucial to sustain erythropoiesis in mice. *Haematologica* 106**,** 795-805.

Nai, A., Lidonnici, M.R., Rausa, M., Mandelli, G., Pagani, A., Silvestri, L., Ferrari, G., Camaschella, C., 2015. The second transferrin receptor regulates red blood cell production in mice. *Blood* 125**,** 1170-1179.

Nandar, W., Neely, E.B., Unger, E., Connor, J.R., 2013. A mutation in the HFE gene is associated with altered brain iron profiles and increased oxidative stress in mice. *Biochimica et biophysica acta* 1832**,** 729-741.

Ndayisaba, A., Kaindlstorfer, C., Wenning, G.K., 2019. Iron in Neurodegeneration - Cause or Consequence? *Frontiers in neuroscience* 13**,** 180.

Nemeth, E., Tuttle, M.S., Powelson, J., Vaughn, M.B., Donovan, A., Ward, D.M., Ganz, T., Kaplan, J., 2004. Hepcidin regulates cellular iron efflux by binding to ferroportin and inducing its internalization. *Science (New York, N.Y.)* 306**,** 2090-2093.

Nicolas, G., Chauvet, C., Viatte, L., Danan, J.L., Bigard, X., Devaux, I., Beaumont, C., Kahn, A., Vaulont, S., 2002. The gene encoding the iron regulatory peptide hepcidin is regulated by anemia, hypoxia, and inflammation. *The Journal of clinical investigation* 110**,** 1037-1044.

Ohgami, R.S., Campagna, D.R., Greer, E.L., Antiochos, B., McDonald, A., Chen, J., Sharp, J.J., Fujiwara, Y., Barker, J.E., Fleming, M.D., 2005. Identification of a ferrireductase required for efficient transferrin-dependent iron uptake in erythroid cells. *Nature genetics* 37**,** 1264-1269.

Papanikolaou, G., Pantopoulos, K., 2005. Iron metabolism and toxicity. *Toxicology and applied pharmacology* 202**,** 199-211.

Papanikolaou, G., Pantopoulos, K., 2017. Systemic iron homeostasis and erythropoiesis. *IUBMB life* 69**,** 399-413.

Pellegrino, R.M., Boda, E., Montarolo, F., Boero, M., Mezzanotte, M., Saglio, G., Buffo, A., Roetto, A., 2016. Transferrin Receptor 2 Dependent Alterations of Brain Iron Metabolism Affect Anxiety Circuits in the Mouse. *Scientific reports* 6**,** 30725.

Pellegrino, R.M., Riondato, F., Ferbo, L., Boero, M., Palmieri, A., Osella, L., Pollicino, P., Miniscalco, B., Saglio, G., Roetto, A., 2017. Altered Erythropoiesis in Mouse Models of Type 3 Hemochromatosis. *BioMed research international* 2017**,** 2408941.

Petrak, J., Vyoral, D., 2005. Hephaestin--a ferroxidase of cellular iron export. *The international journal of biochemistry & cell biology* 37**,** 1173-1178.

Philpott, C.C., Ryu, M.S., Frey, A., Patel, S., 2017. Cytosolic iron chaperones: Proteins delivering iron cofactors in the cytosol of mammalian cells. *The Journal of biological chemistry* 292**,** 12764-12771.

Piperno, A., Pelucchi, S., Mariani, R., 2020. Inherited iron overload disorders. *Translational gastroenterology and hepatology* 5**,** 25.

Plays, M., Müller, S., Rodriguez, R., 2021. Chemistry and biology of ferritin. *Metallomics : integrated biometal science* 13.

Protchenko, O., Baratz, E., Jadhav, S., Li, F., Shakoury-Elizeh, M., Gavrilova, O., Ghosh, M.C., Cox, J.E., Maschek, J.A., Tyurin, V.A., Tyurina, Y.Y., Bayir, H., Aron, A.T., Chang, C.J., Kagan, V.E., Philpott, C.C., 2021. Iron Chaperone Poly rC Binding Protein 1 Protects Mouse Liver From Lipid Peroxidation and Steatosis. *Hepatology (Baltimore, Md.)* 73**,** 1176-1193.

Quiles Del Rey, M., Mancias, J.D., 2019. NCOA4-Mediated Ferritinophagy: A Potential Link to Neurodegeneration. *Frontiers in neuroscience* 13**,** 238.

Raha-Chowdhury, R., Raha, A.A., Forostyak, S., Zhao, J.W., Stott, S.R., Bomford, A., 2015. Expression and cellular localization of hepcidin mRNA and protein in normal rat brain. *BMC neuroscience* 16**,** 24.

Rauner, M., Baschant, U., Roetto, A., Pellegrino, R.M., Rother, S., Salbach-Hirsch, J., Weidner, H., Hintze, V., Campbell, G., Petzold, A., Lemaitre, R., Henry, I., Bellido, T., Theurl, I., Altamura, S., Colucci, S., Muckenthaler, M.U., Schett, G., Komla Ebri, D., Bassett, J.H.D., Williams, G.R., Platzbecker, U., Hofbauer, L.C., 2019. Transferrin receptor 2 controls bone mass and pathological bone formation via BMP and Wnt signaling. *Nature metabolism* 1**,** 111-124.

Rhodes, S.L., Buchanan, D.D., Ahmed, I., Taylor, K.D., Loriot, M.A., Sinsheimer, J.S., Bronstein, J.M., Elbaz, A., Mellick, G.D., Rotter, J.I., Ritz, B., 2014. Pooled analysis of iron-related genes in Parkinson's disease: association with transferrin. *Neurobiology of disease* 62**,** 172-178.

Rishi, G., Secondes, E.S., Wallace, D.F., Subramaniam, V.N., 2016. Normal systemic iron homeostasis in mice with macrophage-specific deletion of transferrin receptor 2. *American journal of physiology. Gastrointestinal and liver physiology* 310**,** G171-180.

Rodriguez, A., Pan, P., Parkkila, S., 2007. Expression studies of neogenin and its ligand hemojuvelin in mouse tissues. *The journal of histochemistry and cytochemistry : official journal of the Histochemistry Society* 55**,** 85-96.

Roetto, A., Di Cunto, F., Pellegrino, R.M., Hirsch, E., Azzolino, O., Bondi, A., Defilippi, I., Carturan, S., Miniscalco, B., Riondato, F., Cilloni, D., Silengo, L., Altruda, F., Camaschella, C., Saglio, G., 2010. Comparison of 3 Tfr2-deficient murine models suggests distinct functions for Tfr2-alpha and Tfr2-beta isoforms in different tissues. *Blood* 115**,** 3382-3389.

Roetto, A., Mezzanotte, M., Pellegrino, R.M., 2018. The Functional Versatility of Transferrin Receptor 2 and Its Therapeutic Value. *Pharmaceuticals (Basel, Switzerland)* 11.

Roskams, A.J., Connor, J.R., 1994. Iron, transferrin, and ferritin in the rat brain during development and aging. *Journal of neurochemistry* 63**,** 709-716.

Rouault, T.A., 2013. Iron metabolism in the CNS: implications for neurodegenerative diseases. *Nature reviews. Neuroscience* 14**,** 551-564.

Ryu, M.S., Zhang, D., Protchenko, O., Shakoury-Elizeh, M., Philpott, C.C., 2017. PCBP1 and NCOA4 regulate erythroid iron storage and heme biosynthesis. *The Journal of clinical investigation* 127**,** 1786-1797.

Santambrogio, P., Levi, S., Cozzi, A., Rovida, E., Albertini, A., Arosio, P., 1993. Production and characterization of recombinant heteropolymers of human ferritin H and L chains. *The Journal of biological chemistry* 268**,** 12744-12748.

Sheng, M., Greenberg, M.E., 1990. The regulation and function of c-fos and other immediate early genes in the nervous system. *Neuron* 4**,** 477-485.

Silvestri, L., Pagani, A., Nai, A., De Domenico, I., Kaplan, J., Camaschella, C., 2008. The serine protease matriptase-2 (TMPRSS6) inhibits hepcidin activation by cleaving membrane hemojuvelin. *Cell metabolism* 8**,** 502-511.

Skouta, R., Dixon, S.J., Wang, J., Dunn, D.E., Orman, M., Shimada, K., Rosenberg, P.A., Lo, D.C., Weinberg, J.M., Linkermann, A., Stockwell, B.R., 2014. Ferrostatins inhibit oxidative lipid damage and cell death in diverse disease models. *Journal of the American Chemical Society* 136**,** 4551-4556.

Sripetchwandee, J., Wongjaikam, S., Krintratun, W., Chattipakorn, N., Chattipakorn, S.C., 2016. A combination of an iron chelator with an antioxidant effectively diminishes the dendritic loss, tau-hyperphosphorylation, amyloids-β accumulation and brain mitochondrial dynamic disruption in rats with chronic iron-overload. *Neuroscience* 332**,** 191-202.

Vela, D., 2018. Hepcidin, an emerging and important player in brain iron homeostasis. *Journal of translational medicine* 16**,** 25.

Wallace, D.F., Summerville, L., Subramaniam, V.N., 2007. Targeted disruption of the hepatic transferrin receptor 2 gene in mice leads to iron overload. *Gastroenterology* 132**,** 301-310.

Wang, W., Knovich, M.A., Coffman, L.G., Torti, F.M., Torti, S.V., 2010. Serum ferritin: Past, present and future. *Biochimica et biophysica acta* 1800**,** 760-769.

Ward, R.J., Zucca, F.A., Duyn, J.H., Crichton, R.R., Zecca, L., 2014. The role of iron in brain ageing and neurodegenerative disorders. *The Lancet. Neurology* 13**,** 1045-1060.

Wilkinson, J.t., Di, X., Schönig, K., Buss, J.L., Kock, N.D., Cline, J.M., Saunders, T.L., Bujard, H., Torti, S.V., Torti, F.M., 2006. Tissue-specific expression of ferritin H regulates cellular iron homoeostasis in vivo. *The Biochemical journal* 395**,** 501-507.

Wilkinson, N., Pantopoulos, K., 2014. The IRP/IRE system in vivo: insights from mouse models. *Frontiers in pharmacology* 5**,** 176.

Wu, X.G., Wang, Y., Wu, Q., Cheng, W.H., Liu, W., Zhao, Y., Mayeur, C., Schmidt, P.J., Yu, P.B., Wang, F., Xia, Y., 2014. HFE interacts with the BMP type I receptor ALK3 to regulate hepcidin expression. *Blood* 124**,** 1335-1343.

Wyss-Coray, T., 2016. Ageing, neurodegeneration and brain rejuvenation. *Nature* 539**,** 180-186.

Xiao, X., Dev, S., Canali, S., Bayer, A., Xu, Y., Agarwal, A., Wang, C.Y., Babitt, J.L., 2020. Endothelial Bone Morphogenetic Protein 2 (Bmp2) Knockout Exacerbates Hemochromatosis in Homeostatic Iron Regulator (Hfe) Knockout Mice but not Bmp6 Knockout Mice. *Hepatology (Baltimore, Md.)* 72**,** 642-655.

Yang, W.S., Stockwell, B.R., 2008. Synthetic lethal screening identifies compounds activating iron-dependent, nonapoptotic cell death in oncogenic-RAS-harboring cancer cells. *Chemistry & biology* 15**,** 234-245.

Yu, S., Feng, Y., Shen, Z., Li, M., 2011. Diet supplementation with iron augments brain oxidative stress status in a rat model of psychological stress. *Nutrition (Burbank, Los Angeles County, Calif.)* 27**,** 1048-1052.

Zecca, L., Fariello, R., Riederer, P., Sulzer, D., Gatti, A., Tampellini, D., 2002. The absolute concentration of nigral neuromelanin, assayed by a new sensitive method, increases throughout the life and is dramatically decreased in Parkinson's disease. *FEBS letters* 510**,** 216-220.

Zecca, L., Stroppolo, A., Gatti, A., Tampellini, D., Toscani, M., Gallorini, M., Giaveri, G., Arosio, P., Santambrogio, P., Fariello, R.G., Karatekin, E., Kleinman, M.H., Turro, N., Hornykiewicz, O., Zucca, F.A., 2004a. The role of iron and copper molecules in the neuronal vulnerability of locus coeruleus and substantia nigra during aging. *Proceedings of the National Academy of Sciences of the United States of America* 101**,** 9843-9848.

Zecca, L., Youdim, M.B., Riederer, P., Connor, J.R., Crichton, R.R., 2004b. Iron, brain ageing and neurodegenerative disorders. *Nat Rev Neurosci* 5**,** 863-873.

Zechel, S., Huber-Wittmer, K., von Bohlen und Halbach, O., 2006. Distribution of the iron-regulating protein hepcidin in the murine central nervous system. *Journal of neuroscience research* 84**,** 790-800.

Zhang, D.L., Ghosh, M.C., Rouault, T.A., 2014. The physiological functions of iron regulatory proteins in iron homeostasis - an update. *Frontiers in pharmacology* 5**,** 124.

Zhao, N., Gao, J., Enns, C.A., Knutson, M.D., 2010. ZRT/IRT-like protein 14 (ZIP14) promotes the cellular assimilation of iron from transferrin. *The Journal of biological chemistry* 285**,** 32141-32150.

Zucca, F.A., Segura-Aguilar, J., Ferrari, E., Muñoz, P., Paris, I., Sulzer, D., Sarna, T., Casella, L., Zecca, L., 2017. Interactions of iron, dopamine and neuromelanin pathways in brain aging and Parkinson's disease. *Progress in neurobiology* 155**,** 96-119.